OXYGEN AND HYDROGEN ISOTOPE RATIOS IN CHERTS AND RELATED ROCKS

Thesis by

LeRoy Paul Knauth

In Partial Fulfillment of the Requirements

For the Degree of

Doctor of Philosophy

California Institute of Technology

Pasadena, California

1973

(Submitted August 7, 1972)

ACKNOWLEDGEMENTS

I wish to express my deepest appreciation to Dr. Samuel Epstein for his guidance and encouragement. I also thank him for the use of his laboratory facilities and the freedom to develop the course of this investigation. Many of his ideas and suggestions have been incorporated into this research.

My sincere thanks go to the following people:

Dr. Heinz Lowenstam for contributing several important samples and for many useful discussions about cherts, carbonates, and the history of the earth;

Mrs. Jane Young for examining, preparing, and isotopically analyzing the carbonate samples, and for general inspiration;

Mr. Joop Goris for patiently performing nearly all of the CO_2 mass-spectrometric analyses;

Mr. Victor Nenow for his many frustrating hours trying to teach me electronics;

Mr. Curtis Bauman for constructing the metal parts of the oxygen-extraction apparatus;

Drs. R. N. Clayton, H. Craig, H. P. Taylor, Jr., and L. T. Silver for helpful discussions;

Drs. E. C. Perry, J. Schopf, J. Verhoogen, W. Newman, L. T. Silver, J. Lawrence, and Mr. H. Emerson for contributing samples;

My parents, Mr. and Mrs. W. T. Knauth, who made possible the use of a vehicle for the 11,000 mile collecting trip;

Mr. Richard Forester, who spotted a mistake in my procedure for going through the maze of isotopic correction factors;

Mrs. Jan Scott for drafting a number of the diagrams;

Mrs. Jan Zawacki for her devoted labor in typing this thesis with uncanny speed and accuracy;

and the staff and students at Caltech for all that I have learned from them.

Finally, I would like to thank Mrs. Bep Bingham for making the writing of this thesis possible by loaning me her set of Willson "Sound-Silencer" ear muffs which helped shut out the incredible din generated continuously by irresponsible personnel on the Caltech campus.

During part of this research I was supported by a National Defense Education Act fellowship. Research funds were provided by Dr. Samuel Epstein from NSF grant GA-31325X and from grants given by the Atomic Energy Commission.

ABSTRACT

The feasibility of making meaningful measurements of the deuterium content of water extracted from hydrous silica has been evaluated by a series of dehydration and isotope exchange experiments. A new experimental technique, called Differential Isotopic Analysis (D.I.A.), has been developed which allows the isotopic exchange characteristics of water in different sites in hydrous silica to be determined. This method involves the sampling of successive increments of water driven off during heating of the silica and the measurement of δD for these water samples. The isotopic pattern established for the δD-values of successively driven-off samples varies markedly, depending on the degree to which the water in silica has been exchanged with deuterium-rich water in controlled experiments. The fraction of the water or hydroxyl groups that is most resistant to exchange and most difficult to drive off is that water or hydroxyl group most likely to contain the hydrogen which was in equilibrium with the waters from which the silica formed.

Granular microcrystalline quartz, the most common constituent of chert, has been found to contain hydroxyl groups particularly suitable for hydrogen isotope analyses. Cherts of a given age consisting of granular microcrystalline quartz free of organic matter yield an approximate linear

relationship between δD and δO^{18} of the total oxygen. The line thus defined is parallel to the δD-δO^{18} relationship for meteoric waters, but has an intercept which is age-dependent. The isotope data indicate that, for many cherts, the diagenetic transformation of opal to granular microcrystalline quartz occurred in the presence of meteoric waters. The displacement with time of the δD-δO^{18} relationship is interpreted as being due to the effect of past climatic temperature changes on the temperature-dependent isotopic fractionation factors for D/H and O^{18}/O^{16}. The variations in O^{18}/O^{16} and D/H ratios of cherts and other forms of hydrous silica have been investigated and have been used to deduce climatic temperature variations for the central and western United States over geologic time.

The chert-water oxygen isotope fractionation with temperature was estimated from published experimental data and from the isotopic compositions of cherts which formed at approximately known temperatures. The fractionation is

$$1000 \ln \alpha\, O^{18}/O^{16}\ (\text{chert-water}) = 3.09\ (10^6\ {}^{\circ}K^{-2}) - 3.29$$

This equation was used to calibrate the temperature dependence of the variation with time of the δD-δO^{18} linear relationships for cherts, assuming that the variations are due entirely to climatic temperature fluctuations and that the oceans have not changed isotopically with time.

Temperatures deduced for chert formation indicate that the average past climatic temperatures for the central and western United States decreased from 34°C to 20°C through the Paleozoic, increased to 35° - 40°C in the Triassic, and then decreased to the present day value of 13° - 15°C. Temperatures in the Precambrian for this region may have reached over 50°C at 1.3 billion years, although temperatures similar to those of the Phanerozoic Era are inferred at 2 billion years and 1.2 billion years. Extremely cold temperatures deduced for deep ocean water from the oxygen isotopic composition of several samples of opal-CT (1.2 wt.% H_2O) in deep sea sediments indicates the possibility of ice caps at the close of the Cretaceous and at the beginning of the Oligocene. Granular microcrystalline quartz in deep sea sediments often forms during deep burial at elevated temperatures and cannot be used to deduce deep ocean temperatures.

Cherts are usually not in isotopic equilibrium with their coexisting carbonates, and the somewhat insensitive chert-calcite oxygen isotope fractionation thus cannot be used to obtain meaningful temperatures. Calcitic Crinoid fragments in a chert nodule from the Mississippian Burlington limestone yielded an oxygen isotopic temperature of 25°C, indicating that fossil fragments encased within chert nodules may be protected from post-depositional exchange with ground waters and thus suitable for isotopic paleo-

temperature analysis.

Most forms of opal are so hydrous that meaningful δ-values cannot be ascertained with existing analytical techniques. Hyalite opal presents the fewest difficulties since it contains less than 3% H_2O. In spite of the analytical difficulties, δ-values for amorphous silica qualitatively reflect the isotopic composition of the waters and temperatures of formation.

TABLE OF CONTENTS

Chapter I

INTRODUCTION

1.1 Stable Isotopes and the Chert Problem

In 1935 Urey and Greiff showed that theoretical differences in the chemical properties of the isotopes for an element were probably large enough to cause isotope fractionation during natural processes. However, extensive studies of variations in the ratios of stable isotopes did not begin until A. O. Nier developed the double-collecting mass spectrometer which allowed rapid and precise measurement of relative isotope abundances (Nier, 1947). Using a mass spectrometer which had been modified by McKinney et al. (1950) to give increased precision, Epstein et al. (1951, 1953) established a relationship between temperature and relative O^{18} abundance in calcium carbonate in marine shells. This relationship was used by Urey et al. (1951) to deduce the temperatures of the Upper Cretaceous oceans. At the same time, Silverman (1951) showed that the O^{18}/O^{16} ratio in silicate minerals varied significantly and could be useful in elucidating geologic processes.

Since these developments, the field of isotope geochemistry has expanded rapidly. Variations in the isotopic composition of hydrogen, oxygen, and carbon have been used extensively to obtain significant information useful in solving a host of geologic problems. The breadth of recent

research in stable isotope geochemistry is illustrated by the numerous references given by Clayton (1971).

Among sedimentary materials, those which have been studied the most by stable isotope methods are the carbonates and, to a lesser extent, the clay minerals. The present work on authigenic silica was initiated to further extend the understanding of oxygen and hydrogen isotope variations in sedimentary rocks. It will be shown that the isotopic variations of hydrogen and oxygen in authigenic silica are probably related to past climatic temperatures and the isotopic history of the hydrosphere.

Sedimentary silica is commonly referred to as "chert" although a variety of other terms have been used. These rocks are chemically simple, consisting only of hydrous SiO_2. They are distinguished from the mechanically deposited sandstones of similar composition by the fact that they have been chemically precipitated from an aqueous solution. They are found as important constituents of the geologic column over all of geologic time. Once crystallized, these materials become highly insoluble, highly impermeable, and very resistant to alteration. This suggests that their isotopic composition may be well preserved, and therefore of use in deducing the original conditions associated with their deposition.

Most previous information regarding the nature of

cherts has typically been based on careful field and petrographic observations. The interpretation of these observations are often ambiguous, and considerable controversy has arisen concerning the origin of most forms of chert. Chemical analyses of this material have revealed little or no major variation. This chemical monotony has greatly inhibited geochemical investigations of cherts. An understanding of the isotopic variations thus takes on added importance as an additional approach to the solution of problems associated with chert genesis.

1.2 Research Objectives

I. The first objective of this research was to evaluate the possibility of making meaningful measurements of the D/H ratio of water extracted from cherts and opals. These measurements should aid the interpretation of any observed isotope variations.

II. The second objective consisted of determining the isotopic variation in a suite of silica samples specially collected for the following purposes: (1) to ascertain the range of natural variations in the isotopic composition of well-preserved cherts collected from a variety of sediments of all ages, (2) to determine the effects of low-grade metamorphism and hydrothermal activity on the isotope ratios of cherts, (3) to determine whether the waters involved in chert or opal formation were marine

or non-marine, (4) to indicate whether the original isotope ratios in marine cherts have been preserved with time and can be used to place constraints on the isotopic history of the oceans, and (5) to deduce possible temperatures of formation of individual cherts and opals.

III. The final objective was to examine the O^{18}/O^{16} and C^{13}/C^{12} ratios in calcites and dolomites coexisting with cherts to determine if the quartz-calcite oxygen isotope geothermometer could be used for obtaining reliable temperatures of chert formation. This additional data should also provide pertinent information concerning chert genesis.

1.3 Notation

The most desirable method of reporting the isotopic composition of a substance is to express it as a ratio, such as O^{18}/O^{16}, D/H, etc. Unfortunately, such a ratio is experimentally difficult to measure. However, variations in these ratios among different substances can be measured precisely by use of the double-collecting mass spectrometer originally designed by Nier (1947) and modified by McKinney et al. (1950). These variations are normally reported as the per mil (.1%) difference between the absolute ratio of the unknown sample and the absolute ratio of an arbitrary standard. This difference is known as a δ-value, and is expressed as

$$\delta \text{‰}_{std}\ X = \left[\frac{\text{Ratio X} - \text{Ratio std}}{\text{Ratio std}}\right] 10^3$$

X = sample std = standard

Positive δ-values usually indicate an enrichment of the heavier isotope in the sample relative to the standard, while negative δ-values indicate relative depletion. If the absolute ratio of the standard is known it is possible to use the above equation to determine the absolute ratios of samples for which the δ-value has been determined. At present, values for the absolute ratios of the standards commonly used are known with insufficient precision. It is therefore necessary to report δ-values rather than absolute ratios. Fortunately, as long as all the isotope ratios measured on the mass spectrometer are related to the true ratio by a constant (but unknown) multiplicative factor, the precision of the δ-values is the same as for those cases where the absolute ratios are known.

In this work

$$(1\text{-}1) \qquad \delta O^{18} = \left[\frac{O^{18}/O^{16}_{sample} - O^{18}/O^{16}_{SMOW}}{O^{18}/O^{16}_{SMOW}}\right] 10^3$$

where SMOW is Standard Mean Ocean Water, as defined by Craig (1961b).

$$(1\text{-}2) \qquad \delta D = \left[\frac{D/H_{sample} - D/H_{SMOW}}{D/H_{SMOW}}\right] 10^3$$

$$(1\text{-}3) \qquad \delta C^{13} = \left[\frac{C^{13}_{\text{sample}} - C^{13}/C^{12}_{\text{PDB}}}{C^{13}/C^{12}_{\text{PDB}}} \right] 10^3$$

The C^{13}/C^{12} standard (PDB) is carbon dioxide prepared by reacting 100% H_3PO_4 with PDB calcium carbonate at 25.2°C. PDB consists of Cretaceous belemnites, Belemnitella americana, from the Peedee formation of South Carolina.

The per mil difference between δ-values for two substances, A and B is sometimes referred to as the "fractionation" between A and B. This quantity ($\delta_A - \delta_B$) is frequently replaced by the symbol Δ_{A-B}. The term "fractionation" is distinct from the term "fractionation factor" (α), which represents the partition of the isotope ratios between two phases and will be discussed later.

1.4 Previous Work Involving Stable Isotope Studies of Silica

Although there has been no systematic survey of the isotopic composition of cherts and opals, some data for various types of sedimentary silica do exist. The results of this previous work are summarized below.

1. O^{18}/O^{16} in silica. Silverman (1951), in an early survey of the distribution of oxygen isotopes in natural silicates, observed that samples of Dover flint and Miocene diatomite yielded the largest O^{18}/O^{16} ratios of any materials sampled. This result suggested that the O^{18}/O^{16}

ratio in terrestrial rocks is greatest for silica precipitated in the ocean. Recently, however, O'Neil and Hay (1971) have measured even greater O^{18}/O^{16} ratios in cherts which are associated with the alkaline lakes of East Africa. These authors suggested that O^{18}-rich brines were involved in the chert formation, accounting for the "heavy" values.

2. The use of cherts in isotope thermometry. Shortly after analytical methods for precise δO^{18} measurements were developed, a number of cherts were analyzed in attempts to use quartz-calcite fractionations for temperature determinations. Clayton and Epstein (1958) observed that at low temperatures, the Δ-quartz-calcite is about 7 for "unaltered" cherty limestones and that this fractionation decreases for samples known geologically to have formed at higher temperatures. This result was in good agreement with the behavior suggested by theoretical isotope considerations, and led to a study of the hydrothermal alteration of the Leadville Limestone (Engel et al. 1958). This work yielded the following results relevant to the present investigation. First, it was observed that cherts in unaltered beds of this Mississippian limestone were very uniform in δO^{18} along and across bedding over large areas. This suggests that in a survey of cherts a δO^{18} measurement of a given chert sample might be representative of cherts over areas the size of an outcrop or larger, thereby eliminating the need for massive sampling.

Secondly, δ-values of the unaltered cherts were about 6‰ more negative than values expected for "normal" marine carbonate and silica. This difference was attributed to probable isotope exchange of the original sedimentary constituents with ground waters after lithification of the rock. The result, however, pointed out the need for an extended survey of cherts and limestones to find out if this discrepancy was true for all ancient limestones and cherts, or if it was an anomaly peculiar to the Leadville Limestone.

Thirdly, it was observed that hydrothermal activity and metamorphism could obliterate the original δ-values of chert and carbonate; the more water involved in the hydrothermal activity, the greater the amount of alteration. Taylor and Coleman (1968) also observed that this was true in the case of bedded cherts metamorphosed in the blueschist facies. Engel et al, found that the δO^{18} alteration was useful in that they could use the new quartz-calcite oxygen isotope fractionations to estimate approximate temperatures and degree of isotopic equilibrium obtained during the metamorphism.

3. Chert in iron formations. Previous work on the isotopic composition of cherts in iron formations was largely concerned with the readjustment of δO^{18} values during metamorphism and the possibility of using the quartz-

magnetite oxygen isotope fractionation to determine metamorphic temperatures. James and Clayton (1962) observed that the oxygen isotope ratios of bedded cherts in Precambrian iron formations could be altered at temperatures below 250°C. However, Sharma et al. (1965) claimed that the O^{18}/O^{16} ratio of meta-cherts in the Quebec iron formation largely reflected the original values in spite of a regional metamorphism to amphibolite facies.

Becker (1971) performed oxygen and carbon isotope analyses on an extended suite of samples from the two billion year old Hemersley Iron Province in western Australia. The bedded cherts, carbonates, and iron oxides in this formation are considered one of the least altered and best preserved of the Precambrian iron formations. Becker, however, concluded that massive isotope exchange had occurred during a low-grade metamorphism lowering the δO^{18} of the cherts and carbonates uniformly by eleven to fourteen per mil. Using newly calculated quartz-water and magnetite-water fractionations, he concluded that much of the iron-formation had equilibrated at 280°C. The original sedimentary oxygen isotope record was thus considered destroyed. The carbon isotope record, however, was shown to be preserved and indicative of a closed-basin origin for these sediments.

The results of isotope work on "chert"-bearing iron-

formations are thus somewhat different with regard to the redistribution of oxygen isotopes during metamorphism. Either certain conditions were drastically different for the different formations (e.g. amount of water involved), or else there are alternative explanations for the isotope data. This question will be examined later.

4. Cherts in limestones. Most of the chert in the sedimentary column occurs in limestones. It is usually found there in the form of nodules, thin beds, silicified fossils, and finely disseminated grains. Very little stable isotope work has been done on these kinds of chert.

(a) Savin and Epstein (1970b), in their general survey of oxygen and hydrogen isotopes in sedimentary materials, analyzed a suite of silicified Devonian brachiopods. They observed a wide range of oxygen isotopic compositions, and were able to conclude that these replacements had occurred at temperatures below 100°C. The variations of the measured values were attributed to complicated processes involving dehydration of amorphous silica or silicifation of the fossils in the presence of fresh water after lithification and uplift.

(b) Degens and Epstein (1962) analyzed a series of thirty-five coexisting Phanerozoic limestones and cherts for O^{18}/O^{16} ratios. The data suggested a time trend in which the O^{18}/O^{16} ratio of both cherts and

limestones decreased with increasing age of the samples. The authors interpreted this trend as post-depositional exchange with ground waters depleted in O^{18}. In their interpretation older samples had longer times to suffer such exchange and thus had been altered the most. This work suggested that cherts had as poor an isotopic memory as the easily exchangeable limestones.

5. Bedded cherts. δO^{18} measurements for six Precambrian and two Devonian samples of bedded chert were made by Perry (1967). He also observed suggestion of a time trend in which the more ancient cherts were depleted in O^{18}. A number of arguments were advanced by him against the explanation that the trend was due simply to cherts exchanging with ground waters over long periods of time. Assuming that these cherts were of marine origin and had formed in approximate isotopic equilibrium at low temperatures, he interpreted the variation as representing a progressive change in the oxygen isotopic composition of the ocean with time. This change was attributed to progressive outgassing of the mantle, adding water richer in O^{18} to a primordial ocean depleted in this isotope.

Continuing this study of ancient cherts, Perry and Tan (1972) made a more detailed analysis of carbon and oxygen isotopes in the early Precambrian bedded-metachert sequences in South Africa. These authors argued that the

pre-metamorphic O^{18} values of the cherts had been largely preserved and were approximately 17‰ lower than values for modern oceanic silica. Again, assuming that these cherts were precipitated from ocean water at temperatures comparable to present day temperatures, they concluded that the δO^{18} of the early Precambrian oceans was fifteen to seventeen per mil lighter than present ocean water and that the model of Perry (1967) was a valid explanation for these data. Thus, these two studies of ancient cherts were presented as arguments that oxygen isotope analyses of cherts could be used to establish the rate of mantle outgassing and the growth of the earth's oceans.

6. Biogenic silica. More recent sediments frequently contain large amounts of biogenic opal. After similar measurements by Silverman (1951) and Degens and Epstein (1962), Savin (1967) measured an ocean-core sample composed almost entirely of the siliceous debris of organisms. He obtained a considerably lower O^{18}/O^{16} ratio than similar materials analyzed by Degens and Epstein who had dehydrated the samples. The difficulties in analyzing extremely hydrous silica were thus illustrated.

Mopper and Garlick (1971) found that the water component of oceanic radiolaria caused δO^{18} analyses of these materials to be irreproducible. This poor reproducibility inhibits the use of radiolaria for isotopic paleotemperature

investigations. Nevertheless, they observed that Pleistocene radiolarians were enriched in O^{18} relative to recent radiolarians in the same oceanic core sample by about 2‰. This enrichment was attributed to post-depositional exchange at bottom temperatures or early diagenetic redistribution of the silica. Their measurement of the fractionation between present day ocean water and biogenic silica of 36 to 38‰ corresponds closely to a value of +36‰ for authigenic oceanic quartz crystals measured by Garlick (1969).

7. Hydrogen isotopes in cherts. A search of the literature revealed that almost no previous work had been done on hydrogen isotopes in cherts or opals. This is perhaps not surprising since so little is known about the isotopic variations during the process of extracting water from hydrous silica as well as the lack of substantive information regarding the hydration states of this water in cherts and opals.

For purposes of structural determinations, Micheelsen (1966) attempted to replace with deuterium the hydrogen of H_2O and OH in flints from the Cretaceous chalks of Denmark. After boiling in D_2O for three weeks, infrared measurements on the flints showed that some of the H_2O molecules and none of the hydroxyls had been replaced by D_2O. This result hampered Micheelsen's extensive study of the various

OH sites, but provided evidence that hydroxyls in cherts were not labile and thus could be useful for hydrogen isotope studies of natural samples, a very important result for the present investigation.

1.5 Summary of Previous Work

Work done prior to this investigation had firmly established the following points.

1. The fractionation for silica-water in the temperature range 0-20°C is approximately 36-40‰, making most forms of precipitated silica richer in O^{18} than other terrestrial materials.

2. This initially large δO^{18} value for cherts can be significantly lowered by metamorphic and hydrothermal processes. This alteration leaves little trace of the primary δO^{18} values, but can frequently be useful in determining metamorphic temperatures.

3. The hydrous component of opaline silica makes accurate δO^{18} analysis of this material exceedingly difficult.

Less firmly established is the observation that natural samples of silica display a systematic variation in O^{18}/O^{16} ratio, with the oldest samples containing the least O^{18}. Explanations of this apparent trend were incomplete, especially in discriminating between the isotope

effects of metamorphism, post-depositional exchange, primary environment, and evolutionary trends in the thermal and isotopic history of the hydrosphere. The fundamental questions left unanswered by these efforts concerned (1) an understanding of the basic controls on the original isotopic composition of cherts, and (2) the extent to which these values have been altered by subsequent events. It is to these questions that much of the following research has been directed.

Chapter 2

REVIEW OF SILICA IN SEDIMENTS

2.1 Introduction

In order to better understand the meaning of isotope analyses of cherts and opals it is worthwhile to consider some mineralogic and petrologic aspects of these substances. Hydrous SiO_2 (silica) occurs in several mineralogical varieties, many of which are amorphous. The paragenesis of silica varieties in a particular deposit reflects the conditions of its formation as well as the subsequent diagenetic and metamorphic history. It is therefore necessary to clarify the mineralogical character of silica before attempting to understand its isotopic composition. Also, because of its variable water content, there are analytical problems associated with the measurement of δ-values for several of these varieties of silica. Measurements of the isotopic composition of silica for which the mineralogical character has not been considered may thus be erroneous.

Cherts and opals are found in a great variety of marine and fresh water sediments. Many of the occurrences are the result of diagenesis and may have had different diagenetic histories. Conclusions deduced for one geologic setting may not apply to another setting. It is thus

desirable to distinguish between the different modes of occurrence of silica in sediments to provide a framework for a meaningful interpretation of the isotope data.

The terminology used to describe samples in this thesis is in accord as much as possible with usage in the more recent literature. The term "silica" simply refers to hydrous SiO_2 without specific reference to the mineralogical form. "Chert" refers to crystalline forms, and "opal" is used as an inclusive term for amorphous silica.

2.2 Mineralogy of the Chemical Siliceous Sediments

Silica occurs naturally in crystalline and amorphous forms. The crystalline forms can be represented by three petrographic end members: granular microcrystalline quartz (Keller, 1941), chalcedony or chalcedonic quartz (Folk and Weaver, 1952), and megaquartz (Folk, 1950).

A. Granular microcrystalline quartz. The most common constituent of nodular and bedded cherts is granular microcrystalline quartz. This material consists of interlocking, anhedral grains of α-quartz, 2-30μ in size. Petrographically, these individual grains are characterized by the presence of undulatory extinction and have very diffuse grain boundaries.

Micheelsen (1966), utilizing a variety of analytical techniques, has made an exhaustive study of the structure of granular microcrystalline quartz as it occurs in the

dark flints from Stevns, Denmark. In his structural model, the granular microcrystalline quartz grains are each built up of piles of plates of α-quartz parallel to (0001). The plates have a mean thickness of about 600Å, and their faces are covered with Si-OH groups. Adjacent plates are joined by a monolayer of water. The presence of water results in alternating plates of right and left-handed quartz forming twins according to the Brazil law. Individual plates contain sub-grains and are finely divided by twin faults. Additional Si-OH groups are present along these fault-planes. His proposed sites for these particular hydroxyls are shown in figure 2-1.

Using a combination of infrared and thermogravimetric techniques, Micheelson concluded that these cherts contained .27% H_2O and 1.0% water by weight in the form of hydroxyls bonded to silicon. As noted earlier, he could not exchange the OH with D_2O at 101°C.

Micheelson finally proposed that these granular microcrystalline quartz grains might have formed by the epitaxial replacement of consolidated silica gel (called "subsidiary cryptocrystalline silica", a disordered intergrowth of cristobalite and tridymite (A. Tovborg Jensen et al., 1957; and Micheelson, 1966)).

The extent to which Micheelson's structural model applies to granular microcrystalline quartz in other cherts

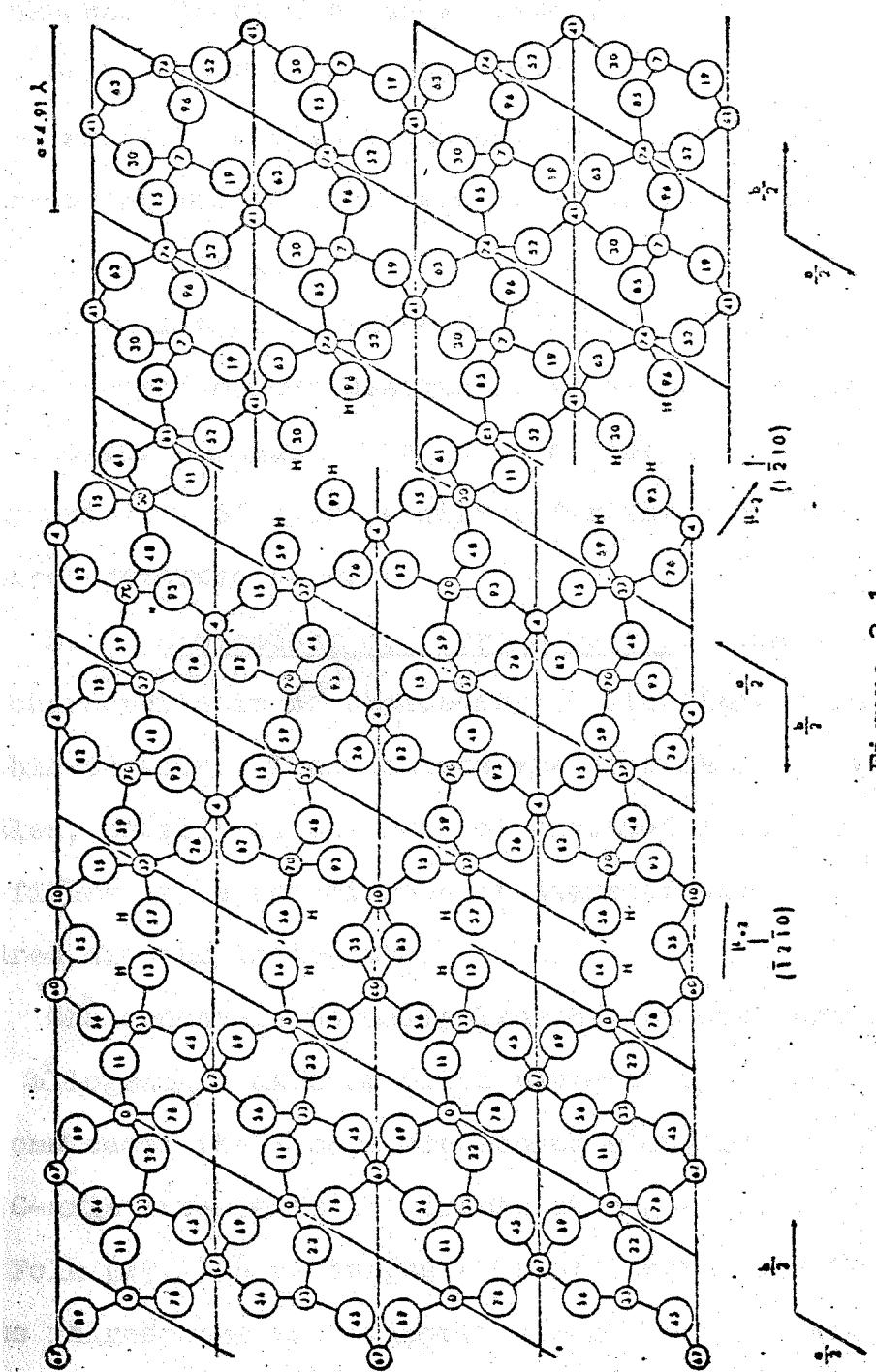

Figure 2-1

STRUCTURAL MODEL FOR PLATE OF α-QUARTZ IN FLINT FROM STEVNS, DENMARK (MICHELSEN, 1966)

is unknown. As will be shown later, most cherts contain considerably less total water than the 1.3% by weight described above. In all liklihood, this is due to loss of water during partial recrystallization of the granular microcrystalline quartz.

In this thesis, Micheelson's model is considered to define the end-member designated as granular microcrystalline quartz. Granular microcrystalline quartz is the most important form of hydrous silica for the purposes of the research reported here.

B. Chalcedony or Fibrous Quartz. The distinguishing characteristic of chalcedony is its fibrous appearance in thin-section. These fibers are seen as radiating bundles, usually in the form of cavity-filling spherulites. The fibers are a few microns in diameter and several hundred microns in length.

Chalcedony is normally length-fast with the C crystallographic axis oriented perpendicular to the fibers. In some cases the fibers are length slow, indicating that the C-axis intersects the fibers at angles of 90^{o}. Pittman and Folk (1971) have suggested that length-slow chalcedony forms in response to "evaporite-prone" environments, while length-fast chalcedony is characteristic of non-evaporite environments.

Folk and Weaver (1952) have observed that the fibrous

nature of chalcedony is not apparent under the electron microscope. They noted numerous fluid filled bubbles approximately 1 micron in diameter. The authors suggested that water was present in these cavities accounting for the brownish color and the reduced density and refractive index of chalcedony relative to quartz. Pittman (1959) failed to see these bubbles in chalcedony from the Edwards Limestone, Texas, indicating the fluid-filled inclusions may not be a general characteristic of fibrous quartz. No other information is available on the actual water content of chalcedony. This results from the fact that chalcedony is much less abundant than granular microcrystalline quartz in nearly all cherts, and thus hard to separate in large amounts for analysis. As noted in Chapter 9, Tertiary chalcedony in deep sea sediments has 1 wt-% water in the form of hydroxyls bonded to silicon.

As already mentioned, chalcedony usually occurs as a cavity-filling, and it is the most common fossil-replacement material. Folk and Weaver (1952) have suggested that chalcedony will usually form in preference to the other forms of quartz when free growth space is available. Indeed, such growth space may be a prerequisite for chalcedony formation. Fibers of chalcedony frequently grade outward into well-defined α-quartz (here called megaquartz).

Chalcedony was rarely a major constituent of the materials studied in this research. However, it was abundant in several samples and required special consideration.

C. Megaquartz. Authigenic grains of non-fibrous quartz which do not possess the undulatory extinction and other characteristics of granular microcrystalline quartz are here referred to as megaquartz. Folk (1950) has defined this material as the "coarse-grained, non-cherty authigenic quartz of sedimentary rocks".

Megaquartz exists in all grain sizes, and is characterized petrographically by its uniform extinction and well defined, frequently subhedral, grain boundaries. It occurs as a recrystallization product of granular microcrystalline quartz and chalcedony, and also occurs as drusy quartz, authigenic quartz crystals, quartz overgrowths, and geode quartz. Megaquartz is frequently seen filling former cavities in cherts. It is a common replacement mineral of fossils, but is less abundant than chalcedony in this respect. Little quantative information on the water content of megaquartz is available.

Metamorphosed cherts consist almost entirely of megaquartz. However, in well-preserved cherts, this form of crystalline silica is usually a minor constituent. In ancient cherts it is sometimes hard to distinguish this authigenic material from recrystallized granular micro-

crystalline quartz. Thus, it can be difficult to accurately assess the state of chert preservation on petrographic bases alone.

In this research the distinction between cherts composed of megaquartz and cherts composed of other forms of silica is particularly useful for evaluating the state of preservation of ancient cherts. This evaluation is extremely important for the interpretation of the isotopic composition of silica.

2.3 Opaline Forms

The amorphous variety of silica is usually called opal, although a large number of local and non-standardized terms are frequently used.

Jones and Segnit (1971) have recently presented a classification of opal based upon X-ray diffraction patterns. They observed that natural opals fall into three groups: opal-C (well-ordered α-cristobalite), opal-CT (disordered α-cristobalite, α-tridymite), and Opal-A (highly disordered, near amorphous). Samples which display only a few diffuse bands in X-ray patterns appear as close-packed aggregates of silica spheres when viewed with the electron microscope (Jones et al., 1964). Weaver and Wise (1972) have reported that silica with X-ray patterns corresponding to opal-CT (as given by Calvert, 1971) is in the form of cristobalite in spherules 10 to 12 μm in

diameter.

Opal is the most hydrous form of silica. Water contents vary from about one weight percent for some forms of opal-CT (see Chapter 9) to twelve weight percent for biogenic opal. The structural nature of this water has not been investigated thoroughly, and is largely unknown. Infrared spectra, however, reveal the presence of OH groups bonded to silicon (Keller et al., 1952; Keller and Pickett, 1949; Sun, 1962), but most of the water is considered to be chemically unbound (Jones et al., 1963).

In this research, the relative amounts of bonded and unbonded water have been investigated by stable isotope experiments and will be discussed in detail later. The results suggest that some opaline material contains as much as two percent bonded water, probably in the form of Si-OH groups.

2.4 The Chemistry and Marine Chemistry of the Silica System

A full understanding of the distribution of silica in sediments, its paragenesis of mineralogical forms, and its isotopic composition is greatly dependent upon an understanding of its chemistry in aqueous solutions.

Attempts to make experimental studies of silica formation are impeded by the fact that laboratory precipitation of silica at low temperatures usually produces a

colloid rather than an aggregate of granular microcrystalline quartz. Electrolytes can be used to flocculate the sol, but the resulting silica gel bears little resemblance to naturally occurring cherts and opals. However, MacKenzie and Gees (1971) have recently observed identifiable quartz crystals precipitated directly from sea water at room temperatures. The crystals are euhedral and should thus be considered a sub-microscopic variety of megaquartz.

Krauskopf (1959) has reviewed the aqueous solubility relations of silica. He concluded that at 25°C amorphous silica has a surprisingly high solubility of 100 - 140 ppm, while quartz falls in the range 6 - 14 ppm. Stober (1967), however, showed that the true solubility relations of silica were obscured by the condensation of hydrated amorphous silica on the surfaces of the solids. This layer ends further dissolution of the underlying surface and controls the two-phase equilibrium. Thus, experiments involving crystalline silica at room temperature do not yield the desired solubility relationships for quartz. The result is that inorganic precipitation of silica in natural environments cannot presently be understood completely in terms of known experimental relationships.

Silica occurs in solution as monomeric silicic acid, H_4SiO_4 (Iler, 1955). Above pH 9, the extensive ionization of silicic acid causes an enormous increase in the

solubility of all forms of silica. Alkaline waters are thus frequently invoked to explain silica mobilization in diagenesis. A large reduction in the pH of alkaline silica-rich waters passing through a carbonate deposit should cause carbonate to dissolve and silica to precipitate. This mechanism is frequently invoked as an explanation for the silification of limestones.

The marine chemistry of silica is an extremely complicated subject which has provoked considerable controversy. A knowledge of the marine chemistry of silica is fundamental to the question of whether cherts form by direct precipitation from ocean water or whether they form diagenetically during burial. Fresh waters flowing into the ocean contain soluble silica concentrations generally 10 to 15 times that of surface-water in the open ocean (Bien et al., 1958). There is no sign of accumulation of soluble silica in surface sea-water in spite of the fact that ocean water is remarkably undersaturated with respect to silica. Thus, there is somewhere an effective sink for soluble silica in the ocean.

The exact nature of this sink is presently being debated between two schools of thought. One school holds that biogenic consumption completely accounts for the low oceanic silica concentrations (Calvert, 1968; Harriss, 1966; Fanning and Schink, 1969). In particular, Lisitisyn

(1967) and Lisitisyn et al. (1967) have shown that biologic precipitation and redistribution of silica occur on a truly colossal scale in the present-day oceans. Data presented by these authors convincingly demonstrate that silica secreting organisms are capable of utilizing all of the soluble silica supplied by rivers and streams to the ocean.

Burton and Liss (1968) have criticized some of these results, and MacKenzie and Garrels (1966) have argued that the amount of silica supplied to the sea over geologic time greatly exceeds that which is observed as chemical siliceous sediments in the geologic column. These authors conclude that only about 10% of the incoming silica is consumed by organisms with the remainder entering into reactions with clays and bicarbonate.

MacKenzie et al. (1967) have argued that the formation of silicates (clays, zeolites) are the major controlling factors of silica concentration in the ocean. In addition, Bien et al. (1958) have given strong evidence suggesting uptake of silica through adsorption by oceanic clay minerals. Thus, a satisfactory understanding of the relative roles of organic versus inorganic removal of silica from the oceans is still unavailable. It is, however, clear that, due to its undersaturation, silica cannot precipitate inorganically from the present-day ocean. Furthermore, it is clear that organisms are introducing

tremendous amounts of silica into modern sediments.

2.5 Paragenesis

Abundant field, petrographic, and experimental studies have demonstrated that silica in sediments is initially deposited as amorphous opal which subsequently undergoes a complicated series of transformations. These transformations have been most recently documented by Ernst and Calvert (1969) and Heath and Moberly (1971) for post-Jurassic deposits containing abundant biogenic silica. The sequence is biogenic opal ⟶ opal-CT ⟶ granular microcrystalline quartz (the authors use different terms). Concerning the second conversion, Heath and Moberly observed in thin-section "saw-tooth contacts" between opal-CT and granular microcrystalline quartz, which they considered "classic solid-solid inversion fronts".

Concerning the first step, Weaver and Wise (1972) observed with the scanning electron microscope that opal-CT in deep sea sediments consisted of fine crystallites of cristobalite growing in spherules of diameter 3 to 10 μ. They concluded that the cristobalite is a chemically precipitated authigenic mineral. In a strict sense silica never really suffers a major dehydration in going from biogenic opal, with 10 wt-% water, to granular microcrystalline quartz, with 1 wt-% or less. Instead, the very

hydrous material is dissolved and reprecipitated as a relatively anhydrous phase which subsequently inverts to granular microcrystalline quartz.

The above paragenesis for silica is not unique. As already mentioned, MacKenzie and Gees (1971) have shown that megaquartz can precipitate directly from sea-water at room temperature. In addition, chalcedony commonly lines the walls of cavities and is frequently assumed by chert petrographers to be a primary precipitate.

All forms of silica can be converted to megaquartz by metamorphism or by deep burial over long periods of time. It is the end-product of paragenetic silica transformations. Some possible pathways in the paragenesis of silica are summarized in figure 2-2.

2.6 Modes of Occurrence of the Chemical Siliceous Sediments

A. Introduction - For purposes of this discussion, the natural occurrences of the chemical siliceous sediments have been divided into sixteen groups. These groups are listed in table 2-1, together with an indication of the kind of silica most commonly observed for each occurrence. In addition, the table indicates the supposed nature of the water, either marine or non-marine, from which the silica precipitated.

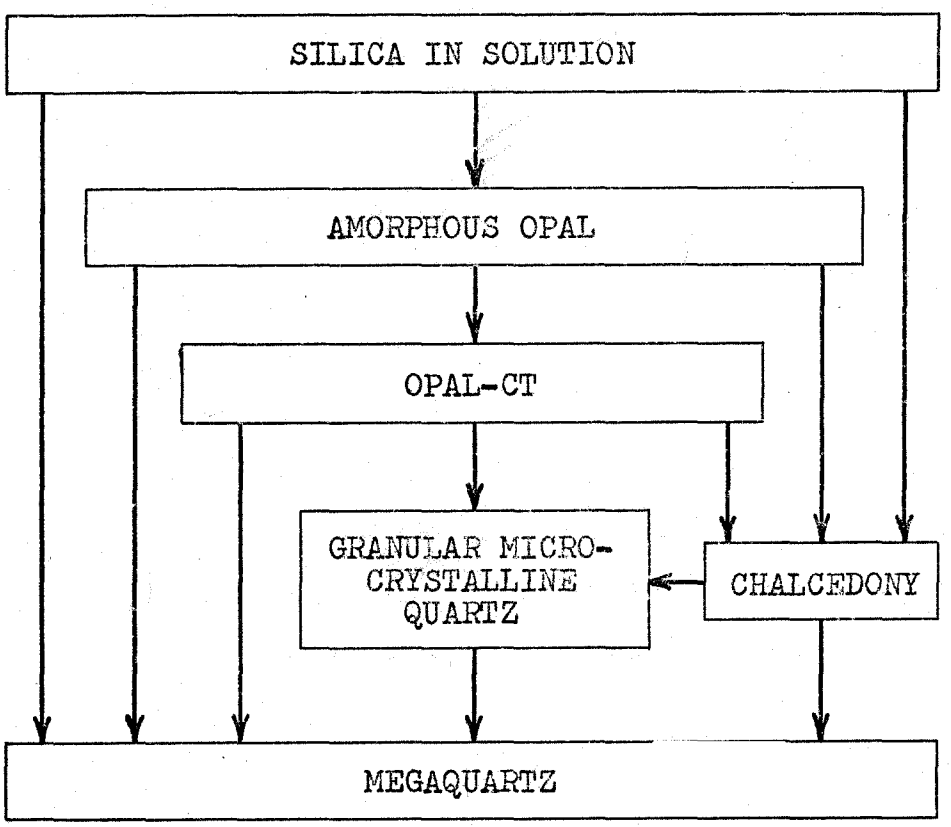

Figure 2-2

POSSIBLE PATHWAYS IN THE
PARAGENESIS OF AUTHIGENIC SILICA

Table 2-1

VARIETIES OF SILICA IN SEDIMENTS

	Opal	Granular Microcrystalline Quartz	Chalcedony	Mega Quartz	Marine	Fresh Water
1. Modern organisms	X				X	X
2. Diatomites	X				X	X
3. Chert in limestone		X	usually minor	usually minor	X	X
4. Bedded cherts		X		usually minor	X	
5. "Volcanic" cherts		X			X	?
6. Silicified wood	X	X	X	X		X
7. Silicified fossils			X	X	?	X
8. Iron formations		X		X	?	?
9. Flint		X	X		X	
10. Silica cement	X	X	X	X	?	X
11. Geodes				X		X
12. Porcellanite		X			X	X
13. Inorganic opal	X					X
14. Joides "cherts"	X	X	X	X	X	
15. "Magadi cherts"		X	?			X
16. "Tripoli" & "sheet cherts"		X		X		X
17. Drusy quartz				X	X	X
18. Silicified fault zones	X			X		X

B. Diatomites - The great abundance and accumulation of diatoms in present day waters and sediments would appear to suggest that similar occurrences should be common in the geologic record. Surprisingly, this is true only of the Tertiary. This fact can be attributed to the evolutionary history of the Diatomaceae. They appear first in Liassic time, but have become abundant only since late Cretaceous (Lowenstam, 1963). Since then, diatomaceous deposits, both fresh-water and marine, have been widespread. Most of these deposits are extremely well preserved, consisting of fragile opaline tests of a variety of species of diatoms.

Beds of diatomite range in thickness from a few inches to many tens of feet thick. They are frequently interbedded with carbonates, shales, and volcanic material. With time it is thought that the opaline silica will be diagenetically mobilized and reprecipitated as massive beds of chert composed of granular microcrystalline quartz (Ernst and Calvert, 1969). Bramlette (1946) has observed and described certain details of this process as it occurs in the Monterey formation, California. Alteration of the silica appears to have occurred only along bedding planes and fractures through which warm or alkaline waters have percolated (Ernst and Calvert, 1969).

In short, it appears that diatomaceous accumulations of biogenic silica could have been the dominant silica occurrence during the Tertiary, but before then they were unimportant to non-existent. It could be argued that diagenesis and recrystallization have completely obliterated any trace of these fragile structures, thereby accounting for the apparent absence of these materials. However, this has not been the case for radiolarians, sponge spicules, and even more delicate life-forms. Conclusions concerning chert genesis based on these extremely recent and temporally restricted occurrences of diatomites should be applied with great caution to the more common occurrences of silica in the geologic record.

c. Modern organisms. The present day oceans contain a truly immense number of silica-secreting organisms. Litisitsyn et al. (1967) and Litisitsyn (1967) have made an exhausitive study of the distribution and form of silica suspended in the ocean and contained in modern oceanic sediments. They observe that the most common silica producers are the diatom algae, and that these organisms account for more than 70% of the modern accumulation of oceanic silica. Second in importance are the radiolaria, followed by the siliceous sponges. Silicoflagellates also precipitate silica, but on a much reduced scale. Recently, Lowenstam (1971) has observed silica being produced by gastropods,

and there is evidence of silica production on a minor scale in higher organisms (Iler, 1955).

Silica precipitation by organisms is always opaline. The tests, skeletons, and shell fragments of these organisms frequently accumulate in substantial thicknesses of biogenic opal spread continuously over enormous areas of the ocean floors. The principal areas of accumulation are in the form of belts extending along certain latitude parallels, and in some places completely encircle the earth. Two of the main belts are subpolar, and one is equatorial.

The distribution of silica-secreting organisms is primarily dependent upon the supply of organic nutrients. The supply of nutrients is related to the large scale circulation of the oceans. The areas of upwelling are the areas richest in nutrients and thus richest in silica-producing organisms. Litisitsyn (1967) has discussed at length the additional complex factors controlling the ultimate distribution of the biogenic siliceous sediments.

Diatoms are also the primary users of silica in fresh waters. They have been shown to be surprisingly abundant and are the dominant control on the soluble silica concentration of rivers and lakes (Wang and Evans, 1969; Holland, 1969).

D. Cherts in limestones. Perhaps the most remarkable accumulation of silica in sediments is the

occurrence in limestones of nodules, sheets, lenses, and extensive beds of granular microcrystalline quartz. The silica in this association usually goes under the name of "chert".

The most distinctive of the chert forms are the nodular cherts. These consist of oblate spheroids with the major axis lying in the bedding plane. They exist in a variety of sizes, usually from several centimeters to a meter in width. The color and luster of the cherts are also variable ranging from translucent or white to a dull jet-black. The limestone may contain only a few scattered nodules or, in some cases, may contain more than 50% chert by volume.

The well-known black chert nodules in the Cretaceous chalks of northwestern Europe are referred to as "flint". These nodules contain abundant remains of silica sponges and are usually distributed along bedding planes. They are here considered simply as another form of chert in carbonate rocks.

Biggs (1957), Pittman (1959), Carrozi (1960), and others have described the petrography of some typical nodular cherts. The relationships observed are extremely variable and hard to interpret. Petrographic work usually reveals the presence of variable amounts of carbonate in the form of fossils, relict bedding planes, dolomite rhombs, cavity fillings, veins, and numerous patches of uncertain

origin. Frequently, carbonate fossils are beautifully preserved in the chert while the surrounding carbonate has been totally recrystallized or dolomitized. Fossils found in chert nodules are always of the same kind as found in preserved portions of the host limestone. Mineralogically, the chert consists predominantly of granular microcrystalline quartz with subordinate amounts of chalcedony and megaquartz. The chalcedony and megaquartz nearly always occur in cavities or in fossil casts. Opal and Opal-CT are very rare. Granular microcrystalline quartz in the extremely ancient and thermally disturbed nodular cherts tends to be partially recrystallized to form megaquartz. Nodules completely recrystalled in this manner tend to be extremely rare.

The statements made thus far concerning the nodular cherts apply equally as well to the thin beds, lenses, and veins of chert also found in the limestones. Apparently these materials are simply irregular chert accumulations which formed in the same manner as the nodules.

Early workers were divided in opinion as to the genesis of cherts in limestones. Tarr (1926) headed a school of thought which argued that these siliceous materials had precipitated inorganically from the ancient oceans as globules of silica gel and had subsequently crystallized to form chert. Van Tuyl (1918) represented those who

considered cherts to be secondary features of replacement origin. More recent workers seem to agree that most nodular cherts are clearly secondary, having replaced the portions of the limestone in which they are found. The time of this replacement is thought to have been extremely early, while the limestone was still largely unlithified. The beds, lenses, and nodules are thus considered to be diagenetic but penecontemporaneous with carbonate sedimentation (see White, 1947; Biggs, 1957; Harris, 1958; Bissell, 1959; or Dapples, 1967). Of course, this conclusion need not apply to all cherts in limestones.

The source of the silica for cherts in limestones is not generally agreed upon. Lowenstam (1942) has argued convincingly that biogenic silica in the form of opaline sponge spicules is the silica source of some silurian cherts. Dapples (1959), Bissell (1959), Biggs, (1957), Walker (1960), and others have argued that silica is frequently non-biologic, and can be attributed to inorganic colloidal precipitation, volcanically-derived silica, and diagenetic reactions with silicate minerals. These authors, however, have probably underrated the tremendous ability of organisms to add silica to sediments. This is especially probable in view of the recent findings of Litisityn (1967) concerning the enormous input of biogenic silica to recent sediments.

Dapples (1959, 1967) has discussed silicification of

carbonates in terms of the various sedimentary environments and geosynclinal zones. He believes that there is strong suggestion that such silicification becomes more extensive progressing from cratonic sediments to miogeosynclinal sediments to eugeosynclinal sediments. Such a sequence may be due to an additional source of silica for the eugeosynclinal accumulations or may reflect depositions from deeper water from which carbonate has dissolved due to pressure effects.

In conclusion, it seems likely that most cherts in limestones form diagenetically soon after deposition in the sediments. The opaline remains of silica secreting organisms are mobilized, and this silica, together with silica derived from other sources, is redeposited in the form of nodules, lenses, and along bedding planes. Probably the newly formed silica is also opaline and crystallizes with time to form granular microcrystalline quartz.

E. Bedded cherts. Beds of chert are very common in sedimentary rocks of all litholigies and of all ages. These beds vary from the thin, discontinuous sheets, already mentioned in connection with the carbonate rocks, to the massive layers of novaculite which are spread aereally over thousands of square kilometers. In addition to these are the bedded cherts interlayered with shales, siltstones, iron formation, and volcanic materials. Petrographically,

the bedded cherts consist of granular microcrystalline quartz with impurities of carbonate, iron oxides, organic matter, and various amounts of clastic materials.

E-1. Novaculites. Novaculites are usually considered to be the pure, thick and geographically extensive variety of bedded cherts. They consist of continuous beds of granular microcrystalline quartz with frequent radiolarian and sponge remains. The Caballos-Arkansas Novaculite is the best studied example of this material, though opinion is still widely divided regarding its origin. Goldstein (1959) suggested that the granular microcrystalline quartz resulted from alteration of extensive volcanic ash falls in a submarine environment. McBride and Thompson (1970) argued that the novaculite was originally a deep-sea accumulation of biogenic silica. Folk (1970), however, has concluded that at least part of the Caballos novaculite accumulated as a tidal flat deposit.

E-2. Radiolarian cherts. Radiolarian cherts are beds of granular microcrystalline quartz containing abundant fossil radiolarians. The chert is frequently interbedded with pillow lavas and volcanic materials. Such occurrences have been described by Davis (1918), Sampson (1923), and Fagin (1962). The beds of chert are thought to have originated from abyssal accumulations of siliceous oozes, although the association with basalt has suggested

that some silica may have been derived from volcanic materials.

E-3. Siliceous shales, Porcellanites. Beds of chert occurring within shale sequences are common. These frequently grade into siliceous shales and lose their identity as authigenic silica accumulations. Impure cherts of this sort are frequently termed Porcellanites. Dapples (1967) has pointed out that the association of chert with shale is more common among eugeosynclinal sediments, although the association is very widespread. He cites evidence supporting the idea that much of the silica in such cherts has been introduced diagenetically, and that it may have replaced initial carbonate beds. Keller (1941) studied a widespread Permian occurrence of this type and concluded that the silica was probably a primary inorganic precipitate.

E-4 Volcanic cherts. Frequently, impure beds of essentially non-fossiliferous chert are found in extensive successions of lavas and tuffs. These are sometimes stained red by iron-oxides and are then referred to as jasper. More often they are blue-green, or even black. They contain abundant material thought to be altered volcanic ash and glass. Muller and Ferguson (1939) have observed strata with every gradation from pure chert to andesite tuffs and tuffaceous slates. Bedded cherts such as these have almost surely resulted from alteration of volcanic ash.

E-5. Bedded cherts in iron formations. Bedded cherts of the Precambrian are frequently found intimately interlayered with sedimentary iron deposits. These are the well known iron formations and are of great economic and scientific importance. They have been extensively studied. Most of the chert in these units consists of megaquartz. Granular microcrystalline quartz can still be observed in thin sections of these cherts and it is likely that these ancient chert units have been extensively recrystallized.

The temporal restriction of the iron formations to the Precambrian, combined with their worldwide occurrence, seems to indicate that special worldwide conditions or processes were operative during the time of their deposition. James (1966) and Govett (1966) have reviewed the problems associated with the development of iron formations. Considerable controversy surrounds explanations of the origin of these rocks, especially concerning the role of biologic activity, the oxygen content of the Precambrian atmosphere, the source of the iron and silica, the site of deposition, and subsequent metamorphic alteration of the mineralogy. It is not certain whether these rocks were deposited in a marine environment (James, 1954), an alkaline lake (Eugster, 1969), a fresh-water lake (Hough, 1958), or as an evaporite deposit (Trendall and Blockley, 1970).

The preservation of microfossils in the granular

microcrystalline quartz of iron formations (Barghoorn and Tyler, 1965) raises certain questions concerning the paragenesis of the silica phases. Oehler and Schopf (1971) have shown experimentally that it is possible that the blue-green algae seen in these rocks were preserved by the following steps: (1) permeation of living algae by a solution of colloidal silica; (2) conversion to a solid gel; and (3) transformation to granular microcrystalline quartz. This is essentially the same mechanism proposed for the development of granular microcrystalline quartz in cherts of all ages.

F. Silicified fossils. Silicified fossils are exceedingly common in the sedimentary column, especially in carbonate rocks. In thin section it is seen that most silicified fossil material is composed of chalcedony and megaquartz. Frequently the megaquartz is aligned in radial aggregates in a manner suggesting that it is recrystallized chalcedony. Often, however, the megaquartz is subhedral, suggesting that it developed without a chalcedonic precursor. In these circumstances, it appears likely that the original fossil material was dissolved by percolating solutions leaving a cavity in which silica was subsequently deposited. Granular microcrystalline quartz is frequently seen engulfing and replacing carbonate fossils, but it usually serves to destroy the form of the shell material rather than preserve

it. To a first approximation, granular microcrystalline quartz can be considered to be absent from the common silicified fossils.

The replacement of fossils by silica frequently occurs with only minor silicification of the matrix carbonate. However, chert nodules containing preserved calcitic shell fragments are a common occurrence, indicating that the matrix was replaced before the shells.

Dapples (1967) has indicated that there is no consistent sequence of silicification of fossil shells with respect to species and concluded that the crystal habit or composition of the carbonate is not the controlling factor. The preferential replacement of certain types of shells may be related to the amount of organic matter present at the time of silicification, the state of preservation of the original microstructure and mineralogy, or the quantity and source of silica being precipitated.

The time of silicification in the diagenetic history of the sediment is uncertain and is undoubtedly variable. Cloud and Barnes (1946) have pointed out that silicified fossils are not known in subsurface rocks from the Ellenburger group of central Texas, though they are common in outcrop. Much replacement probably occurs in the weathering cycle, but much might also occur in early diagenesis.

G. Silicified organic remains.

G-1. Petrified wood. Cell by cell replacement of wood by silica is a common occurrence, especially in Tertiary sediments. Opal and chalcedony are the two most common forms of silica found in silicified wood. The opaline replacements vary greatly in their color, texture, and purity. Gem opal is not uncommon in such occurrences. The more ancient examples of silicified wood are composed largely of chalcedony and recrystallized chalcedony. The "recrystallized chalcedony" bears the spherulitic form of chalcedony but lacks the fine fibrous structure, and should be considered a fine-grained variety of megaquartz. Iron oxides, calcite, and organic matter coexist with these crystalline forms of petrification. The silica paragenesis in these materials was probably colloidal silica ⟶ opal ⟶ chalcedony-quartz.

Silicified wood occurs in two distinct associations. In one, such as the "petrified forests" of Yellowstone Park and at Florissant, Colorado, silicified tree stumps are enclosed in volcanic ash and breccia. In the other, such as the "petrified forest" of Arizona, logs are enclosed in fluvatile sandstones and shales. Waters passing through these surrounding materials had evidently become saturated with silica, possibly due to high pH. It is possible that the decaying wood caused the pH to decrease locally, precipitating amorphous silica. The extremely local nature of

any such chemical relationship is emphasized by the frequent cell-by-cell replacement, and the observation by Ward (1895) of a tree trunk lying across a contact between sands and clays in which the part enclosed in the sands was silicified, while the part in the clays was lignitized.

G-2. Silicified insects. Silica can also be found in various other petrified remains. Palmer (1957) has described Miocene insects and spiders which have been replaced by chalcedony. His careful observations reveal that silicification may not have been the first step in the replacement of the arthropods. In particular, replacement by an unidentified brown organic compound seems to precede the formation of the chalcedony. Palmer insists that these specimens do not result from the filling of cavities left by leaching the organic material away. "The replacement occurred soon after death, or in such a chemical environment that internal organs in many instances had not disintegrated."

H. Inorganic opal deposits. Apparently inorganic opal deposits are exceedingly widespread in Cenozoic deposits. The most common occurrence of such opal is in volcanic rocks or in sedimentary sections containing volcanic materials. In this association it usually occurs as a cavity filling and has probably formed during the low temperature weathering of the volcanic material, although hydrothermal deposits are also possible. Geysers and related

hot waters, rich in silica dissolved at high temperatures, are known to precipitate opal (e.g., the "geyserite" of Yellowstone Park).

Swineford and Franks (1959) have described a rare occurrence of opal beds thought to be related to soil-forming processes. In addition, Pittman (1959) has reported opal in the weathered surfaces of a cherty limestone.

Peterson and Von der Borch (1965) have observed opal precipitating in lakes associated with the Coorong Lagoon of South Australia. Dolomite, magnesite, and magnesian calcite are also being deposited there. The authors suspect that high pH (9.5 to 10.2) stages of the lakes causes dissolution of detrital silicates. Lowering of the pH and drying of the lakes causes precipitation of the opal. This work is particularly important as it is a definite example of silica being inorganically accumulated in a carbonate deposit.

I. Silica cement. Silica is the most common constituent of sandstone cements. All of the mineralogical varieties of silica occur in this fashion. It most commonly forms as euhedral, optically continuous overgrowths on the detrital quartz grains. The quartz cement may also occur as minute crystals forming fringes around the grains or as an irregular mosiac in the former pore space (see Hatch et al., 1938, for illustration). Granular microcrystalline quartz and chalcedony are observed separately and together as

cementing materials, though these occurrences are somewhat unusual (Pettijohn, 1957). Opal is very uncommon as a silica cement, though it has been described in Cenozoic sediments by Swineford and Franks (1959), Pöhlmann (1886, p. 247), and others. Pettijohn (1957) has noted that opal-cemented sands are commonly associated with volcanic ash beds.

Other cementing minerals, especially calcite, often (1) occur with, (2) replace, or (3) are replaced by silica. The paragenesis of these minerals is difficult to ascertain petrographically, but it is clear that silica is often the first to form and is later replaced by calcite. Siever (1959) made an extensive study of silica cementation in some Pennsylvanian sandstones and suggested that silica cement usually formed during shallow burial, was partially replaced by carbonate during deep burial, and further deposited in small amounts during uplift. It is clear that silica cements in any sandstone are likely to have had a complicated history involving several generations of deposition and removal.

The source of silica for these cements is uncertain, but is probably a combination of partial solution of the detrital quartz and the introduction of silica-rich waters derived from other units.

Tallman (1949) has observed that the older sandstones

are cemented primarily with silica, while younger sandstones tend to be cemented with carbonate. This may indicate that diagenetic conditions in the past were more conducive to silica cementation than to carbonate cementation. Alternatively, it could mean that carbonate cements tend to be replaced with silica over geologic time.

J. Geodes. A common and spectacular occurrence of silica is in the form known as "geode quartz" or, when colored, "agate". Geodes are globular bodies of quartz which occur in former miarolitic cavities of lava-flows and in a variety of cavities in sedimentary rocks. Quartz and chalcedony are the mineralogic varieties of silica found in these occurrences. Hayes (1964) distinguishes geodes from vugs containing "drusy" quartz on the basis that geodes have discrete outer layers of mineral matter, usually composed of chalcedony, whereas drusy quartz is deposited directly on the carbonate. Beautifully formed euhedral quartz crystals commonly project into empty spaces in the centers of geodes, and are a favorite of mineral collectors.

In sedimentary rocks, geodes are most commonly found in argillaceous carbonates. The best studied example of argillaceous carbonates is the Warsaw formation at the junction of Iowa, Illinois, and Missouri. Van Tuyl (1916, 1925) made an extensive study of these geodes and concluded that they had originated from solution of syngenetic calcerous

concretions followed by infilling of quartz. Robertson (1951, 1944), however, hypothesized that such geodes resulted from primary precipitation of silica gel from the ocean followed by subsequent crystallization. Hayes (1964) studied these geodes extensively and found all gradations from early diagenetic carbonate concretions to quartz-lined geodes. He concluded that the following sequence of events had occurred:

(1) carbonate concretions form diagenetically in the sediment;

(2) chalcedony replaces the surface of the concretion to form a shell of silica;

(3) as silicification proceeds inward, the form of silica tends toward spherulitic chalcedony and euhedral megaquartz;

(4) before complete silicification, the core calcite is dissolved;

(5) large quartz crystals subsequently grow in the cavity.

Geodes in volcanic rocks have been studied to a lesser degree, and they undoubtedly form as a cavity-filling. Nacken (Correns, 1969) concluded that the concentrically-banded agates found in such rocks had to form above the critical temperature of water (375°C) to produce the banding, but below 575°C to account for the low-temperature variety

of quartz. Correns (1969) explains certain planar layers in other varieties of agates as being due to deposition from an aqueous phase. He suggested that the banding was due to "rhythmic deposition from solution diffusing through the siliceous mass, analogous to the formation of Liesegang rings."

K. "Drusy" quartz. Irregular cavities in carbonate rocks are frequently found to be lined with euhedral crystals and aggregates of quartz. Such quartz is called "drusy" quartz. The quantity of this quartz appears to be greater in samples which have been extensively weathered (e.g. Cloud and Barnes, 1946, p. 95). It may thus be considered to form during the weathering cycle, although not necessarily the present-day weathering cycle. Dake (1930, p. 115) observes that druses from the Cambrian potosi formation are found as rounded detrital clasts in the overlying Ordovician Gasconade Formation. If the druses formed during weathering, then they formed during a Cambrian or early Ordovician weathering cycle.

L. Silica earth and weathering residues. Unusual but economically important siliceous "soils" consisting entirely of disaggregated granular microcrystalline quartz are here called "silica earth". This material has been referred to by a large number of colloquial terms, most commonly "tripoli", "ganmister", "cotton chert", and

"soft silica". The most notable occurrence is in southern Illinois where Lamar (1953) has described it as a soil-like material consisting of chert particles averaging 1 to 5 microns in diameter. Weller and Ekblaw (1940) and Lamar (1953) have shown that this siliceous earth is the in-situ weathering residue of local paleozoic chert-rich limestones. In their interpretation, the flat-lying cherty carbonates had been entirely removed by ground waters leaving behind an accumulation of highly fractured chert beds and nodules. Intensive leaching of the chert caused it to disaggregate and to produce the silica earth.

Samples of this material were obtained for the present study. Examination of unweathered portions of the limestone units reveal that unaltered cherts contain a great amount of fine-grained carbonate. It is the leaching of this carbonate which apparently causes the chert to disaggregate.

Also in southern Illinois, Lamar (1953) observed frequent concentrations of nodules and pillow-like masses of chert in the soil horizons. Ruby (1952, p. 44) described similar occurrences in western Illinois, some at least 40 feet thick. Apparently these occur when the chert itself is sufficiently free of finely-disseminated carbonate, making it highly resistant to leaching and consequent disaggregation while the enclosing limestone is entirely removed by ground waters. Both authors suggest that silica is remobilized

and deposited within and around the chert residuum during the weathering cycle, producing local lithification of the outcrop. Ruby, in particular, ascribes the origin of much of the chert to such secondary processes. Bain and Ulrich (1905) observed that certain vesicular cherts 2 - 3 feet thick in Ordovician limestones in Missouri disappeared altogether when followed beneath the surfaces of outcrops, suggesting that in some cases chert development is entirely surficial.

The lithification of chert residues is carried to its greatest extent in the case of the sheet cherts of southwestern Missouri. Here, Robertson (1967) showed that one such extensive sheet over 20 feet thick had resulted from solution of the carbonate constituents from normal cherty limestones, subsequent collapse of the residual chert beds and nodules, and cementation by silica.

The extent to which similar processes as those described above have acted to produce beds of chert in older rocks of the sedimentary column has not been studied. Many of the morphological features of ancient deposits resemble strongly some of those observed for the weathered deposits. In particular, a frequent sequence observed in carbonate deposits involves a gradual increase of chert content going upsection until complete beds of chert occur. It is possible that these sequences represent the lithified products of

ancient weathering surfaces in which the carbonate had been gradually leached away as described above. It is not inconceivable that many bedded chert deposits have resulted in this fashion.

M. Deep sea cherts. Siliceous rocks have recently been recovered from drill cores of the Deep Sea Drilling Project (Joides). These "cherts" range in age from pre-upper Cretaceous to mid-Tertiary and are found to be common and widely distributed in deep-sea sediments, occurring in siliceous oozes, chalks, silts, and clays. Calvert (1971) has clarified the nature of the silica phases in these sediments. True "cherts" have been found only in the older pre-upper Cretaceous sediments. These are described as being "quartzitic", while the younger materials are composed of opal-cristobalite, as revealed by X-ray diffraction, and are not cherts in the strictest sense.

Heath and Moberly (1971) have examined cherts obtained from cores in the western Pacific. These authors conclude that biogenic opal in the sediments has been dissolved and reprecipitated as "cristobalite" (opal-CT ?) which then inverts to "quartz" (granular microcrystalline quartz). Von der Borch et al. (1971) postulated the same sequence for cherts from east central Pacific basin sediments.

Samples of deep-sea cherts were obtained for this study. Further discussion based on observations of these samples is given in Chapter 9.

The presence of minor amounts of granular microcrystalline quartz and abundant opal suggests that biogenic silica undergoes diagenetic alteration in the deep-sea marine environment on a time-scale of greater than 60 million years. This is significantly slower than similar processes observed in fresh-water environments. Considerable study of the deep-sea cherts is desirable as it will undoubtedly yield much significant information regarding the whole question of silica diagenesis and consequently of chert genesis.

N. Inorganic cherts from alkaline lakes. Chert beds and nodules consisting of granular microcrystalline quartz occur in the sediments of alkaline lakes in East Africa. Eugster (1967) has identified two new hydrous sodium silicates, $NaSi_7O_{13}(OH)_3 \cdot 3H_2O$ (magadiite) and $NaSi_{11}O_{20.5}(OH)_3 \cdot 3H_2O$ (kenyaite) among these lake beds. The cherts of Lake Magadii occur as small nodules in beds of this material or in horizons stratigraphically equivalent with them (Eugster, 1969). In dilute acids, magadiite and kenyaite can be converted to a crystalline hydrate of silica, $6SiO_2 \cdot H_2O$.

Eugster has proposed that magadiite is a primary precipitate of the alkaline lakes. Where percolating ground waters have subsequently removed the sodium, the magadiite has been converted to kenyaite and then to chert. Hay (1968) observed similar associations in other lakes in East

Africa. He concluded that some of the chert may have formed from magadiite in lake-bottom sediments without a leaching mechanism, although he cannot explain an alternative mechanism. In addition, Hay observed an additional silica phase, chalcedony, lining trona molds in the cherts.

Eugster (1969) has suggested that chert formation in these lakes is analogous to chert formation in the Precambrian iron formations.

2.7 Evolution of the Silica System

The sedimentary record yields evidence that there have been three major silica associations which have evolved through geologic time. The first of these is the chert-iron association of rocks usually older than 2 billion years. Although the record of these ancient rocks is scanty and biased completely toward shield deposits, it seems that the dominant occurrence of sedimentary silica was in association with iron-formations.

As carbonate deposition began and iron formations waned, the great bedded-chert sequences gave way to the development of nodular cherts in limestones. By Paleozoic time, nodular cherts in limestones were exceedingly common. Though quantitative information is lacking, there seems to be some suggestion that the amount of chert in limestone reached a maximum in the late Paleozoic and that it has been since declining. In any case, it is apparent that silica

as a separate phase most commonly occurred in carbonate rocks from about 2 billion years to at least 60 million years B.P.

Since the end of the Mesozoic, the diatoms have sc proliferated that nearly all dissolved silica in natural waters is being utilized by these organisms. Thus, since the beginning of the Cenozoic, the major silica deposits have been in the form of diatom accumulations.

It is conceivable that silica-secreting sponges developed and proliferated with the onset of limestone evolution and accounted for the large amount of chert associated with carbonate. Lowenstam (1961) has suggested that with the onset of diatoms the sponges declined rapidly, accounting for the most recent silica-displacement from chert in limestone to biogenic accumulations. The ancient Precambrian association of chert with iron formations may have been due to the absence of silica-secreting organisms combined with peculiar oceanic and atmospheric chemistry. In any case, it is probable that the evolution of organic activity combined with diagenetic modification has been mainly responsible for the distribution and type of the common silica occurrences.

2.8 Summary Statement

The above discussion concerning samples of hydrous silica is the first attempt at reviewing the chemistry,

mineralogy, and occurrence of silica in a manner that might be useful for isotope investigators. This review served as a guide for the collection of samples used in this research, and has been used throughout the text that follows as a source of reference for the discussion of the isotope data.

Chapter 3

THEORY

3.1 Introduction

The mass differences of the different isotopes of a given element result in small differences in the chemical properties of the different isotopic molecules. This is due primarily to the effect of mass on the vibration frequencies of the various bonds involved. The differences in chemical properties lead to fractionations of the isotopes in chemical reactions. The degree of fractionation is a function of the mass of the nuclides, the temperature, and various kinetic factors. Usually, reactions involving the lighter nuclides, of atomic number 20 or less, display fractionations which can be measured by existing techniques. Some of the theoretical aspects behind such fractionations will now be briefly considered.

3.2 Equilibrium Isotope Fractionation

The equilibrium partition of the stable isotopes of an element between two compounds can be thought of in terms of an "exchange reaction" of the sort

$$(3\text{-}1)\quad aAX_n + bBX^*_m \leftrightharpoons aAX^*_n + bBX_m \qquad an = bm$$

in which X is an element common to all moledules in the reaction. X, however, consists of two isotopes, the heavier being denoted by the asterisk. Thus, AX^*_n is a molecule containing the heavier isotope of X exclusively.

The equilibrium constant for this reaction is

$$K = \frac{\left[AX^*_n\right]^a \cdot \left[BX_m\right]^b}{\left[AX_n\right]^a \cdot \left[BX^*_m\right]^b} = \frac{\left(Q_{AX^*} / Q_{AX}\right)^a}{\left(Q_{BX^*} / Q_{BX}\right)^b}$$

where Q = statistical mechanical partition function.

A fundamental problem of theoretical isotope considerations is to relate terms in this expression to measurable properties. The relationships most commonly used today were given by Bigeleisen and Mayer (1947) and Urey (1947) who related the partition functions to the frequencies of vibration of nonlinear, polyatomic molecules. Since these frequencies can be deduced from infrared spectra, they were able to evaluate K for a variety of ideal gas reactions at various temperatures. Their work indicated that ℓnK should vary as $1/T$ for low temperatures and as $1/T^2$ for high temperatures.

Solids present a more complicated problem since the exact spectrum of the many different vibration frequencies is usually not known. In certain cases, the appropriate vibration frequencies can be approximately deduced from heat capacity data. McCrea (1950) and Becker (1971) have combined such data with spectroscopic data and various assumptions concerning the nature of lattice vibrations to evaluate the appropriate partition functions for several solids of geologic interest. However, such calculations

alone usually do not agree exactly with experimental data.

The quantity determined experimentally is the fractionation factor, α. For two phases in equilibrium, α expresses the measured isotope distribution in the two phases. For equation 3-1

$$\alpha_{AX-BX} \equiv \frac{\left(\frac{X^*}{X}\right)_{AX}}{\left(\frac{X^*}{X}\right)_{BX}}$$

In other words, α is the ratio of the isotopic species X, X* in compound AX divided by the ratio of the same isotope species of compound BX.

α can be related to K for reaction 3-1 by realizing that if the isotopes are randomly distributed through the molecules, then for reaction 3-1

$$\frac{\left[AX^*_n\right]}{\left[AX_n\right]} = \frac{[X^*]^n}{[X]^n} = \left(\frac{X^*}{X}\right)^n$$

Thus

$$\alpha_{AX-BX} = \frac{\left(\frac{X^*}{X}\right)_{AX}}{\left(\frac{X^*}{X}\right)_{BX}} = \frac{\left(\frac{\left[AX^*_n\right]}{\left[AX_n\right]}\right)^{1/n}}{\left(\frac{\left[BX^*_m\right]}{\left[BX_m\right]}\right)^{1/m}} = \frac{\left(\frac{\left[AX^*_n\right]}{\left[AX_n\right]}\right)^{a(1/an)}}{\left(\frac{\left[BX^*_m\right]}{\left[BX_m\right]}\right)^{b(1/bm)}}$$

$$= K^{1/an} = K^{1/bm}$$

In experiments, the δ-values of the equilibrating phases are measured and from these, α is determined. The

δ notation is defined on page 4. In terms of reaction 3-1, α is related to δ by

$$\alpha_{AX-BX} = \frac{1 + \frac{\delta X^*_{(AX)}}{1000}}{1 + \frac{\delta X^*_{(BX)}}{1000}}$$

where

$$\delta X^*_{(AX)} = 10^3 \left(\frac{\frac{X^*}{X}_{(AX)} - \frac{X^*}{X}_{(std)}}{\frac{X^*}{X}_{(std)}} \right)$$

More simply, an approximate relationship between α and δ is as follows:

$$\ell n\, \alpha_{AX-BX} = \ell n\, \alpha_{AX-std} - \ell n\, \alpha_{BX-std}$$

$$\cong \frac{\delta X^*_{AX} - \delta X^*_{BX}}{1000}$$

$$\delta X^*_{AX} - \delta X^*_{BX} \cong 1000\ \ell n\, \alpha_{AX-BX}$$

[Thus, the "fractionation" of isotopes (Δ) between two substances is equal to 1000 ℓn of the "fractionation factor" (α).]

Comparisons of equilibrium constants determined experimentally with those predicted from theory usually reveal good agreement in the case of ideal gases, but very poor agreement in reactions involving solids.

The variation of the isotope equilibrium constant with temperature has many applications to geologic problems and has been investigated by many workers. Most geologic

reactions of interest involve solids, and the variance of α with temperature has usually been investigated experimentally rather than theoretically. Nevertheless, theoretical treatments are very useful in predicting the qualitative distribution of isotopes in solids.

Substitution of isotopes should not change the volume in solids. Thus, the equilibrium constant should be largely independent of pressure. It has been shown that this is true for the isotopic fractionation of oxygen between bicarbonate and water to 4 kilobars (Hoering, 1961), and between calcium carbonate and water to 20 kilobars (Clayton et al., 1972). Garlick et al. (1971), however, have suggested that certain eclogites derived from the upper mantle showed evidence of an original 3 per mil difference between crystals and melt due to pressure effects. However, measurable pressure effects on the isotope equilibrium constant do not exist over the pressure range encountered in the upper crust.

3.3 Specific Considerations for Silica in Sediments

An understanding of the isotope data for silica in sediments is greatly aided by some of the following theoretical and experimental considerations. Oxygen isotope equilibrium relations for two systems which are of utmost importance to this research are the equilibrium fractionations between quartz-water and calcite-water.

Clayton et al. (1972) have recently measured equilibrium constants for oxygen isotope exchange between quartz and water over the temperature range 195°C to 750°C. Quartz does not equilibrate in the laboratory at lower temperatures. Becker (1971), however, has invoked a multiplicative factor upon his theoretical calculations for quartz-water fractionations to bring them into agreement with experimental values and has thus extended the range of values for the quartz-water fractionation factor to 0°C. His calculated relationship is shown in figure 3-1. Becker does not indicate how accurate this relationship is.

Equilibrium fractionation factors for oxygen isotopes in the calcite-water system in the temperature range 0° - 500°C were most recently calculated and determined experimentally by O'Neil et al. (1969). The fractionation factors are represented by the equation

$$1000 \ln \alpha_{C\text{-water}} = 2.78 (10^6 T^{-2}) - 3.39$$

The quartz-water and calcite-water systems can be combined to give fractionation factors between quartz-calcite over the temperature range 0° - 500°C by the equation

$$1000 \ln \alpha_{Q\text{-}C} = .60 (10^6 T^{-2}) \quad \text{(Clayton et al., 1972)}$$

In addition to these equilibrium relationships, there are several possible kinetic processes that may affect the oxygen and hydrogen isotope relationships in cherts. The

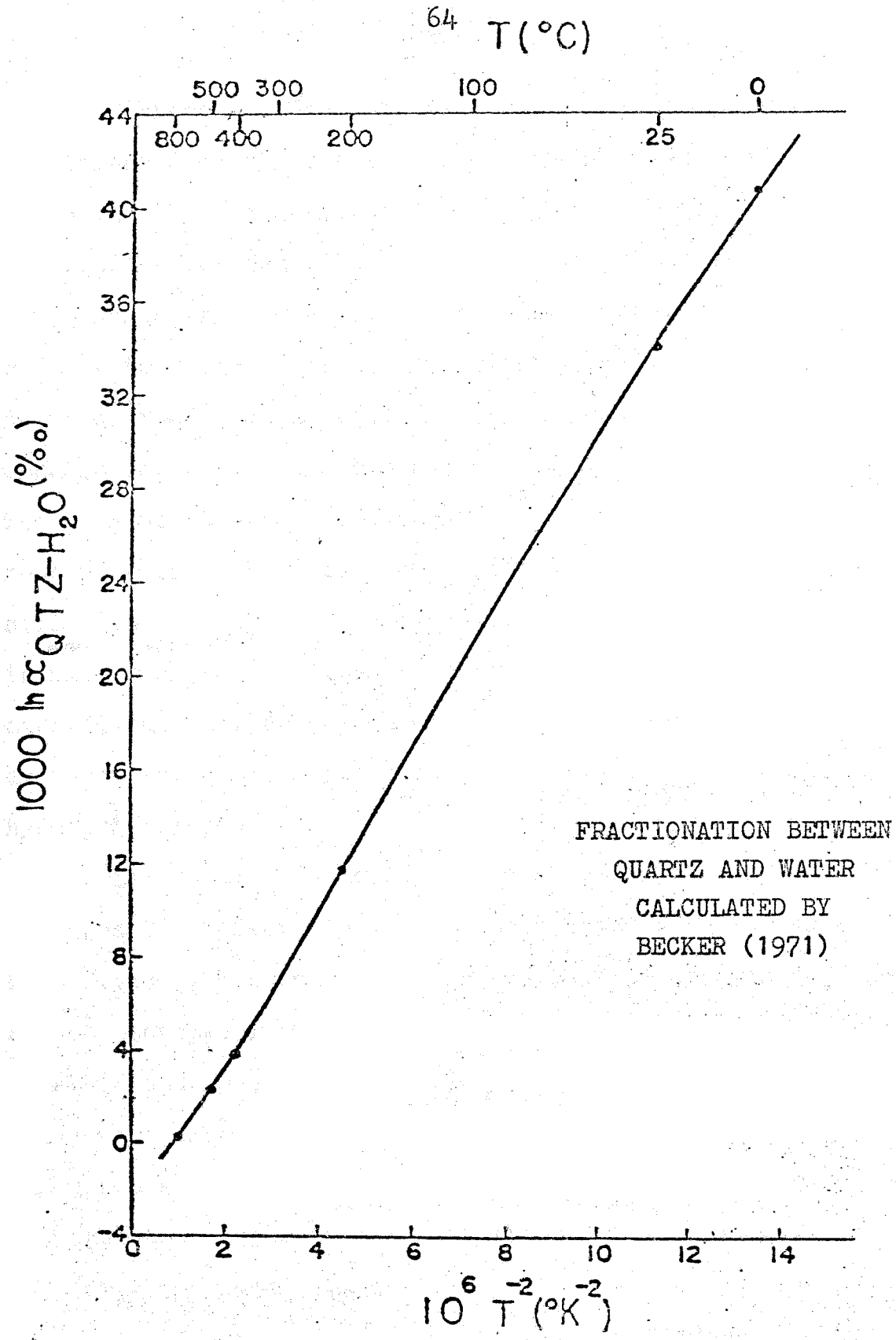
T(°C)
500 300
100
0
800 400
200
25
44
40
36
32
28
24
20
16
12
8
4
0
-4
1000 lnαQTZ-H2O(‰)
0
2
4
6
8
10
12
14
10^6 T^-2(°K^-2)
FRACTIONATION BETWEEN
QUARTZ AND WATER
CALCULATED BY
BECKER (1971)

Figure 3-1

first of these concerns the fact that much silica is precipitated by organisms. There may be vital effects which initially fractionate the isotopes in a manner unlike the equilibrium described above. Biological precipitation of silica always occurs in waters undersaturated with respect to silica. Its dissolution in such waters after death of the organism is greatly impeded by thin films of organic matter or metallic surface complexes (Lewin, 1961). The presence of these substances may also affect the isotope reactions associated with the silica. In addition, biogenic silica is very hydrous. Dehydration of this material either in nature or in the laboratory may cause fractionation, significantly altering the original isotope ratios of the oxygen in the silica and the hydrogen in the residual hydroxyl groups.

The isotopic composition of natural silica is further expected to reflect the isotopic composition of the waters from which it precipitated. The variations of hydrogen and oxygen isotopes in meteoric waters are well understood (Epstein and Mayeda, 1953; Friedman, 1953; Friedman et al., 1964; Dansgaard, 1964; and Craig, 1961a). Craig (1961a) has given a least squares linear relationship between hydrogen and oxygen isotopes in these waters. This is

$$\delta D = 8 \delta O^{18} + 10$$

This relationship is very important for this research and

will be used throughout the text. It will be referred to as the "meteoric water line". Craig's data are reproduced in figure 3-2 to show the scatter in δ-values of the natural water samples used to establish the above relationship. Any hydrous minerals which form in equilibrium with these waters must also display at least this amount of scatter.

3.4 Isotope Relationships in Hydrous Minerals

At equilibrium the oxygen and hydrogen isotopic composition of natural hydrous minerals is dependent upon temperature and the isotopic composition of the waters with which they have equilibrated. The effects of these parameters are shown in figure 3-3. A graph of this sort can show simultaneously the D/H and O^{18}/O^{16} ratios of natural waters and hydrous minerals. Ocean water and the meteoric water line are plotted in figure 3-3 along with a family of curves for hydrous minerals formed in equilibrium with ocean water and meteoric waters at the temperatures T_1, T_2, and T_3. The position of the hydrous mineral line relative to the meteoric water line is plotted to the lower right of the meteoric water line because Savin (1967) and Savin and Epstein (1970a) have shown that the total oxygen in most clay minerals is enriched in O^{18}, and hydrogen in the hydroxyl groups is depleted in deuterium. It will be shown later that this is apparently true for hydrous silica as well.

If it is assumed that at temperature T_1 the isotopic

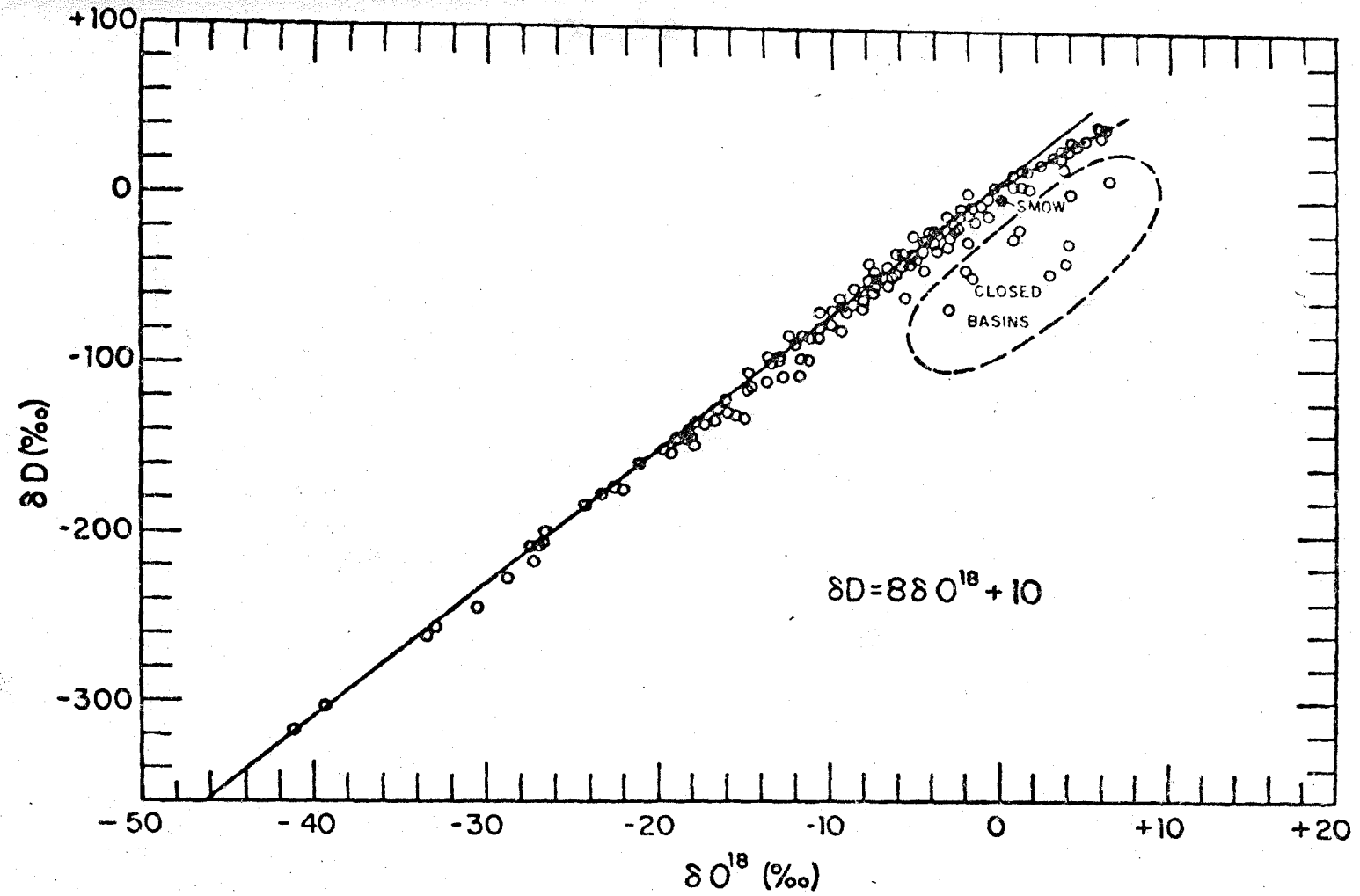

Figure 3-2

δD AND δO^{18} VARIATIONS IN PRECIPITATION AND METEORIC WATERS

(From Craig 1961)

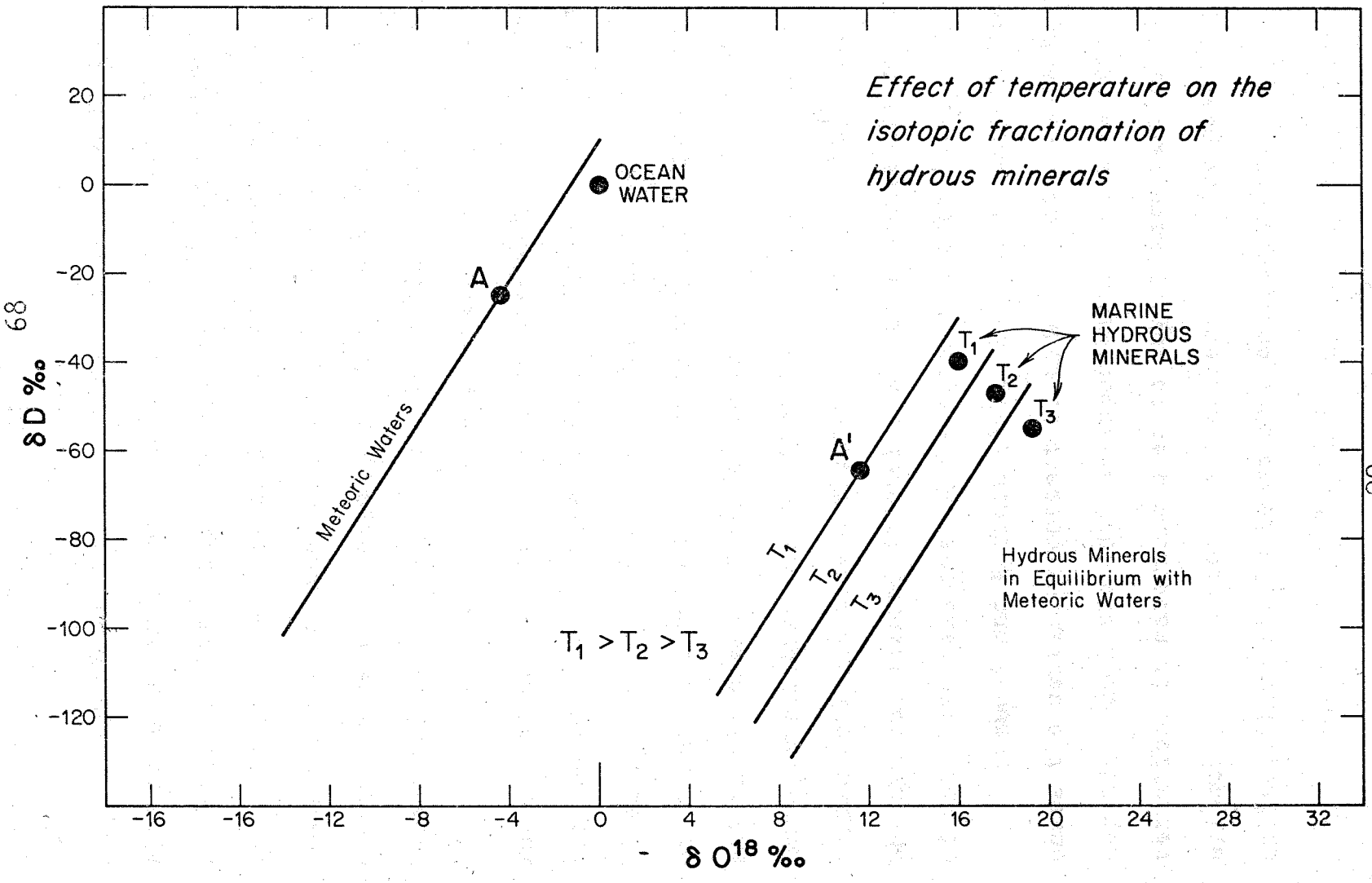
Effect of temperature on the isotopic fractionation of hydrous minerals
OCEAN WATER
A
Meteoric Waters
MARINE HYDROUS MINERALS
T1
T2
T3
A'
T1
T2
T3
Hydrous Minerals in Equilibrium with Meteoric Waters
T1 > T2 > T3
δ D ‰
- δ O18 ‰
20
0
-20
-40
-60
-80
-100
-120
-16
-16
-12
-8
-4
0
4
8
12
16
20
24
28
32

Figure 3-3

composition of some given hydrous mineral in equilibrium with ocean water is represented by point T_1, then at the same temperature this mineral in equilibrium with fresh water with isotopic composition A would be represented by A^1. δ-values for various samples of this mineral forming in meteoric waters at temperature T_1 would be represented as a line parallel to the meteoric water line. At lower temperatures this line would be displaced away from the meteoric water line due to the temperature dependence of the fractionation factors (Savin and Epstein, 1970). This is represented by lines T_2 and T_3, where $T_1 > T_2 > T_3$. The temperature dependence of α may be expected to vary for different hydrous minerals, but in all cases, α varies inversely to the temperature. Large temperature changes over the whole earth's surface during geologic time would thus affect both δO^{18} and δD in the hydrous mineral in such a way as to shift the position of this line relative to the meteoric water line.

Suzuoki and Epstein (1972) have shown that in many cases the deuterium content of hydrous silicates is also dependent upon the cation composition. Possible compositional variations in materials used to investigate past climatic effects must therefore be considered. In the case of pure silica, there should be no such complications.

3.5 Factors Affecting the Isotopic History of the Hydrosphere

Ocean water is currently thought to be depleted in O^{18} by 7‰ and enriched in D by 30 to 70‰ relative to mantle or "juvenile" water (Sheppard and Epstein, 1970; Epstein and Taylor, 1967). It is possible that the difference in the isotopic composition of ocean water and mantle water is a result of complicated isotopic fractionations during the formation of the primordial ocean. It is also possible that ocean water originally had an isotopic composition similar to mantle water and that some process or processes have altered this original isotopic composition. The factors which might affect the isotopic history of the oceans can be postulated, but the extent of their relative importance is subject to much speculation.

A. Review of previous work concerning isotopic history of the oceans. The initial concern over the isotopic history of the ocean resulted from the early paleotemperature investigations of Urey et al. (1951). The authors speculated that Precambrian processes had fixed the O^{18}/O^{16} ratio of the ocean, and that this ratio had remained unchanged since the Cambrian. Silverman (1951), however, observed that O^{18} was concentrated in sediments and suggested that sedimentation had caused a decrease in the O^{18}/O^{16} ratio of ocean water with time.

Compston (1960) measured δO^{18} values for well-preserved Premian brachiopods and found them to be similar to present day values. From this he assumed that the Premian oceans were isotopically similar to the present oceans. Lowenstam (1961) likewise concluded that the amount of O^{18} in the oceans had changed little since Late-Paleozoic, this being based upon similarities in the systematics of Sr, Mg, and O^{18}/O^{16} in Premian and Recent brachiopods.

Weber (1965) observed that ancient limestones and dolomites are depleted in O^{18} and suggested that this is due to the increase with geologic time of O^{18} in the ocean. Fritz (1971) also argued that isotope data on dolomites require a lower O^{18}/O^{16} ratio for the ancient oceans. Perry (1967) proposed that this ratio had increased with time, the cause being the input of O^{18}-rich mantle water by primary outgassing or by cycling of ocean water through the mantle (Perry and Tan, 1972; Chase and Perry, 1972). Savin and Epstein (1970a) observed that 1390 million year-old glauconites were depleted in O^{18} and enriched in D relative to Cenozoic glauconites. Consequently, they suggested that the oceans at that time may have been 30‰ richer in D and 6‰ poorer in O^{18}.

Muehlenbachs (1971) proposed that the O^{18}/O^{16} ratio of ocean water has been held constant by its continuous involvement in the metamorphism of ocean basalts.

Longinelli (1966) concluded from a study of O^{18} in phosphates that the oceans had decreased by 5 - 9 per mil since the Jurassic, but he has recently indicated that his measurements were inaccurate (Longinelli and Nuti, 1972).

Wenner and Taylor (1972) offered the suggestion that the isotopic composition of possible meteoric waters involved in the alteration of certain Precambrian rhyolites was so enriched in O^{18} that Precambrian ocean waters may have been O^{18}-rich relative to the present day ocean

It is known that concentration of water in the ice caps depletes the oceans in O^{16}. The maximum amount of this depletion during the Pleistoiene ice ages is not certain. Emialiani (1970) claims a .5 per mil depletion and Dansgaard and Tauber (1969) claim 1.2 per mil or more. Over geologic time these excursions of the oceanic O^{18}/O^{16} ratio due to ice cap formation are short-lived and are not a major factor in the long-term isotopic history of sea water.

It is clear from the previous work that no agreement exists concerning the isotopic history of ocean water. The suggested δO^{18} values for the ancient oceans cover the range of possibilities including positive values, negative values, and present-day values.

B. Models for the isotopic history of the hydrosphere. Several models for the isotopic history of the hydrosphere can be generated on the basis of the

investigations mentioned above. These can be tested against the isotope results obtained in the present study.

Any change in the isotopic composition of the ocean will result in a concomitant shift of the meteoric water line on a $\delta D - \delta O^{18}$ diagram. Any shift of this meteoric water line will be reflected in the isotope ratios of hydrous minerals which form in equilibrium with these waters. If a given family of hydrous minerals always formed at the same temperature, then any displacement with geologic time of the locus of δD-δO^{18} values could be interpreted as resulting from a shift in the meteoric water line. This shift could, in turn, be interpreted as a change in the isotopic composition of ocean water.

The most obvious problem with this approach to the study of the isotopic history of ocean water is that displacements of the hydrous mineral locus due to temperature fluctuations (figure 3-3) may exceed any displacements due to changes in the isotopic composition of the oceans. This problem is especially severe because isotope fractionations vary greatly at the low temperatures characteristic of sedimentary mineral formation. However, changes in the isotopic composition of ocean water as large as those proposed by Perry (1967) would result in noticeable shifts of the δD-δO^{18} locus for isotopically preserved cherts and other hydrous minerals which formed under sedimentary conditions, in spite of possible large climatic temperature fluctuations in the history of the earth.

If the isotopic composition of the present ocean has been determined only by the addition of mantle water rich in O^{18} and depleted in D relative to that of an ancient ocean, a fairly specific shift of the meteoric water line can be considered. This model is shown in figure 3-4. In this figure the present-day meteoric water line is shown together with the locus of δ-values for present-day hydrous minerals and the range of δ-values proposed for mantle water. Ancient ocean δ-values must fall along a line passing through the mantle δ-values and the present δ-value according to a simple mixing model. The position of δ-values for the oceans at past times τ_1 and τ_2, $\tau_1 > \tau_2$, are shown together with their associated meteoric water lines, A and B respectively. The corresponding loci of δ-values representing the hydrous minerals at time τ_1 and τ_2 are lines A' and B' respectively. The amount of added mantle water necessary to shift the δD or δO^{18} of ocean water by a given amount can be calculated from the expression

$$\delta_{\substack{\text{present}\\\text{ocean}}} = X\,(\delta_{\substack{\text{mantle}\\\text{water}}}) + (1 - X)\,(\delta_{\substack{\text{past}\\\text{ocean}}})$$

X = mole fraction of mantle water added to ancient ocean.

An additional factor which might effect the δD history of the oceans is the preferential escape of hydrogen from the atmosphere after photodissociation of water vapor. This process will enrich the oceans in deuterium with time.

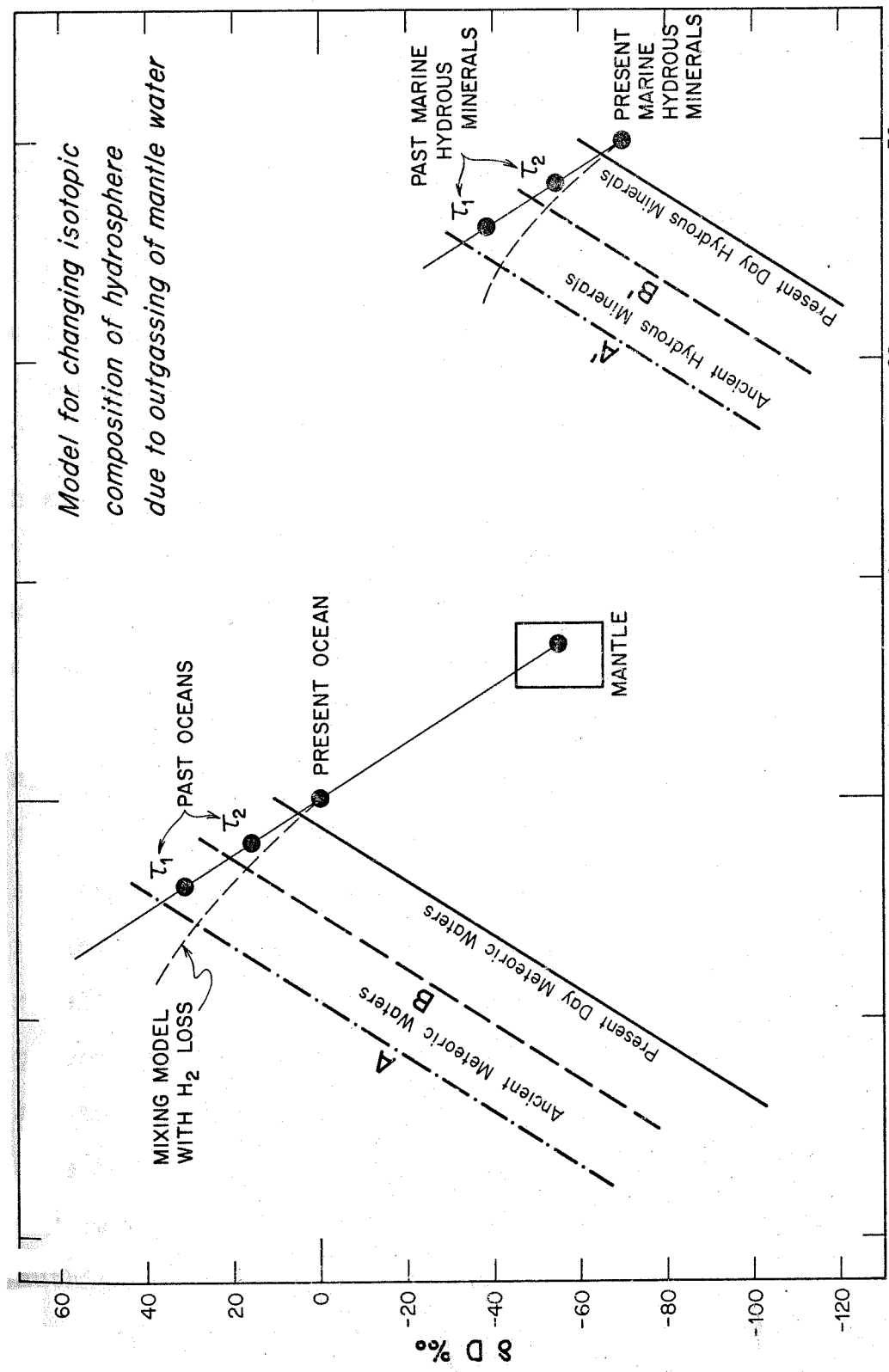
Model for changing isotopic composition of hydrosphere due to outgassing of mantle water
PAST MARINE HYDROUS MINERALS
PRESENT MARINE HYDROUS MINERALS
Present Day Hydrous Minerals
Ancient Hydrous Minerals
A'
B'
τ1
τ2
PAST OCEANS
PRESENT OCEAN
MANTLE
MIXING MODEL WITH H2 LOSS
Present Day Meteoric Waters
Ancient Meteoric Waters
A
B
δ D ‰
δ O18 ‰
60
40
20
0
-20
-40
-60
-80
-100
-120
30
20
10
0
-10
-20

Figure 3-4

The exact amount of enrichment is unknown due to uncertainties in the fractionation associated with photodissociation and uncertainties in the rate of hydrogen loss over geologic time. The qualitative effect would be similar to that shown by the dashed line in figure 3-4. This, too, would be reflected in the isotopic composition of the hydrous minerals as shown.

The process of sedimentation will affect the isotopic history differently. In this case, O^{18} and hydrogen will become progressively depleted in the oceans with time. A model for this process is shown in figure 3-5. Ancient oceans at past times τ_1 and τ_2, $\tau_1 > \tau_2$, are shown with their associated meteoric water lines. Sedimentation of minerals rich in O^{18} and poor in deuterium depleted these oceans in O^{18} and enriched them in deuterium, causing the shifts shown. The locus of δ-values for subsequent generations of hydrous minerals are shifted to the left as a result of the changing oceanic δ-values. The exact displacements of the loci depend upon which hydrous minerals are the predominate authigenic minerals at any given geologic time because the fractionation factors vary for different minerals. The important point is that sedimentation of authigenic O^{18}-rich and deuterium-poor minerals causes nearly the exact opposite trend in displacements of the locus of hydrous mineral δ-values with time as compared with the

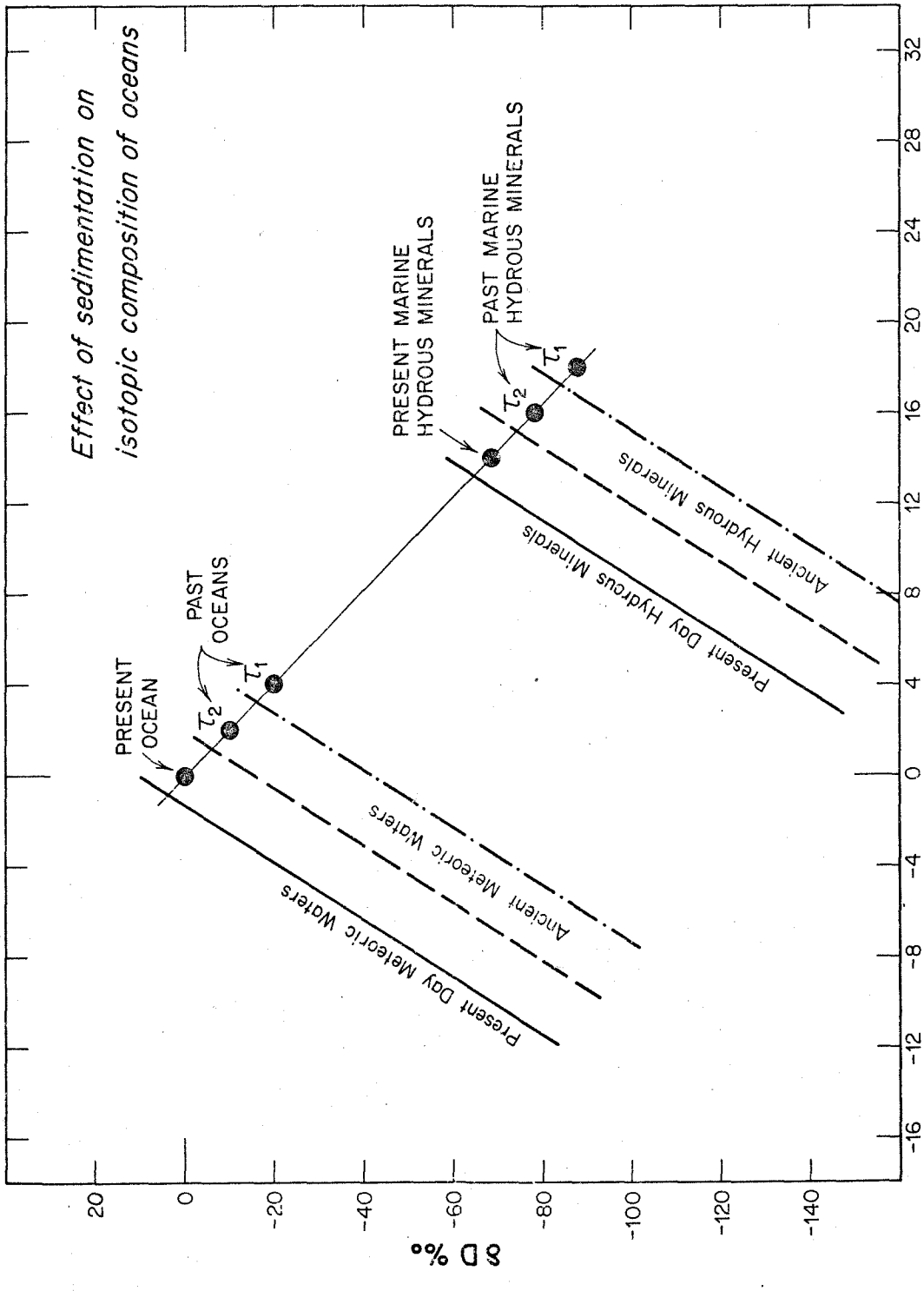
Effect of sedimentation on isotopic composition of oceans
PRESENT OCEAN
PAST OCEANS
τ_2
τ_1
PRESENT MARINE HYDROUS MINERALS
PAST MARINE HYDROUS MINERALS
Present Day Meteoric Waters
Ancient Meteoric Waters
Present Day Hydrous Minerals
Ancient Hydrous Minerals
δD ‰
δ O18 ‰
20
0
-20
-40
-60
-80
-100
-120
-140
-16
-12
-8
-4
0
4
8
12
16
20
24
28
32

Figure 3-5

mantle-input model described above.

It should be noted that all of the processes mentioned above may be occurring simultaneously. It is also possible that these processes produce such small isotopic effects that the oceans have not changed isotopically with time. In this case there should be no observed shift with time in the $\delta D - \delta O^{18}$ locus of a given hydrous mineral. If displacements in the locus of δ-values for some hydrous mineral, such as chert, can be established, then it can be determined which, if any, of these models is applicable.

Chapter 4

ANALYTICAL TECHNIQUES

4.1 Sample Collection

The majority of specimens analyzed in this work were collected by the author from outcrops in the central and western United States. The geologic column in these regions contains beautifully exposed and well-studied examples of almost all the silica occurrences described in Chapter 2. Most of the samples were obtained during a three-month, 11,000 mile collecting trip during the summer of 1971. Sample localities were selected after an intensive three-month survey of the geologic literature of the western United States. The sample localities and references are listed in Appendix I together with pertinent petrographic and field data.

At each outcrop the horizons of interest were thoroughly searched for chert occurring in the form of nodules, beds, and irregular accumulations which are clearly unrelated to tectonic fractures, hydrothermal veins, and surface silicification. Where weathering or other alteration was evident, examples of the altered as well as the "fresh" material were collected. Criteria for judging the degree of weathering of chert are difficult to specify. In deeply weathered carbonate outcrops, dark cherts will frequently have lighter-

colored rhinds, the so-called "patinated" cherts. In other outcrops such color variations are frequently unrelated to the surfaces and are then poor weathering criteria. The resistance to hammer blows is a possible criterion for "freshness", for some cherts tend to fracture and disaggregate during the weathering cycle. However, the factors controlling the physical strength of cherts have never been evaluated, and it does not follow that a chert which fractures easily has been extensively weathered.

Whenever possible, localities were selected which had been well-studied by previous workers, with measured stratigraphic sections being the most desirable. The locality of collection was determined as accurately as available topographic maps would allow. This collection is strongly biased in favor of pure, hard cherts which occur in carbonate rocks.

Several samples were obtained from various donors. The criteria for collection, the exact location, and the geologic circumstances for these samples is less well known, but all available information is listed with the sample description.

4.2 Laboratory Examination and Preparation of the Samples

Samples selected for analysis were usually broken up and fed through a large jaw-crushing machine, resulting in a tray filled with cm-sized chips. These chips were then sorted out according to color and translucence. This

usually resulted in three or less groups of chips from the same sample. Three or four pieces the size of pin-heads were then ground up in a steel mortar for each of the groups. These were examined petrographically in a 1.540 refractive index oil to ascertain the sample purity and mineralogy. The group of chips containing the least amount of impurities was then smashed in a hardened-steel mortar and ball-pestel. The resulting powder was sieved, retaining two size-fractions, 100 - 200 mesh, and < 200 mesh. The <200 mesh fraction was then treated with 1:5 HCl to remove carbonates and steel-fragments from the crushing process. This sample was rinsed twice with triply-distilled water and allowed to air dry. Many of the extremely fine grains were usually floated off during the rinsings. The treated powders were then stored in screw-cap vials until analyzed. Thin-sections of the uncrushed original sample were made for many of the samples.

4.3 Oxygen Extraction from Silica

Oxygen isotope analyses are made on a gas-source mass spectrometer which uses CO_2 as the working gas. CO_2 is a chemically stable gas easily manipulated in vacuum lines, and its isotopic molecules have masses occurring in a "clean" part of the mass spectrum ("background" masses in the spectrometer result from hydrocarbons, atmospheric constituents, and various impurities in the high-vacuum system). It is therefore required to convert the oxygen in

silica to gaseous CO_2 without altering its O^{18}/O^{16} ratio.

The various methods used to extract oxygen from silicates for isotopic analysis are the carbon reduction method (Clayton and Epstein, 1958), the bromine-pentafluoride method (Clayton and Mayeda, 1963), or the fluorine method (Taylor and Epstein, 1962). The fluorine and bromine-pentafluoride methods have proved the most successful and are now widely used in a routine fashion. Oxides and silicates are reacted with excess fluorine or bromine-pentafluoride at 400° - 500°C in nickel reaction vessels to produce free oxygen and fluorides. The gaseous reaction products are passed through traps cooled to liquid nitrogen temperatures (-196°C) to remove SiF_4 and HF while allowing O_2 and F_2 to pass. The F_2 is removed by allowing it to react with KBr to form HF and Br_2. The Br_2 is then frozen out, and the remaining O_2 gas is reacted with carbon to produce CO_2, which can then be analyzed mass spectrometrically.

A. Fluorine method. The high vacuum apparatus shown in figure 4-1 was specially constructed in a fashion very similar to that of Taylor and Epstein (1962). The apparatus was suitable for use of either fluorine or bromine-pentafluoride as the reaction reagent. Sample powders are loaded into the reaction vessels in a glovebox containing P_2O_5 - dried air. This precaution is necessary since fluoride coatings of the metallic parts when exposed to the

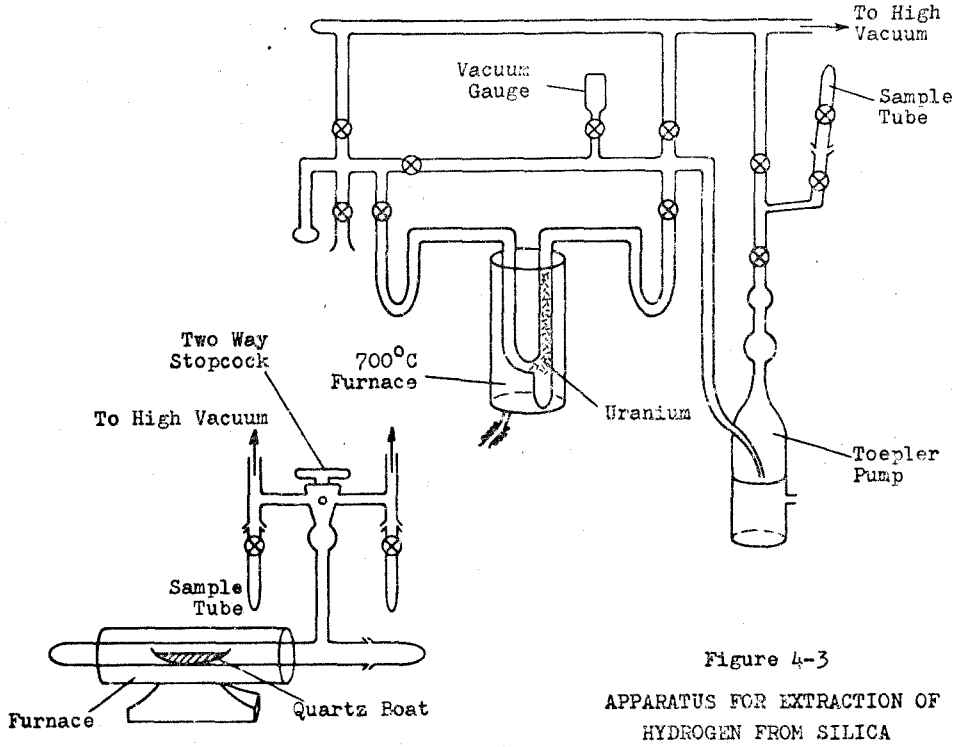

Figure 4-3

APPARATUS FOR EXTRACTION OF HYDROGEN FROM SILICA

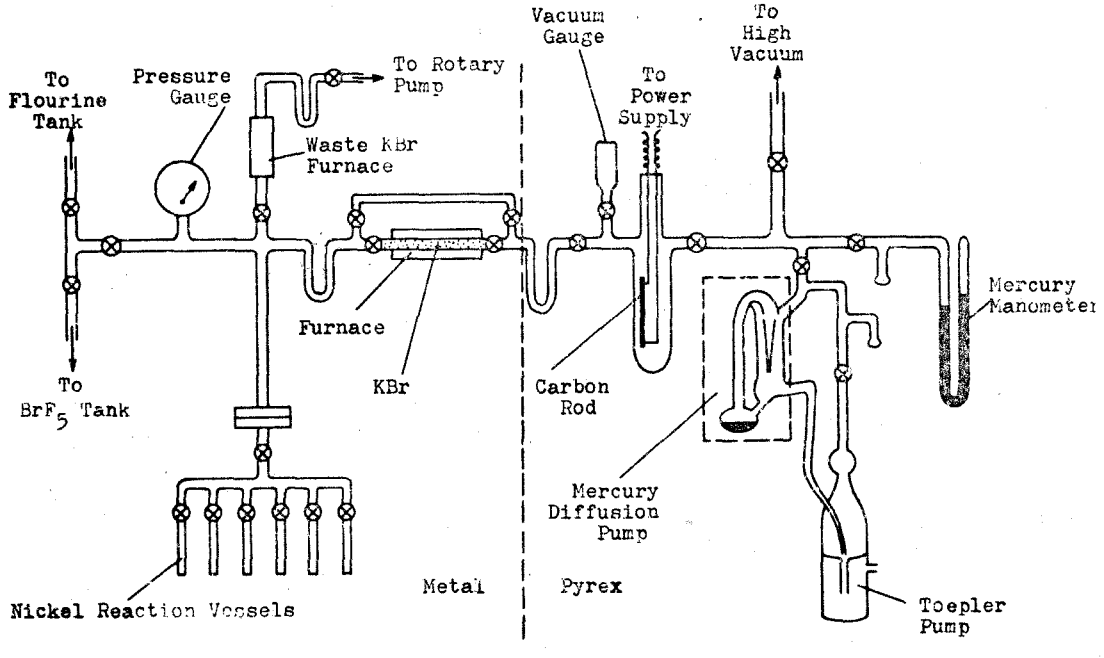

Figure 4-1

APPARATUS FOR EXTRACTING OXYGEN FROM SILICA AND CONVERTING TO CO_2

moist atmosphere will hydrate and liberate contaminating oxygen during fluorination of the sample.

Taylor and Epstein (1962) have described most of the details of the procedure for the fluorine method used here. Additional procedures and variations of technique used in this work are described below. Since all of the samples analyzed were almost identical chemically, the same procedure could be used routinely.

About 2 moles of F_2 are required for reaction with one mole of $SiO_2 \cdot nH_2O$ ($n << 1$ for natural samples). This corresponds to about 3×10^{-5} moles F_2 per milligram SiO_2. Since 20 - 30 mg of sample were typically used for an analysis, the stoichometric requirement of fluorine is 6.5×10^{-4} to 1×10^{-3} moles F_2. A reagent excess of a factor of 1.5 to 2 was found to be sufficient to obtain 100% yields for samples of sedimentary silica. This amount of fluorine could be placed in the reaction vessels and measured by means of the pressure gauge (2/3 atmosphere of fluorine in 50 cc vol. at 20°C = 1.4×10^{-3} moles F_2). An additional fluorine excess was not desirable since it increased the rate of consumption of the KBr, and produced excess pressures at 450°C which might result in leakage.

B. Contamination of the reagent. The fluorine gas used in this work contained small amounts of nitrogen and oxygen. The oxygen in the fluorine was carefully measured

and found to be .31% of the volume. The isotopic composition was determined to be δ_{SMOW} = +7.4‰. All oxygen isotope analyses were corrected for this contaminant, a correction which usually amounted to about .2‰.

C. CO_2 purification. Trace amounts of fluorine and bromine may contaminate the final CO_2 and affect the isotope analysis. These can be removed by cycling the CO_2 through a mercury diffusion pump with a Toepler pump. This is done on a separate part of the same vacuum line while the next oxygen sample is being converted to CO_2. Parts of the walls of a new diffusion pump turned yellow after several samples were cycled, showing that this step is indeed necessary.

D. Bromine-pentafluoride method. The use of BrF_5 is a satisfactory method for oxygen extraction from silica only if quantitative yields are obtained. Garlick and Epstein (1967) have shown that non-quantitative yields due to insufficient reaction time and insufficient temperature result in anomalous δ-values, while this is not true in the case of fluorine extractions.

The BrF_5 method is advantageous in that the KBr furnace is unnecessary, resulting in faster diffusion of O_2 and quicker conversion times. However, routine use of this method was found to be unsatisfactory in the present case. A series of quartz standards were reacted at 470 - 580° C as specified in the procedure of Clayton and Mayeda (1963).

Erratic yields and anomalous δ-values resulted as shown in figure 4-2. Since the proper reagent excess, temperature, and reaction times were used, the method was considered unreliable and was abandoned. Successful BrF_5 extractions are widely reported for SiO_2 analyses, and it is not known why the method failed in this case. The same standards prepared by the fluorine method consistently yielded δO^{18} values with a reproducibility of $\pm$ .2‰ for yields greater than 95%.

4.4 Water and Hydrogen Extraction

Hydrogen occurs in hydrous silica in the form of OH and H_2O. This water may be extracted by heating the sample in a high vacuum and condensing the water in liquid nitrogen-cooled traps. Hydrogen in this water is liberated for analysis with the gas-source H_2-mass spectrometer by reacting it with pure uranium at 700°C in the manner of Godfrey(1962). A schematic illustration of the high vacuum apparatus for the water extraction and hydrogen liberation is shown in figure 4-3. The exact procedures for water extraction varied, depending on the type of sample and the kind of experiment.

4.5 Correction Factors and Numerical Conversions for Isotopic Analysis of CO_2.

A detailed discussion of mass spectrometer correction

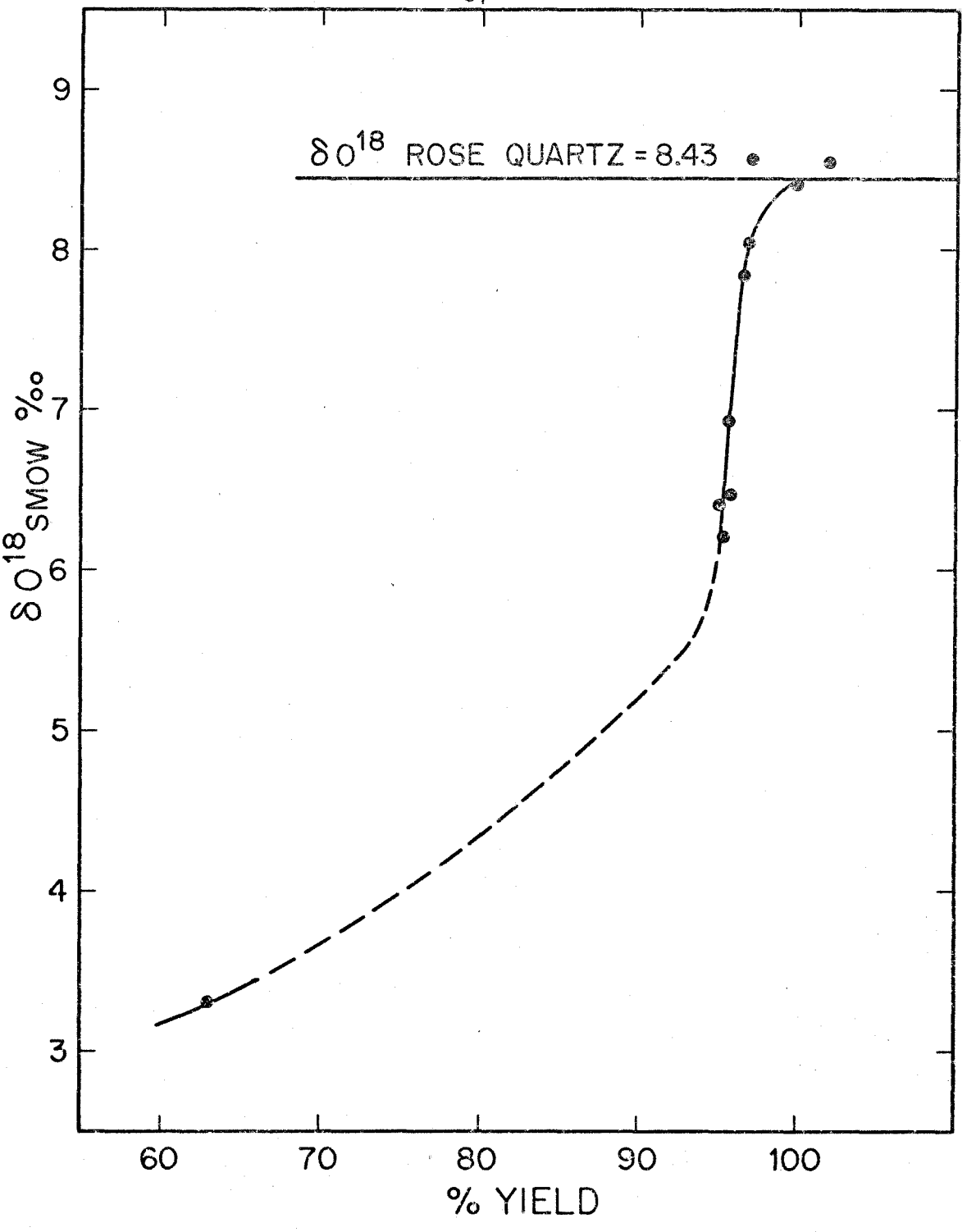

Figure 4-2

ISOTOPIC EFFECTS OF NON-QUANTITATIVE OXYGEN YIELDS FROM ROSE QUARTZ WHEN USING BrF_5 AS REAGENT

factors and numerical conversions is given in Appendix II. A summary of the relevant equations used for correcting the raw mass-spectrometric data and converting them to SMOW is given here.

A. Background and leakage correction. The combined correction factor for leakage of the glass inlet valves as derived in the appendix is

$$(4\text{-}1) \qquad \delta_m = \left[1 + \frac{44B}{44 - 44B}\right] \delta_{raw}$$

where 44B = voltage of mass-44 Beam with both valves closed

44 = voltage mass-44 beam with standard-side valve open.

This correction was usually about .1 - .5‰ for sedimentary silica.

B. C^{13}, O^{17} correction. The appropriate corrections for C^{13} and O^{17} in the mass-spectrometer ion beam have been given by Craig (1957) for cases where PDB calcite is the working standard. Since PDB calcite was not used as the working standard in this research, it was necessary to evaluate new correction factors. The C^{13} and O^{17} abundances in the Caltech working standard relative to the abundances in PDB calcite were determined from measured values of ΔO^{18} PDB-Caltech working std. and ΔC^{13} PDB-Caltech working std. Using these abundances and the relationships given by Craig (1957), the following correction factors for C^{13} and O^{17} were obtained:

$$(4\text{-}2) \qquad \delta_c O^{18} = 1.0014 \ \delta_m O^{18} + .009 \ \delta C^{13}$$

$$(4\text{-}3) \qquad \delta_c C^{13} = 1.0695 \ \delta_m C^{13} - .0348 \ \delta O^{18}$$

δ_m = δ-value corrected for all instrumental errors,

δ = corrected for raw δ-values (the multiplicative factors here are so small that it makes no difference whether δ is the corrected or uncorrected value.

These corrections usually changed the δ-values by less than .1‰.

δ-values corrected as above are the precise isotope differences between sample and working standard.

C. Special corrections for CO_2 obtained by the fluorine method. Every sixth silica sample analyzed by the fluorine method was a sample of Rose Quartz Standard with a δO^{18}-value of +8.43‰ on the SMOW scale as measured by H. P. Taylor, Jr. (unpublished data). The difference in δO^{18}-values between the sample and this standard (both measured on the same day) is

$$(4\text{-}4) \qquad \delta O^{18}_{x\text{-SMOW}} - \delta O^{18}_{\text{rose qtz-SMOW}} = \left[1 + \frac{1}{10^3} \ \delta O^{18}_{\text{std-SMOW}}\right] \left[\delta O^{18}_{x\text{-std}} - \delta_{\text{rose qtz-SMOW}}\right]$$

where $\delta O^{18}_{\text{std-SMOW}} = 24.5‰ = \delta O^{18}_{\text{SMOW}}$ value of Caltech working standard

Each sample contained 4.3 μm of impurity O_2 from the fluorine. The δO^{18} value for this O_2 was +7.4‰. The "blank" correction is thus

$$(4\text{-}5) \quad \delta_{c'} = \frac{\delta_c O^{18} - \left(\frac{4.3}{4.3 + \mu m}\right)\left(7.4\right)}{1 - \frac{\mu m}{4.3 + \mu m}}$$

where $\mu m = CO_2$ yield in μm.

As mentioned previously, this correction usually amounted to about .2‰ for sedimentary silica.

All of the correction factors above may be combined to give

$$(4\text{-}6) \quad \delta O^{18}_{x\text{-SMOW}} = \left\{\left[1 + 10^{-3}\,(\delta_{\text{std-SMOW}})\right]\left[1.0014\right]\left[1 + \frac{44B}{44-44B}\right]\left[\delta_{x\text{-std}} - \delta_{\text{rose qtz-std}}\right] + \delta_{\text{rose qtz-SMOW}} - \left(\frac{31.7}{4.3 + \mu m}\right)\right\}\left(1 - \frac{\mu m}{4.3 + \mu m}\right)^{-1}$$

For each sample the measured quantities were μm, 44B, $\delta_{x\text{-std}}$, and $\delta_{\text{rose qtz-std}}$ (measured every 5 samples). This equation was routinely solved by entering the appropriate values into a Hewlett-Packard 9100A desk computer programmed with equation 4-6.

D. Conversion factors for carbonates. The following numerical values were used to convert δO^{18} measurements of CO_2 derived from carbonates by the phosphoric acid method to δO^{18}-values for carbonate on the SMOW scale.

$\alpha_{CO_2\text{-calcite}} = 1.01008$ (Sharma and Clayton, 1965)

$\alpha_{CO_2\text{-dolomite}} = 1.01090$ (Sharma and Clayton, 1965)

$\alpha_{CO_2\text{-SMOW}} = 1.0407$ (O'Neil and Epstein, 1966)

4.6 Correction Factors for Isotopic Analysis of Hydrogen

The hydrogen mass-spectrometer used in this work is of the Nier type with side arm, and measures the ratio of the mass-3 beam (HD) strength to the mass-2 (H_2) beam strength. H_3^+ ions are produced in the source and contaminate the mass-3 beam. This contaminating component can be corrected for, using the pressure effect method described by Friedman (1953).

δ-values corrected for H_3^+ must be further corrected for background and leakage of the glass inlet valves. This correction may be expressed as

$$(4\text{-}7)\quad \delta_{c\text{-std}} = \left[1 + \frac{(2)b}{(2) - (2)b}\right] \delta_{m\text{-std}}$$

(2)b = background mass-2 ion current with inlet valves closed

(2) = mass-2 ion current of standard or sample (these are set equal)

$\delta_{c\text{-std}}$ = corrected δ-value

$\delta_{m\text{-std}}$ = δ-value corrected for H_3^+

The working standard used for this work had $\delta_{SMOW} = -69.7‰$.

This value, δ_c, can be substituted into the usual change-of-standard equation (Craig, 1957) to give

$$\delta_{c\text{-SMOW}} = \delta_{c\text{-std}} - 69.7 + 10^{-3} (-69.7) (\delta_{c\text{-std}})$$

$$\delta_{c\text{-SMOW}} = \left[-68.63\right] \delta_{c\text{-std}} \tag{4-7}$$

Chapter 5

SPECIFIC TECHNIQUES FOR THE HYDROGEN ISOTOPE ANALYSES OF HYDROUS SILICA

5.1 Introduction

Before meaningful isotope analyses can be made on water extracted from hydrous silica it is necessary to consider how the water is held in this material. Water in hydrous silica may occur as structurally essential hydroxyl groups and hydrates in various sites and as adsorbed and mechanically trapped H_2O. The isotopic composition of these different waters may vary, depending upon possible different fractionation factors between water and the different sites. Furthermore, some of this water may exchange readily with ground waters, or may exchange in the laboratory during chemical and physical treatments. In summary, it is first necessary to understand the nature of the water in the material to be analyzed. Secondly, techniques must be established for isolating the different kinds of waters present in the material. Thirdly, it must be established which water does not undergo isotopic exchange during laboratory procedures and treatments. Finally, it is desirable to know if any of this water is resistant to exchange with ground waters over geologic time.

As was discussed in Chapter 2, little is known about the structural state or nature of water in naturally-

occurring silica other than that deduced by Micheelson for Danish flints. Therefore, the following experiments were performed to provide information concerning the nature of water in silica and to develop an appropriate method of water extraction. The problem of whether or not the water in silica exchanges with ground waters over geologic time is not easily solved by laboratory experiments and will be discussed after isotopic data for silica from sediments of many ages has been presented.

5.2 Extremely Hydrous Amorphous Silica

Most of the experiments which were done to decipher the nature of water in amorphous silica were performed on a sample of Miocene diatomite, #287, from the Monterey formation at the Palos Verdes Hills, California. The diatomite contains a few sponge spicules and there is probably a small amount of organic matter also present. The silica is isotropic under crossed nichols. A pure, white sample of diatomite which was collected from a quarry face was selected for the experiments. This sample was chosen for the experiments because it is a type of silica representative of the natural samples of amorphous silica being investigated in this research.

A. Differential isotopic analysis (D.I.A.). The first experiment done on the diatomaceous earth involves the stepwise heating of the sample during which the water

liberated is collected and analyzed for δD. The purpose of this technique is to ascertain the manner in which water is isotopically fractionated as it is removed from the sample. Since differential thermal analyses of hydrous minerals reveal that water in different structural sites is given off at different temperatures, it is desirable to see if this is also the case for silica. It is possible that the fractionation pattern during dehydration differs for the different sites. This method combines Differential Thermogravimetric Analysis with isotope analysis of the water as it is extracted, and is hereafter called Differential Isotopic Analysis (D.I.A.).

Two variations of this method can be used. In one, the temperature is raised to a specified value and all water that can be liberated at this temperature is collected and isotopically analyzed. The temperature is then raised to some higher value, and the water again collected. This procedure is continued until the sample is completely dehydrated. A D.I.A. performed in this manner has the disadvantage that large amounts of water may be given off over a very narrow temperature range and are thus all included in one fraction. In such a case it is not possible to observe the isotopic enrichment pattern as the sample is dehydrated. This difficulty can be eliminated by taking a new fraction as soon as a specified amount of water has been extracted from the

sample. In this way, all fractions would contain about the same amount of water, though there may be several fractions taken for the same temperature.

In the more detailed procedure for the D.I.A. experiments, about .5 grams of hydrous silica were placed in a nichrome bucket which was suspended from a quartz spring by a nichrome wire as shown in figure 5-1. Water is liberated from the sample when it is heated in the furnace. The water is condensed in one of two sample tubes cooled with liquid nitrogen. As the silica sample gives off water, it loses weight and the loss is recorded by the quartz spring balance. The amount of rise depends on the amount of water lost, and this can be accurately calibrated. The sensitivity of the quartz spring balance was such that a 2 mg weight loss would cause the bucket to rise 1 division on a reticle scale that could be read accurately to .1 division. A 2 mg weight loss corresponds to approximately 100 μmoles of water. Thus, a water loss as small as 2 μmoles from the sample could be measured with this technique.

After the desired amount of water was liberated and collected, the two-way stopcock was turned, diverting the flow to the other sample tube. Meanwhile, the sample tube containing the collected sample was removed and replaced with a new tube in preparation for the next fraction.

When the sample bucket ceases to rise, the temperature

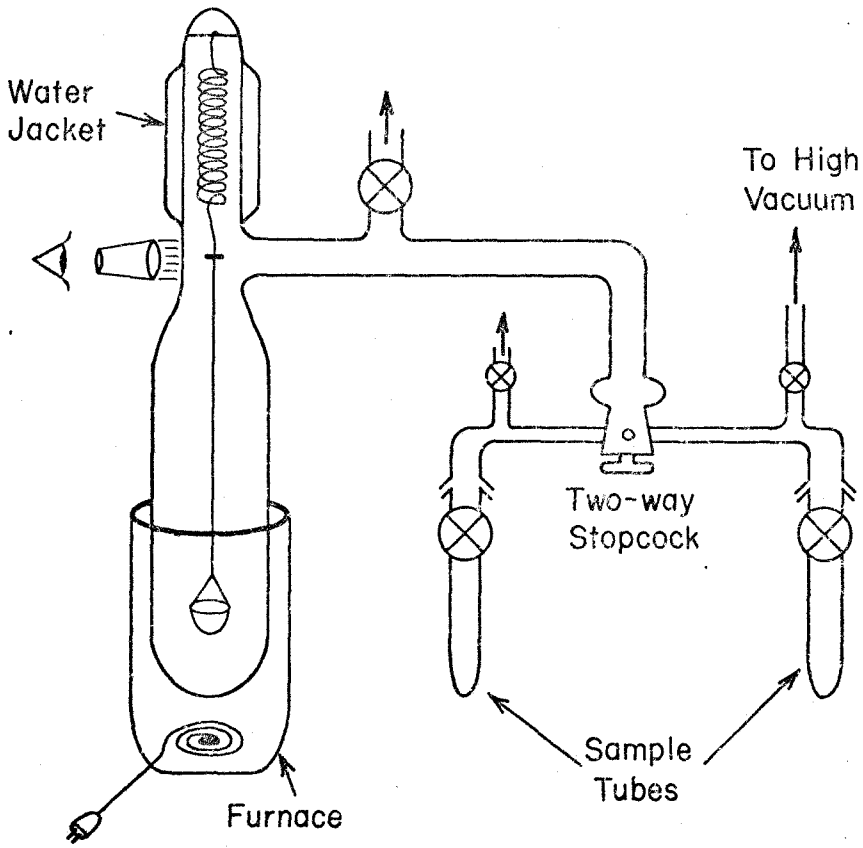

Figure 5-1

APPARATUS FOR DIFFERENTIAL ISOTOPIC ANALYSIS (D.I.A.)
USING QUARTZ SPRING BALANCE

of the furnace is increased causing more water to be liberated. This procedure is continued until all the water is liberated from the sample. The result of the procedure is a set of water samples of equal volumes obtained at progressively higher temperatures. These water samples are analyzed for δD by the methods discussed in section 4.4. In practice, it was found that the quartz spring began to heat up in spite of the water jacket at furnace temperatures above $300^{o}C$. This causes the spring to stretch, thereby slowing the rate of ascent of the sample bucket, resulting in a false determination of the actual water loss.

The results of this procedure for the untreated diatomite sample are presented in table 5-1 and plotted graphically in figure 5-2. The graph shows the hydrogen-isotope enrichment pattern for samples plotted sequentially from left to right. The total water content of opaline silica at room temperature is largely dependent on the relative humidity to which the sample was exposed before dehydration. In this and most subsequent experiments, the samples were allowed to air dry and were placed in the vacuum line and evacuated. For the experiments illustrated in figure 5-2, collection of the first water sample began after a vacuum of about 10^{-2} mm was reached. This starting point varied from experiment to experiment, and because it is desirable to compare the D.I.A. pattern from experiment to experiment, it was

Table 5-1

DIFFERENTIAL ISOTOPIC ANALYSIS (D.I.A.)
OF MONTEREY DIATOMITE #278

Fraction	Temperature Interval	Time Interval	Yield $\mu m/mg$	δD_{SMOW}‰
1	21°C	0^h10^m	.253	- 75.1
2	21°	11^m	.317	- 47.9
3	21-55	1^h04^m	.298	- 17.2
4	55-87	1^h10^m	.344	- 6.8
5	87-97	59^m	.293	- 37.1
6	97-102	1^h34^m	.363	- 41.6
7	102-130	58^m	.288	- 43.9
8	130-158	31^m	.312	- 40.1
9	158-169	28^m	.350	- 42.7
10	169-176	38^m	.261	- 46.6
11	176-218	57^m	.229	- 45.7
12	218-294	33^m	.183	- 56.1
13	294-360	1^h17^m	.177	- 80.4
14	360-404	19^m	.075	- 92.0
15	404-514	22^m	.199	- 99.8
16	514-735	23^m	.379	-104.2
17	735	40^m	.086	-109.8
18	735-846	36^m	.065	-101.8
19	846-982	3^h01^m	.022	- 75.4

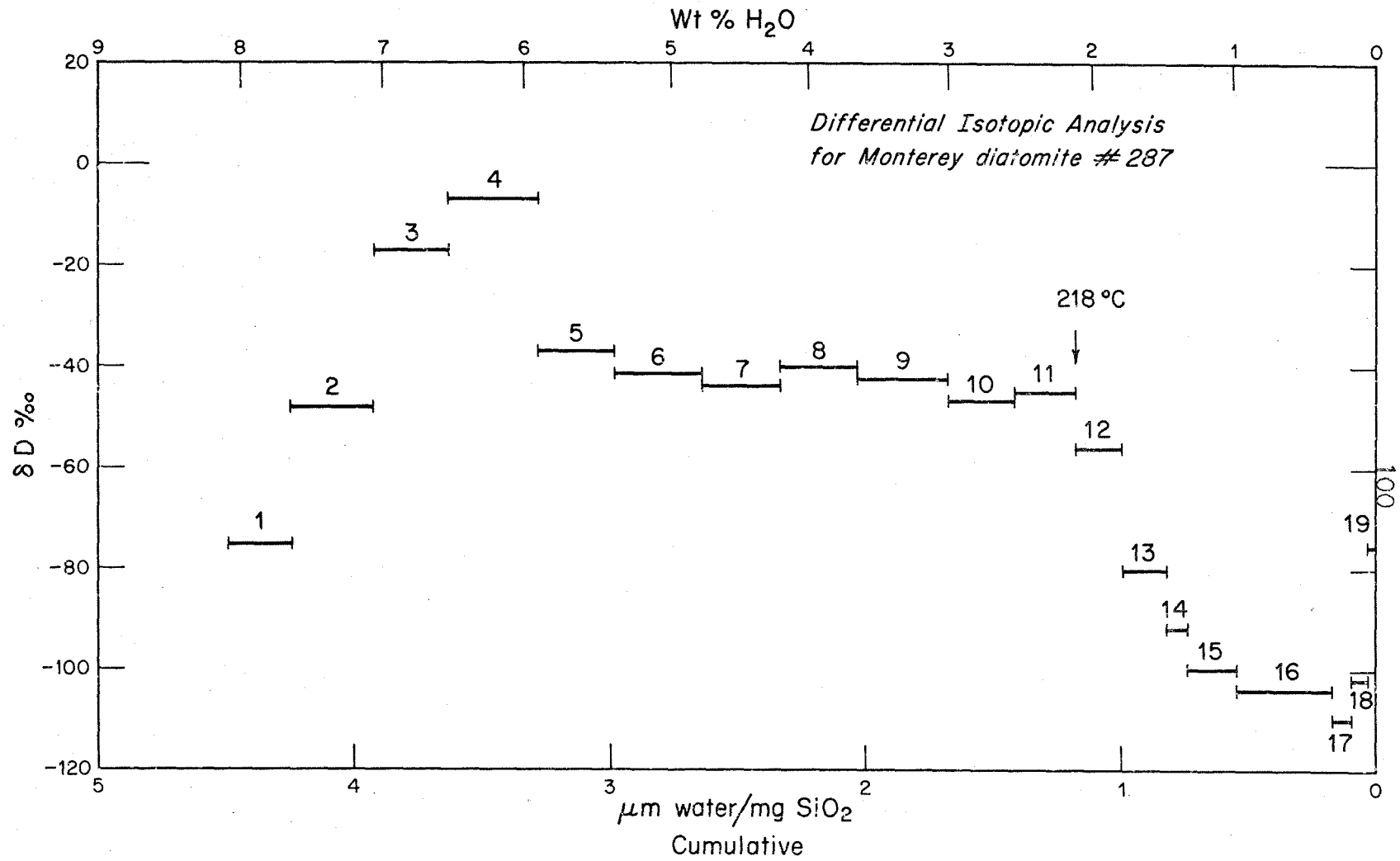
Wt % H_2O
9
8
7
6
5
4
3
2
1
0
20
0
-20
-40
-60
-80
-100
-120
δ D ‰
Differential Isotopic Analysis
for Monterey diatomite #287
218 °C
1
2
3
4
5
6
7
8
9
10
11
12
13
14
15
16
17
18
19
100
5
4
3
2
1
0
μm water/mg SiO_2
Cumulative

Figure 5-2

found convenient to plot the numerical values of the abscissa from right to left.

The first four fractions in figure 5-2 show a continuous enrichment in deuterium as the sample is dehydrated. The next seven fractions, from 87° to 218°, are relatively uniform isotopically with $\delta D \cong -43‰$. The next six fractions, from 200° to 735°, decrease continuously in δD; and the last two fractions, between 735° and 982°, show a large increase in δD.

The range in δD for water fractions extracted in this manner is 105‰. If it is desired to assign a single δD-value for the water in diatomite, the value will depend critically upon the initial and final temperatures of dehydration.

These data suggest that water occurs in diatomite in at least three different sites or hydration states, here referred to as waters I, II, and III. Water I comes off at the lowest temperatures, fractions 1 - 4, and can be interpreted as H_2O loosely bound or mechanically trapped. If H_2O is subjected to distillation and the vapor is removed from the system as it is formed, then the residual liquid water will become progressively enriched in the heavier isotopes (O^{18}, D). δD in fractions of the vapor successively sampled will become more positive. The fractionation pattern for the first four fractions in this experiment shows this

successive enrichment, supporting the idea that most of the water extracted below 87° is structurally non-essential.

Water II is liberated between 87° and 218° and appears to have $\delta D \cong -43‰$. Above 218° there is suggestion of a third water, water III, beginning to be outgassed which has a very low δD-value ($<100‰$). The enrichment pattern is suggestive of a mixing curve between water II and water III, in which water III becomes a more appreciable component at higher temperatures. The deuterium enrichment of the final two fractions is not understood. The water in these fractions may have been derived from an additional site or a site newly created during exposure to high temperatures. It is also possible that the enrichment is an experimental artifact due to problems associated with the extraction procedure for analyzing small amounts of water represented by these fractions.

As a check on the reproducibility of the total isotopic enrichment pattern and the effect of pre-treatment of the sample, several more aliquots of this diatomite were dehydrated and the water analyzed.

The procedure used for these experiments involved placing the sample in a quartz boat and heating with a furnace as shown in figure 4-5. Further use of the tedious procedure using the quartz spring was unnecessary because the amount of water released by the diatomite at various

temperatures could be ascertained from the known water release pattern shown in table 5-1 or figure 5-2.

Figures 5-3, 5-4, and 5-5 show the results of these experiments superimposed on the data of figure 5-2. A two-fraction dehydration of the untreated diatomite shown in figure 5-3 yielded a fraction for 25° - 193° and 193° - 1000°. Each cut is seen to be isotopically and volumetrically equal to the sum of cuts obtained in the previous detailed dehydration, which indicates the reproducible nature of the dehydration experiment.

One aliquot of the diatomite was soaked in chlorox, rinsed in distilled water, and allowed to air-dry. A D.I.A. was performed on this sample, giving the data shown in figure 5-4. The similarity between the chlorox treated and untreated D.I.A. curves indicate that water I and water II have been affected isotopically only to a small degree. The high-temperature fraction of this D.I.A. pattern (> 200 - 300°C) seems to reproduce that of the untreated sample, suggesting that water III is largely unaffected by the treatment.

Figure 5-5 shows results of a D.I.A. performed on a sample of the diatomite treated in 1:5 HCl, rinsed with distilled water, and air-dried. Water outgassed below 200°C is isotopically different from that of the untreated sample, again suggesting that the water liberated below 200°C

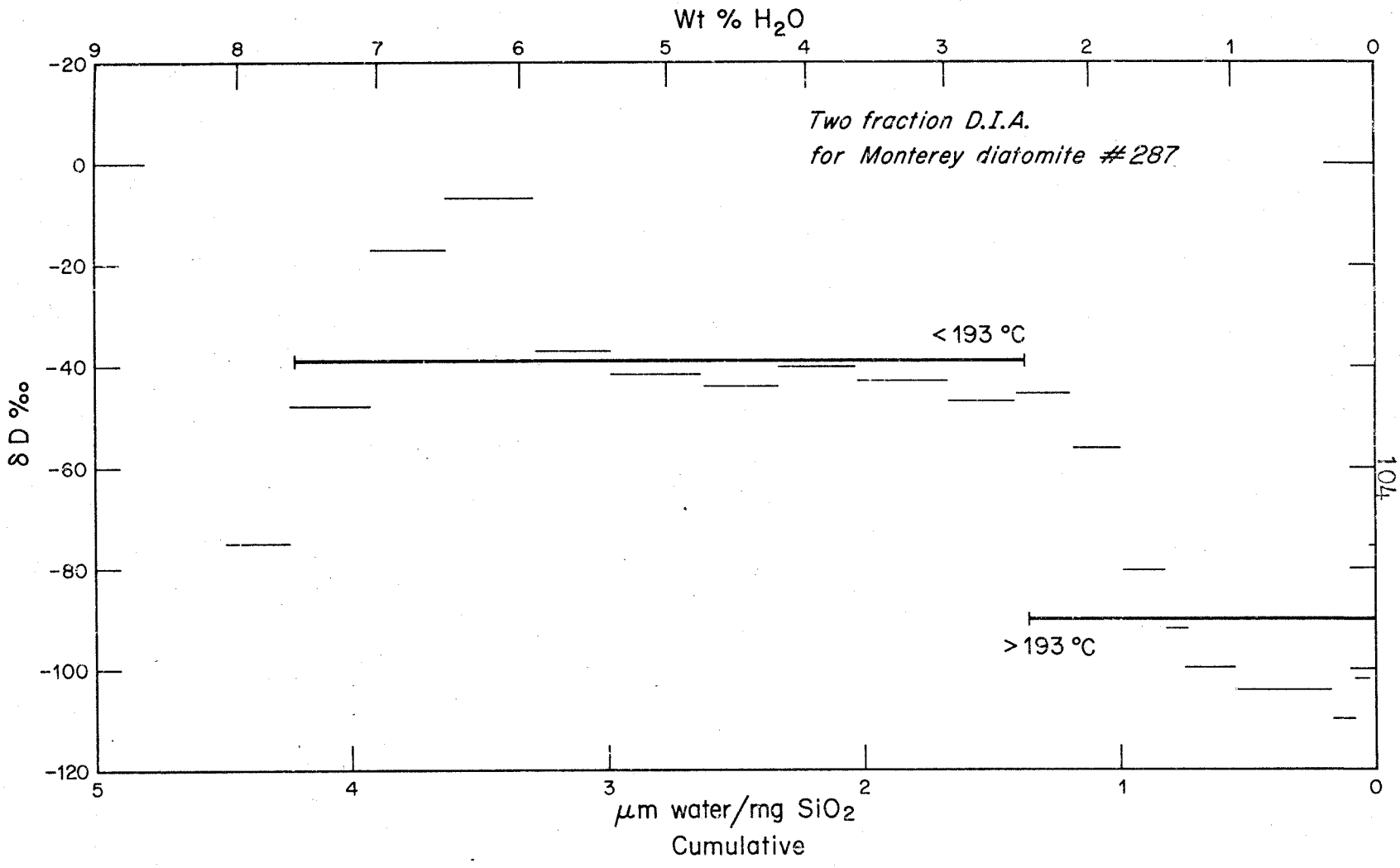
Wt % H_2O
9
8
7
6
5
4
3
2
1
0
-20
0
-20
-40
-60
-80
-100
-120
δ D ‰
Two fraction D.I.A.
for Monterey diatomite #287
< 193 °C
> 193 °C
5
4
3
2
1
0
μm water/mg SiO_2
Cumulative

Figure 5-3

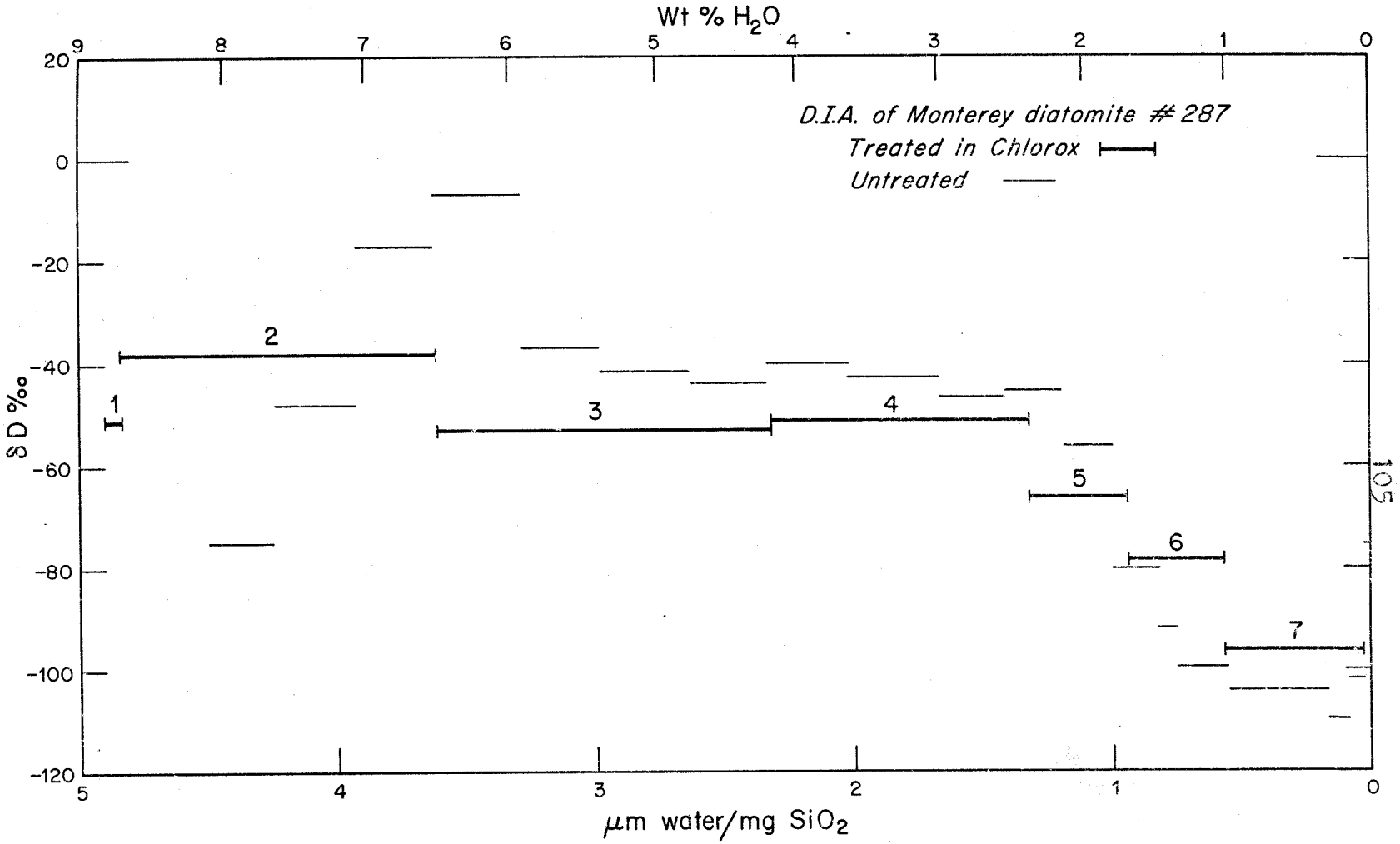
Wt % H_2O
9
8
7
6
5
4
3
2
1
0
20
0
-20
-40
-60
-80
-100
-120
δD ‰
D.I.A. of Monterey diatomite #287
Treated in Chlorox
Untreated
1
2
3
4
5
6
7
5
4
3
2
1
0
μm water/mg SiO_2
Cumulative
105

Figure 5-4

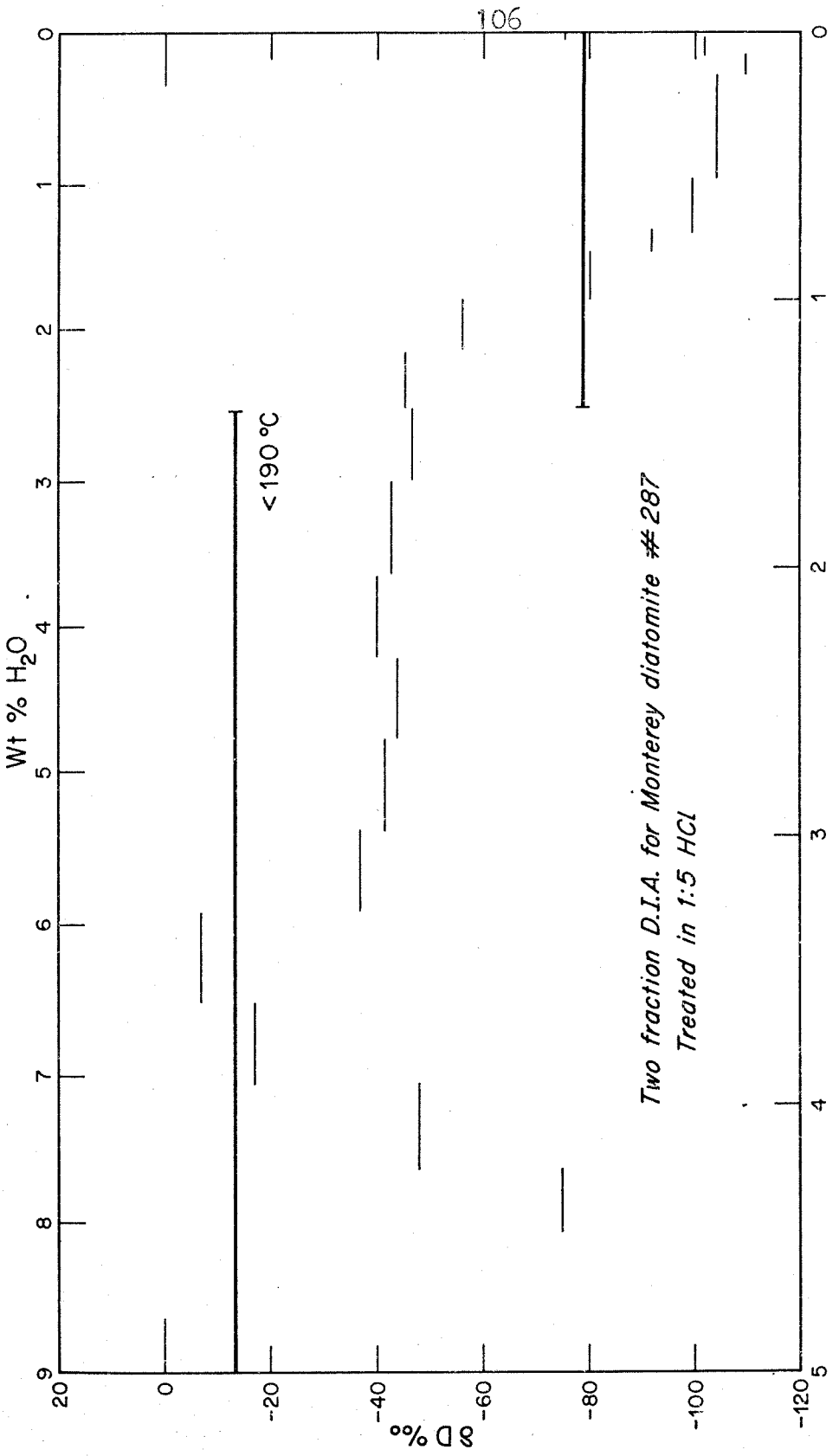
Wt % H_2O
δD ‰
μm water/mg SiO_2
Cumulative
<190 °C
Two fraction D.I.A. for Monterey diatomite #287
Treated in 1:5 HCl

Figure 5-5

exchanges, while the water liberated above 200°C does not.

From these experiments it is not certain if the reagent or the repeated rinsings are responsible for the exchange. The data strongly indicate, however, that much of the water liberated below 200° C has little ability to resist exchange. The necessity of doing exchange experiments with water of known isotopic composition was therefore clearly indicated. These are discussed in the following section.

B. Low temperature exchange experiments on Monterey diatomite. Water in silica which exchanges at room temperature is isotopically of no geologic interest since D/H measurements of this water merely reflect the D/H ratio of the laboratory air, treatment solutions, or the last rainfall on the outcrop. Water in silica which does not exchange at room temperature may also be of little geologic interest if it exchanges at higher temperatures or over long periods of geologic time at lower temperatures.

B-1. Procedure. Approximately .5 gram of sample was placed in a vessel of the type shown in figure 5-6. 5 cc of water of $\delta D = +1715‰$ was introduced into the vessel, representing a 120-fold excess over the amount of H_2O in the sample. A cap with a stopcock and vacuum join was placed on the vessel. The sample was allowed to exchange overnight at room temperature with the D-enriched water. The exchanged sample could not be dried in the air since this

Figure 5-6

VESSEL FOR 25°C EXCHANGE EXPERIMENTS

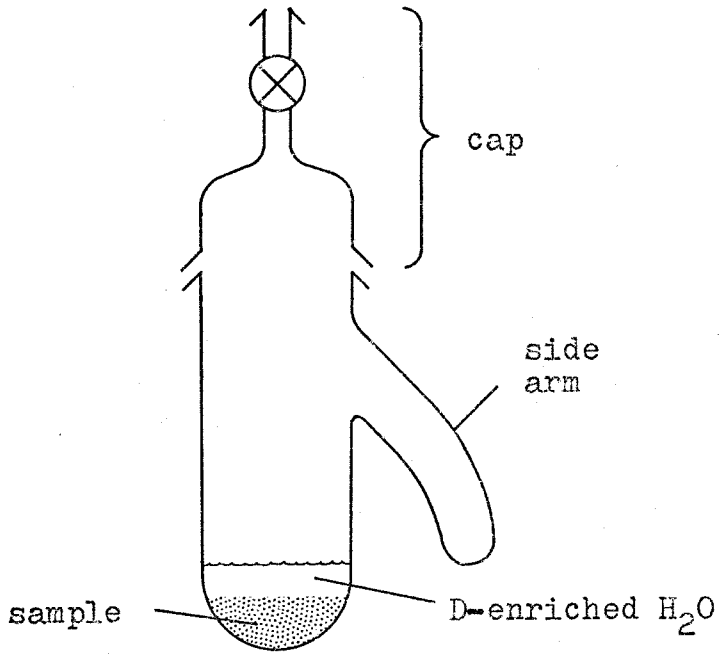

would result in back-exchange of the sample with water vapor in the air. Consequently, the water and sample were frozen with LN_2, the vessel placed on a vacuum line, and the vessel evacuated. The LN_2 cold trap was then transferred to the side arm. As the frozen sample and water warmed up, the water distilled into the side arm until dry. The cap was then removed and the sample quickly dumped into a quartz boat and placed in the water extraction apparatus of figure 4-3. In this procedure, the sample was exposed to atmospheric H_2O for only one or two minutes. A D.I.A., as described on page 102, was then performed.

B-2. Results. The results of the D.I.A. are indicated in table 5-2 and are shown in figure 5-7 together with the D.I.A. for the unexchanged sample. Because the

Table 5-2

DIFFERENTIAL ISOTOPIC ANALYSIS FOR MONTEREY DIATOMITE EXCHANGED AT ROOM TEMPERATURE WITH DEUTERIUM-ENRICHED WATER (+1715‰)

Fraction	Temperature Interval	Time Interval	Yield μm/mg	δD_{SMOW}‰
1	26°C	1^h40^m	.099	1808
2	26-66	22^h50^m	.915	1299
3	66-114	1^h15^m	.599	520
4	114-154	1^h55^m	1.212	98.8
5	154-218	50^m	.273	34.1
6	218-311	1^h40^m	.300	40.4
7	311-574	3^h15^m	.717	32.5
8	574-1000	3^h50^m	.261	0.9

water used for the exchange was very deuterium-enriched, the scale of the ordinate in figure 5-7 is greatly expanded. The results clearly show that water released from the silica at the lower temperatures has suffered the most exchange. It is clear, however, that water outgassed over the whole temperature range has been exchanged to some extent.

The isotopic enrichments of subsequent samples in the stepwise dehydration are here much too large to be due to isotopic fractionation associated with equilibrium or kinetic isotope effects resulting from vapor-hydrate or

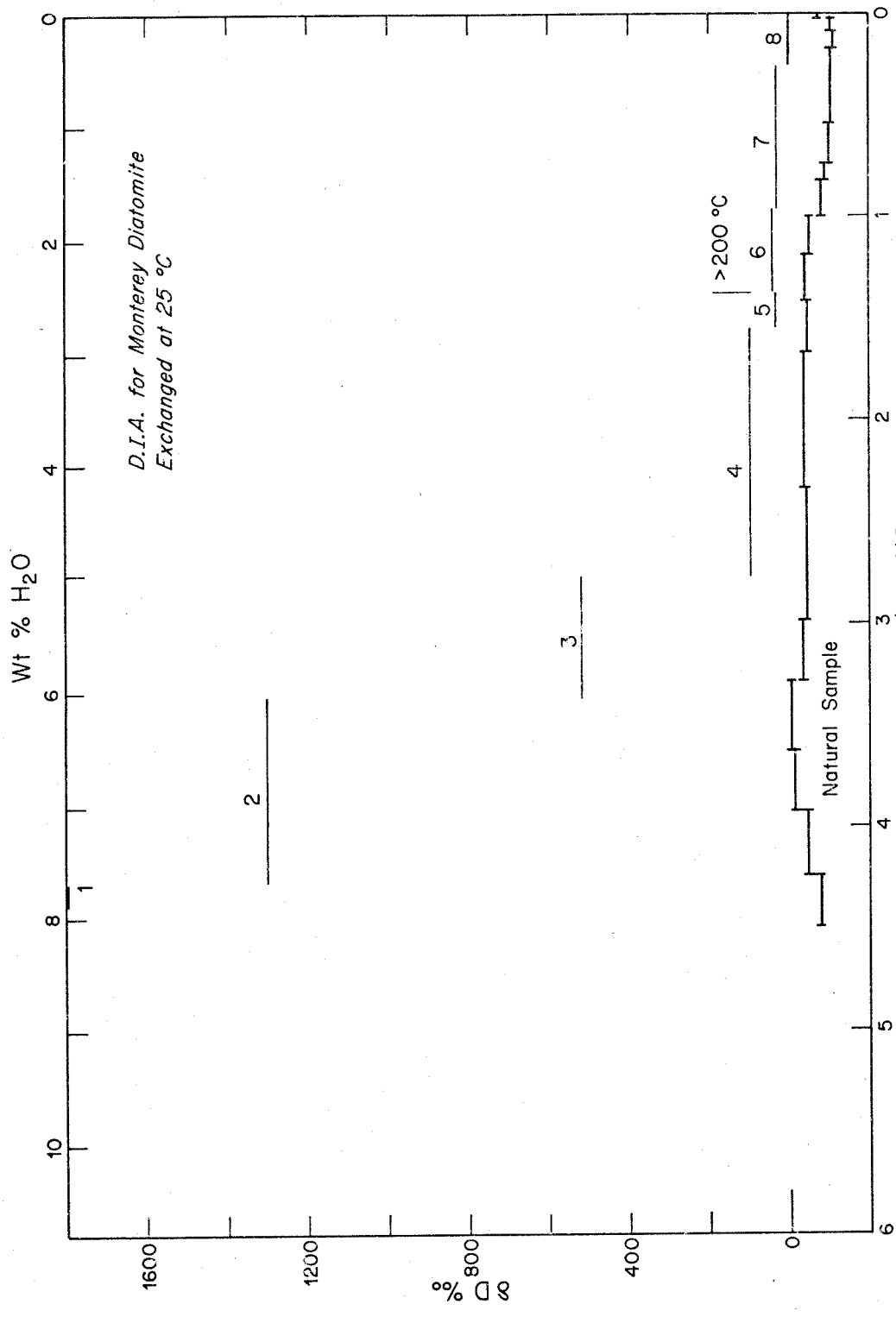
D.I.A. for Monterey Diatomite
Exchanged at 25 °C
Wt % H_2O
δD ‰
μm water/mg SiO_2
Cumulative
Natural Sample
>200 °C
1
2
3
4
5
6
7
8

Figure 5-7

vapor-hydroxyl fractionations. Maximum possible fractionations associated with these or analogous processes are probably on the order of those observed in the case of Raleigh distillation of water, about 200 to 300 per mil (Epstein, 1959). The isotopic variations of figure 5-7 must therefore be due to mixing of waters which have or have not exchanged to various degrees. In other words, the heavy δD for a given fraction cannot be due to fractionation associated with dehydrations, but must represent a mixture of water derived from sites which have exchanged and sites which have not exchanged.

The relative amount of exchanged and unexchanged water for a given fraction can be calculated from the following equation which is valid for obtaining the combined δ-value of any two waters or gases of known isotopic composition which are mixed together.

$$(5\text{-}1) \qquad \delta_t = X_1 \delta_1 + (1 - X_1) \delta_2$$

where δ_1 = δ-value of water #1

δ_2 = δ-value of water #2

δ_t = combined δ-value

X_1 = mole fraction of water #1

X_2 = mole fraction of water #2

The difference in exchangeability of these two waters may result because they are in different sites, different hydration states (OH or bonded H_2O), or exchange at different rates due to their structural positions. The important fact is that some of the water exchanges rapidly and the relative amount can be determined from equation 5-1.

The actual amounts of exchanged and non-exchanged water in a given fraction can be calculated using the relative amounts (X_1, $1 - X_1$) and the actual water yield of the fraction. The results of this calculation performed for all the fractions are given in table 5-3 and plotted as a histogram in figure 5-8.

The shape of a histogram depends greatly upon the temperature intervals chosen, and can give a misleading view of the water release as a function of temperature. For example, in figure 5-8, careless examination of the shape of the upper histogram might suggest that most of the "non-exchangeable" water in diatomite is outgassed above 300°C where, in fact, this is not true. A more convenient graphic representation of these data is obtained by plotting the first derivative of the cumulative curve for the experimental data. The area under the resulting curve is equal to the amount of water outgassed over the temperature range given.

The cumulative curve for the two "sites" (exchangeable and non-exchangeable) is plotted in figure 5-9. The first derivative for this curve was obtained by constructing tangents at 50°C intervals. The results are plotted in figure 5-10.

The maxima and minima of figure 5-10 undoubtedly shift to slightly higher and lower temperatures depending on the rate of heating. For example, the peak of curve II at 150°C

Table 5-3

VALUES USED FOR CALCULATIONS OF ACTUAL AMOUNT OF EXCHANGED AND NON-EXCHANGED WATER FOR EACH FRACTION IN D.I.A. OF TABLE 5-2, AND RESULTS OF THE CALCULATION

Fraction	Temperature	δ_t ‰	δ_1 ‰	δ_2 ‰	X_1	$X_1(\frac{\mu m}{mg})$ m/mg	$(1-X_1)$	$(1-X_1)\frac{\mu m}{mg}$ m/mg
1	26°C	1808	1715	--	1.0	.099	--	0
2	26-66	1299	1715	- 20	.76	.70	.24	.22
3	66-114	520	1715	- 30	.32	.19	.68	.41
4	114-154	99	1715	- 40	.08	.10	.92	1.12
5	154-218	34	1715	- 45	.04	.01	.96	.26
6	218-311	40	1715	- 50	.05	.02	.95	.29
7	311-574	33	1715	- 85	.07	.05	.93	.67
8	574-1000	0	1715	-105	.06	.02	.94	.25

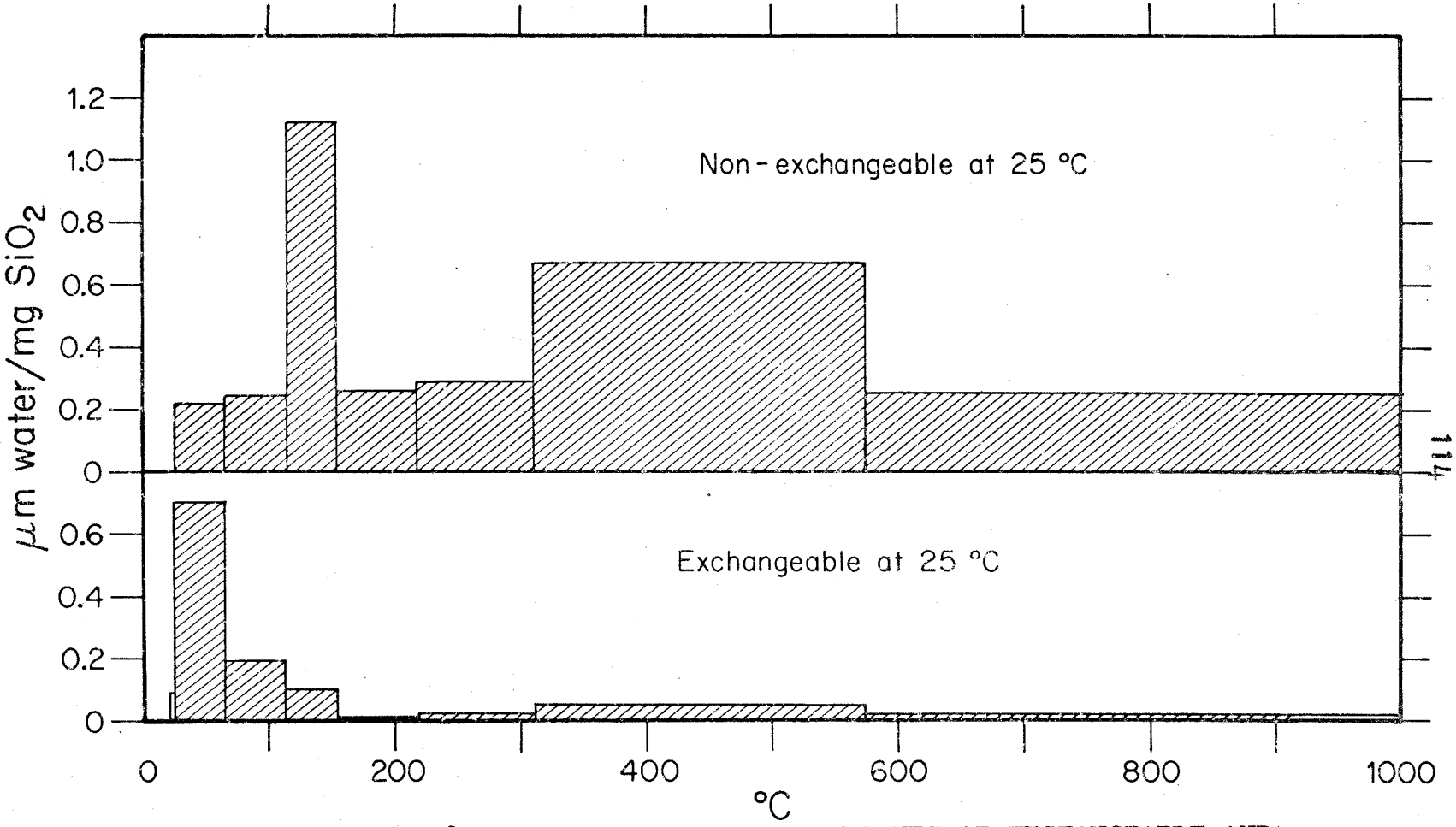

Figure 5-8: HISTOGRAMS SHOWING AMOUNTS OF EXCHANGEABLE AND NON-EXCHANGEABLE WATER RELEASED AT SUCCESSIVELY HIGHER TEMPERATURES FOR MONTEREY DIATOMITE EXCHANGED OVERNIGHT WITH D-ENRICHED WATER AT 25°C

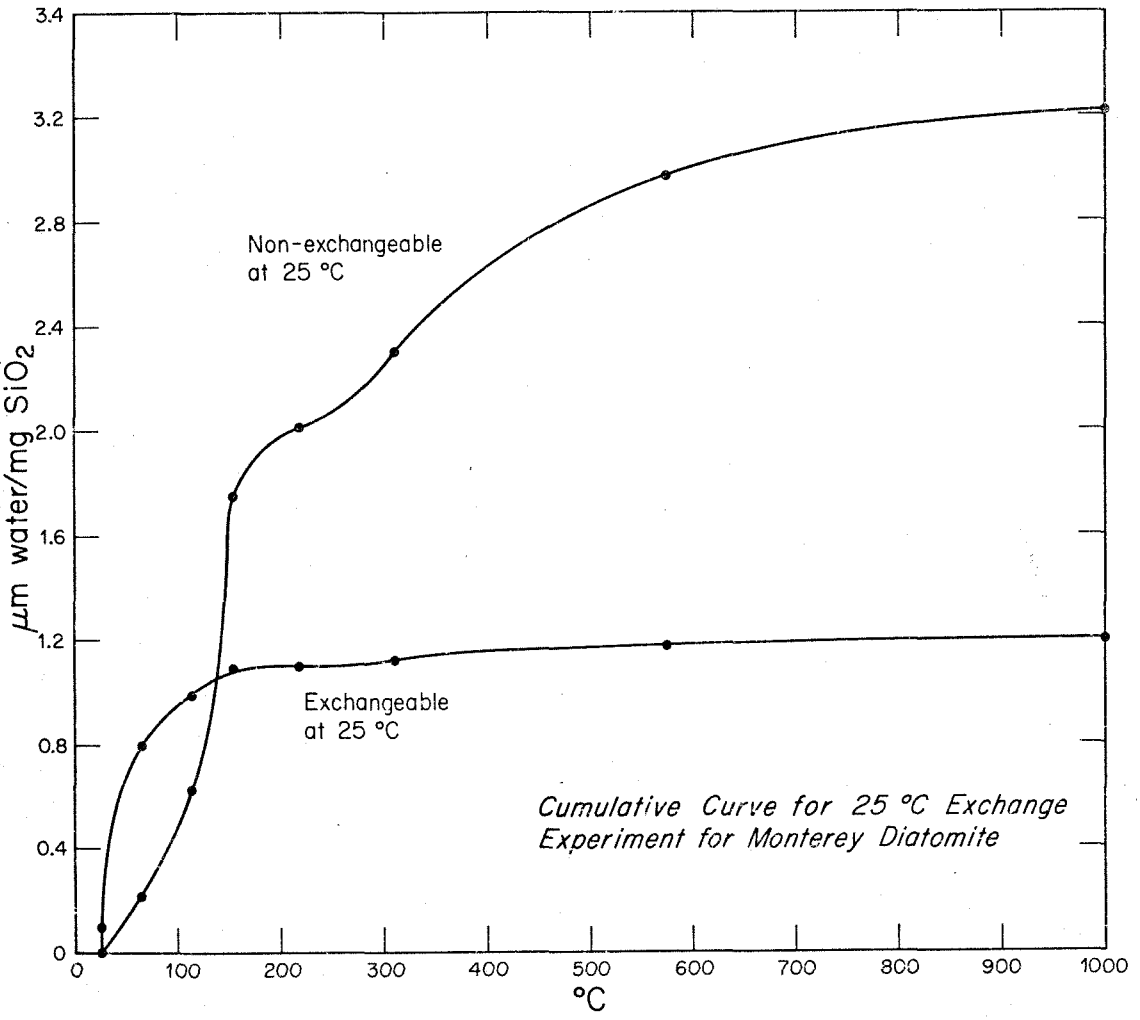

Figure 5-9

CUMULATIVE CURVES FOR μm/mg OF EXCHANGEABLE AND NON-EXCHANGEABLE WATER RELEASED AT SUCCESSIVELY HIGHER TEMPERATURES FOR MONTEREY DIATOMITE EXCHANGED OVERNIGHT WITH D-ENRICHED WATER AT 25°C

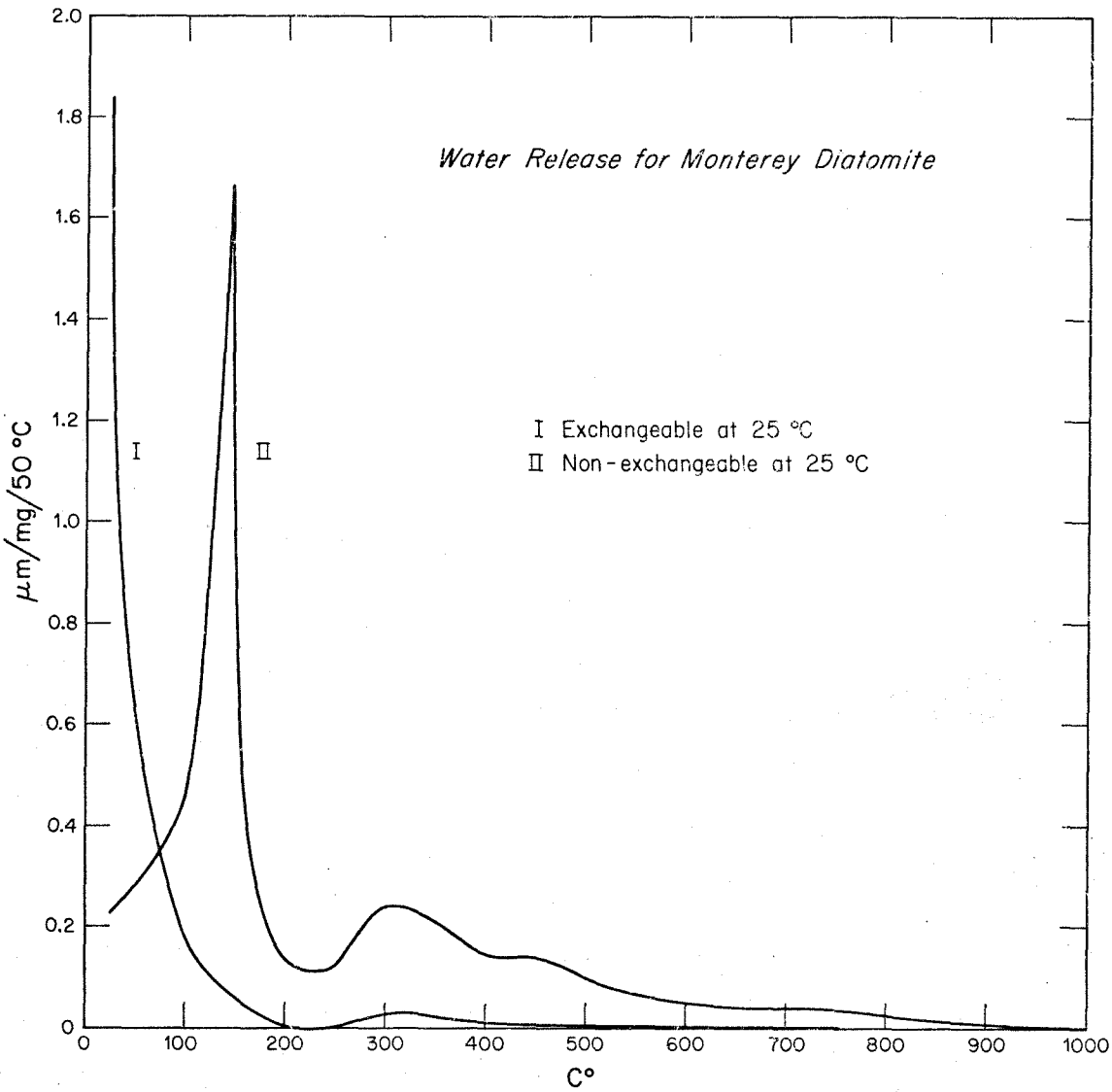

Figure 5-10

WATER RELEASE FOR MONTEREY DIATOMITE.
AREA UNDER CURVE EQUALS AMOUNT OF
WATER RELEASED BETWEEN 25° AND 1000°C.

could probably be shifted to 50°C or less if the sample were left at a low temperature for an extremely long time. This was, in fact, observed in experiments to be discussed later. The qualitative relationship between temperature and dehydration pattern, however, is clear and suggests that the room-temperature exchangeable fraction is almost entirely removed in vacuum below 200°C. This readily removed water is probably very loosely bound or mechanically trapped H_2O. The small rise in curve I appearing at around 300°C may be due to easily exchangeable hydroxyls or may be more tightly bound H_2O or OH which formed during heating and before all the H_2O had been removed. The two peaks of curve II, the non-exchangeable fraction, suggest a loosely bound H_2O component which can be removed below 200°C and a more tightly bound water removable at higher temperatures, probably in the form of hydroxyl groups.

B-3. Conclusions regarding the room temperature exchange experiments. The results of the experiment described above suggest that there is no one temperature at which the exchangeable fraction can be completely separated from the non-exchangeable fraction by the D.I.A. method. However, extensive pumping under vacuum or heating to about 75°C removes most of the easily exchangeable water. The combined δ-value of the remaining water may be considered to be geologically meaningful. Its δD-value is independent

of any water exposed to the sample during collection, storage, or analysis. Whether this water retains its δ-value during prolonged exposure to ground waters or higher temperatures is a question that must be decided from the natural data or deduced from the exchange experiments described below.

Reference to figures 5-4 and 5-5 suggests that some exchange of the water fraction released below 200°C in curve II of figure 5-10 has been due to the chlorox and acid treatments. In this connection, Lewin (1961) has observed that the rate of dissolution of diatomaceous silica is enhanced after acid treatments, suggesting that certain cations may normally be adsorbed on the silica surface (accounting for the low solubility rate of silica in sea water). The enhanced exchange capability after acid treatments may be similarly due to removal of any such protecting cations.

C. 100°C exchange experiments on Monterey diatomite. The effect of temperature on the exchangeability of hydrogen isotopes in water contained in Monterey diatomite was studied in a series of exchange experiments at 100°C. The primary purpose of these experiments was to determine how much of the water which does not exchange at room temperature (curve II of figure 5-10) would do so at 100°C.

C-1. Procedure. .5 to 1.5 grams of diatomite were placed in glass bulbs along with 8 to 13 ml of heavy water ($\delta D = +1715‰$). The glass bulbs, shown in figure 5-11,

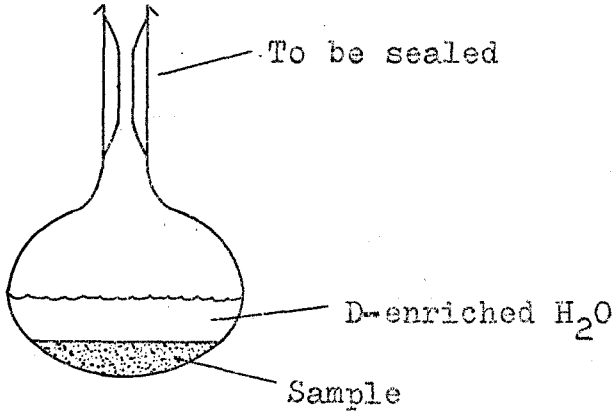

Figure 5-11

GLASS BULBS FOR 100°C EXCHANGE EXPERIMENTS

were connected to a high vacuum line, the water-sample mixture was frozen with LN_2, and the remaining air was pumped out. The neck on each glass bulb was then sealed off. The bulbs were then placed in a boiling water bath and allowed to exchange for the desired interval of time. The experiment for each sample was terminated by removing the bulb from the 100°C bath and by breaking off the neck of the bulb. The contents of the bulb were then removed and the sample was dried in various ways to be described. A D.I.A. was then performed on the dry sample.

C-2. Results. Data for the D.I.A. for each experiment are presented in tables 5-4, 5-5, 5-6, 5-7, and

Table 5-4

DIFFERENTIAL ISOTOPIC ANALYSIS FOR MONTEREY DIATOMITE EXCHANGED 4,252 HOURS AT 100°C
(Curve B in figure 5-12)

Fraction	Temperature	Time Interval	Yield μm/mg	δD_{SMOW}‰
1	24°C	28^h25^m	.34	1714.9
2	24-119	7^h20^m	1.92	1731.9
3	119°	112^h35^m	.61	1671
4	119-181	22^h50^m	.13	1624
5	181-248	51^h35^m	.20	---
6	248-314	17^h15^m	.15	1013
7	314-536	18^h0^m	.67	999.9
8	536-742	17^h15^m	.21	933.9
9	742-1000	3^h0^m	.03	584.6

Table 5-5

D.I.A. FOR MONTEREY DIATOMITE EXCHANGED 700 HOURS AT 100°C, AIR DRIED
(Curve C in figure 5-12)

Fraction	Temperature	Time Interval	Yield μm/mg	δD_{SMOW}‰
1	25-95°C	37^m	1.88	474.6
2	95-211	1^h30^m	2.32	1516.7
3	211-316	43^m	.33	1157.2
4	316-445	50^m	.36	738.1
5	445-643	1^h20^m	.49	810.9
6	643-776	2^h01^m	.17	875.5
7	776-1022	2^h49^m	.06	700.0

Table 5-6

D.I.A. FOR MONTEREY DIATOMITE EXCHANGED 328.5 HOURS AT 100°C, AIR DRIED 240 HOURS
(Curve D in figure 5-12)

Fraction	Temperature	Time Interval	Yield μm/mg	δD_{SMOW}‰
1	22-63°C	1^h23^m	1.01	218.3
2	63-127	2^h26^m	1.35	569.1
3	127-135	20^m	.16	---
4	135-143	38^m	.56	1234.4
5	143-163	34^m	.31	1408.1
6	163-178	26^m	.22	1418.8
7	178-192	54^m	.15	---
8	192-223	45^m	.16	1168.2
9	223-322	41^m	.29	940.9
10	322-492	1^h48^m	.48	631.7
11	492-678	3^h55^m	.39	683.5
12	678-777	1^h08^m	.09	717.6
13	777-902	1^h57^m	.04	592.2
14	902-981	3^h0^m	.02	592.9

Table 5-7

D.I.A. FOR MONTEREY DIATOMITE EXCHANGED 333 HOURS AT 100°C, AIR DRIED IN OVEN AT 100°C
(Curve E in figure 5-12)

Fraction	Temperature	Time Interval	Yield μm/mg	δD_{SMOW}‰
1	23-102°C	16^h0^m	.658	95.9
2	102-159	4^h0^m	.242	926.2
3	159-198	3^h50^m	.197	1073.7
4	198-283	3^h33^m	.197	794.9
5	283-418	1^h42^m	.337	448.3
6	418-496	12^h0^m	.378	450.4
7	496-790	4^h20^m	.356	530.5
8	790-1060	3^h32^m	.041	488.0

are plotted graphically in figure 5-12. The D.I.A. data for untreated diatomite already presented in table 5-1 and figure 5-2 are shown again as curve A for reference in figure 5-12. δD variations for this D.I.A. are small in comparison to the large deuterium enrichments in the samples experimentally exchanged at 100°C. The data for curve B can be used together with the results of the preceding sections to propose a model for the hydration states in diatomite. The model should then explain the results represented by curves C, D, and E.

C-2a. Curve B. The D.I.A. pattern represented as curve B is the one obtained for diatomite exchanged for

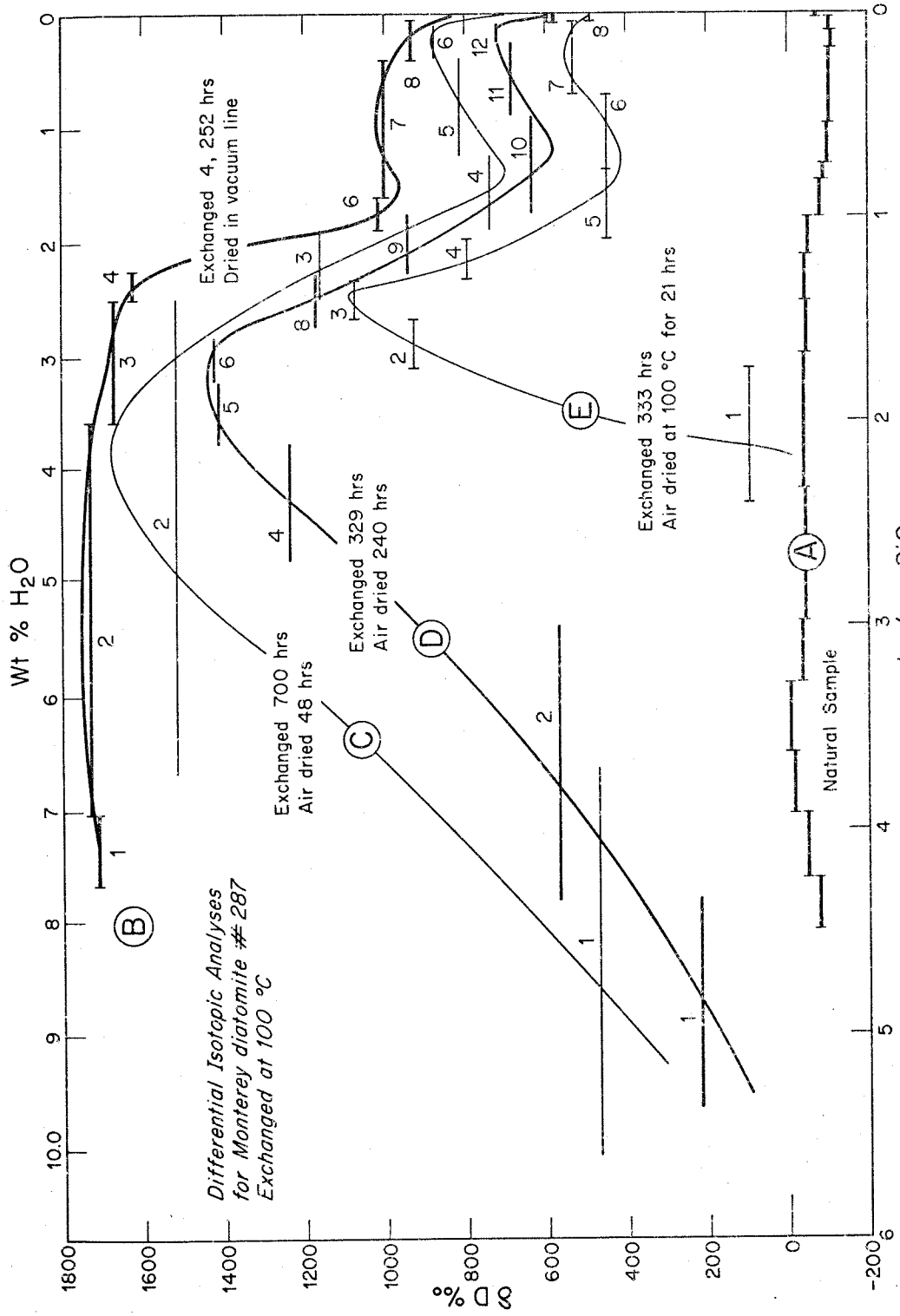
Wt % H_2O
μm water/mg SiO_2
Cumulative
δD ‰
Differential Isotopic Analyses
for Monterey diatomite #287
Exchanged at 100 °C
Exchanged 4, 252 hrs
Dried in vacuum line
Exchanged 700 hrs
Air dried 48 hrs
Exchanged 329 hrs
Air dried 240 hrs
Exchanged 333 hrs
Air dried at 100 °C for 21 hrs
Natural Sample
A
B
C
D
E

Figure 5-12

4,252 hours. For this experiment an attempt was made to prevent exposure of the exchanged sample to laboratory air during drying. The previous procedure for drying the sample was used (section 5.2-B), except that the sample was not dried to completion in the vessel with the side-arm (figure 5-6). The still-wet sample was removed and inserted into the vacuum line furnace (figure 4-3). Further drying of the sample was accomplished by extremely slow pumping. Unfortunately, this procedure allows a considerable vapor pressure of deuterium-enriched water to develop in the vacuum line. It will be shown in section 5.3-A-4 that this causes considerable hydration of the glass walls and vacuum grease with heavy water which subsequently exchanges with the "unexchanged" water outgassed from the diatomite at higher temperatures. In other words, a very considerable isotopic "memory effect" is introduced by this drying procedure, and this effect causes the subsequent fractions of the D.I.A. to be more enriched in deuterium than the actual water outgassed from the sample. The result is that the data shown for each fraction of curve B are undoubtedly somewhat heavier than the true δ-values. Curve B, therefore, represents maximum isotopic exchange under the conditions described. The true D.I.A. pattern is either coincident with curve B or falls below it by some unknown amount. In spite of this error introduced into the experiment, it is readily apparent that

waters outgassed at temperatures above 200°C have exchanged to only a small degree with the heavy water, even after 4,252 hours at 100°C. The relative amount of exchanged and unexchanged water for a given fraction can be calculated using equation 5-2, assuming that the δ-value of the cut represents a mixture of heavy water (δ D = +1715‰) and unexchanged water with a δD-value given by curve A. This calculation performed for all the cuts is given in table 5-8 and the results plotted as a histogram in figure 5-13. The cumulative curve is shown in figure 5-14 and the derived water-release pattern is shown in figure 5-15.

Figure 5-15 shows that nearly all of the more "loosely-bound" water released below 200°C is exchangeable at 100°C. About 70% of the water released above 200°C is unexchanged. Comparison of these data with the exchange experiment at 25°C (figure 5-10) shows that the total water yield is somewhat less in the case of the sample exchanged at 100°C. Approximately 16% less water was released above 200°C for the sample exchanged at 100°C. Water released below 200°C is the same to within 2% for the two experiments. This result suggests that heating for 6 months in boiling water alters the character of the diatomite with regard to the amount of water located in the more strongly bonded sites. The effect is to reduce the amount of water that is held by biogenic silica at room temperature.

Table 5-8

VALUES USED FOR CALCULATION OF ACTUAL AMOUNT OF EXCHANGED AND NON-EXCHANGED WATER FOR EACH FRACTION IN D.I.A. OF TABLE 5-4, AND RESULTS OF THE CALCULATION

Fraction	Temperature	δ_t ‰	δ_1 ‰	δ_2 ‰	X_1	$X_1(\frac{\mu m}{mg})$	$(1-X_1)$	$(1-X_1)\frac{\mu m}{mg}$
1	24°C	1715				.34		
2	24-119	1715				1.92		
3	119°	1671	1715	- 40	.97	.59	.03	.02
4	119-181	1624	1715	- 45	.95	.12	.05	.01
5	181-248	missing, estimate from figure 5-12				.06		(.03)
6	248-314	1013	1715	- 60	.60	.09	.40	.06
7	314-536	1000	1715	-100	.61	.41	.39	.26
8	536-742	934	1715	-100	.57	.12	.43	.09
9	742-1000	585	1715	-100	.38	.01	.62	.02

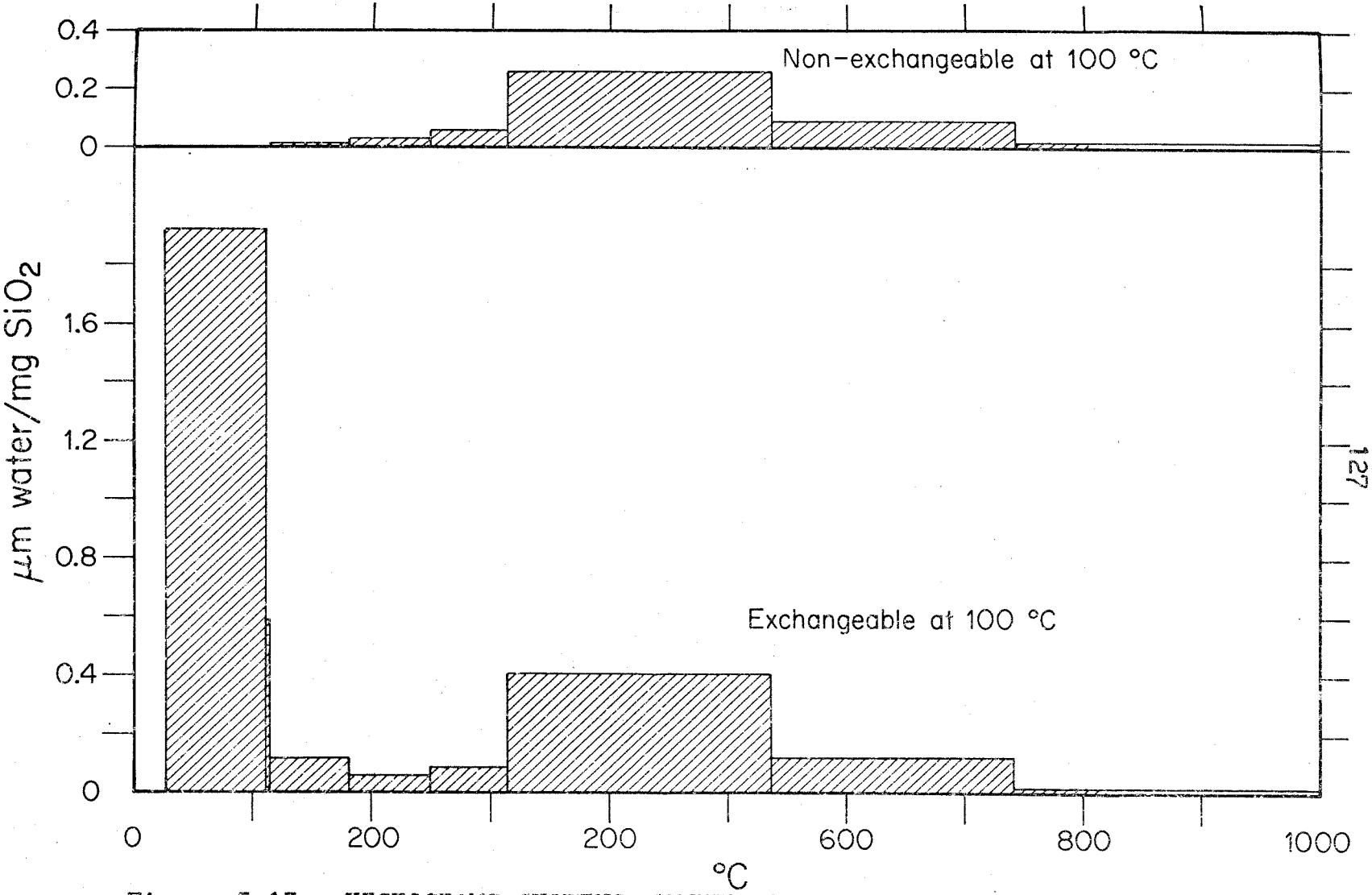

Figure 5-13: HISTOGRAMS SHOWING AMOUNTS OF EXCHANGEABLE AND NON-EXCHANGEABLE WATER RELEASED AT SUCCESSIVELY HIGHER TEMPERATURES FOR MONTEREY DIATOMITE EXCHANGED 4,252 HOURS WITH D-ENRICHED WATER AT 100°C

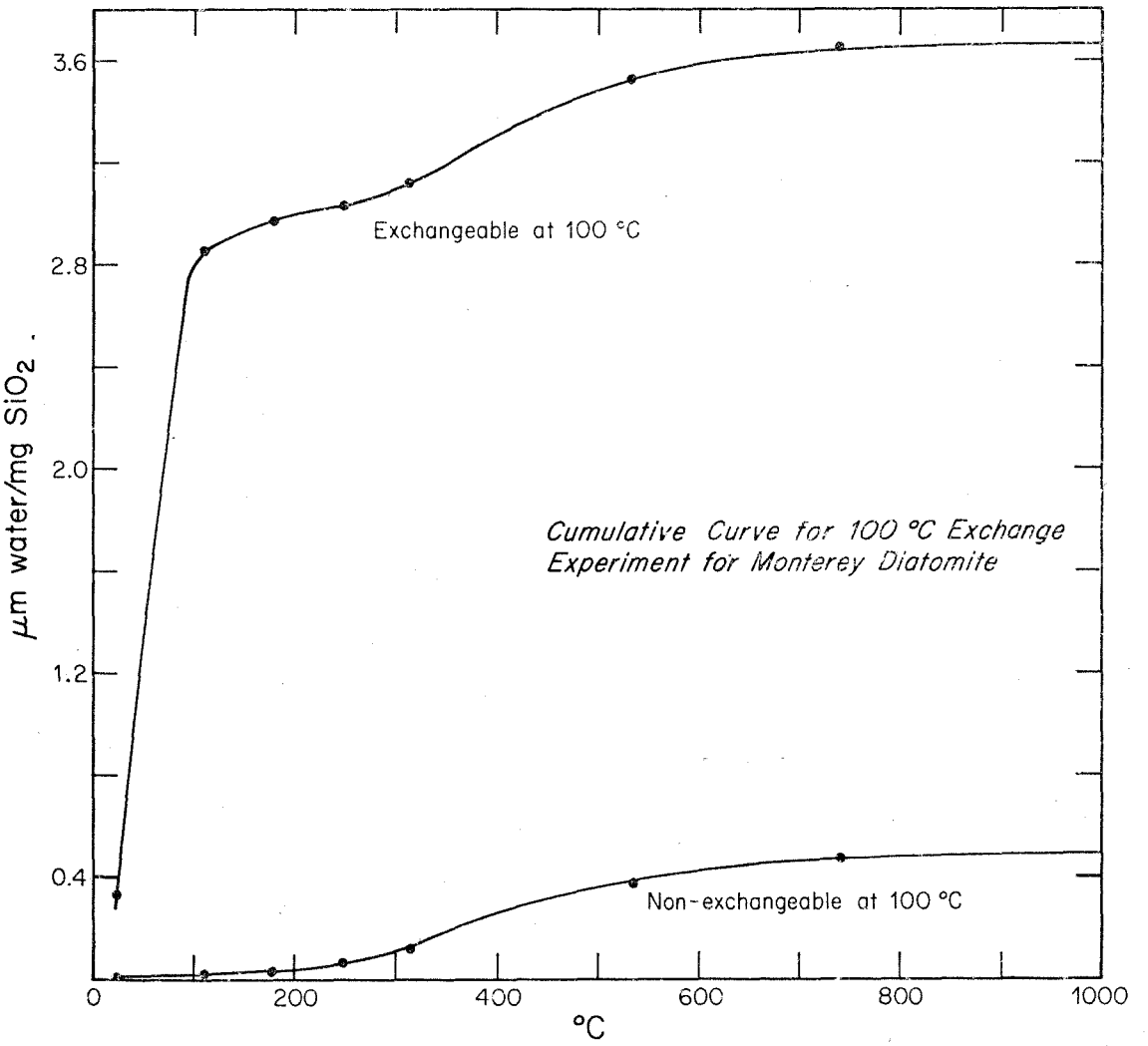

Figure 5-14

CUMULATIVE CURVES FOR μm/mg OF EXCHANGEABLE AND NON-EXCHANGEABLE WATER RELEASED AT SUCCESSIVELY HIGHER TEMPERATURES FOR MONTEREY DIATOMITE EXCHANGED 4,252 HOURS WITH D-ENRICHED WATER AT 100°C

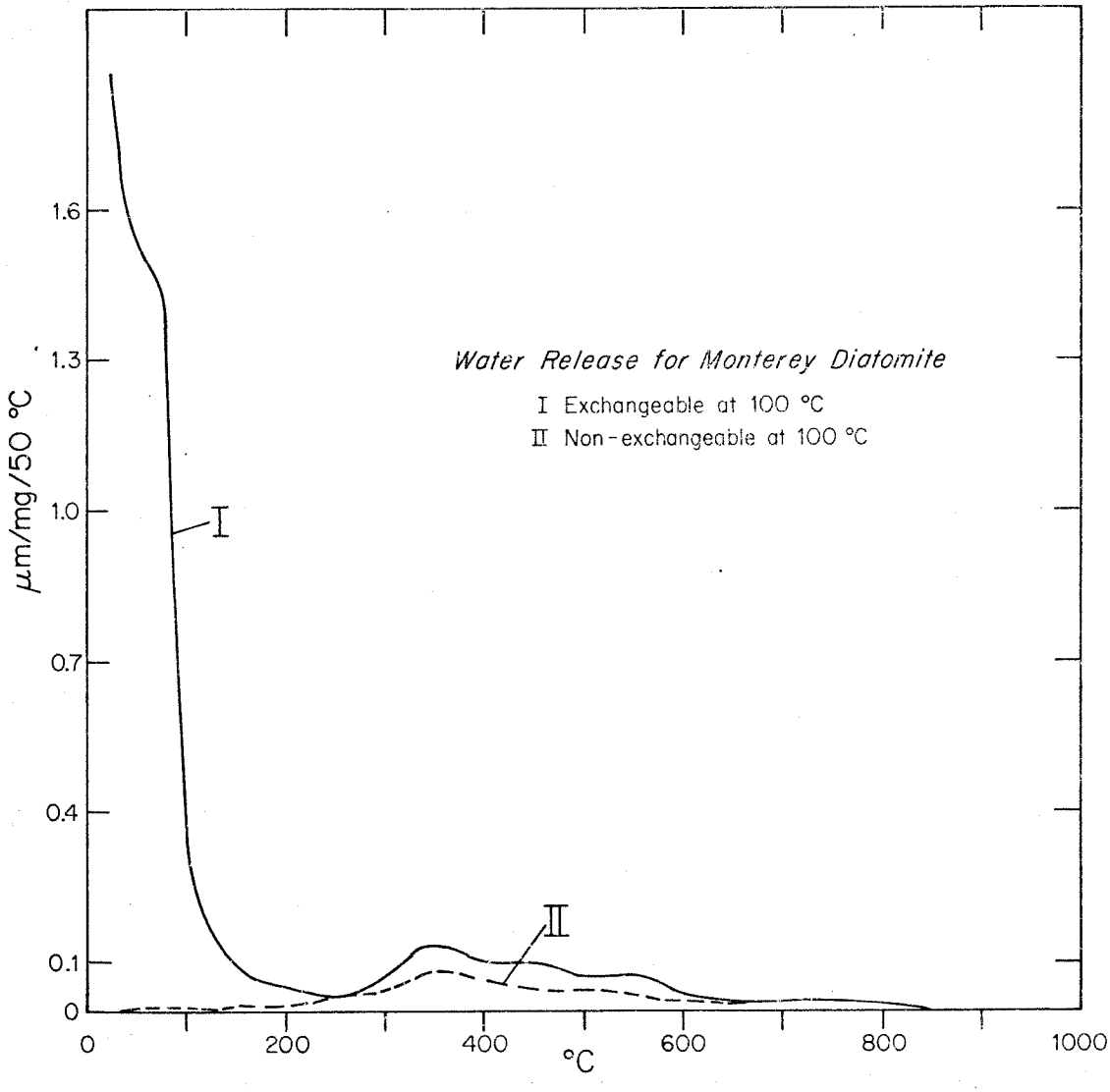

Figure 5-15

WATER RELEASE FOR MONTEREY DIATOMITE.
AREA UNDER CURVE EQUALS AMOUNT OF
WATER RELEASED BETWEEN 25° AND 1000°C.

The curve representing the exchangeable water component of figure 5-15 (curve I) is the sum of the curve representing water which exchanges at 25°C (curve I, figure 5-10) and the curve representing water which exchanges at 100°C. The curve representing water which exchanges at 25°C can be subtracted from curve I of figure 5-15 to produce a representation of the water release from the site or sites which are exchangeable at 100°C but not at 25°C. This has been done to give the curves shown in figure 5-16. The integral of each curve equals an amount of water (in μm/mg) with the designated exchange characteristics.

An alternative method for deriving these curves can be obtained by using curve II of figure 5-10. This curve, representing the amount of non-exchangeable water at 25°C, is the sum of the curve for water which will exchange at 100°C and the curve for water which will not exchange at 100°C. The 100°C non-exchangeable fraction is known from figure 5-15 (curve II), and can be subtracted from curve II of figure 5-10 to yield the 100° exchangeable fraction. The result of this subtraction is shown in figure 5-17.

The curves for the 100°C exchangeable fraction as derived by these two independent methods have somewhat different characteristics. The following differences are significant.

(1) The low temperature water release peak

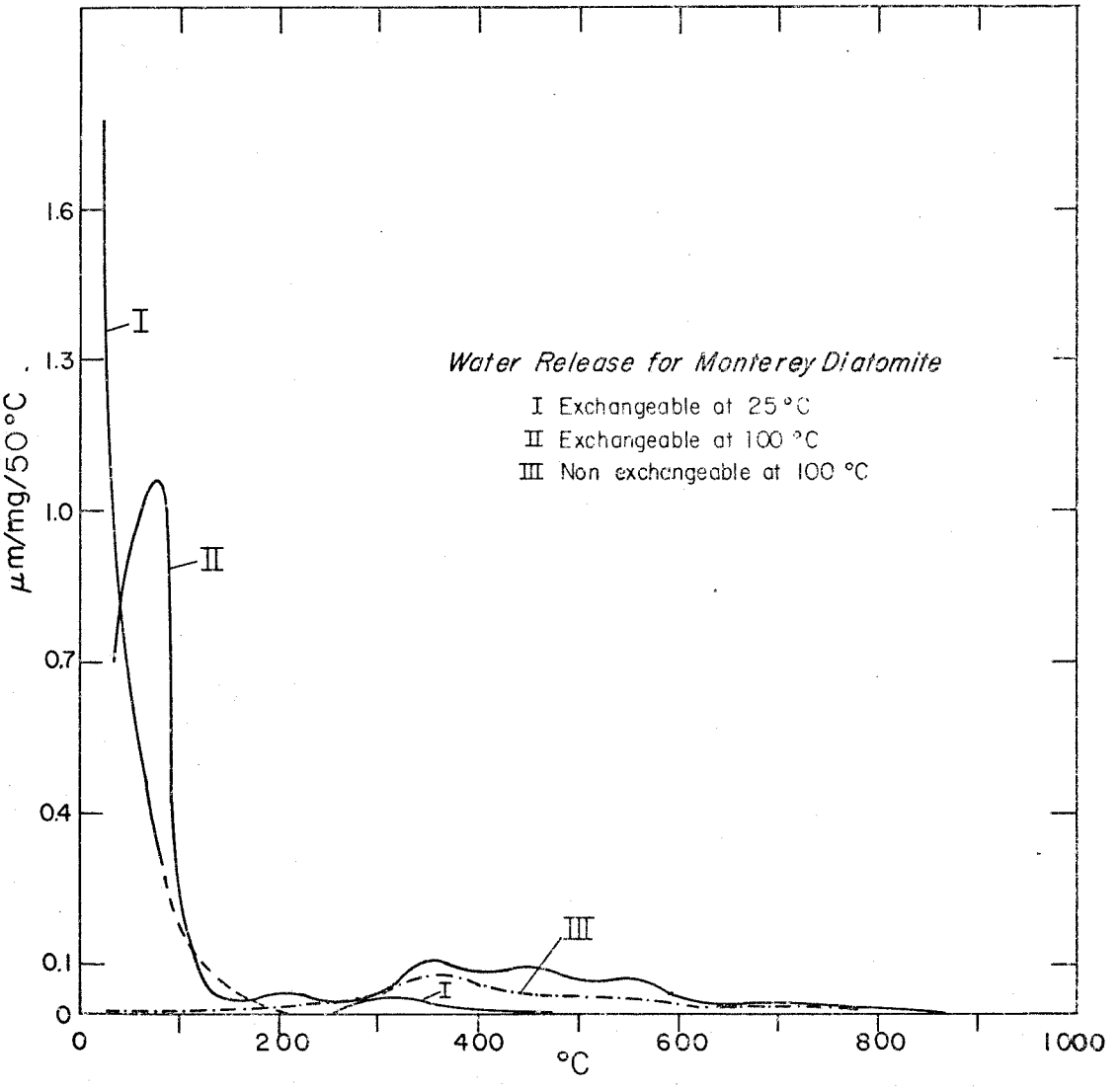

Figure 5-16

WATER RELEASE FOR MONTEREY DIATOMITE.
AREA UNDER CURVE EQUALS AMOUNT OF
WATER RELEASED BETWEEN 25° AND 1000°C.

CURVE II DERIVED BY SUBTRACTING CURVE I OF
FIGURE 5-10 FROM CURVE I OF FIGURE 5-15

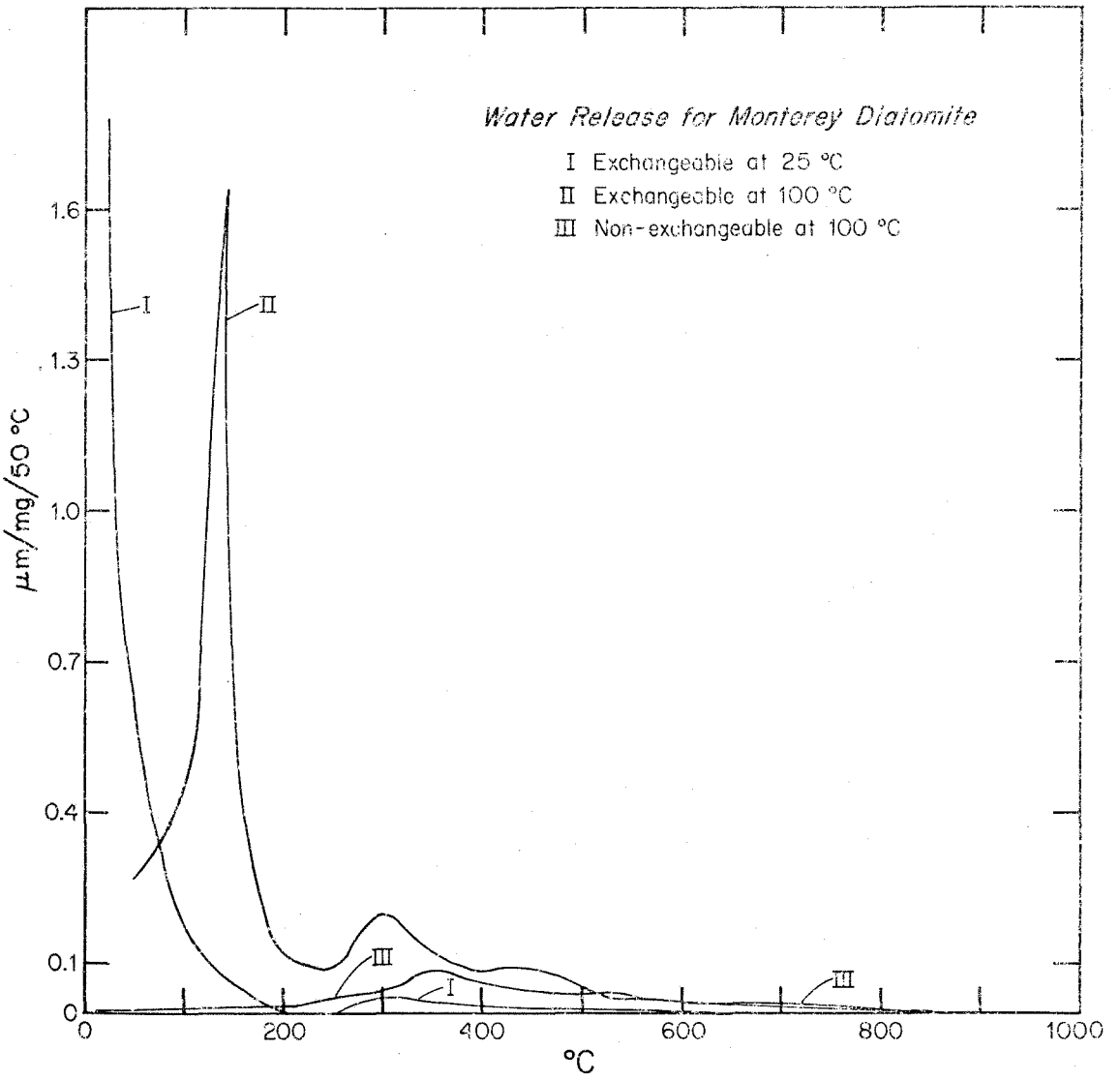

Figure 5-17

WATER RELEASE FOR MONTEREY DIATOMITE.
AREA UNDER CURVE EQUALS AMOUNT OF
WATER RELEASED BETWEEN 25° AND 1000°C.

CURVE II DERIVED BY SUBTRACTING CURVE II OF
FIGURE 5-15 FROM CURVE II OF FIGURE 5-10

occurs in figure 5-16 at about 75°C, while in figure 5-17 it is sharply defined at approximately 150°C. This difference is probably due to differences in the rates of dehydration. As shown in table 5-4, the sample from which the curves of figure 5-16 were derived was allowed to dehydrate for a total of 148 hours below 119°C. In the case of figure 5-17, the sample was allowed to dehydrate for only 25 hours (see table 5-2). The longer heating period at 119°C allowed a greater dehydration of water from the 100°C exchangeable site. This result shows the effect of the heating rate on the dehydration characteristics of this material.

The longer outgassing time below 100°C probably shifted curve I significantly to the left. The cross-over between curves I and II between 110° and 175°C for figure 5-16 is therefore probably incorrect.

(2) The second difference is the absence in figure 5-16 of a maximum in the curve at 300°C. This maximum is a major feature of the curve in figure 5-17, and its absence in figure 5-16 explains the 16% reduction in the water yield mentioned above. The absence of this maximum cannot be explained as a result of the heating rate on the D.I.A. since the maximum is not displaced, but is entirely absent. Apparently, the hydroxyls responsible for this maximum are removed during structural changes associated

with boiling the sample in water for 6 months.

Model of the hydration states. The results shown in figure 5-17 allow considerable insight into the nature of water in biogenic silica. The curves of figure 5-16 are not used because curve II was derived from data based upon diatomite which had been structurally altered by extended exposure to water at 100°C. The curves of figure 5-17 are considered to be the best representation of the water release patterns from naturally occurring, unaltered diatomite.

Assuming that water released below 200°C occurs as H_2O and water released above 200°C as hydroxyl, then the following points seem likely.

(1) Hydroxyls occur in three different sites. Approximately .18 wt.% water exists as surface hydroxyls which exchange readily at room temperature. This figure is derived by integrating the high temperature ($>200^{\circ}C$) portion of curve I in figure 5-16. Approximately 1.3 wt.% water occurs as hydroxyls in more protected sites. These hydroxyls interact with any surrounding water at 100°C within 6 months. Approximately .88 wt.% water (the integral of curve III, figure 5-17) exists as hydroxyls in internal sites, highly protected from any surrounding water. These hydroxyls had not exchanged at 100°C after at least 6 months of interaction with deuterium-rich water.

(2) At least 1.98 wt.% of the water in

diatomite occurs as mechanically trapped or adsorbed H_2O. This figure represents the amount of this water which cannot be removed from the sample by outgassing in vacuum at 25°C. Natural samples exposed to air contain an amount of this water which is dependent upon the humidity.

(3) Approximately 3.60 wt.% of the water in diatomite occurs as H_2O groups within the silica or in sites otherwise protected from interaction with any external water. At temperatures of 100°C these H_2O groups exchange with any surrounding water.

These results have been derived entirely from consideration of figure 5-17 which was, in turn, derived from the data of tables 5-1, 5-2, and 5-4. These hydration characteristics of Monterey diatomite are summarized graphically in figure 5-18.

C-2b. Curves C, D, and E in figure 5-12. Curves C and D are D.I.A. patterns for samples of the Monterey diatomite exchanged at 100°C with deuterium-enriched water and then air-dried for different lengths of time. Curve E is the D.I.A. pattern for a sample of the diatomite which was exchanged at 100°C for about the same length of time as the sample giving curve D, but was dried in a 100°C drying oven exposed to laboratory air. This method of drying allowed the sample to back-exchange at 100°C with water vapor in the laboratory air.

Figure 5-18

HYDRATION CHARACTERISTICS OF WATER IN MONTEREY DIATOMITE

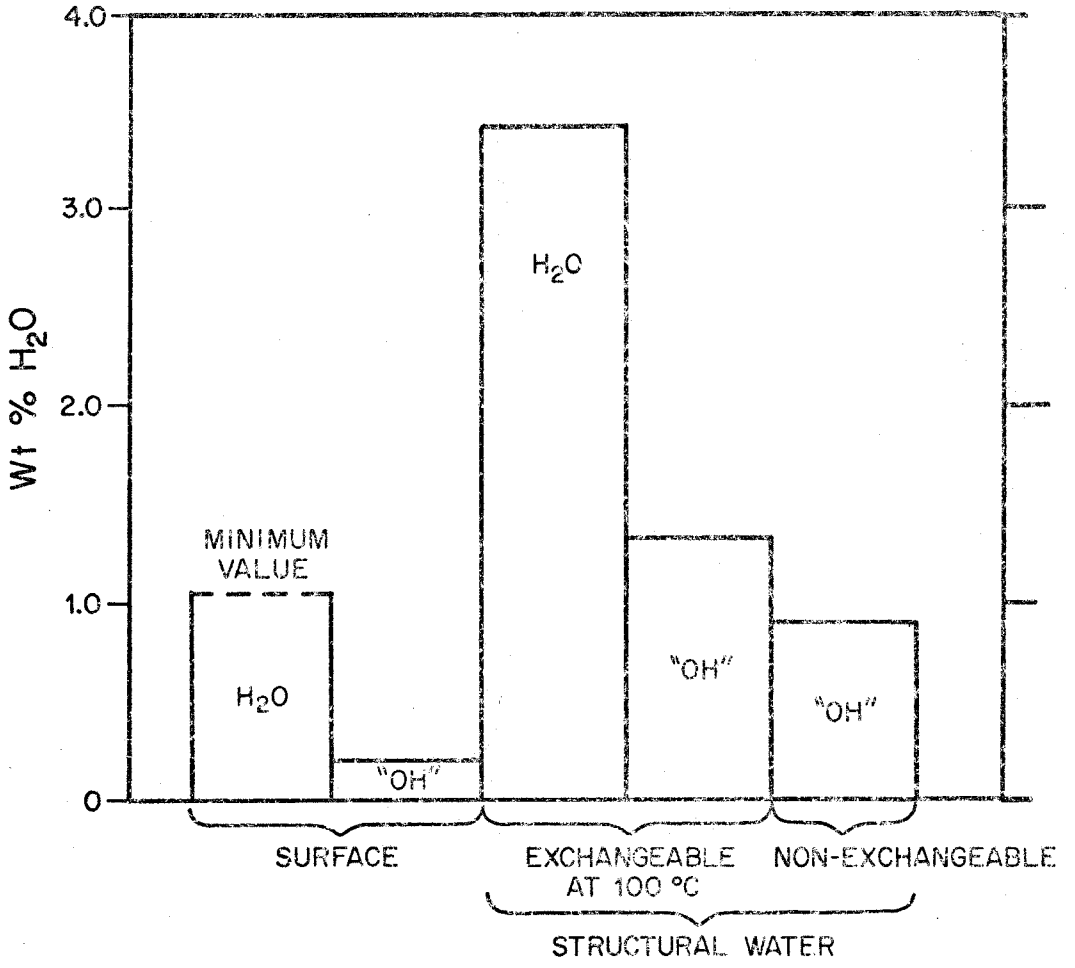

"OH" = water released above 200°C

Considering first the high temperature fractions ($>200^{\circ}C$) represented by the last 1.4 $\mu m/mg$ of water derived during dehydrations B, C, and D, it is apparent that the samples which were exchanged with heavy water for the longest period of time suffered the most deuterium enrichment. Water extracted above $200^{\circ}C$ for diatomite exchanged 329 hours (curve D) has a δD-value of approximately +700‰. This represents 39% exchange with the heavy water. After 700 hours, this δD-value is approximately +800‰, or 44% exchange; and after 4,252 hours it is +1000‰, or 55% exchange. Presumably the corresponding part of curve E (fractions $>200^{\circ}C$) was exchanged to $\delta D = +700‰$, but began to exchange back during $100^{\circ}C$ drying to a value near that of water vapor in the laboratory air ($\approx -100‰$). 21 hours of such exchange apparently lowered the δD-value by about 200‰, representing an exchange of 11%. The rate of exchange of the high temperature fraction (assumed to be hydroxyl) is shown in figure 5-19.

Below $200^{\circ}C$ the D.I.A. patterns clearly show the effects of exchange which occurred during drying in the presence of water vapor in air. Curve D, the D.I.A. pattern for diatomite dried in air for 240 hours, shows this effect more strongly than curve C, which is for diatomite exposed to air for only 48 hours. The corresponding section of

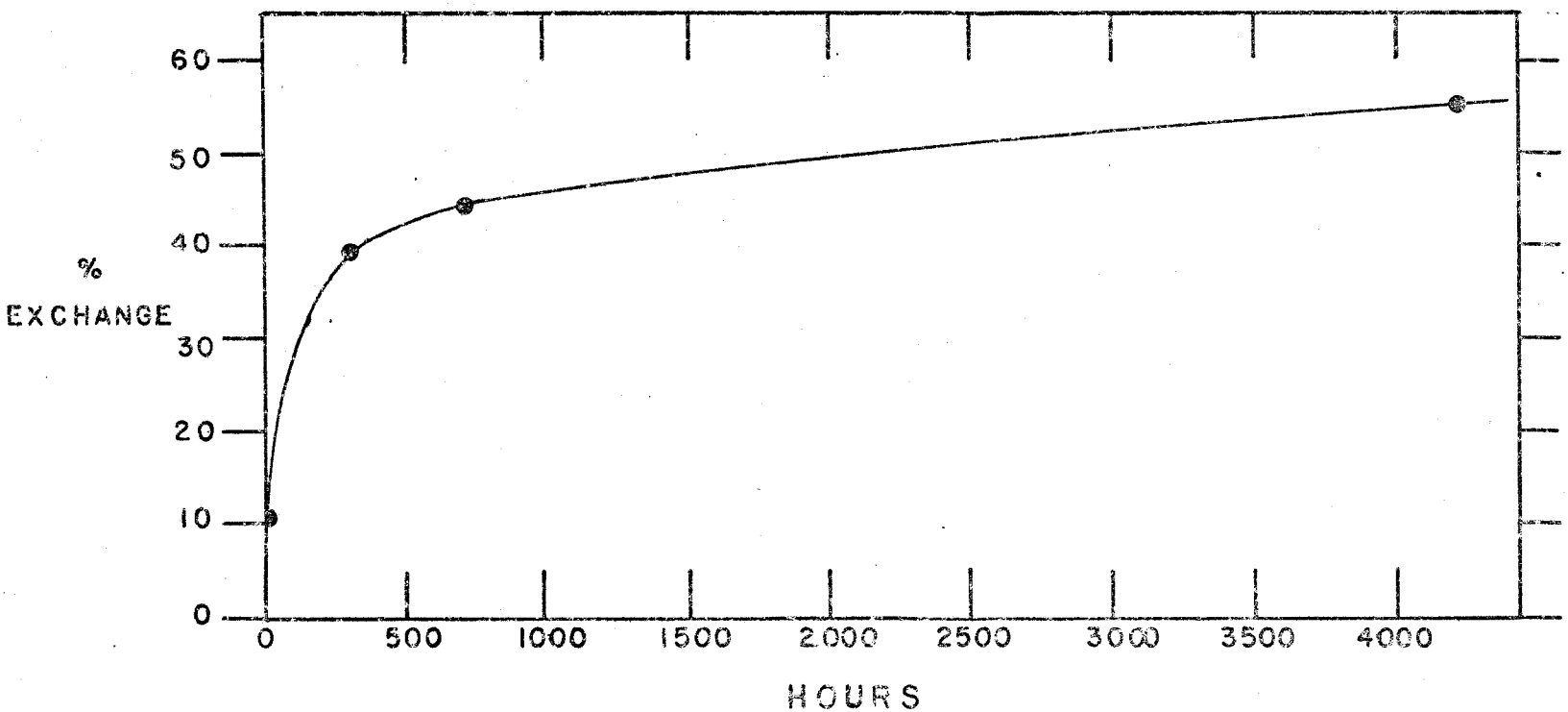

Figure 5-19

RATE OF EXCHANGE OF "HYDROXYL" IN MONTEREY DIATOMITE

curve E has also been extensively "back-exchanged" with water vapor in the drying oven, although most of this low-temperature, easily exchangeable water has been removed in the drying oven.

The behaviour described above can be understood in terms of the water release patterns shown in figures 5-16 and 5-17.

Curve D can be explained by assuming that the adsorbed and trapped water represented by curve I, figure 5-17, was exchanged to $\delta D = +1715$, but re-equilibrated with atmospheric water vapor during the drying period. The initial fraction of the D.I.A. contained water largely composed of this re-equilibrated water yielding a δD-value of +278‰. As the temperature was increased and further fractions collected, more water was released from the "site" represented by curve II, figure 5-17. Water in this "site" should have exchanged to the heavy value, but should not have back-exchanged with laboratory water vapor during drying. Therefore, the progressive enrichment in deuterium shown in curve D for fractions approaching 200°C is satisfactorily explained by the water release patterns of figure 5-17.

Above 200°C curve D shows δD-values indicating that about half the water in the diatomite has exchanged with the heavy water. This result can be understood from the water release patterns in figure 5-16 or 5-17, which show that

above 200°C about half the water should exchange at 100°C and half should not. Curve D as well as all those in figure 5-12 shows an isotopic minimum between 300° and 400°C, indicating that the greatest proportion of unexchanged hydroxyl groups is outgassed over this temperature range.

Curve C is qualitatively similar to curve D. It can be explained exactly as curve D was explained if it is assumed that the shorter drying time did not allow complete exchange of the adsorbed and trapped water with the atmospheric water vapor.

It was hoped that the non-essential and easily exchangeable water fraction of this diatomite could be removed at low temperatures allowing the more geologically meaningful water fraction to be collected separately. However, as shown by the water release patterns for unheated diatomite in figure 5-17, water from the various sites is outgassed simultaneously as the temperature is raised. Heating to 50°C will remove a large fraction of the trapped and adsorbed H_2O without significantly dehydrating the other sites. Above this temperature the more essential water components begin to outgas along with further dehydration of the labile components.

It is clear from the above result that if natural samples of biogenic silica have been exposed to ground waters at 100°C, then the bulk of the water extracted

from them has been profoundly altered. The fact that significant exchange occurs rapidly at 100°C leaves open the strong possibility that exposure of the material to low temperature ground waters over geologic time could also result in significant exchange.

D. Summary of the experimental results on diatomite.

(1) Water in Monterey diatomite occurs in at least 5 different forms with regard to hydration state and exchange properties. These are shown graphically in figure 5-18.

(2) Experimental water release patterns as a function of temperature for those sites with similar exchange properties are best represented in the case of naturally occurring diatomite as shown in figure 5-17. The precise shape of these curves is a function of the rate of dehydration, but their general form is not.

(3) Adsorbed and mechanically trapped water can be largely removed by vacuum pumping overnight at room temperature.

(4) Natural samples which have been heated to 100°C by warm ground waters have largely lost their original δD values.

5.3 Crystalline Silica

The three most common crystalline forms of silica have been described in section 2.2. Two of these forms, chalcedony

and granular microcrystalline quartz, contain water and are the subjects of the following experiments aimed at determining the amount of water which would exchange during acid treatments, rinsings, and exposure to laboratory air. Only room temperature exchange experiments were done using the procedure described in section 5.2-B. The crystalline forms of silica contain much less water than the amorphous forms, and it is necessary to use larger samples to obtain amounts of water large enough for D.I.A. A 600-fold excess of heavy water ($\delta D = +1715$) was used for the exchange reservoir.

A. Chalcedony.

A-1. Sample description. Megascopic amounts of fibrous quartz are not common, and no chert collected for this research was entirely composed of this material. (Megascopic amounts of chalcedony were obtained from a deep-sea chert sample in the final days of this research, but too late to perform experiments on.) Therefore, the chert sample containing the most chalcedony of any collected was used in this experiment. The results are therefore not applicable to pure chalcedony, but are nevertheless useful for evaluating isotopic data on natural samples which contain abundant amounts of it.

A chert nodule, sample #171 from the Mississippian Burlington Formation, was used for the following exchange experiments. The sample was collected from a quarry face

just west of Hardin, Illinois. The precise location is given in Appendix II.

The chert nodule is composed of 60% unusually well preserved calcite crinoid plates, 30% chalcedony, 5% granular microcrystalline quartz, and 5% megaquartz. In former cavities the chalcedony often grades into megaquartz and much is very fine-grained, apparently grading into granular microcrystalline quartz. A small amount of opal may be present, but the total water content of the sample is typical of nodular cherts in limestones (see Chapter 6).

A-2. Sample preparation. Powdered material for the exchange experiments was selected from stored powders routinely prepared as described in section 4.2.

A-3. D.I.A. A D.I.A. was obtained for the natural sample (free of carbonate) and is shown in table 5-9 and figure 5-20. Unlike the diatomite, successive cuts show a continuous decrease in δD-values. From these data alone it is uncertain whether the trend represents mixing of various amounts of water derived from sites with $\delta D = \approx -45‰$ and $-80‰$, or whether the trend represents a fractionation pattern associated with dehydration of a single site.

A-4. Exchange experiment at 25°C. The sample was allowed to exchange overnight, was decanted, and was placed directly into the vacuum line without being dried

Table 5-9

D.I.A. FOR CHERT COMPOSED LARGELY OF CHALCEDONY #171

Fraction	Temperature	Time Interval	Yield µm/mg	δD_{SMOW}‰
1	25-113°C	5^h40^m	.030	-42.32
2	113-203	2^h35^m	.016	-45.90
3	203-316	3^h05^m	.013	-54.17
4	316-559	3^h05^m	.090	-58.22
5	559-1000	5^h	.030	-76.74

in any way. Drying was accomplished by extremely slow pumping. Air in the line is slowly evacuated by this procedure, but free water in the wet powder quickly volatilizes and saturates the vacuum line. This water of $\delta D = +1715‰$ was in contact with the glass walls and stopcock grease for approximately 3 hours until the sample was dry. The D.I.A. derived by subsequent heating of the sample is presented in table 5-10 and is shown as curve II of figure 5-21. (The D.I.A. of figure 5-20 is replotted as curve I for reference.)

This result indicated far more exchange than expected. It was suspected that the glassware and stopcock grease had been strongly hydrated by the prolonged exposure to the heavy water, and that the sample water which subsequently outgassed during the D.I.A. had partially exchanged with this water.

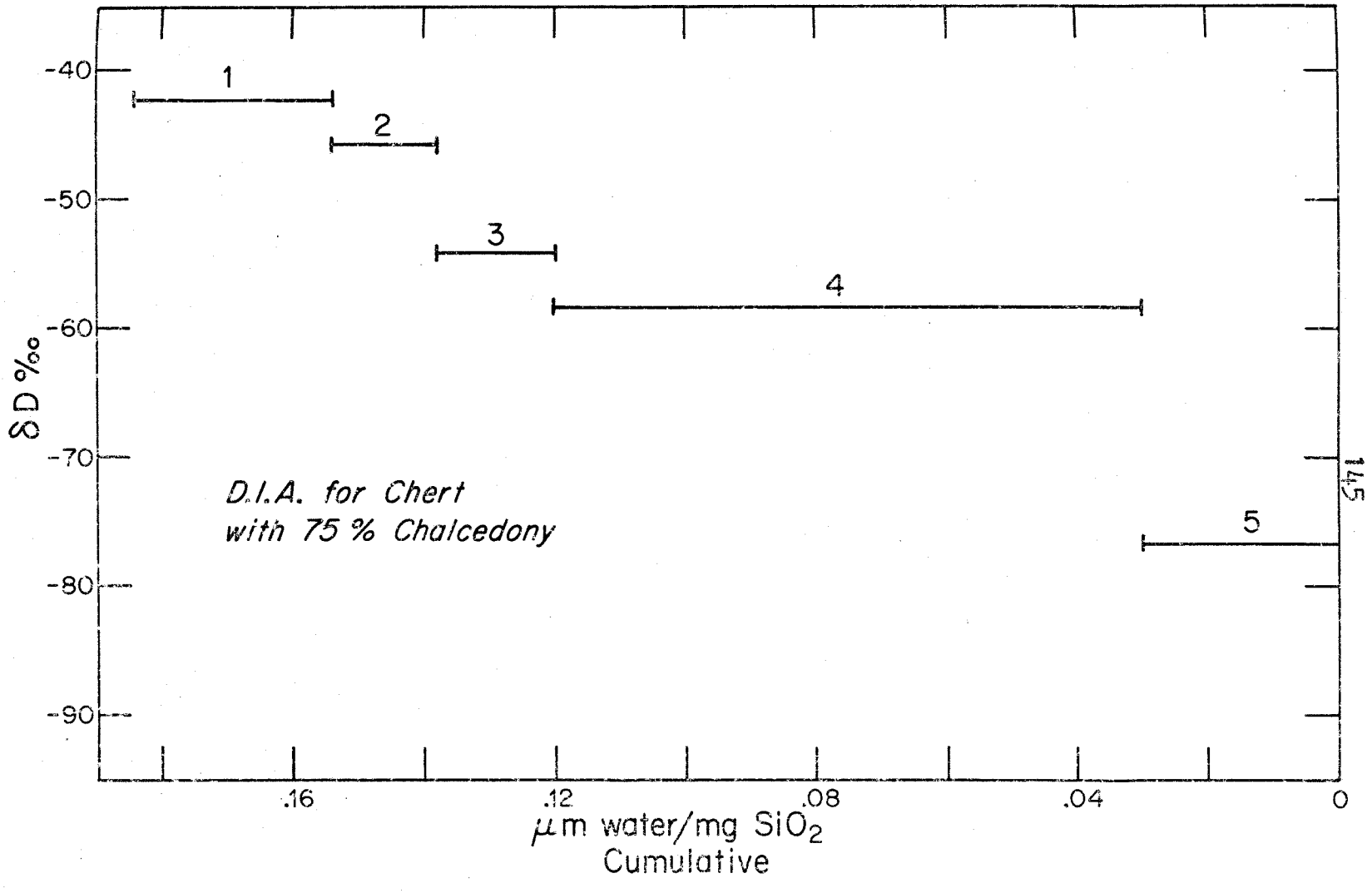
-40
-50
-60
-70
-80
-90
δD ‰
1
2
3
4
5
D.I.A. for Chert
with 75 % Chalcedony
.16
.12
.08
.04
0
μm water/mg SiO2
Cumulative
115

Figure 5-20

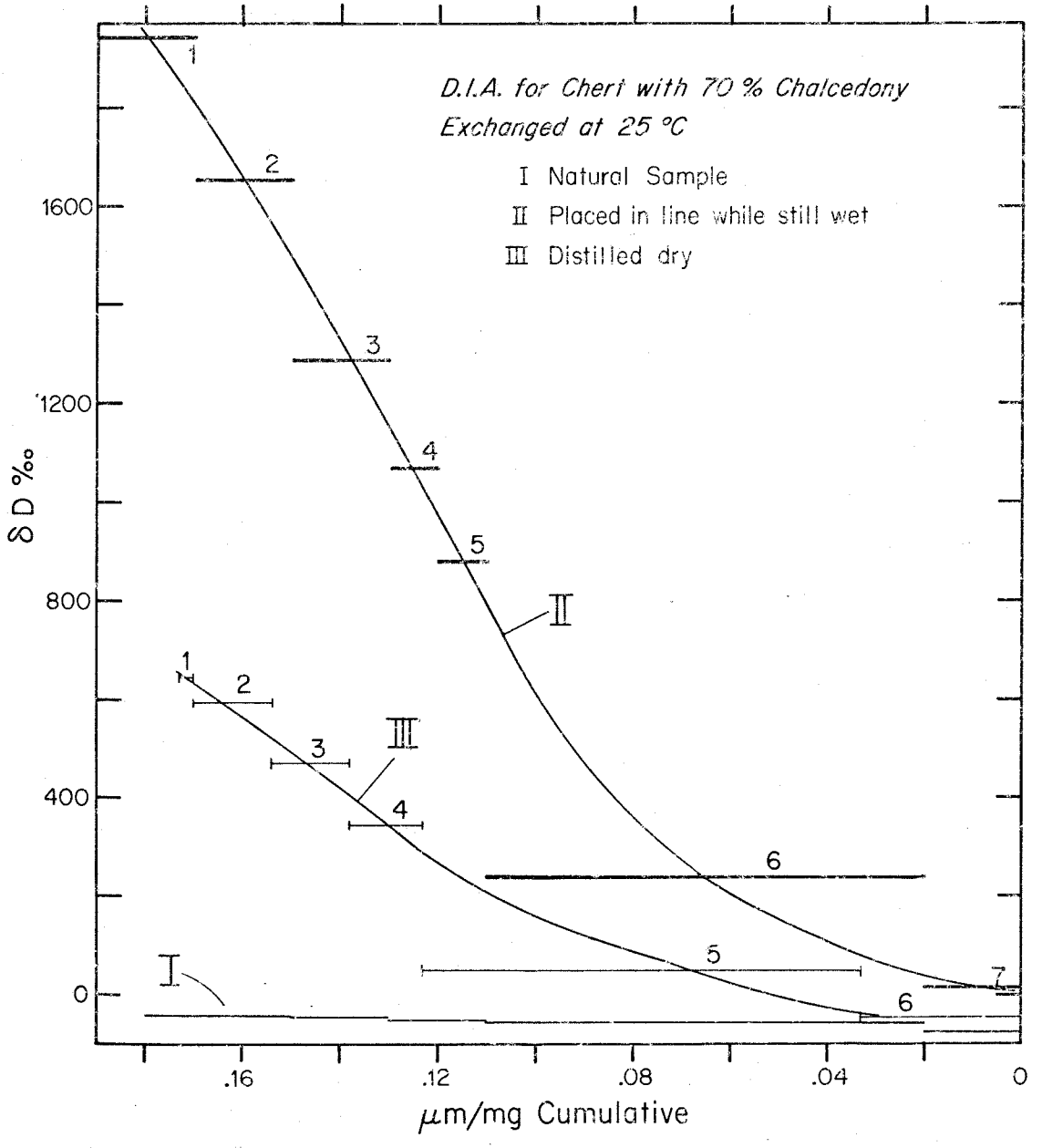

Figure 5-21

DIFFERENTIAL ISOTOPIC ANALYSES FOR CHERT WITH 70% CHALCEDONY EXCHANGED FOR 12 HOURS AT 25°C WITH D-ENRICHED WATER (δD = +1715‰)

Table 5-10

D.I.A. FOR CHALCEDONY-RICH CHERT #171
EXCHANGED WITH D-ENRICHED WATER (δD = +1715‰)
AT 25°C, PLACED IN EXTRACTION LINE WET

Fraction	Temperature	Time Interval	Yield μm/mg	δD_{SMOW} ‰
1	25°C	18^h22^m	> .2	1958
2	25-59	24^h0^m	.011	1657
3	59-124	72^h20^m	.016	1289
4	124-229	4^h30^m	.01	1068
5	229-314	3^h35^m	.009	879
6	314-510	16^h0^m	.092	240
7	510-1000	4^h53^m	.023	18

The experiment was repeated, with the exception that the sample was dried to completion at 25°C by the distillation procedure in section 5.2-B before placing it in the extraction line. This procedure prevented any unusual hydration of the vacuum line from occurring. The D.I.A. then obtained is presented in table 5-11 and shown as curve III of figure 5-21. Significantly less exchange is inferred from this D.I.A. than that suggested by the previous experiment. This result clearly indicates that a severe analytical "memory effect" is introduced into the experiment if a significant vapor pressure of water is allowed to develop in a vacuum line such as this.

The D.I.A. represented by curve III may be interpreted as the result of simultaneous outgassing of water from two

Table 5-11

D.I.A. FOR CHALCEDONY-RICH CHERT #171
EXCHANGED WITH D-ENRICHED WATER (δD = +1715‰)
AT 25°C, DISTILLED DRY

Fraction	Temperature	Time Interval	Yield μm/mg	δD_{SMOW}‰
1	24-68°C	4^h0^m	.009	644
2	68-112	7^h0^m	.016	593
3	122-231	4^h0^m	.016	470.5
4	231-313	6^h15^m	.015	345.5
5	313-535	4^h	.090	50.3
6	535-1000	3^h30^m	.033	-44.6

sites. One site contains water which is labile and easily exchangeable. The other is unexchanged. Water outgassed at the lower temperatures contains more of the labile water than that outgassed at higher temperatures.

In order to verify this interpretation, the dehydrated sample was again placed into enriched water, allowed to rehydrate overnight, and dried in the same manner as described above. The sample, when heated again to 1000°C, yielded only .015 μm/mg water. In this case the amount was too small for isotopic analysis. If it is assumed that this small amount of water which rehydrated the sample was adsorbed water, it is possible to perform a mass balance calculation to see if this adsorbed water is the exchangeable component in the room temperature exchange experiment. The

δD-value for the total water extracted from the natural sample (0.184 μm/mg) is -57‰ (curve I, figure 5-24). Assuming that 0.015 μm/mg water (the adsorbed water) in the natural sample exchanged completely with the heavy water, then from equation 5-2 the δD-value for the total water should be +192‰. δD for the total water extracted from the natural sample exchanged overnight with heavy water is +170‰ (curve III, figure 5-21). This approximate agreement between the calculated and measured δD-value strongly suggests that the interpretation is correct that the D.I.A. given as curve III represents a mixing curve between exchanged surface water which outgases primarily at low temperatures and unexchanged water which outgases primarily at high temperatures. Water release curves as a function of temperature for these two waters can be derived as before (section 5.2-B). Results of the calculations for each fraction are given in table 5-12. The histograms, cumulative curves and the final water release curves are shown in figures 5-22, 5-23 and 5-24, respectively.

Figure 5-24 shows that most of the non-exchangeable water is released above 200°C. The results suggest that most of the water in fibrous quartz is in the form of hydroxyl groups which are protected from interaction with surrounding water. Exchangeable water is outgassed along

Table 5-12

VALUES USED FOR CALCULATION OF ACTUAL AMOUNT OF EXCHANGED AND NON-EXCHANGED WATER FOR EACH FRACTION IN D.I.A. OF TABLE 5-11 AND RESULTS OF CALCULATION

Fraction	Temperature	δ_t ‰	δ_1 ‰	δ_2 ‰	X_1	$X_1(\frac{\mu m}{mg})$	X_2	$X_2(\frac{\mu m}{mg})$
1	25-68°C	644	1715	-40	.39	.004	.61	.005
2	68-122	593	1715	-40	.36	.006	.64	.010
3	122-231	470	1715	-45	.29	.005	.71	.011
4	231-313	345	1715	-50	.22	.003	.78	.012
5	313-535	50	1715	-60	.06	.005	.94	.085
6	535-1000	-45	1715	-80	.02	.001	.98	.032

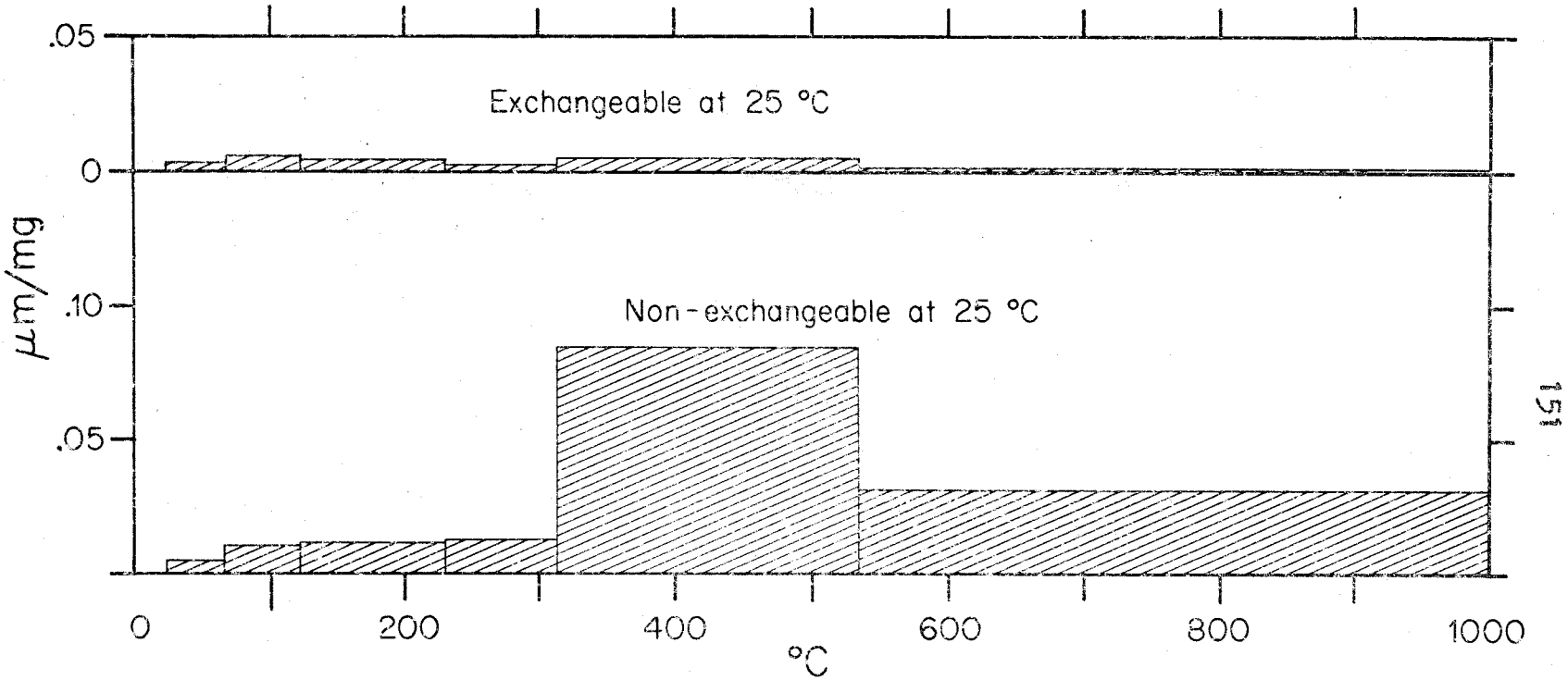

Figure 5-22

HISTOGRAMS SHOWING AMOUNTS OF EXCHANGEABLE AND NON-EXCHANGEABLE WATER RELEASED AT SUCCESSIVELY HIGHER TEMPERATURES FOR CHERT CONTAINING 70% CHALCEDONY WHICH WAS EXCHANGED OVERNIGHT WITH D-ENRICHED WATER AT 25°C

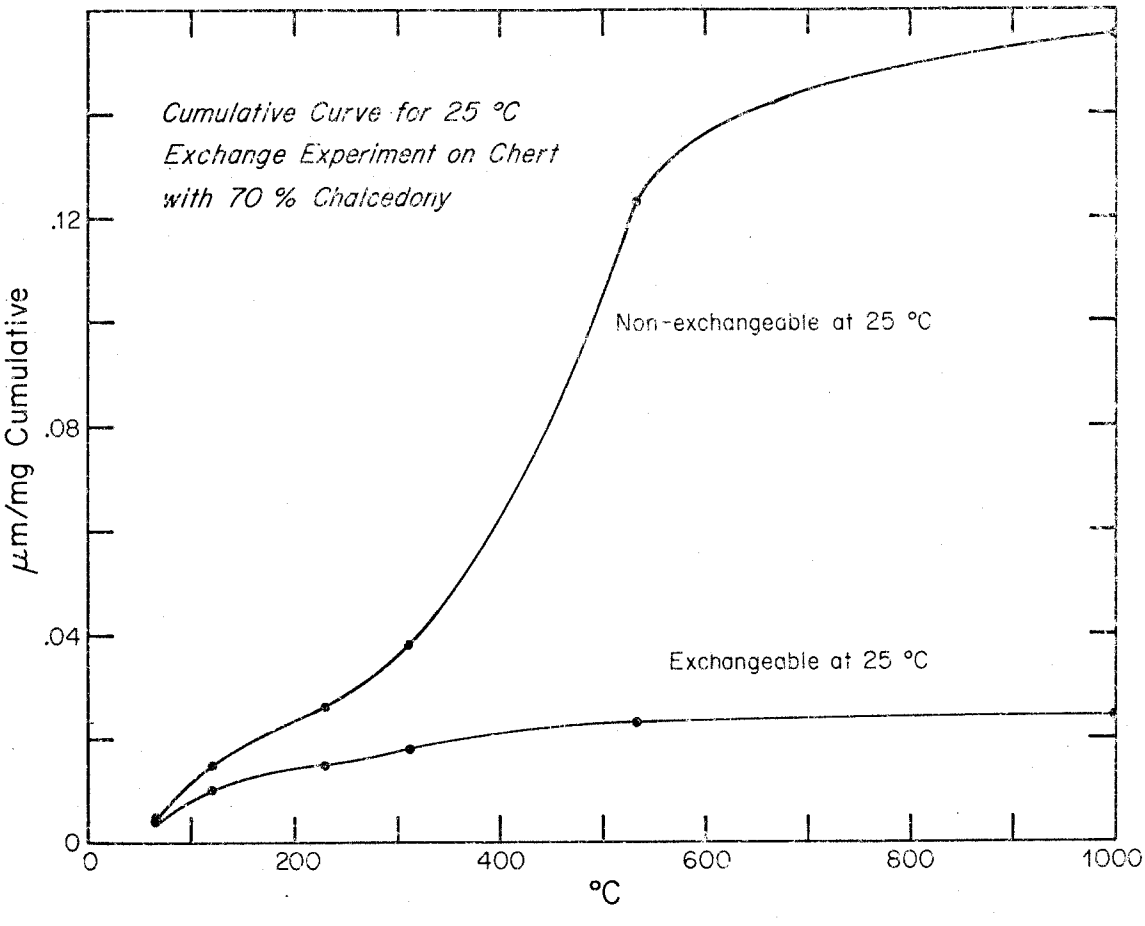

Figure 5-23

CUMULATIVE CURVES FOR μm/mg OF EXCHANGEABLE AND NON-EXCHANGEABLE WATER RELEASED AT SUCCESSIVELY HIGHER TEMPERATURES FOR CHERT CONTAINING 70% CHALCEDONY WHICH WAS EXCHANGED OVERNIGHT WITH D-ENRICHED WATER AT 25°C

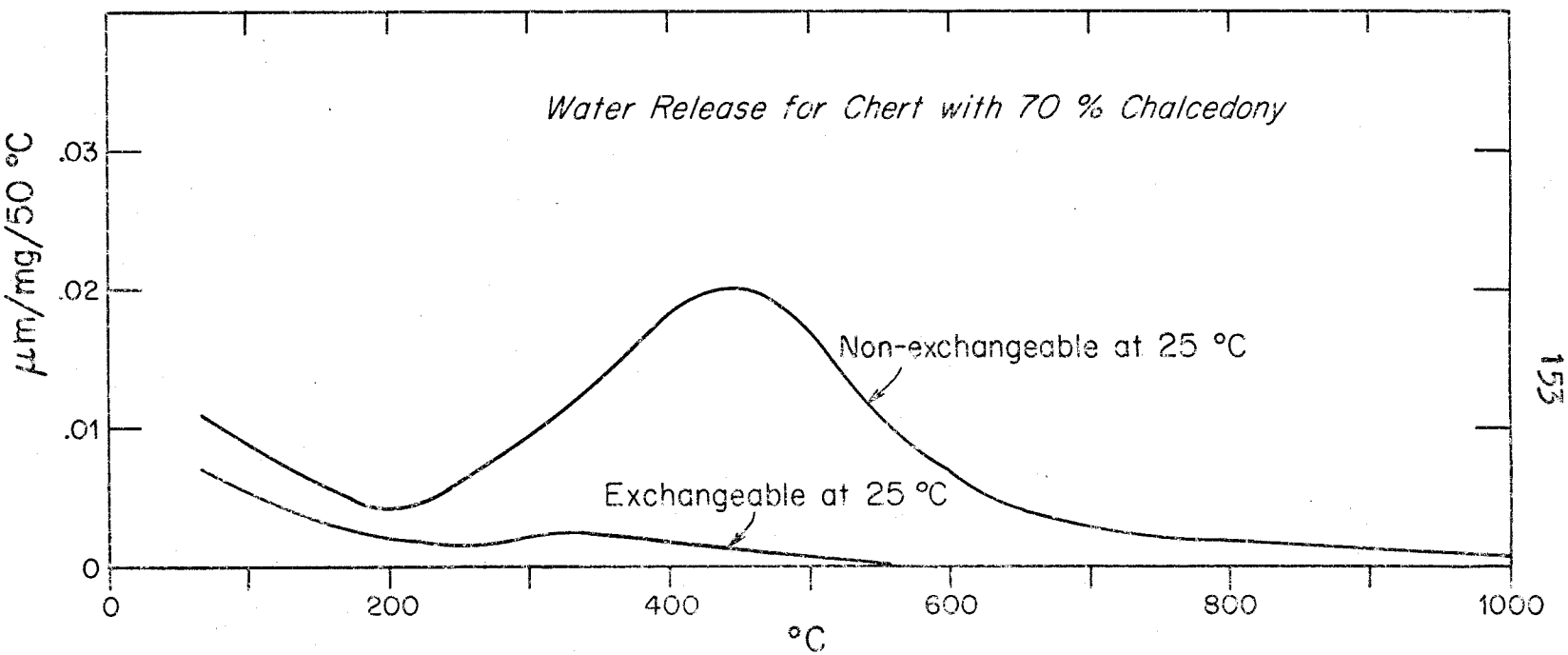

Figure 5-24

WATER RELEASE FOR CHERT WITH 70% CHALCEDONY.
AREA UNDER CURVE EQUALS AMOUNT OF
WATER RELEASED BETWEEN 25° AND 1000°C.

with this non-adsorbed water at nearly all temperatures and it is thus not possible to completely separate the two waters thermally.

The above experiments show that for samples crushed to <200 mesh, water extracted from hydroxyl sites in cherts composed largely of fibrous quartz will be contaminated by water which has been isotopically exchanged during acid treatments, rinsings, and exposure to laboratory air. The effect of this water on the isotopic analyses depends upon the difference between its δD-value and that of the hydroxyl. D/H measurements on cherts composed predominantly of fibrous quartz are thus suspect. More precise measurements on these materials could possibly be made for samples sufficiently free of carbonate as to not require fine-crushing for acid-treatments.

B. Granular Microcrystalline Quartz

B-1. Sample description. The exchange experiments for granular microcrystalline quartz were performed on a sample of Precambrian chert from the Mescal limestone in southern Arizona. The sample was collected from outcrops on the south canyon face at Roosevelt Dam, east of Phoenix. Chert occurs here as thin beds in the limestone. The sample used here was taken from a 2-inch thick white translucent bed which showed a "pinch and swell" structure. Petrographically, the sample consists predominately of granular microcrystalline quartz. Former cavities in the chert

are filled with megaquartz, and some are lined with small amounts of chalcedony. Irregular patches of very fine-grained carbonate are commonly seen in thin section. The granular microcrystalline quartz may be somewhat finer-grained than most cherts, but otherwise the texture is characteristic of most cherts in limestones. The water content is .5 wt.%, a typical value for cherts in limestone.

B-2. Sample preparation. Material for the exchange experiments was selected from powders routinely prepared as described in section 4.2.

B-3. D.I.A. A D.I.A. with two fractions for the unexchanged sample is shown in table 5-13 and figure 5-25, curve I.

B-4. Exchange experiment at 25°C. The sample was allowed to exchange with deuterium-rich water overnight and was distilled dry by the method described in section 5.2-B. The results of the D.I.A. for the exchanged material are presented in table 5-14 and illustrated as curve II,

Table 5-13

D.I.A. FOR GRANULAR MICROCRYSTALLINE QUARTZ, #34

Fraction	Temperature	Time Interval	Yield $\mu m/mg$	δD_{SMOW}‰
1	25-349°C	5^h30^m	.114	-62.82
2	349-1000	2^h10^m	.141	-102.89

Table 5-14

D.I.A. FOR GRANULAR MICROCRYSTALLINE QUARTZ #34 EXCHANGED OVERNIGHT WITH DEUTERIUM-ENRICHED WATER (δD = +1715‰) AT 25°C

Fraction	Temperature	Time Interval	Yield µm/mg	δD_{SMOW}‰
1	23-63°C	14^h	.005	+211.52
2	63-125	5^h20^m	.008	+236.26
3	125-221	5^h25^m	.042	+ 23.33
4	221-301	3^h40^m	.058	- 50.03
5	301-550	6^h35^m	.088	- 51.26
6	550-1000	3^h30^m	.069	- 55.11

figure 5-25. These results show that a small amount of exchange has occurred, especially for water released below 200°C. The dehydrated sample was placed in deuterium-enriched water overnight to see if any rehydration would occur. .007 µm/mg of water was extracted from the sample so treated. To determine if this water is the easily exchangeable component responsible for the exchange seen in figure 5-25, the following mass balance calculation can be made.

The δD-value for total water extracted from the unexchanged sample is -84.98‰. If .007 µm/mg of water in this sample exchanges to +1715‰, the resultant total δ-value of the sample would be -36‰ (derived with

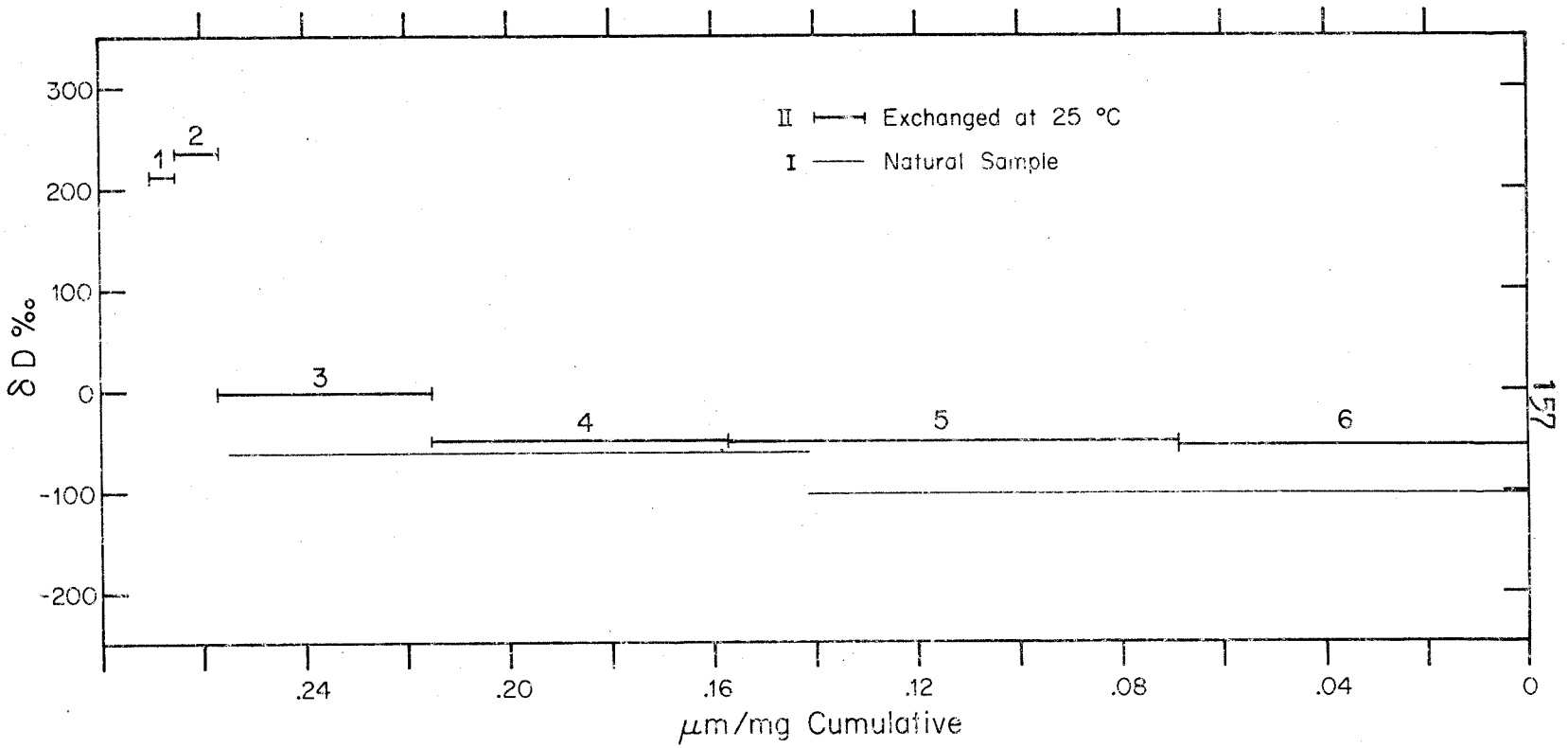

Figure 5-25
DIFFERENTIAL ISOTOPIC ANALYSES FOR
GRANULAR MICROCRYSTALLINE QUARTZ

equation 5-2 and data in table 5-13). The observed total δ-value (fraction 1-6 for curve II, combined) is -27‰, in close agreement with the computed value. This result indicates that the exchangeable water component is the fraction which rehydrates and is probably surface water largely in the form of H_2O.

Water release patterns as a function of temperature may be derived from this experiment as was done previously. Results of the calculations are given in table 5-15. The histograms, cumulative curves, and final water release curves are shown in figures 5-26, 5-27, and 5-28.

B-5. Discussion. The results shown in figure 5-28 show that nearly all of the water derived from granular microcrystalline quartz is liberated above 200°C and does not exchange during exposure to liquid water at 25°C, even when the sample is in the form of fine powder. This suggests that the water occurs as hydroxyls within the silica structure, in agreement with the conclusion of Micheelson (1966) (see section 2.2-A). The small amount of exchangeable water is apparently that water which is adsorbed on the surfaces of the grains. Most of the labile and exchangeable water in granular microcrystalline quartz is removed by exposure to high vacuum at room temperatures. Water derived from this material by further heating is water which has not been isotopically altered during the sample preparation.

Table 5-15

VALUES USED FOR CALCULATION OF ACTUAL AMOUNT OF EXCHANGED AND NON-EXCHANGED WATER FOR EACH FRACTION IN D.I.A. OF TABLE %-14 AND RESULTS OF THE CALCULATION

Fraction	Temperature	δ_t ‰	δ_1 ‰	δ_2 ‰	X_1	$X_1(\frac{\mu m}{mg})$	$(1-X_1)$	$(1-X_1)\frac{\mu m}{mg}$
1	25-63°C	211.52	1715	- 60	.13	.001	.85	.004
2	63-125	236	1715	- 60	.17	.001	.83	.007
3	125-221	23	1715	- 60	.05	.002	.95	.040
4	221-301	-50	1715	- 60	.01	.001	.99	.057
5	301-550	-51	1715	-100	.03	.003	.97	.085
6	550-1000	-55	1715	-100	.02	.001	.98	.068

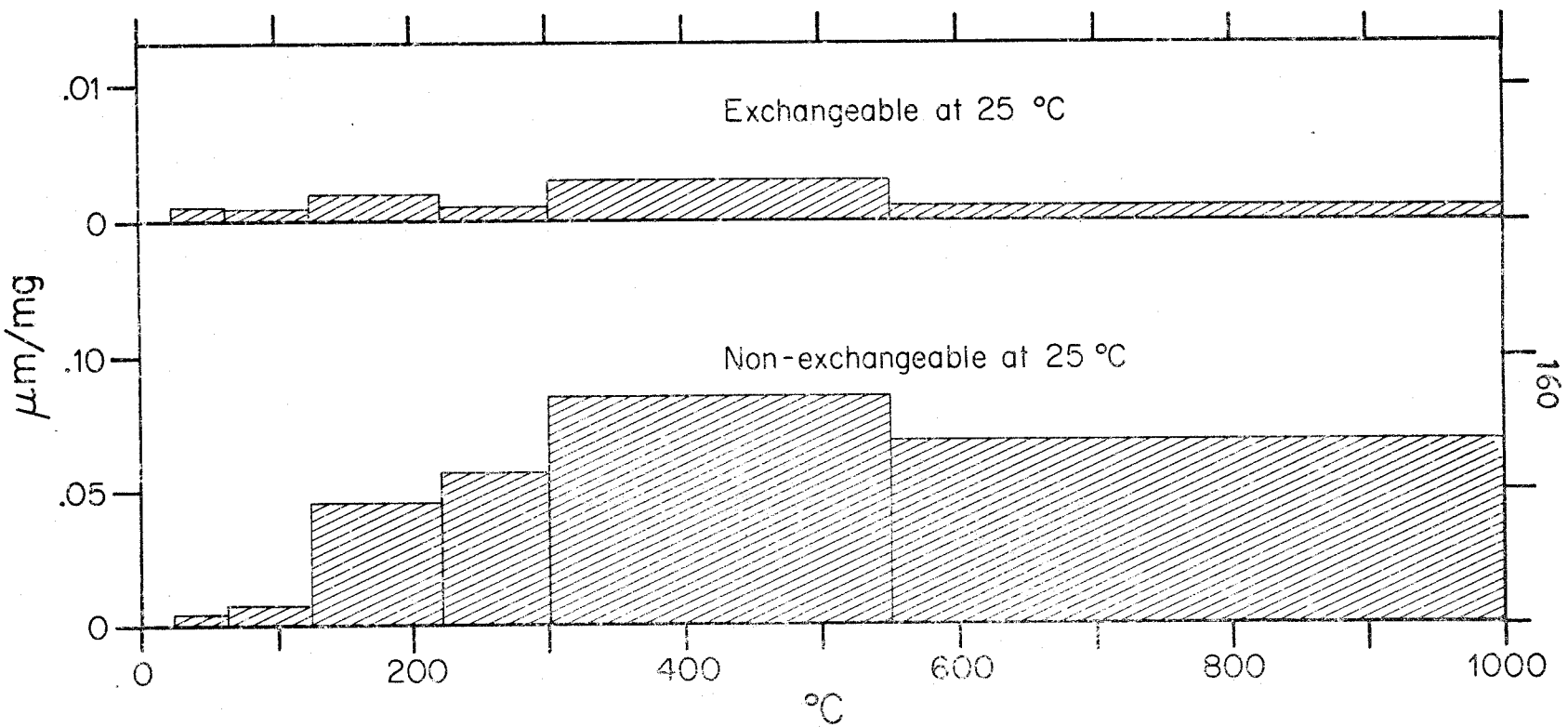

Figure 5-26

HISTOGRAMS SHOWING AMOUNTS OF EXCHANGEABLE AND NON-EXCHANGEABLE WATER RELEASED AT SUCCESSIVELY HIGHER TEMPERATURES FOR GRANULAR MICROCRYSTALLINE QUARTZ WHICH WAS EXCHANGED OVERNIGHT WITH D-ENRICHED WATER AT 25°C

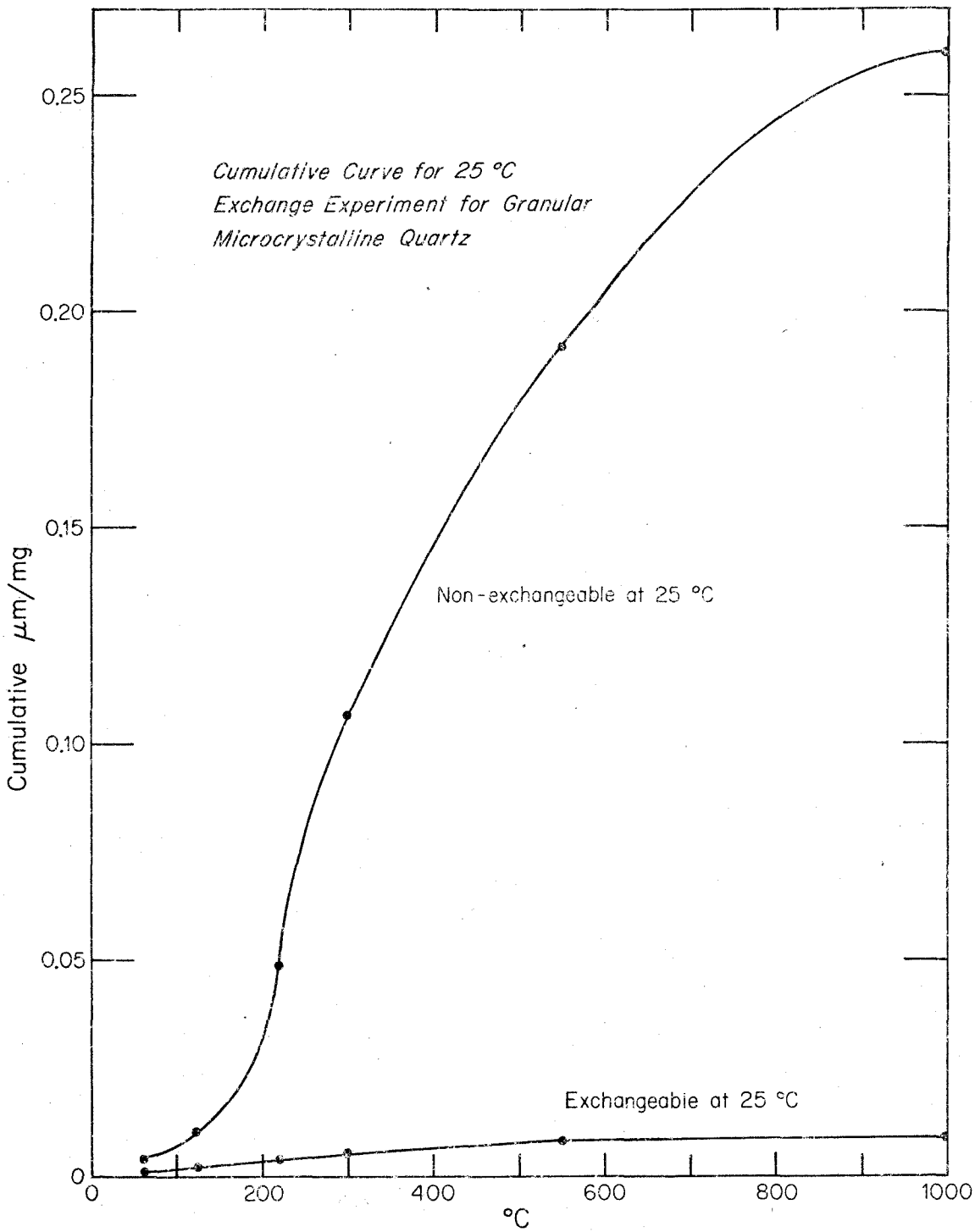

Figure 5-27: CUMULATIVE CURVES FOR μm/mg OF EXCHANGEABLE AND NON-EXCHANGEABLE WATER RELEASED AT SUCCESSIVELY HIGHER TEMPERATURES FOR GRANULAR MICROCRYSTALLINE QUARTZ WHICH WAS EXCHANGED OVERNIGHT WITH D-ENRICHED WATER AT 25°C

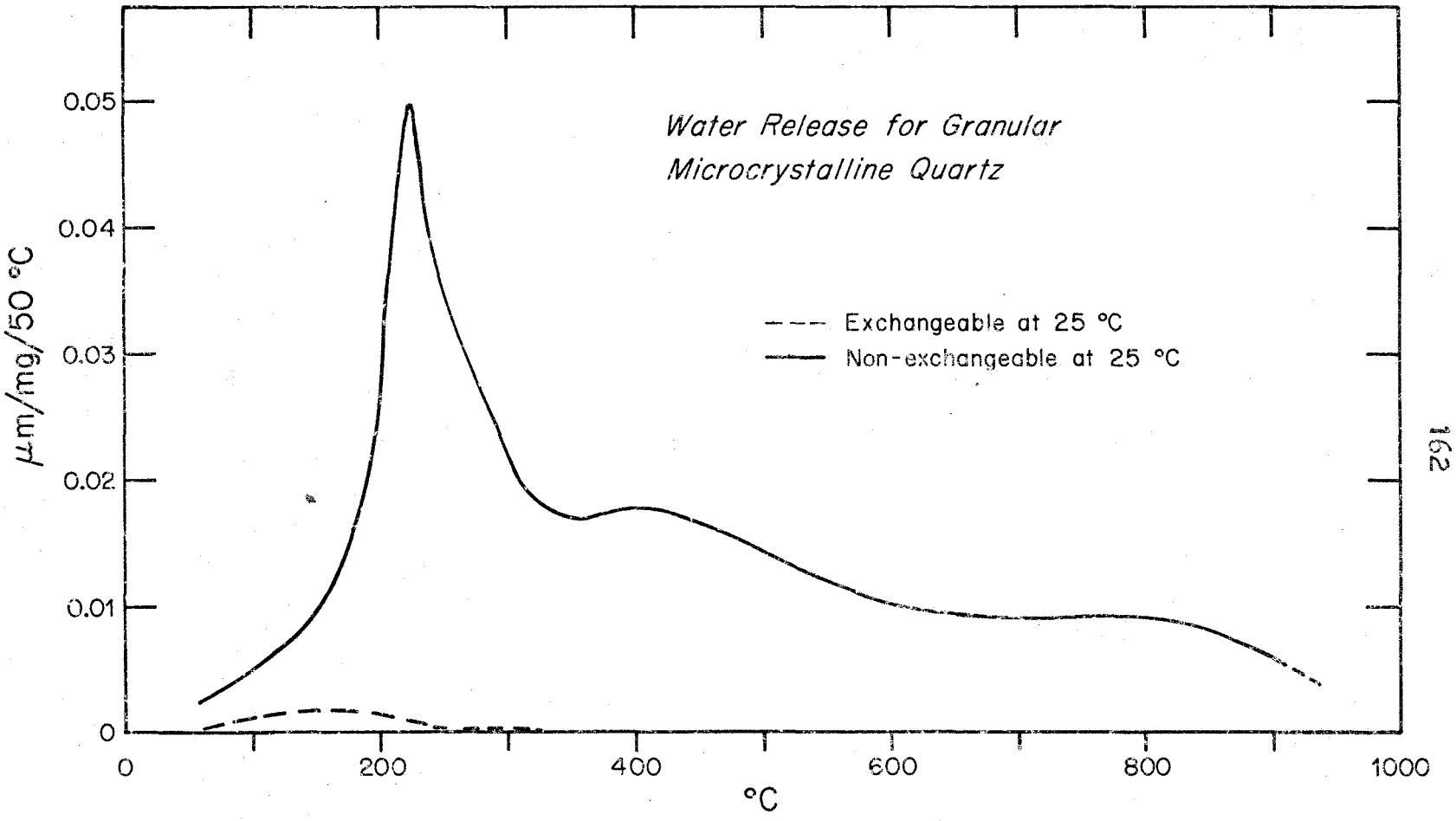

Figure 5-28

WATER RELEASE FOR GRANULAR MICROCRYSTALLINE QUARTZ.
AREA UNDER CURVE EQUALS AMOUNT OF
WATER RELEASED BETWEEN 25° AND 1000°C.

Exchange experiments at 100°C on granular microcrystalline quartz are desirable since information concerning the rate of exchange of the high temperature water fraction could possibly be obtained. One such experiment was started, but it was aborted due to experimental difficulties.

5.4 Conclusions Concerning Isotopic Analyses of Silica

The preceding experiments suggest the following procedures for the isotopic analysis of hydrogen in water contained in silica.

A. Amorphous forms. Most adsorbed, mechanically trapped, and otherwise exchangeable water can be removed from diatomite by pumping under high vacuum for several hours at temperatures between 25° and 50°C. Water extracted above these temperatures can be considered to be geologically meaningful, although this water may not have preserved its initial isotopic ratio over geologic time. Water so extracted is derived from bonded H_2O and hydroxyls in at least 5 sites shown graphically in figure 5-18. Samples collected from sediments known to have experienced temperatures of 100°C during burial have definitely suffered massive exchange of hydrogen isotopes.

The procedures used for diatomite are probably also appropriate for inorganic opals and other forms of biogenic silica. Inorganic opals are much more impermeable than biogenic silica and have a greatly reduced surface area.

These may have preserved their isotope ratios much better than diatomites.

B. Fibrous quartz. Approximately 14% of the water extracted from cherts composed largely of chalcedony after it has been pumped under high vacuum is water which can exchange during handling and treatment. It is not possible to thermally separate this water from the non-exchangeable component. Cherts composed largely of chalcedony are thus somewhat unsuitable for D/H measurements. Approximate δD-values can be obtained if the water used during sample treatments is not drastically different isotopically from the non-exchangeable OH in the fibrous quartz.

C. Granular microcrystalline quartz. Nearly all readily exchangeable water is quickly removed from samples composed predominantly of granular microcrystalline quartz by vacuum pumping at room temperature. Water extracted from such samples at higher temperatures is derived almost entirely from hydroxyl groups within the silica structure. Inasmuch as most cherts are composed of granular microcrystalline quartz, the above result allows rapid and convenient δD measurements to be made on a wide variety of natural samples. The question of preservation of these ratios over geologic time must presently be treated by examination of natural data.

Chapter 6

ISOTOPIC COMPOSITION OF GRANULAR MICROCRYSTALLINE QUARTZ

6.1 Introduction

The isotope results reported in this chapter are primarily for granular microcrystalline quartz. The petrographic and structural character of this material, together with a survey of its mode of occurrence, were discussed in Chapter 2. This form of silica is the most common form of authigenic silica and contains the least amount of adsorbed and exchangeable water.

In practice it is difficult to obtain pure megascopic samples of this material. A typical chert nodule or bed contains carbonate, clay minerals, organic matter, detrital quartz, chalcedony, and megaquartz. In addition, the older cherts are frequently partially recrystallized to megaquartz. The isotopic data obtained for the cherts include some analyses of samples from which these impurities could not be separated. If the impurities appeared to be present in sufficient quantities to affect the isotopic results, they are so indicated. Unless otherwise indicated, the data are for granular microcrystalline quartz which occurs in the form of nodules, beds, and irregular accumulations unrelated to tectonic fractures, hydrothermal veins, and present-day surface silicification.

6.2 Water Contents of Cherts

The water contents of the cherts analyzed in this study are given in figure 6-1. This figure shows the wt.% of non-adsorbed water extracted from natural samples arranged according to their age.

It can be seen from the figure that there is no systematic decrease in the water content of pre-Cretaceous cherts with age. Such a trend might be expected since the amount of recrystallization and annealing of the granular microcrystalline quartz structure should increase with increasing age of the samples. Instead, a large range of water contents is observed for cherts of a single age. These variations are probably related to structural differences of the granular microcrystalline quartz. Variations in the water content are to be expected if the water is non-stoichemetric and is located at point defects, on dislocations, and along lattice faults as proposed by Micheelson (1966).

As seen in figure 6-1, most pre-Tertiary cherts contain less than .5 wt.% water. Cherts with larger amounts of water usually contain large amounts of opaque organic matter visable in thin-section or in grain mounts. It seems likely that this organic matter is the source of the anomalously high water yield in these samples. It is very likely that the water produced by this organic matter

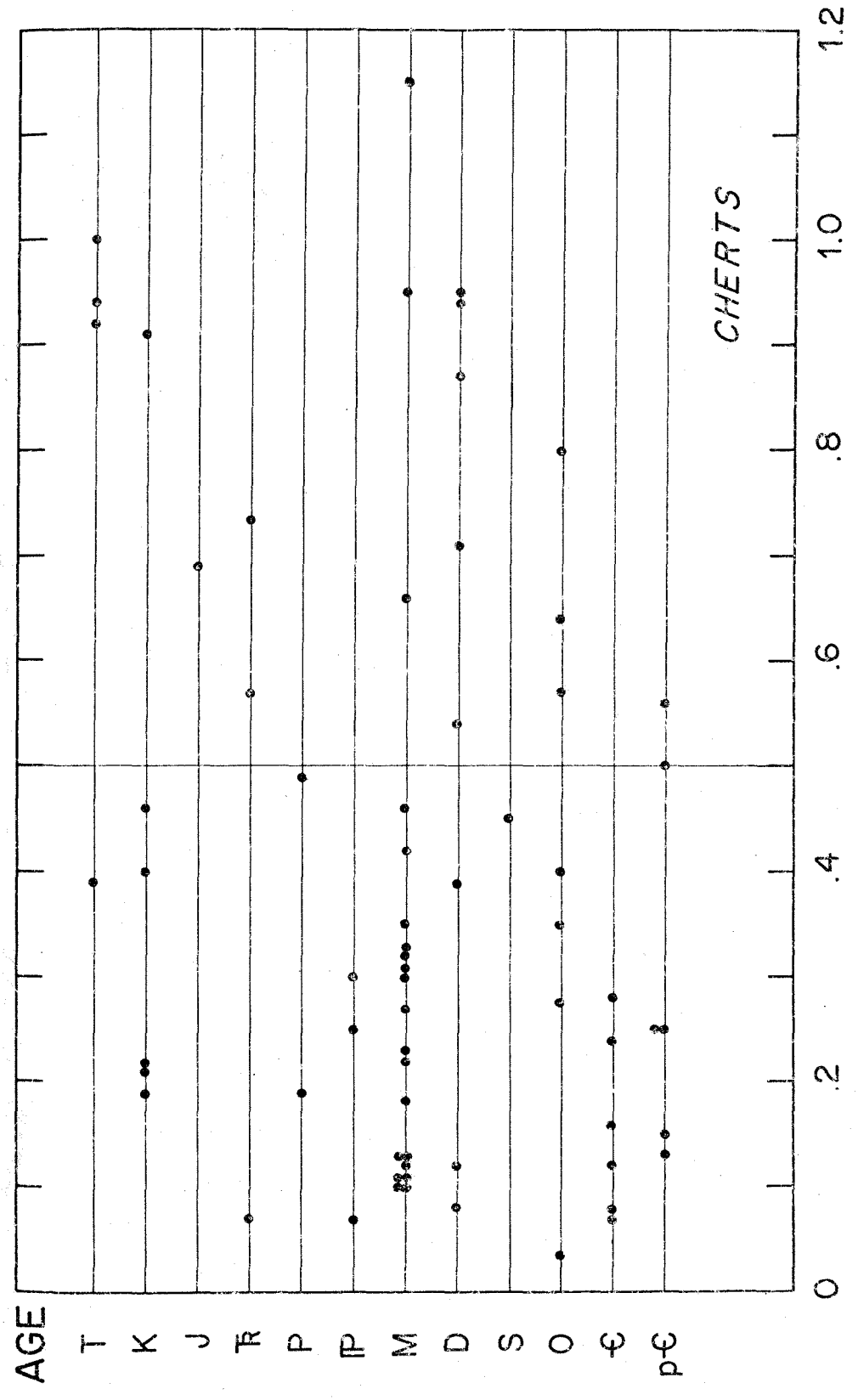

Figure 6-1: WATER CONTENTS OF CHERTS

during dehydration is isotopically dissimilar to the hydroxyl-water of the granular microcrystalline quartz. The meaning of hydrogen isotope analyses of such cherts is thus questionable, depending upon the relative amounts of the dissimilar waters. In the following discussions, all such samples will receive special consideration.

Many cretaceous and younger cherts have water contents of approximately 1% but do not contain visable amounts of organic matter. Instead, these contain small amounts of isotropic to weakly birefrengent silica which is likely to be opal-CT. The water content of opal-CT is somewhat greater than that of granular microcrystalline quartz, and it seems likely that the additional water content of the Cenozoic cherts is due to the presence of opal-CT which has not inverted to granular microcrystalline quartz. In Chapter 9 it will be shown that δD for hydroxyls in opal-CT is isotopically similar to that for coexisting granular microcrystalline quartz when the two form at similar temperatures. Therefore, this material may not be a contaminant from an isotopic point of view.

6.3 Upper Cambrian

Oxygen and hydrogen isotopic data for cherts collected from marine carbonates of Upper Cambrian age are illustrative of the isotope relationships encountered in Phanerozoic samples. δD and δO^{18}-values for samples of this age are

Table 6-1

ISOTOPIC COMPOSITION OF UPPER CAMBRIAN CHERTS

Sample	wt.% H_2O	δD	δO^{18}	T^oC(FW)*	T^oC(Marine)*
1	.08	- 60.4	26.68	34	
2			25.90		
3	.12	- 71.5	25.95	32	
4			27.06		
160	.23	- 50.13	28.30	33	36
161	.07	- 67.9	24.08	38	
220			26.02		
221	.28	- 74.5	26.40	30	
259	.24	-105.3	20.06	37	
325	.16	- 50.5	27.82	34	38

* Explained in section 10.6

given in table 6-1 and are plotted in figure 6-2.

The data points in figure 6-2 form an approximate linear array parallel to the meteoric water line. Two lines are drawn through the data. One is a least-squares fit; the other is a line parallel to the meteoric water line adjusted to fit the data. The close similarity of the two lines strongly suggests that these cherts formed at approximately the same temperature from waters which were isotopically related according to the meteoric water equation given in section 3.4, or the same equation with a different intercept. Samples #325 and #160 define the upper end of this array and thus may have acquired their isotopic compositions in

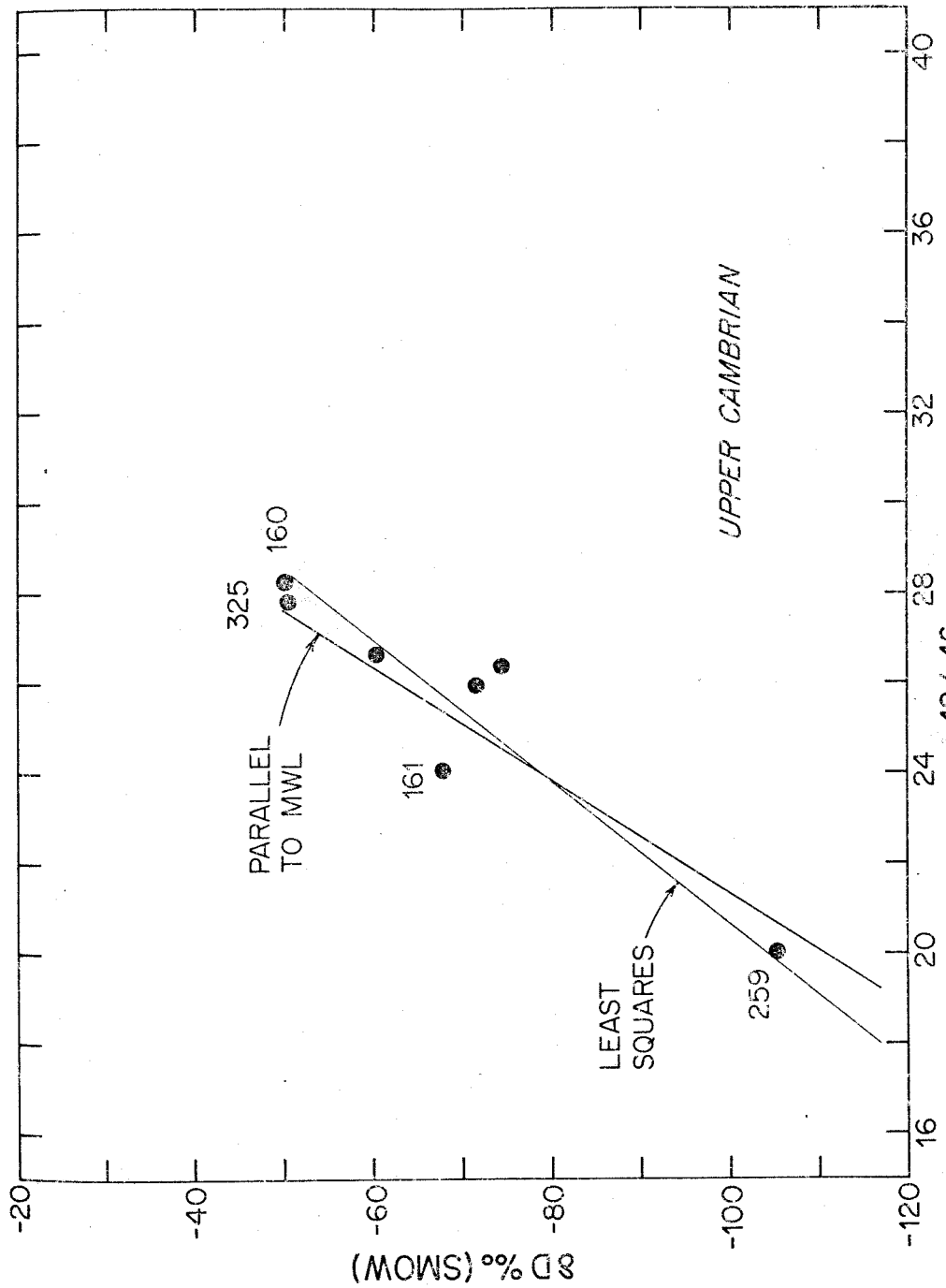

Figure 6-2

ISOTOPIC COMPOSITION OF UPPER CAMBRIAN CHERTS

equilibrium with ocean water. The other samples have clearly been formed from meteoric waters (or ocean water highly diluted with fresh water). It is necessary to emphasize that the formations from which these cherts were collected contain marine fossils and were therefore deposited in ocean water. The fact that cherts have apparently formed from meteoric waters in marine strata is not a contradiction. Instead, it indicates that the cherts have formed epigenetically at a time when meteoric waters were being circulated through the limestone. This is completely consistent with most of the recent hypotheses of chert genesis mentioned in Chapter 2.

Based on their isotopic composition alone, samples #160 and #325 can be considered candidates for true syngenetic cherts. However, it was observed in hand specimen and in thin-section that chert #160 is a silicified oolite. Therefore it, too, is an epigenetic chert. Its position at the positive end of the array leaves open the possibility that the replacement occurred under marine conditions.

No diagnostic petrographic relations are observed for sample #325. It may be a true syngenetic chert. However, it is possible that additional data will yield cherts with more positive δ-values which fall on the line. Samples #325 and #160 are candidates for marine cherts only because they have the most positive δ-values of those measured.

Sample #161, from the Potosi Formation in Missouri, was collected from the same bed and the same outcrop as sample #160. The two samples are different in that #161 contains abundant drusy quartz. Quartz druses such as these are normally thought to have formed by infilling of cavities during weathering. In this case, the Potosi druses are found as clasts in the overlying Ordovician Gasconade Formation. If they formed during a weathering interval, then this interval must have been pre-Ordovician. The isotope data show that #161 indeed formed epigenetically from meteoric waters. The picture that emerges is that the Potosi Formation contains two kinds of cherts. One formed as a result of secondary replacement of carbonate oolites under possible marine conditions. The other formed during a weathering episode in which fresh waters diagenetically altered the formation.

6.4 Ordovician

Isotope analyses were made on samples from the early, middle, and late Ordovician. The results are shown in table 6-2 and are plotted in figure 6-3. The data as a whole are suggestive of a linear array which is not as well defined as that for data for Upper Cambrian cherts. In figure 6-3, a least-squares fit is drawn together with a line parallel to the meteoric water line. These lines are approximately the same as those fitted to the Upper Cambrian data. As in

Table 6-2

ISOTOPIC COMPOSITION OF ORDOVICIAN CHERTS

Sample	wt.% H_2O	δD	δO^{18}	T^oC(FW)	T^oC(Marine)
6	.23	- 89.1	25.45	28	
244	.31	-103	26.86	21	
76	.30	- 52.83	29.66	29	32
81	.80	- 46.4	26.04	40	
85		- 54.1	26.13	38	
93	.03	- 79.3	25.69	31	
94			28.92		
95	.25	- 49.94	29.83	29	33
124	.28	- 44.11	27.79	37	40
158	.40	- 31.2	28.02	40	44
260	.57	-115	17.02	42	
274	.64	- 45	26.94	39	
159			28.34		
101			31.14		

the case of the Upper Cambrian cherts, there is a wide variation in the δO^{18} and δD contents for these samples. If this range of δ-values is interpreted as being due to various amounts of meteoric waters involved in the chert formation, then it is necessary to postulate that temperature differences existed in the waters in which these samples formed. Sample #244, in particular, is greatly displaced from a position in the "linear" array generated by the other samples. A quantitative estimate of the

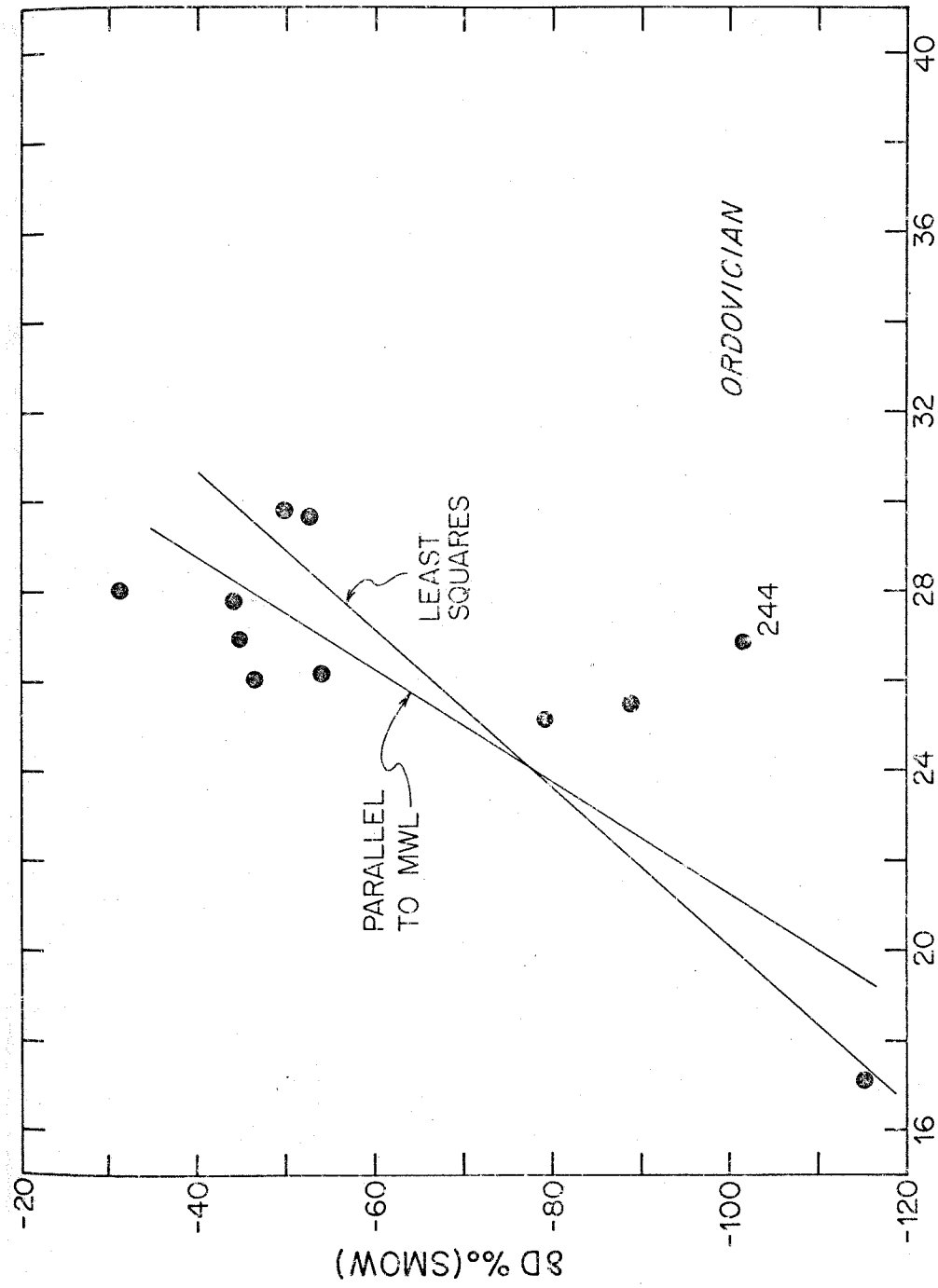

Figure 6-3

ISOTOPIC COMPOSITION OF ORDOVICIAN CHERTS

temperature differentials necessary to produce the observed scatter will be discussed later. The time interval represented by these data is approximately 75 million years (Kulp, 1961), about 2½ times the amount of time represented by the Upper Cambrian data. It is, therefore, not surprising that more scatter is observed, since a longer time is available in which severe climatic changes could have occurred over the area from which these samples were collected.

Of course, it is possible that the original isotope values have been modified since the original crystallization of these cherts, causing the less-systematic results of figure 6-3. This possibility will be considered in detail later.

6.5 Silurian and Devonian

Only one Silurian chert was analyzed, and this datum is included in the discussion of Devonian cherts. The data for this combined time interval of 85 million years are given in table 6-3 and plotted in figure 6-4. The least-squares curves determined for Upper Cambrian and Ordovician cherts are also included in this figure for comparison with the data.

Excluding sample #107, a metamorphosed chert, the data taken together form a group quite distinct from the Lower Paleozoic cherts. The spread in δ-values is greatly

Table 6-3

ISOTOPIC COMPOSITION OF SILURIAN AND DEVONIAN CHERTS

Sample	wt.% H_2O	δD	δO^{18}	$T^{\circ}C$(FW)	$T^{\circ}C$(Marine)
			SILURIAN		
281	.46	-60.2	30.01	26	
			29.87		
			29.80		
282			27.84		
			27.85		
			28.00		
			DEVONIAN		
107	.05	-45.9	21.50	54	
111	.08	-58.0	29.02	29	
139	.87	-37.4	30.1	33	36
268	.75	-52	29.05	31	
272	.12	-67.2	31.65	20	
152	.18	-56.1	31.98	22	25
270a	.35	-68.0	28.6	27	
270b	.45	-61.3	29.8	26	
89			33.64		
101			31.14		

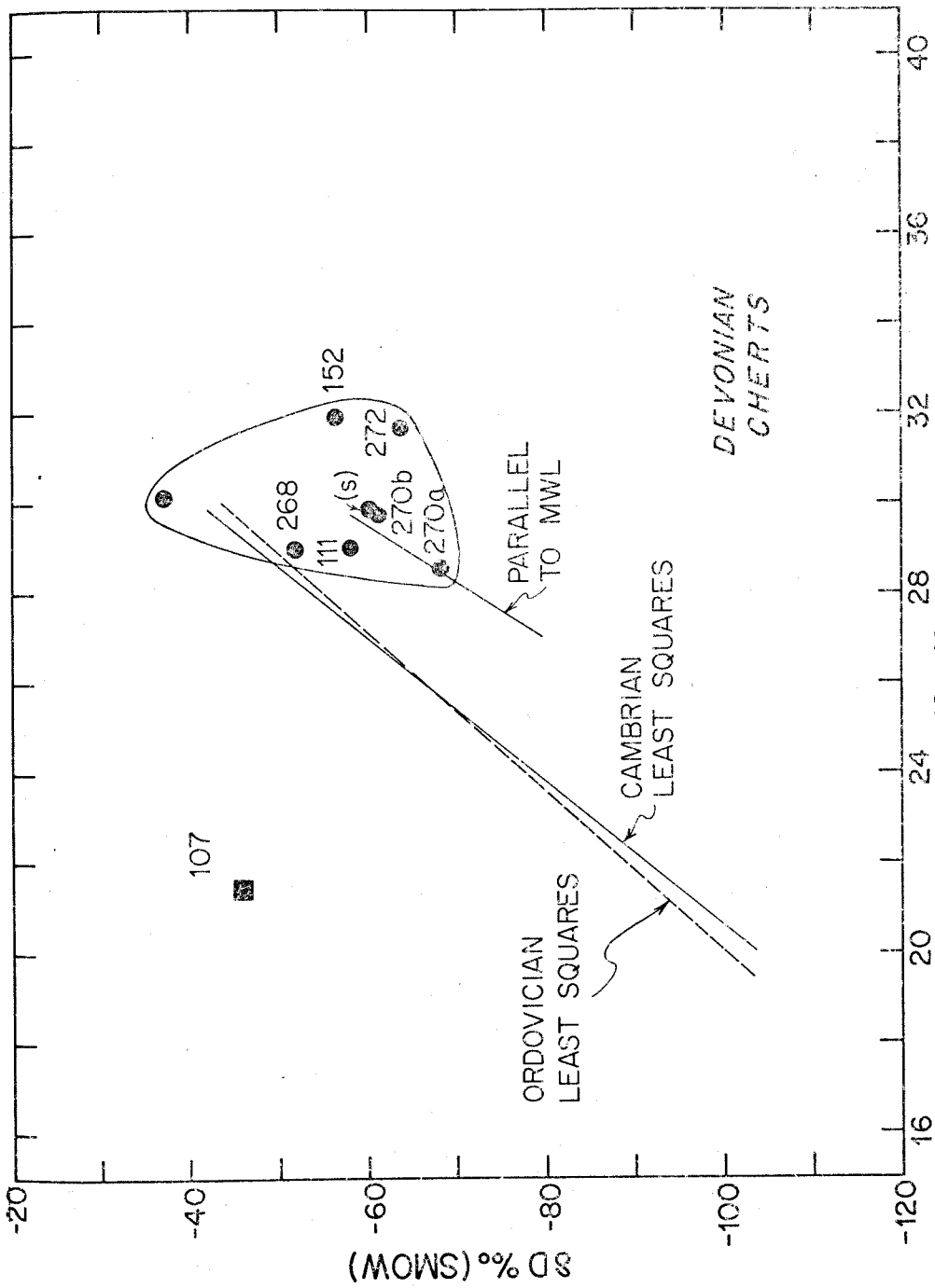

Figure 6-4: ISOTOPIC COMPOSITION OF DEVONIAN CHERTS. #107 IS A METACHERT. SAMPLE (s) IS SILURIAN CHERT #281. LEAST SQUARES LINES FOR CAMBRIAN AND ORDOVICIAN ARE SHOWN FOR REFERENCE.

restricted for these samples with no extremely light values observed. For additional reference, a line parallel to the meteoric water line is shown passing roughly through the data. Due to the restricted range of values, a least-squares fit would be meaningless. The lack of very light δ-values suggests the possibility of a dominantly marine origin for these cherts. Most of these samples are novaculites from the Ouachita system, and it is likely that more extensive sampling of other Devonian cherts would reveal a larger range of values, as in the case of the Lower Paleozoic.

A. Novaculites. The novaculites in figure 6-4 are samples #268, 111, 272, 270a, and 270b. Sample #270 consists of a hand-specimen of Caballos novaculite containing black and green translucent chert. The black chert is sample #270b; the green chert is sample #270a. From the figure it can be seen that the green chert is depleted in D and O^{18} relative to the black chert. A line drawn through these data is remarkably parallel to the meteoric water line. This strongly suggests that the green chert contains a different generation of silica which formed from lighter meteoric waters. The data are consistent with the possibility that the black novaculite is of marine origin and that it has been weathered or altered by meteoric waters to produce its observed isotopic composition.

The variations in δ-values obtained for all the novaculites are significant and may be due to variations in temperature of formation and silica subsequently precipitated from fresh waters.

Sample #107 allows some insight into the effects of metamorphism on the isotopic composition of the novaculites. This chert, also from the Ouachita system, was collected from southeast Oklahoma in an area which has experienced a low-grade regional metamorphism (Goldstein, 1959). Relative to the other novaculites, this metachert is depleted in O^{18} by about 8‰ and enriched in deuterium by about 15‰. The petrographic texture of this chert is quite different from the other novaculite specimens. Most of the silica is in the form of megaquartz rather than the usual granular microcrystalline quartz. This textural change, related to the metamorphism, is similar to that described and illustrated by Goldstein. The effect of low-grade metamorphism on the isotopic composition of cherts can thus be quite drastic. Cherts which have recrystallized to megaquartz can, therefore, be completely unsuitable for isotope studies aimed at elucidating conditions associated with initial chert genesis.

B. Ultra-weathered cherts. Sample #152 was collected from the type of siliceous earth or "tripoli" deposit discussed in section 2.6-L. This particular deposit in southern Illinois is considered to be disaggregated chert

occurring as the in-situ weathering residue of Devonian chert-rich limestones (Lamar, 1953). This sample represents the result of maximum weathering on granular microcrystalline quartz. In refractive index oils, the grains of granular microcrystalline quartz appear to retain their original petrographic characteristics, although a small amount of opal may be present. Isotopically, the sample is slightly enriched in O^{18} and deuterium relative to the other Devonian samples. This result suggests that maximum weathering of chert produces little effect upon the isotopic composition of granular microcrystalline quartz.

6.6 Carboniferous

Isotope data for cherts of Mississippian and Pennsylvanian age are given in table 6-4 and figure 6-5. Cherts consisting entirely of granular microcrystalline quartz free of organic matter define a small domain in figure 6-5. This domain is distinctly separate from the Lower Paleozoic data, but only slightly different from the Devonian data. A linear trend parallel to the meteoric water line is not immediately suggested by these points. Instead, it is possible that the data are grouped about two lines, one the meteoric water line and the other a line given by $\delta D = -6\ \delta O^{18} = +135$, as shown in the figure. This second line forms an upper boundary for all the Carboniferous cherts

Table 6-4

ISOTOPIC COMPOSITION OF CARBONIFEROUS AND PERMIAN CHERTS

Sample	wt.% H_2O	δD	δO^{18}	$T^{\circ}C$(FW)	$T^{\circ}C$(Marine)
		MISSISSIPPIAN			
8	.22	-84.9	28.63	22	
12			29.22		
24	.13	-57.9	29.30	28	
25	.10	-82.1	28.91	22	
35	.11	-57.6	16.10		
36	.13	-66.4	22.08		
41	.46	-63.3	31.33	22	
59	1.15	-38.0	29.06	35	
120	.66	-33.5	29.19	36	
121	.95	-28.8	28.30	40	
128	.18	-50.0	29.62	30	
136	.31	-49.9	31.76	25	28
	.30	-55.9	32.22	22	
137			33.14		
138	.10	-51.9	31.40	25	28
153W	.27	-38.2	34.32		
153G			34.04		
154	.25	-33.3	33.83		
156	.32	-50.8	31.76	25	27
157	.35	-51.5	31.39	25	28
165			31.86		
166			31.91		
167	.42	-62.0	33.42	18	20
169	.30	-57.5	30.72	25	
171	.33	-60.3	32.45	20	23
	.33	-60.1			
		PENNSYLVANIAN			
9	.07	-62.1	33.18	18	21
22	.25	-80.5	29.90	20	
		PERMIAN			
28	.49	-74.8	29.93	22	
209	.19	-96.1	38.90	-2	1
62			31.29		

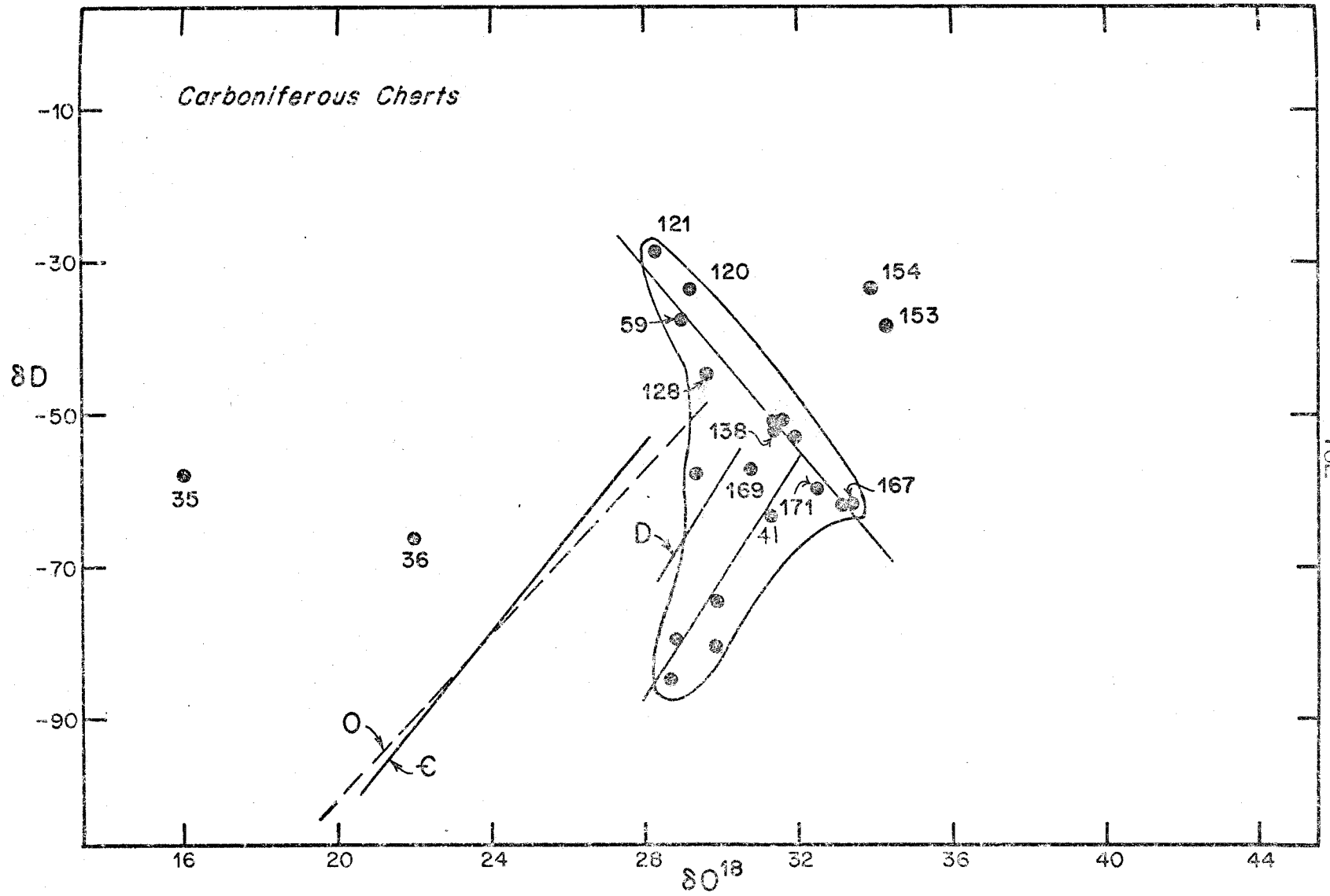

Figure 6-5: ISOTOPIC COMPOSITION OF CARBONIFEROUS CHERTS

except samples #153 and #154. It will be shown later that this line is also an upper boundary for cherts of other ages. In the case of the Mississippian samples, it is significant that samples from the Burlington Formation, #167, 171,169, 138, and 128, all fall on this line. These samples were collected from separate localities in Missouri and Illinois. Here the variations in isotopoc composition cannot be attributed to meteoric waters, since the trend is almost perpendicular to the meteoric water line. Instead, it is entirely possible that the variations are due to chert formation in the Burlington limestone at various temperatures. The position of these data at the "marine-end" of the array suggests that these cherts may have formed under marine conditions.

Samples # 120, 121, and 59 all contain more than .5 wt.% water. These are jet-black cherts with a dull luster and contain small amounts of unidentified reddish-brown material visible in thin-section. It is possible that this material is organic matter and that much of the water collected from these samples has been evolved by pyrolysis during the extraction procedure. If so, the δD determinations for these cherts should not be compared with the cherts largely free of such organic matter. In this respect it is significant that the δD for these samples is greater than for any of the other normal Carboniferous cherts.

On the other hand, these points do fall on the line defining the upper boundary of the Carboniferous data. It is possible that most of the water extracted from these cherts has not been derived from organic matter, and that these data represent cherts which formed at higher temperatures.

Samples #35 and #36 were collected from the hydrothermally-altered Escabrosa limestone in the Tombstone hills, Arizona. These are greatly depleted in O^{18} relative to other Carboniferous cherts. Petrographically, the cherts consist of fine-grained granular microcrystalline quartz cut with a network of microscopic veins composed of megaquartz and possible opal. Though they were collected at the same horizon and within 50 meters of one another, they are very different from each other isotopically. It seems clear that the hydrothermal activity has altered these cherts, resulting in a large depletion in O^{18}. Exchange at elevated temperatures with meteoric or magmatic waters probably caused this depletion.

Sample #41 was also collected from a mineral district, but it has an isotopic composition similar to other Carboniferous cherts. This sample is a nodular chert from the Mississippian Lake Valley limestone at Lake Valley, New Mexico. Petrographically, it is typical granular microcrystalline quartz and, with the exception of some veining,

shows no obvious recrystallization or other alteration related to the extensive mineralization in this area. Many of the cherts in this area occur as layers, veins, and secondary silicification related to faulting and mineralization. The nodular cherts display the same field relations as nodular cherts in normal, unaltered limestones of all ages. These apparently pre-date the mineralization, and were largely unaffected by the hydrothermal alteration of the strata which contain them.

Samples #153 and #154 were collected from the St. Louis Limestone near Jonesburo, Illinois. These cherts are more enriched in deuterium and O^{18} than nearly all of the other Carboniferous cherts. In thin-section, the granular microcrystalline quartz contains abundant cubic crystals of an isotropic mineral (halite ?), length-slow chalcedony, and an unidentified yellow, high index, fibrous mineral. These observations, combined with the observed isotopic enrichments, suggest that these cherts were formed from evaporite waters. Water which has suffered considerable evaporation is markedly enriched in deuterium and O^{18} and could account for the heavy δ-values for these samples. In hand specimen and thin-section, many fossil outlines can be seen in the chert, but any fossils originally present have been entirely silicified. The presence of fossils in what appears to be silicified evaporites suggests a very

complicated history for these samples. The important point for this discussion is that the anomalously heavy isotopic composition of the cherts appears to be related to an evaporite stage in the history of the St. Louis Limestone or an overlying unit.

6.7 Permian

Only one Permian chert was analyzed. Its isotopic composition is given in table 6-4 and is plotted in figure 6-6. It can be seen in the figure that this chert falls in the same range as Carboniferous cherts, and that meteoric water was probably involved in its formation.

Sample #209, also shown in figure 6-6, is a geode and will be discussed in Chapter 8.

6.8 Triassic

Triassic data are given in table 6-5 and are plotted in figure 6-7. The three samples from this period yield a wide spread of δ-values approximately parallel to the meteoric water line. This suggests that meteoric waters were involved in the formation of these samples.

Table 6-5

ISOTOPIC COMPOSITION OF TRIASSIC CHERTS

Sample	wt.% H_2O	δD	δO^{18}	T^oC (FW)
15	.57	-48.6	27.43	36
248	.07	-95.9	17.77	46
252	.73	-82.8	23.70	35

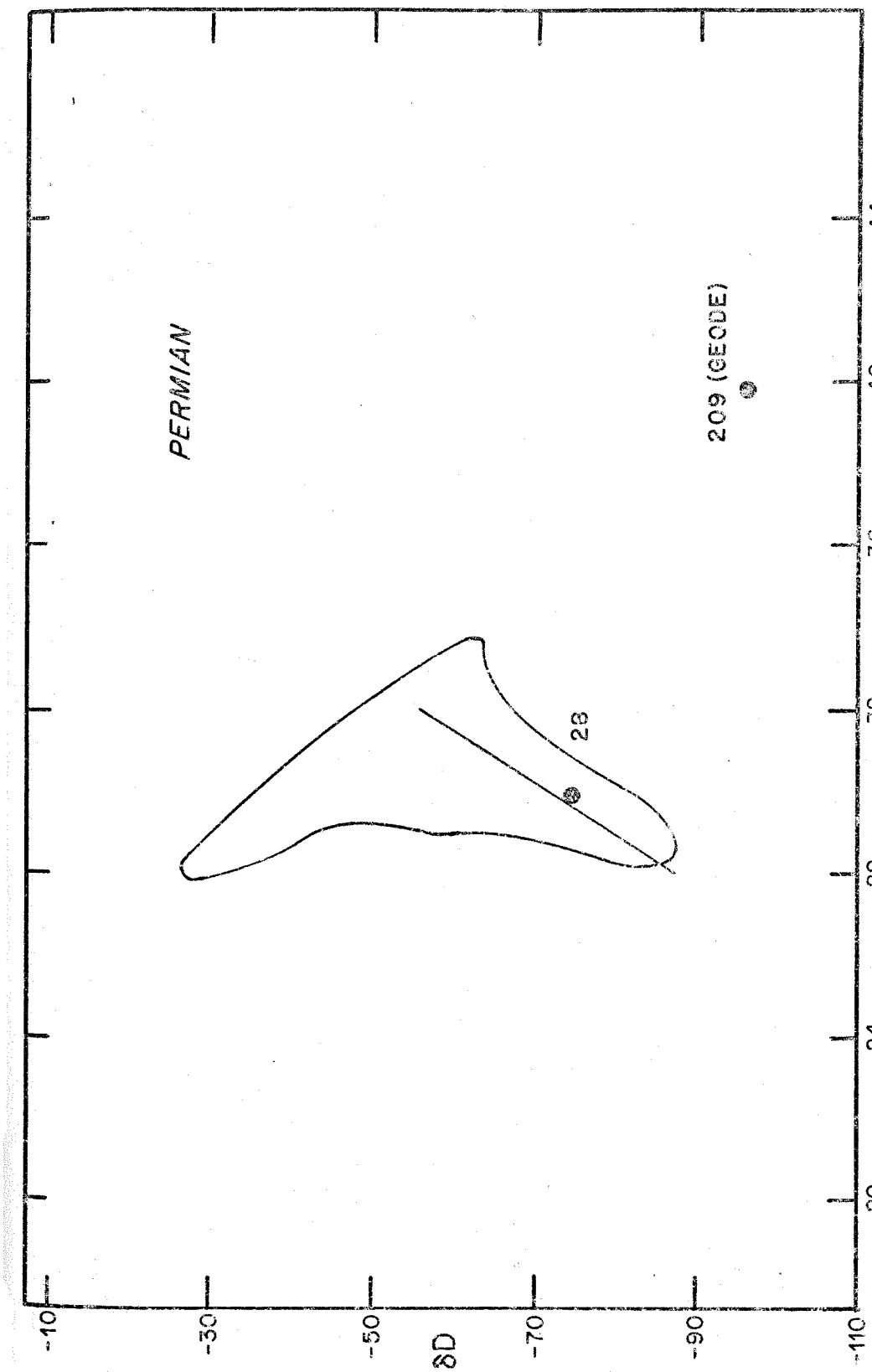

Figure 6-6: ISOTOPIC COMPOSITION OF PERMIAN CHERT

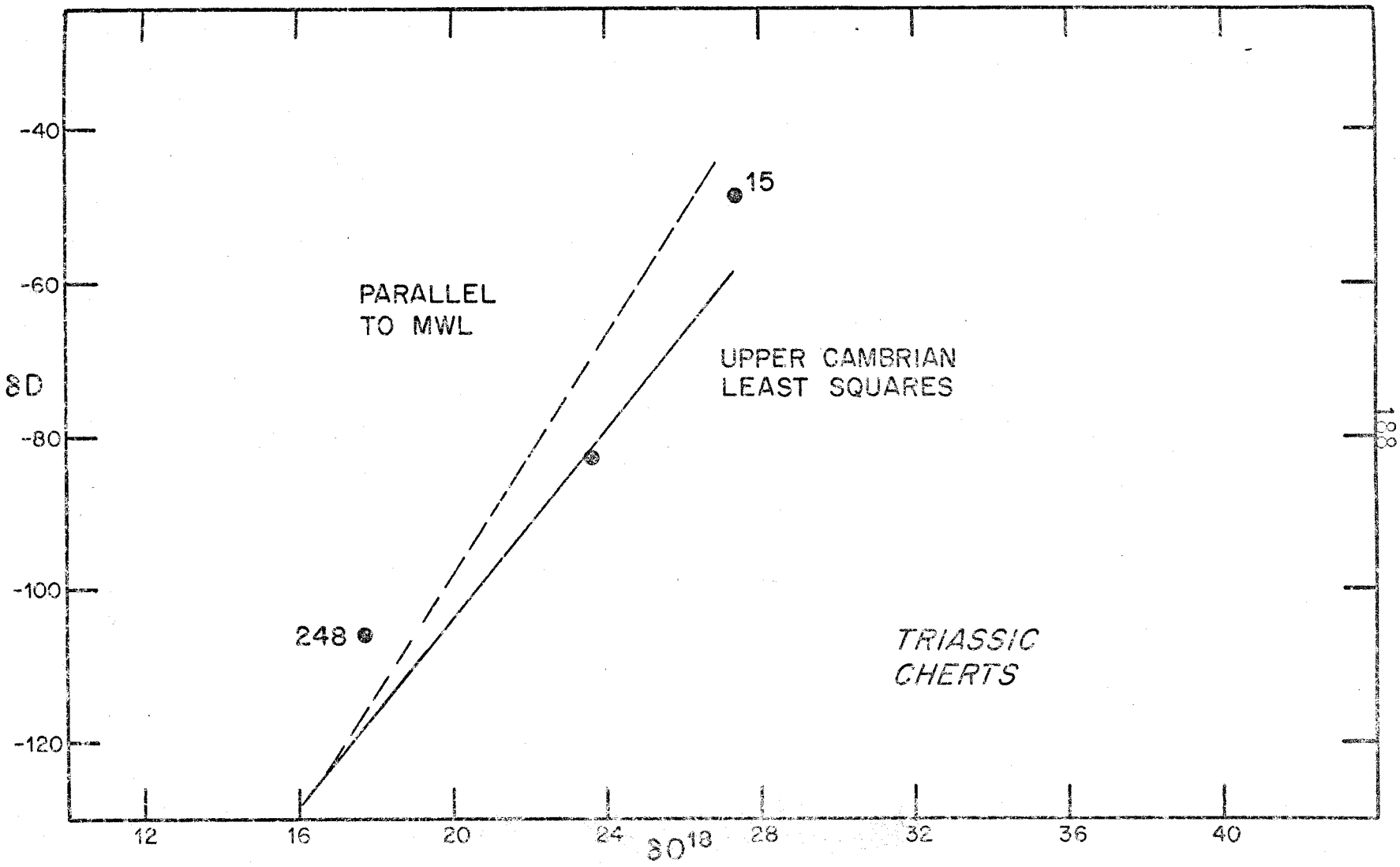

Figure 6-7: ISOTOPIC COMPOSITION OF TRIASSIC CHERTS

Sample #248 is a nodular chert in a carbonate unit. Its isotopic composition is greatly depleted in O^{18} and deuterium, suggesting that it formed from waters which were isotopically very light. In a subsequent chapter it will be shown that consideration of the isotopic composition of the coexisting carbonate for this sample also strongly suggests that the chert formed from isotopically light waters.

Sample #15 is a sample of petrified wood collected from a bentonite deposit in the Chinle formation at Zion Park, Utah. The sample is composed of granular microcrystalline quartz and in thin-section is virtually indistinguishable from normal chert nodules and beds. The grains are elongated and somewhat ragged in a manner strongly suggestive of chalcedony which has recrystallized to granular microcrystalline quartz. The validity of including a petrified wood sample in the present survey is open to question. A different sequence of silica diagenesis with concomitant special isotope effects may have been operative. The fact that this sample is related to the other two in an approximate linear relationship argues against such special effects. The isotopic composition of this sample apparently does not form a class of its own.

The position of sample #15 at the positive end of the array in figure 6-7 suggests that this sample may have formed under marine conditions. However, the Chinle formation is

thought to be a continental deposit (Gregory, 1950). It thus seems likely that Triassic cherts with more positive δ-values are likely to be found and that sample #15 does not define the marine end of the array.

6.9 Cretaceous

Several cherts of Cretaceous age were analyzed. Data for these are given in table 6-6 and are shown in figure 6-8 together with data for Tertiary cherts. Samples #262, 263, and 266 are nodular cherts from the same outcrop in central Texas. Two of these, # 263 and #262, are isotopically the same. Sample #266 is relatively depleted in O^{18} and deuterium and is linearly related to the other two with a slope matching that of the meteoric water line. The isotope data thus suggest that this chert formed at the same temperature as the other two, but in the presence of meteoric water.

Table 6-6

ISOTOPIC COMPOSITION OF CRETACEOUS CHERTS

Sample	wt.% H_2O	δ D	δO^{18}	T°C(FW)	T°C(Marine)
70	.22	-82.8	27.49	25	
262	.40	-67.9	32.65	18	20
263	.21	-64.9	32.62	19	21
266	.19	-72.8	31.57	19	
283	.91	-78.5	33.5	13	16
356	1.00	-79.1	35.90		11
			35.62		

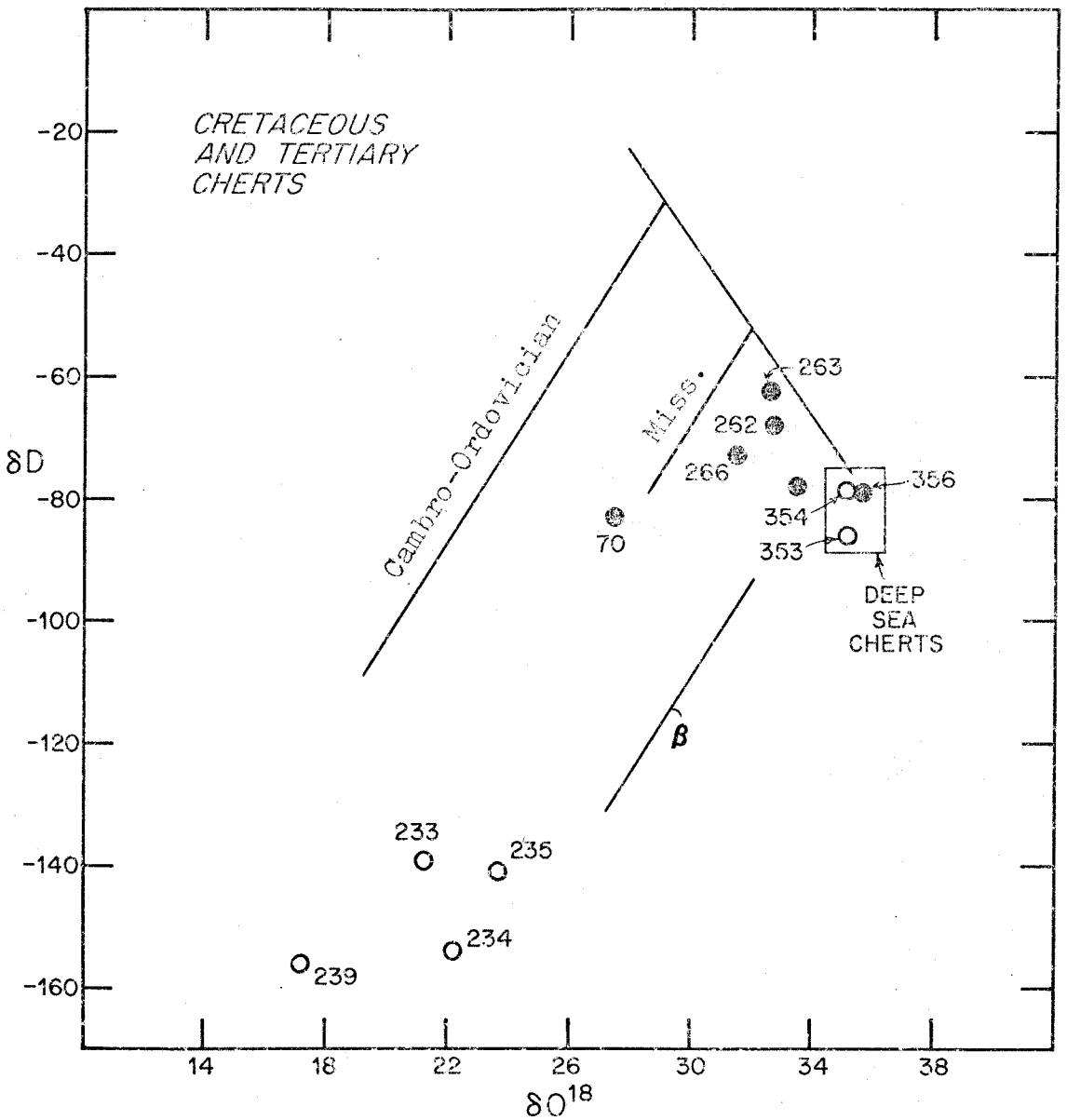

Figure 6-8

ISOTOPIC COMPOSITION OF CRETACEOUS AND TERTIARY CHERTS. OPEN CIRCLES ARE FOR TERTIARY CHERTS; FILLED CIRCLES ARE FOR CRETACEOUS CHERTS.

Sample #70 is a piece of petrified wood collected from a bentonite slope in the Aguja formation, Big Bend National Park, Texas. The Aguja formation contains probable marine and continental deposits. This sample is depleted in O^{18} and D relative to the central Texas cherts, but its isotopic composition does not lie on the locus suggested by the central Texas data. This may indicate that this petrified wood formed from fresh waters at a warmer temperature than the central Texas samples.

Sample #356 is a deep-sea chert from Cretaceous strata at the JOIDES Deep-Sea Drilling Project. This sample has a more positive δO^{18}-value than any observed for cherts collected from continental exposures. The extremely high δO^{18}-value is very likely due to a very low temperature of formation in a marine environment.

The δD value for this sample is not unlike that measured for many of the other Phanerozoic cherts. However, in the previous discussion it has been suggested that only those cherts which define the positive end of the data array for a given period are of possible marine origin. If this is correct, then this "very low-temperature" deep-sea chert is more depleted in deuterium than any of the other marine Phanerozoic samples. This is compatible with the idea that αD chert-water decreases with increasing temperatures, as was observed for other hydrous minerals by Savin and Epstein (1970a).

6.10 Tertiary

δ-values for Tertiary cherts are given in table 6-7 and are plotted in figure 6-8.

Sample #354 is a deep-sea chert from mid-Eocene strata cored at JOIDES site 64. δ-values for this chert are almost identical to the Cretaceous deep-sea chert, #356, and similarly suggest formation from ocean water at very low temperatures. Sample #353 is a deep-sea chert from JOIDES site 70. This sample is composed entirely of fibrous quartz (chalcedony). Nevertheless, both δO^{18} and δD for this sample are very similar to the mid-Eocene chert from site 64.

The fact that the hydrogen in this chert is 80‰ depleted in deuterium relative to ocean water clearly indicates a large fractionation such as that which occurs for hydroxyl groups. The evidence is therefore strong that this

Table 6-7

ISOTOPIC COMPOSITION OF TERTIARY CHERTS

Sample	wt.% H_2O	δD	δO^{18}	T°C(FW)	T°C(Marine)
233	.94	-138.6	21.12	24	
234	1.00	-153.9	22.19	17	
235	1.01	-141.1	23.70	17	
239	.92	-155.9	17.19	18	
354	.92	- 78.9	35.19		12
230			18.07		
236			23.92		
353	1.09	- 85.6	35.19		

water does not occur as fluid inclusions or mechanically trapped H_2O. Such H_2O would have δD-values near that of ocean water. Therefore, the suggestion of Folk and Weaver (1952) that chalcedony contains water in numerous fluid-filled cavities cannot apply to all samples of this material.

Samples #233, 234, 235, and 239 are cherts collected from fresh-water limestones in the Miocene Humbodt formation in northern Nevada. They are greatly depleted in deuterium and O^{18} relative to the deep-sea cherts. This depletion is almost certainly due to their formation from isotopically light meteoric waters.

If the δ-values for samples #354 and #356 are typical of marine cherts formed at ocean bottom temperatures, then line β in figure 6-8 is the probable locus of δ-values for cherts which form from meteoric waters at similar temperatures. The fresh-water Tertiary cherts fall to the left of this line, as would be expected if they formed at warmer temperatures characteristic of continental sedimentation. δ-values for two of these samples, #234 and #235 fall on the same locus as the central Texas Cretaceous cherts. Samples #233 and #239 line up more with the Upper Paleozoic cherts. Formation at temperatures similar to these older rocks is therefore suggested.

6.11 Precambrian Cherts

Studies of the isotopic composition of cherts in

Precambrian rocks are made difficult by several uncertainties. At present, Precambrian strata cannot be dated by means of fossils, and assignments based on lithologic correlations are necessarily suspect (James, 1960). Radiometric age determinations on cross-cutting intrusions and sills are useful in placing age limits on certain strata, but areas with such igneous activity are undesirable areas for chert sampling. Also, the age limits provided by these means frequently encompass hundreds of millions of years, so that the age of a given chert cannot be known accurately.

The preservation of the isotopic composition of silica is very uncertain. Precambrian cherts have had exceedingly long periods of time in which to experience metamorphism, hydrothermal activity, tectonic fracturing, and spontaneous recrystallization. The result is that cherts composed predominantly of granular microcrystalline quartz are less common in Precambrian strata, and are instead largely composed of megaquartz. Isotopic exchange during the transformation from granular microcrystalline quartz to megaquartz is likely to occur if any fluids are present. If the chert recrystallizes any included detrital quartz is also likely to be altered. It thus becomes difficult to petrographically assess the amount of the detrital component in the chert. Samples which are normally rejected for δO^{18} and δD analysis because of the unwanted detrital component might

therefore be mistakingly regarded as pure cherts and analyzed. Detrital quartz is likely to be of igneous and metamorphis origin and thus isotopically very different from authigenic silica. Cherts containing significant amounts of this material would thus be assigned misleading δ-values

A more subtle problem is the question of possible evolutionary trends in the geochemistry of silica diagenesis. In the Precambrian, the most extensive development of chert is associated with the great iron formations. As discussed in Chapter 2, the geologic conditions associated with the deposition, diagenesis, and metamorphism of these rocks is very uncertain. The factors which determine the isotopic composition of the granular microcrystalline quartz in these rocks may be entirely different from those operative in the case of cherts developed in association with carbonates or as independent beds. Nevertheless, granular microcrystalline quartz does exist in Precambrian cherts and several samples were investigated in this research.

Precambrian cherts analyzed for both δD and δO^{18} are listed in table 6-8. These data are plotted in figure 6-9. For reference, the curves obtained for such plots for the Phanerozoic cherts are included in figure 6-9.

Table 6-8

ISOTOPIC COMPOSITION OF PRECAMBRIAN CHERTS

Sample	wt.% H_2O	δD	δO^{18}	Age	T^oC(FW)	T^oC(Marine)
26	.25	-60.0	30.80	≥1.2	24	27
31	.26	-51.1	28.14	≥1.2	33	37
34	.50	-84.9	29.51	1.2	20	
188	.25	-68.0	19.11	1.3±		
			19.51		52	
278	.13	-80.3	17.55	?	53	
300	.56	-73.1	23.61	≈2	38	
304	.15	-56.2	14.91	≈3	72	

Sample #31 and sample #34 are from well-preserved beds of granular microcrystalline quartz occurring in the Mescal limestone, Arizona. Diabase intrusions in nearby correlative rocks have an age of at least 1,200 million years (Silver, 1960). These cherts were collected at Roosevelt Dam, Arizona, from a part of the Mescal limestone which is thought to be exceptionally well-preserved (Shride, 1967, p. 25). Diabase sills do not occur in this immediate area. These cherts have isotopic compositions not unlike those of Phanerozoic samples. Sample #34, in particular, falls on the diagram in a position characteristic of the Post-Jurassic samples.

Sample #26 is a chert from the Bass Limestone exposed at the bottom of the Grand Canyon, Arizona. The Bass

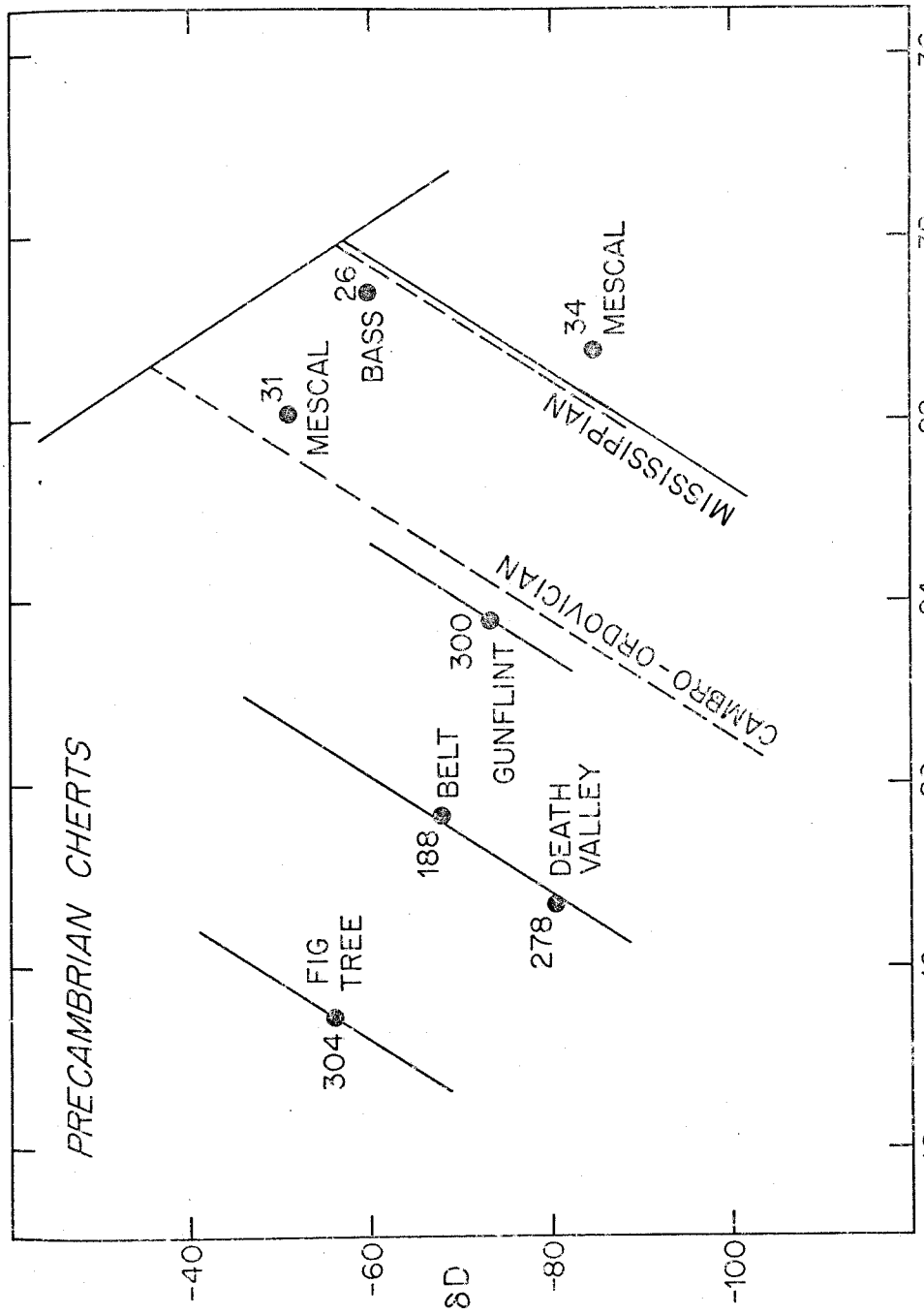

Figure 6-9

ISOTOPIC COMPOSITION OF SEVERAL PRECAMBRIAN CHERTS

Limestone is similar to the Mescal in some respects, and the two may be correlative (Shride, 1967, p. 81). Diabase sills are common in this unit as in the case of the Mescal. The limited exposure from which sample #26 was collected did not have any diabase intrusions, but Maxson (1967) has mapped sills in the next extensive exposure east of this outcrop, a distance of about 8 miles. The sample is considerably recrystallized, and consists predominantly of megaquartz. Surprisingly, this sample is not depleted in δO^{18} as might be expected since it probably recrystallized in response to nearby intrusive activity. Instead, its isotopic composition falls in the range of that characteristic of Upper Paleozoic cherts. It is unlikely that hydrothermal alteration or metamorphism would cause a large increase in the δO^{18} value of chert. The isotopic composition of the water involved in such activity would have to be more enriched in the heavier isotope than any ever measured, deduced, or postulated. It is more likely that the δO^{18} value of this chert is close to its original value, and has been preserved during recrystallization. This suggests that the environment during recrystallization was extremely dry, allowing little or no exchange with a fluid phase.

Of the Precambrian cherts analyzed, this sample falls closest to the isotopic composition of the southern Arizona samples. A line with slope 8 passing through sample #34

very nearly passes through sample #26. It is not inconceivable that these cherts formed at approximately the same temperature from waters isotopically related according to the meteoric water line equation, or one with a similar slope but different intercept. If so, sample #26 formed from possible marine or near-marine waters. Sample #31 does not fall exactly on this line. Its position to the left of this line may mean that it formed at a slightly higher temperature in the presence of fresh waters.

These three samples are remarkable because they show that at least some Precambrian cherts are isotopically indistinguishable from typical Phanerozoic cherts. This result is difficult to explain if the oceans at 1.2 Aeons were depleted in O^{18} by 4 - 5‰ as proposed by Perry (1967). It is also unexpected if cherts exchange with ground waters over geologic time as proposed by Degens and Epstein (1962). However, it is possible that these samples formed from waters enriched in O^{18} by evaporite processes and were initially much heavier. Indeed, Shride (1967, p. 29) has suggested that certain molds in the Mescal cherts represent former halite crystals, and that much of the Mescal Limestone formed under evaporite conditions. Also, Noble (1910, 1914) noted that some chert layers in the Bass Limestone contain small cubic depressions, possibly due to halite crystals. It is, therefore, possible that samples #26, 31,

and 34 are cherts which formed in evaporite environments. However, none of these samples (or any of the others collected from these locations) contain these cubic impressions. Furthermore, these cubes could just as likely be molds of pyrite rather than halite (L. T. Silver, personal communication, also see p. 204). More importantly, the hydrogen isotope data do not suggest an evaporite environment. If the hydrogen isotope ratios have been preserved, the isotopic composition of these samples may be considered indicative of chert formation under possible marine (#26 and #31) and non-marine (#34) conditions at temperatures similar to those associated with typical Phanerozoic cherts. Furthermore, there is no need to invoke isotopically depleted ocean water to explain the isotopic compositions of these samples.

Sample #300 is from the Gunflint Iron Formation and was collected by J. Schopf at Schreiber's Beach, Ontario. The approximate age of the Gunflint is thought to be 1,700 - 2,100 million years (Hurley et al., 1962). Petrographically, this sample is composed predominantly of megaquartz, indicating that the sample has probably been recrystallized. As shown in figure 6-9, this sample is isotopically similar to the Triassic and Lower Paleozoic cherts analyzed in this study. It is depleted in deuterium and O^{18} relative to the inferred values for Triassic and Lower Paleozoic marine cherts. Thus, if the hydrogen isotope data are valid,

this chert appears to have formed from fresh waters at temperatures similar to those of the Triassic and Lower Paleozoic samples. This is a very different interpretation from that of Perry (1967), who suggested that cherts of the Gunflint Iron Formation precipitated from ocean water which was about 10‰ lighter than present day ocean water. This chert is the only example of an iron-formation chert analyzed in this study. The possible non-marine origin of iron-formations is consistent with the idea of Hough (1958) and Govett (1966) that iron-formations may, in some cases, be lacustrine deposits.

Chert #188 is from the Sieyh Limestone in the Lower Belt Series in northwestern Montana. This is a nodular chert composed of granular microcrystalline quartz and occurs in a stromatalitic dolomite. The absolute age of this part of the Belt Series is uncertain, but is thought to be about 1,300 million years (Harrison, 1972). The isotopic composition of this chert defines a point which lies significantly to the left of the δ-values for Phanerozoic cherts as shown in figure 6-9. If its isotopic composition has been preserved, it is likely that this chert formed from meteoric waters at temperatures greater than any of the Phanerozoic samples.

Eslinger and Savin (1971) have argued that parts of the Belt Series reached temperatures of 300°C during burial.

It is unknown if the original isotopic composition of cherts exposed to such high temperatures of burial can be preserved. Exchange of the hydrous component with any fluids present seems likely at these temperatures. However, the silica in this sample has not recrystallized to megaquartz. It was shown in an earlier section that such recrystallization occurs in the case of cherts with thermally altered δ-values. The textural evidence thus suggests that these δ-values may have been preserved. It will be shown in Chapter 7 that the δO^{18} for this sample has certainly not equilibrated with the dolomite at high temperatures because the coexisting dolomite is enriched in O^{18} relative to the chert.

Chert #278 was collected from the Precambrian Beck Spring Formation at Saratoga Springs, Death Valley National Monument, California. The specimen analyzed was composed of about 50% granular microcrystalline quartz and 50% megaquartz. At this locality chert occurs sparsely as small nodules in the Beck Spring dolomite. At the disconformity between the Beck Spring dolomite and the overlying Kingston Peak formation there is a continuous bed of chert grading downward into the dolomite. The abundance of chert along the contact is suggestive of a lag deposit in which much of the underlying carbonate was removed during a pre-Kingston Peak weathering interval. If the topography were extremely

flat, the chert could accumulate and be cemented to form the bed presently observed at the disconformity. More recent occurrences of this sort were described in section 2.6-L. Leith (1925) has described several examples of silicified erosion surfaces in the Precambrian.

The field relations associated with this sample thus suggest the possibility that much of this chert may have formed during a Precambrian weathering episode in the presence of meteoric waters. As shown in figure 6-9, the isotopic composition of this sample is compatible with a meteoric water origin at a temperature of formation warmer than that for the Phanerozoic cherts. This proposed temperature is the same as that proposed for the Belt Series chert, #188.

The age of the Death Valley sample is not known. The Precambrian sedimentary sequence in Death Valley has been correlated with the Belt Series by Dunbar and Waage (1969). However, Wrucke and Shride (1972) have argued that diabase intrusions in this sequence and diabase in the southeastern Arizona Apaché Group are correlative. This would suggest a possible correlation with the Mescal and Bass limestones. Surprisingly, the Death Valley cherts contain the unusual cubic molds described previously for both Arizona cherts. (Acknowledgement to H. Lowenstam, who

spotted these molds while on a field trip with the author at Saratoga Springs). In this case, the molds are extraordinarily well-defined as pyrite molds. Most of them contain the fine striations perpendicular to one another on adjacent faces which are diagnostic of this mineral. Many of the molds are presently filled with limonite. The presence of such molds on the surfaces of chert is extremely unusual, and was not observed in any of the other cherts in this study. The fact that these molds occur in three widely separated localities in rocks which are possibly time correlative is most striking, and may have a greater significance if they formed during Precambrian weathering episodes.

Isotopically, the Death Valley chert is more similar to the Belt chert than to the Arizona samples. However, this presently has little significance with regard to the question of correlation, because rocks of drastically different ages with different geologic settings can have similar isotopic compositions.

Sample #304 is from the 3 billion year old Fig Tree Series in South Africa. It was collected by J. Schopf, who describes it as a bedded chert. Petrographically, it is composed almost entirely of megaquartz, indicating that it has probably been recrystallized to a greater extent than any other chert in this study. Isotopically, the sample falls outside the range of any of the other cherts, and has a

δO^{18}-value typical of cemented sandstones and metamorphic quartz (Savin and Epstein, 1970). The unusual isotopic composition of this sample may be accounted for in several ways. Initially, the original chert could have had δ-values similar to the other cherts in this study. The low-grade metamorphism of the Fig Tree Series could have greatly lowered the δO^{18}-value by exchange with isotopically light waters at elevated temperatures. The fact that the sample has been almost completely recrystallized to megaquartz supports this idea, but as shown previously, is not definitive evidence for isotopic exchange.

It is also possible that the δ-values have been little altered. Perry and Tan (1972) analyzed a number of South African cherts of this age and argued that the δO^{18}-values had been largely preserved in spite of the metamorphism. Assuming this, they suggested that these cherts were marine precipitates which had formed in an ocean depleted by 15‰ relative to present day oceans.

An alternative explanation is that these samples are lake deposits which precipitated at higher temperatures. Indeed, if the δD-value is for preserved hydroxyl groups, then the position of this point in figure 6-9 would suggest deposition from fresh waters at temperatures warmer than for any of the younger cherts in this study.

Positive evidence is lacking that this sample is a

"chert" in the sense of the other samples already considered. The eugeosynclinal metasediments of the Fig Tree Group consist largely of graywackes, carbonaceous argillites, arkoses, argillaceous sandstones, banded iron-bearing carbonaceous cherts, tuffs, and conglomerates (Engle, 1970). The cherts are thus interbedded with clastic deposits and may themselves contain a large detrital component. Usually, detrital grains of quartz in cherts are easy to identify because in thin-section they are relatively large and frequently rounded grains of clear quartz with uniform extinction. However, if the chert has been recrystallized to megaquartz, these detrital grains are no longer easy to identify, especially if they, too, have recrystallized.

As a consequence, the amount of detrital quartz in sample #304 is unknown. In thin-section, there is a suggestion that the recrystallized quartz grains are arranged in sub-planar layers. If these layers are relict bedding planes, this chert may actually be a recrystallized, fine-grained orthoquartzite. If so, it should not be considered in discussions of cherts and their isotopic composition.

6.12 Time Variations of δ-values

In the preceding discussion it has been shown that cherts for a given time period tend to have isotopic compositions which are restricted to certain domains in a δD- δO^{18} plot. These domains are not identical but are different for different geological time periods. This time-shift can be seen by comparing the isotopic compositions of samples from the different time periods as shown in figures 6-9, 6-10, and 6-11. In general, the data for a given time period are clustered about a line parallel to the meteoric water line. The intercept of this line is different for different geological time periods. Several models can explain the variations with time of this δO^{18} vs. δD relationship for the cherts. These will now be considered.

6.13 Climatic Variations

Temperature effects on the hydrogen and oxygen isotopic fractionations were discussed in general terms in section 3.4. Since climatic temperatures of the past are likely to have changed with time, it is of interest to examine the possibility that such temperature variations are the cause of the time shifts in the δD- δO^{18} relationship just noted. Assuming that these shifts are entirely due to climatic variations over the area of sampling, the isotope variations may be understood in the following way.

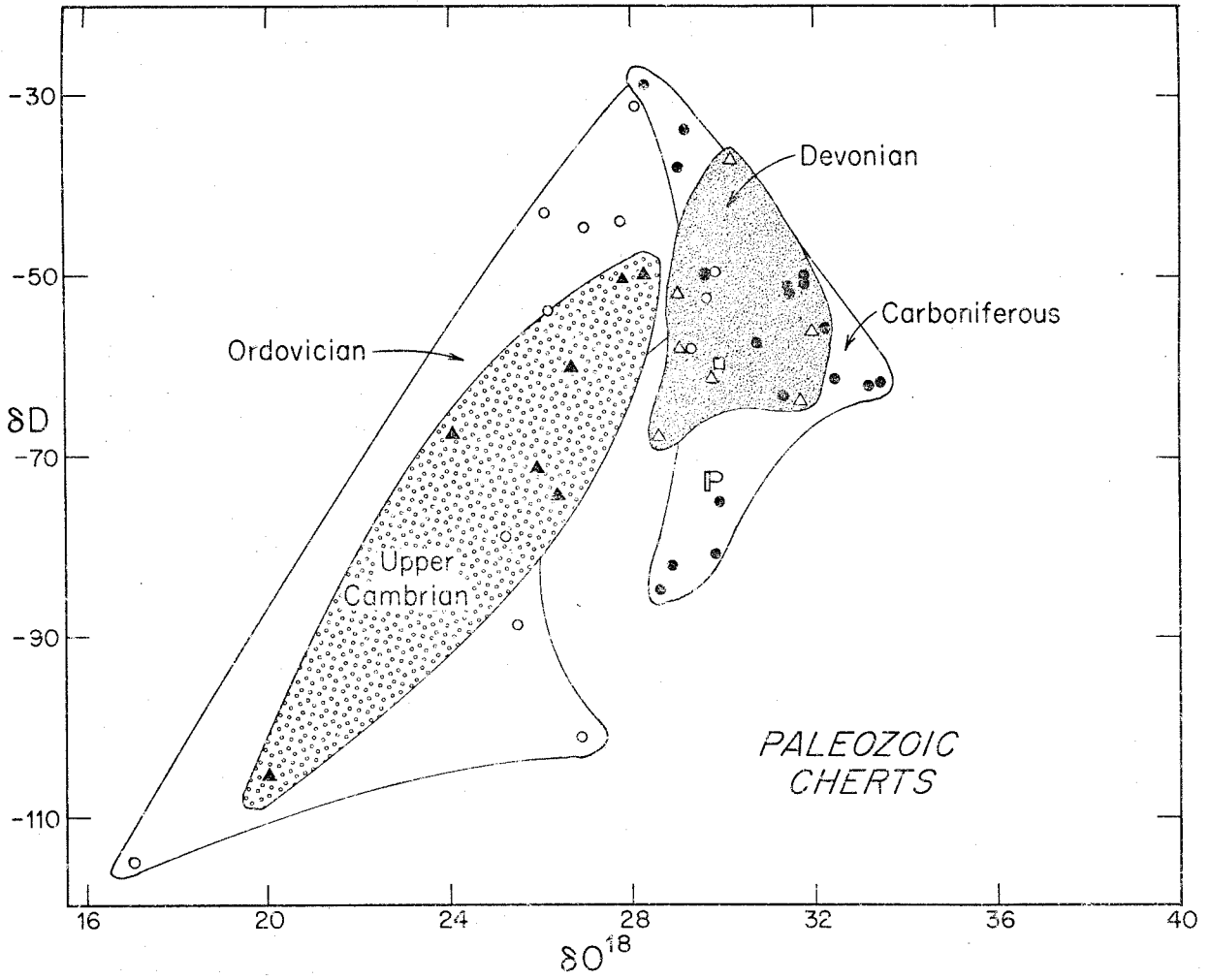

Figure 6-10

ISOTOPIC COMPOSITION OF PALEOZOIC CHERTS. FILLED TRIANGLES ARE FOR THE UPPER CAMBRIAN; OPEN TRIANGLES FOR THE DEVONIAN; OPEN CIRCLES FOR THE ORDOVICIAN; AND FILLED CIRCLES FOR THE CARBONIFEROUS.

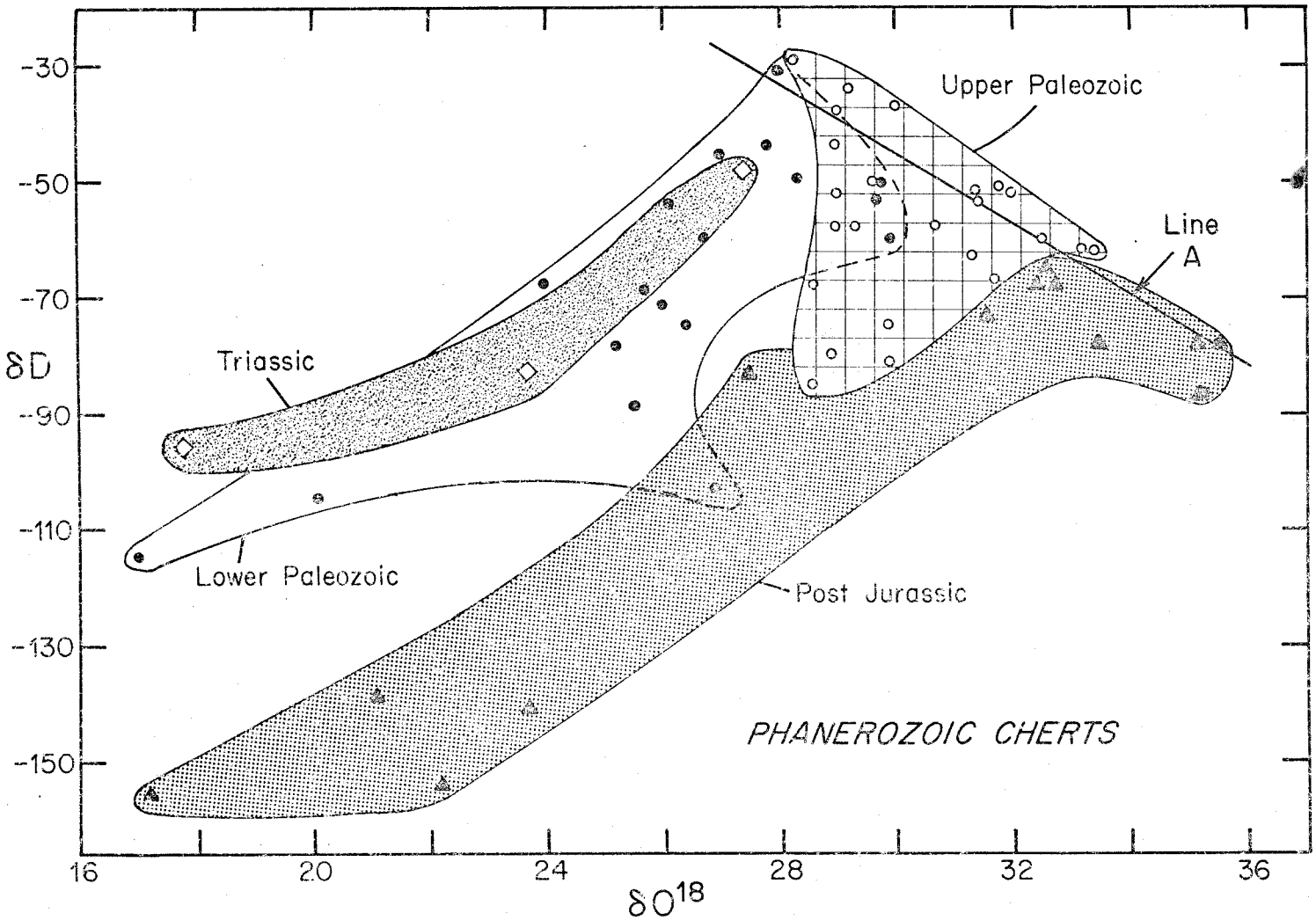

Figure 6-11
ISOTOPIC COMPOSITION OF PHANEROZOIC CHERTS.
THE DOMAINS ARE ELONGATED IN A DIRECTION
PARALLEL TO THE METEORIC WATER LINE.

In figure 3-3, if temperature T_1 is the average temperature over the Central and Western United States for a given time period, then line T_1 represents the locus of isotopic compositions of cherts which form from ocean water and meteoric waters at this temperature. If, in a later period, the average temperature decreases to a value T_2, then the locus of cherts which form at that temperature will shift away from the meteoric water line as shown in the figure. According to this model, the locus of δ-values for cherts should thus shift as a family parallel to the meteoric water line toward and away from the meteoric water line in response to climatic temperature changes over the area of sampling.

It is necessary to clarify exactly what temperature is being indicated according to this model. As pointed out in Chapter 2, it is likely that most cherts form diagenetically before the sediment is lithified. The temperature of chert formation is thus the sediment temperature under conditions of shallow burial.

The sediment temperature down to a few meters will undoubtedly equal that of the bottom water of any overlying water body. Therefore, cherts which form during <u>shallow</u> burial do so at temperatures approximately equal to that of the bottom water of the overlying water.

If the sediments are sub-aerially exposed, the

surface temperature will fluctuate daily and with the seasons. These fluctuations diminish rapidly with increasing depth of the sediment, becoming insignificant below 16 meters (Strahler, 1963, p. 218). Below this depth and before geothermal heating (1°/100 meters) becomes significant, the temperature of the sediment is equal to the yearly average surface temperature. Thus, cherts which form below 16 meters under these conditions do so at the yearly average surface temperature. Chert formation above this depth can occur at a variety of temperatures, but the time-scale of chert formation is probably so long that seasonal temperature changes are averaged out.

From the above considerations it is clear that, in spite of the fact that cherts form during diagenesis, their temperature of formation is probably characteristic of the climatic conditions existing at the site of their formation.

If the climatic variation model is used, the Paleozoic data in figure 6-10 can be explained in the following way. The temperature of formation of the Upper Cambrian and Ordovician cherts analyzed in this study were, on the average, similar. Hence, their isotopic compositions define similar domains parallel to the meteoric water line. In Devonian times, temperatures were cooler, causing the average isotopic composition of the cherts to define a line which is further away from the meteoric water line. In Mississippian

times the temperature dropped further and the average locus of δ-values for these samples shifted further from the meteoric water line. The Triassic data (figure 6-11), being similar to Cambrian and Ordovician data, indicate a climate with temperatures similar to those Periods. δ-values for the Post-Jurassic cherts (figure 6-11) provide a δO^{18}- δD relationship which falls farthest away from the meteoric water line and indicates the coolest temperatures. According to this model, line A of figure 6-11 represents the approximate locus of δ-values for cherts which form under marine conditions.

This reasoning may be extended to the Precambrian cherts shown in figure 6-9. According to this interpretation, the Arizona cherts formed under temperature conditions similar to those encountered in the Carboniferous and Post-Jurassic. The Gunflint is similar to the Triassic and Cambrian, while the others indicate formation at considerably warmer temperatures.

The temperature variations suggested by this model have so far been considered only in qualitative terms. Possible values for these temperatures can be assigned only if the isotopic temperature-fractionation curves for quartz-water are known. Quantitative values for the D/H temperature fractionation between chert and water are completely unknown. In the case of O^{18}/O^{16}, the quartz-water

fractionation has been examined experimentally at high temperatures by Clayton et al. (1972) and calculated for lower temperatures by Becker (1971). As mentioned in Chapter 3, Becker's calculations of the fractionation factors for the isotopes of oxygen between quartz and water were adjusted so that the results would conform to the high temperature experimental results of Clayton et al. It is possible to use Becker's curve (figure 3-1) to assign temperatures to the isotope data for cherts.

In order to do this, it is assumed that (1) line A of figure 6-11 is the locus of isotopic compositions for cherts in equilibrium with ocean water, and (2) the isotopic composition of ocean water has not changed with geologic time and is equal to 0.0 per mil in the SMOW scale.

Numerical results are given below for a number of arbitrary δ-values.

δ	$1000 \ln \alpha$	$\frac{10^6}{{}^\circ K^2}$	${}^\circ C$
38	37.3	12.35	11.6
36	35.4	11.75	18.7
34	33.4	11.12	26.9
32	31.5	10.65	33.4
30	29.6	9.97	43.7
28	27.6	9.37	53.7
26	25.7	8.77	64.7
24	23.7	8.13	77.7

These temperatures are placed next to the locus of supposed marine cherts in figure 6-12 at the appropriate δO^{18}-value. The locus of δ-values for cherts which form from meteoric waters at one of these temperatures is given by a line parallel to the meteoric water line. This line does not pass exactly through the δ-values for the marine chert which forms at this temperature, but is offset in δD by +10‰. This offset reflects the offset of the meteoric water line from SMOW (see figure 3-2).

A number of lines parallel to the meteoric water line and corresponding to the temperatures given above for marine cherts is given in figure 6-12. Also shown in the figure are several domains and points to show the observed variations in the isotopic compositions of cherts. From this figure, temperatures deduced using Becker's curve and the given assumptions can be obtained for several geologic periods.

The average climatic temperature for the Upper Paleozoic is 33°C; for the Lower Paleozoic and Triassic, 44° - 54°C. Precambrian cherts #188 and #278 formed at about 60°C. The deep-sea cherts, instead of having formed at very low temperatures, give temperatures of 19°C.

These temperatures are surprisingly high for climatic temperatures. The 40° - 50°C temperatures indicated for the Lower Paleozoic and Triassic probably exceed the temperature

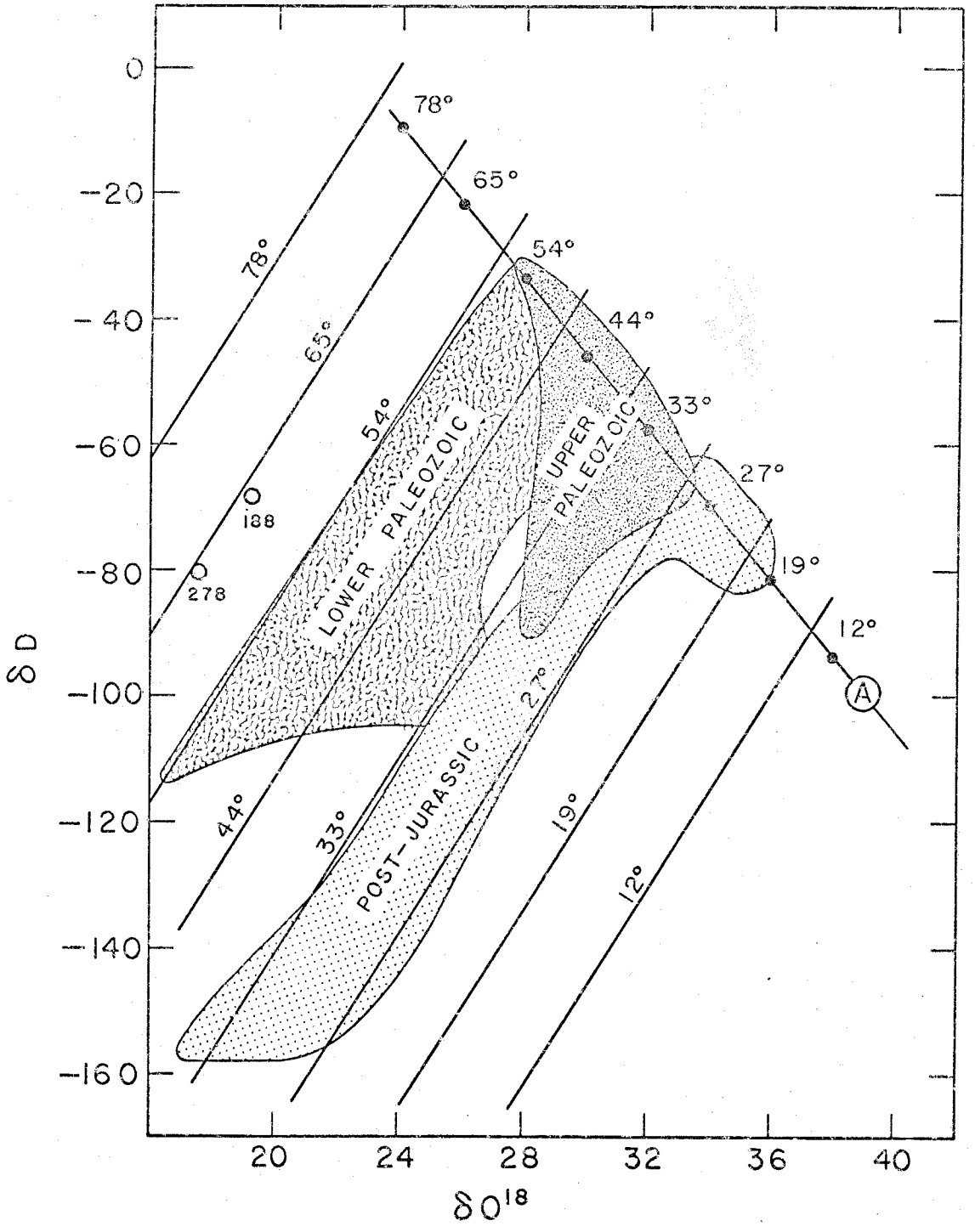

Figure 6-12: TEMPERATURES OF CHERT GENESIS BASED ON THE CALCULATED QUARTZ-WATER OXYGEN ISOTOPE FRACTIONATION OF BECKER (1971). LINE A IS FOR "MARINE" CHERTS.

tolerance of most invertebrate organisms. Also, previous carbonate paleotemperature determinations back to the Permian do not indicate such warm temperatures. It therefore is likely that one of the following conclusions is valid: (1) The isotope variations are not entirely due to climatic variations, (2) Becker's curve is only approximately correct, or (3) Becker's curve is appropriate for pure alpha-quartz, but not for the granular microcrystalline quartz found in cherts.

Another approach to assigning temperatures is to calibrate the natural variations with cherts that formed at known temperatures. Unfortunately, there are no known cherts for which the temperatures of formation are precisely known. However, in Chapters 7 and 9 it will be shown that in several instances temperature limits can be placed on several of the cherts for which the δO^{18}-values have been measured. From this information and certain assumptions concerning the isotopic composition of the hydrosphere, several natural calibration points for the quartz-water oxygen isotope fractionation curve will be proposed. These points are shown in figure 6-13, together with Becker's curve. Also plotted is a straight line which passes roughly through the points for temperatures below 50°C and the high temperature experimental data of Clayton et al. (1972). It is felt that this curve is a more likely approximation to

natural chert samples. The equation is

$$1000 \ln \alpha = 3.09 (10^6 T^{-2}) - 3.29$$

T = temperature in ^{o}K

Figure 6-14 shows the temperatures for marine cherts deduced from this equation assuming that δO^{18} of ocean water has always been 0.0 per mil. The temperature uncertainty shown in the figure corresponds to an uncertainty in the isotopic composition of ocean water of $\pm$1‰.

The model temperatures shown in this figure are not unreasonable estimates for past climates. Most of the samples yield temperatures of 35°C or lower. The Post-Jurassic cherts have temperatures of 10° - 25°C, in approximate agreement with previous carbonate Paleotemperature measurements (Bowen, 1966). The implications of these temperatures and a comparison with the fossil and rock record will be given later. The present discussion is meant only to show that climatic variations provide a viable interpretation of the isotopic data.

Hydrogen isotope fractionation. The possible variation with temperature of δD for cherts in equilibrium with ocean water can be obtained from figure 6-14. It is thus possible to propose a curve for the fractionation of hydrogen isotopes with temperature if it is assumed that δD of ocean water has been 0.0 ‰ over the time interval

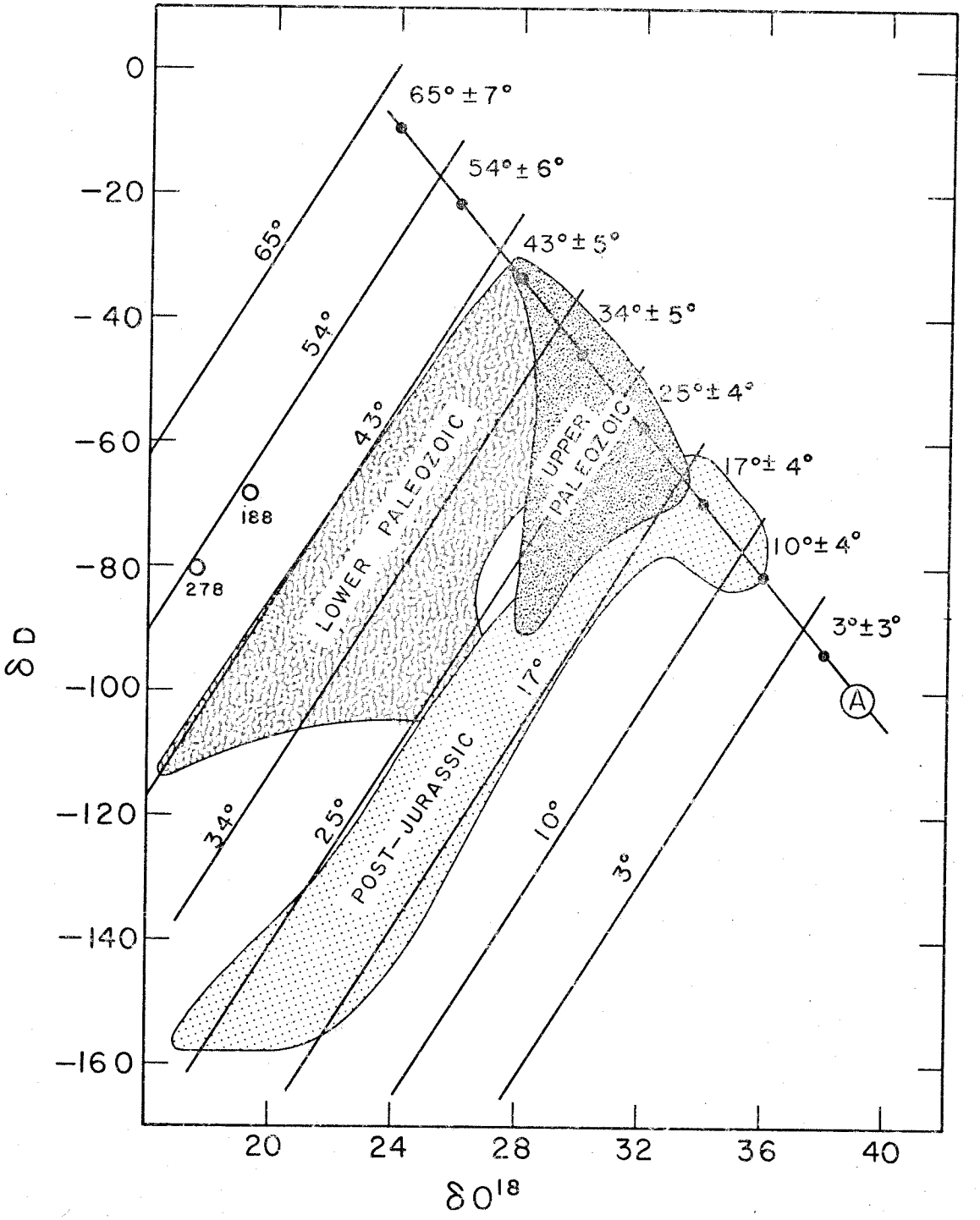

Figure 6-14: TEMPERATURES OF CHERT GENESIS BASED ON THE QUARTZ-WATER OXYGEN ISOTOPE FRACTIONATION SHOWN AS CURVE I, FIGURE 6-13. LINE A IS FOR "MARINE" CHERTS.

represented by the data in figure 6-14. The fractionation with temperature obtained in this fashion is shown in table 6-9 and figure 6-15. For purposes of discussion, the fractionation suggested by Savin and Epstein (1970a) for kaolinite at surface temperatures is indicated in the figure (plotted here as -30‰ at 25°C, but with the possible range indicated by the error bars).

If extrapolated linearly to higher temperatures, this curve indicates 1000 $\ell n \alpha$ D quartz-water = 0 at about 100°C. 1000 $\ell n \alpha$ for most systems is expected to approach zero only at very high temperatures, and it seems unlikely that the silica system should be so unusual. However, if the work

Table 6-9

HYDROGEN ISOTOPE FRACTIONATION WITH TEMPERATURE BETWEEN GRANULAR MICROCRYSTALLINE QUARTZ AND WATER

δD	T°C	1000 $\ell n \alpha$ ^{Hy} chert-water	$\frac{10^6}{(T+273)^2}$
-93	3±3	-97.6	13.4-12.8
-81.5	10±4	-85.0	12.1-12.8
-70	17±4	-72.6	11.6-12.2
-57.5	25±4	-59.2	11.0-11.6
-45.5	34±5	-46.6	10.3-11.0
-33.7	43±5	-34.3	9.7-10.3
-21.5	54±6	-21.7	9.0-9.7

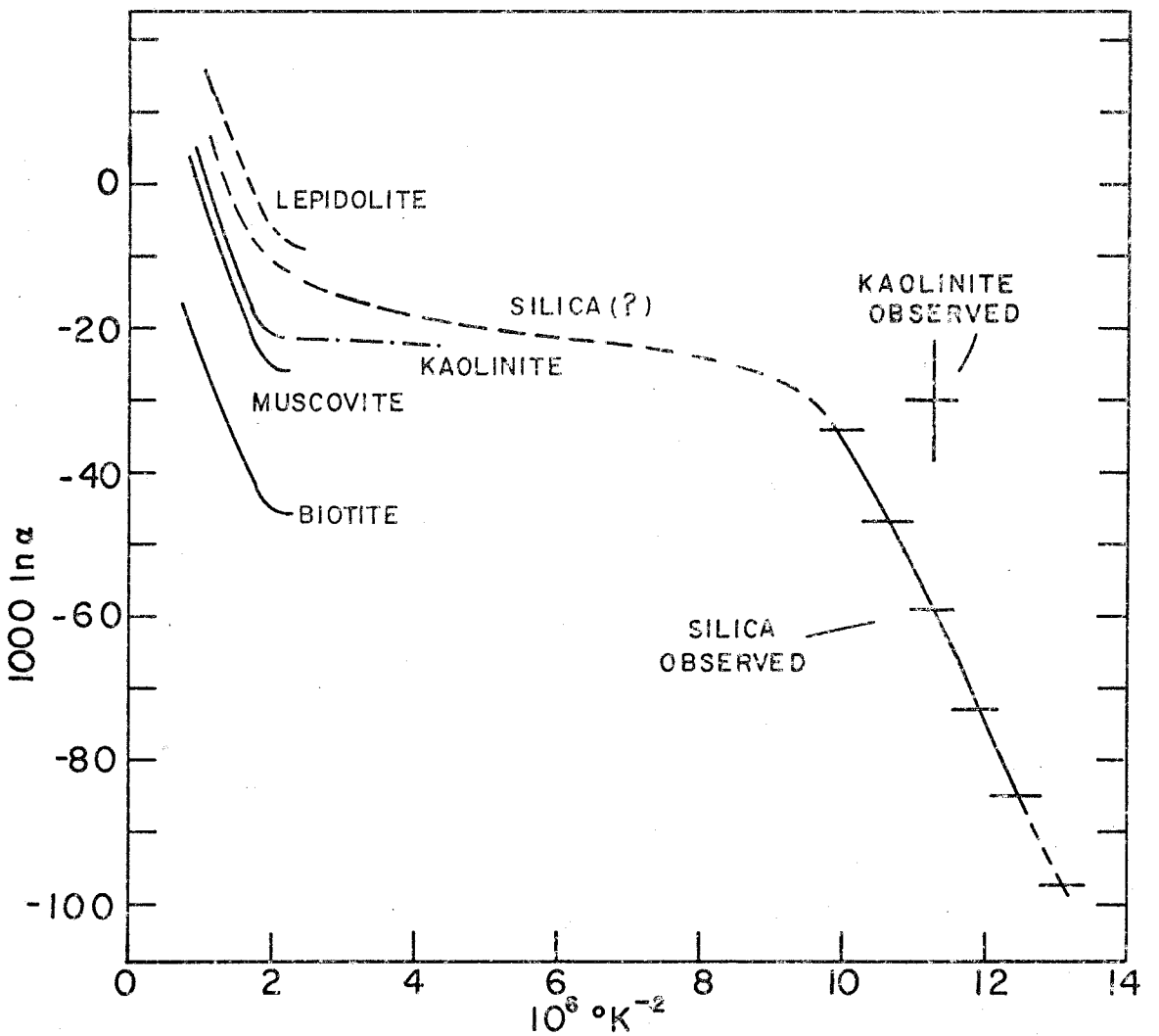

Figure 6-15

POSSIBLE HYDROGEN ISOTOPE FRACTIONATION WITH TEMPERATURE FOR CHERT-WATER. CURVES FOR BIOTITE, MUSCOVITE, KAOLINITE, AND LEPIDOLITE ARE AFTER SUZUOKI AND EPSTEIN (1972). OBSERVED FRACTIONATION AT 25°C FOR KAOLINITE IS FROM SAVIN AND EPSTEIN (1970a).

of Suzuoki and Epstein (1972) is considered, this objection is less serious. These authors showed that if their high temperature experimental fractionations for kaolinite are to be compatible with the low temperature fractionation observed by Savin and Epstein (1970a), then the curve must assume a near-zero slope between 30°C and 400°C. This curve is shown in figure 6-15.

If the silica-water curve behaves similarly, it is possible to deduce its approximate behavior at higher temperatures using the results of Suzuoki and Epstein. They observed that the hydrogen isotope fractionation is dependent upon the cationic composition of the mineral in question, and that it is determined by the mass-to-change ratio of these cations (excluding cases involving hydrogen bonding). In the case of silica, this ratio is similar to that for Al^{+3} and Li^{+1}. Therefore, the high temperature part of the curve for silica should fall in the same region as the kaolinite and lepidolite curves determined by Suzuoki and Epstein. Their curves for several hydrous mineral-water fractionations with temperature are shown in figure 6-15 together with the deduced silica-water curve.

If the silica-water curve shown in the figure is correct, it indicates that cherts formed at sedimentary temperatures in ocean water or meteoric water should <u>never</u> have δD-values more positive than about -25‰. The

greatest values encountered in the preceding survey was -31.2‰, and does not exceed the proposed maximum value.

In conclusion, it may be said that the temperature fractionation curve for hydrogen which arises as a consequence of assuming a climatic change model and the quartz-water oxygen isotope fractionation curve in figure 6-13 is not inconsistent with previous work on other hydrous minerals.

Conclusion for climatic change model. The isotope data obtained for the cherts can be explained if the locus of δD- δO^{18} values is parallel to the meteoric water line at a specified temperature and shifts with time due to climatic variation of the area of sampling. Specific temperatures are assigned in figure 6-14, but must be viewed with caution due to uncertainties used in deducing the quartz-water oxygen fractionation curve at low temperatures. It is more reliable to suggest that if the time-effect seen in the isotopic compositions of cherts is due to climatic temperature variations, then the temperature differences over geologic time are on the order of those shown in figure 6-14.

6.14 Changes in the Isotopic Composition of the Oceans as a Cause of the Isotopic Variations

The effect of possible changes in the isotopic

composition of ocean water with regard to its possible effect on the isotopic composition of cherts was discussed in Chapter 3. In this section, these and other models will be tested against the isotopic composition of the cherts to see which, if any, are viable explanations of the data.

A. Glaciation. Snow and ice presently deposited in the Arctic and Antarctic have δD and δO^{18}-values lighter than -160 and -22 per mil respectively (Craig, 1961a). It follows that during ice ages large amounts of isotopically light water will accumulate at the poles, causing ocean water to be enriched in the heavier isotopes. The amount of enrichment depends upon how much water becomes locked up at the poles. Estimates for the maximum enrichment during the Pleistocene glaciations are .5‰ (Emiliani, 1966), and 1.5‰ (Shackleton, 1967), (Craig, 1965). Even if these estimates are low by a factor of two or three the variations in the isotopic composition of ocean water are too low to account completely for the δO^{18} variations of the cherts. If the combined effect on the hydrogen as well as oxygen isotopes is considered, it is possible to rule out completely the process of glaciation as a major cause of the time-shift of the δ-chert values.

Figure 6-16 shows the meteoric water line and indicates the range of δ-values for the isotopic composition of ocean water which can occur during glaciation

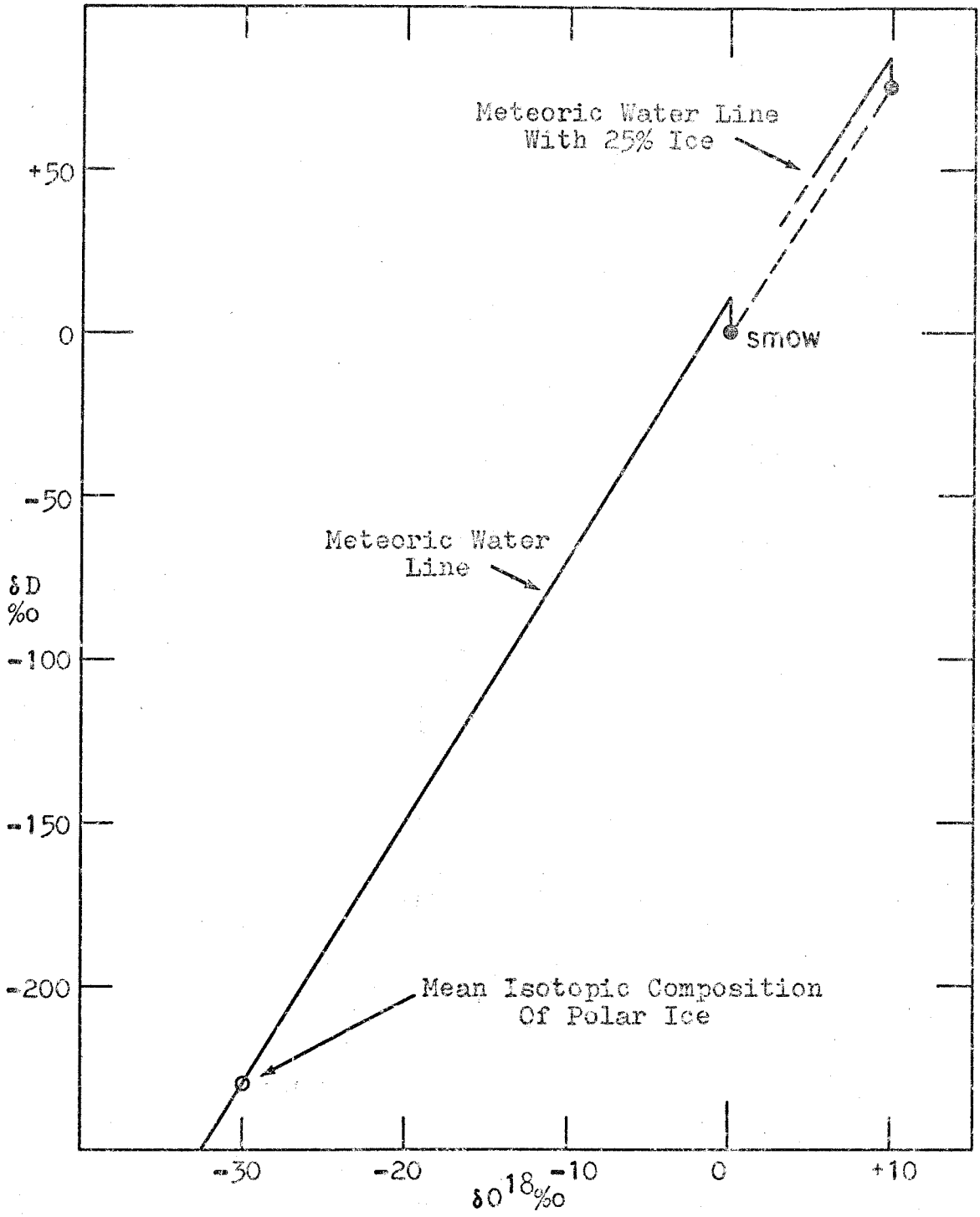

Figure 6-16: CHANGE IN ISOTOPIC COMPOSITION OF OCEAN WATER AND THE METEORIC WATER LINE WHEN 25% OF THE HYDROSPHERE IS ICE

(dashed line). The ocean water values are obtained by subtracting the isotopic composition of polar waters from SMOW. This forces the ocean value away from SMOW along the dashed line. The more polar water subtracted, the greater the displacement of the oceanic value from SMOW.

Point A represents a condition in which about 25% of the hydrosphere is locked up in ice. It can be seen that even with this inconceivable amount of ice the position of the meteoric water line has shifted very little in a direction perpendicular to itself. Thus, glaciation cannot explain the large time-shifts for the locus of chert δ-values.

This argument is valid only if the offset of SMOW from the meteoric water line has remained approximately the same over geologic time. Harmon Craig (personal communication) has suggested that since this offset is due to complicated kinetic effects during evaporation, its magnitude should depend upon wind-speeds, surface temperatures, and other climatic factors. He suggests that variations in these factors constitute a possible explanation for the time-shift of the cherts. This would allow the locus of chert values to move toward and away from the meteoric water line as the offset of SMOW varies. In addition, as the offset increases, the effect of glaciation upon the isotopic composition of the oceans increases.

It is not known how much the offset of SMOW can vary.

At present it is less than the data scatter for natural waters. Until the climatic effects on this offset can be quantitatively understood it is not possible to evaluate this mechanism as an explanation for the time-shift.

The shift in the δ-values of SMOW along the dashed line during major glaciations is a feature which could possibly be obtained from corresponding shifts observed in the δ-values of ancient marine cherts. Although the present data are insufficient in number, examination of figure 6-11 offers some suggestion that the locus of "marine" δ-values for cherts of the Upper Paleozoic are displaced somewhat to the upper right relative to those of the Lower Paleozoic. It is an intriguing possibility that some glaciation greatly preceded the supposed Permian ice age and left its record in the isotopic composition of these cherts.

B. Sedimentation. The effect of sedimentation of hydrous minerals on the isotopic history of the hydrosphere was reviewed and qualitatively considered in section 3.6. A sedimentation model was shown in figure 3-5. According to this model, δ-values for the more recent cherts should lie to the left of those for the older cherts. This is true in a few cases, such as data for the Triassic vs. the 1.2 billion year (?) Arizona cherts. In general, however, the shift is exactly opposite to this. In addition, the observed

shifts equal or surpass the total isotopic effect of sedimentation on the isotopic history of ocean water calculated by Savin and Epstein (1970c) for all of geologic time.

It is clear that this model cannot in itself explain the time-shift of δ-values for the cherts. Although this process is undoubtedly a factor in determining the isotopic composition of the oceans, its effect on the isotopic composition of cherts is clearly minor.

C. Input of mantle water to the oceans. If the time-shift for the locus of δ-values for cherts is a result of shifts in the meteoric water line caused by the addition of mantle water to the oceans, then the change with time of the isotopic composition of cherts should conform to the pattern shown in figure 3-4 and discussed in section 3.5. The locus of chert δ-values should shift such that successive periods lie to the lower right of one another, and the locus of marine cherts should be parallel to the line of slope -8 which passes through mantle water and present day ocean water.

In figure 6-11, line A is the presumed locus of marine cherts. The slope of this line is -7.4. This value is remarkably close to that predicted by the "mantle input" model. As indicated in figure 3-4, the slope of this line may be less negative than -8 if significant amounts of

hydrogen have escaped from the earth. The slope of the locus for marine cherts, being -7.4, is thus compatible with the "mantle input" model.

An objection to this model is that the locus of δ-values for cherts from successive geologic periods do not lie uniformly to the lower right of one another. However, in a general way, the locus of chert δ-values has shifted with time to the lower right. The lack of a uniform time-shift of the cherts may be explained if the "mantle input" model is combined with shifts due to climatic variations. This is not unreasonable, since it would be very remarkable if all cherts formed at the same temperature and thus yielded a set of uniformly shifting loci. The "mantle input" model as discussed in section 3.6-B is thus a viable explanation for at least part of the time-shift.

Muehlenbachs (1971) has argued that water escaping from the mantle is isotopically altered by interaction with near surface rocks. If this is true, then the specific time-shift indicated in figure 3-4 is erroneous, and the mantle input model must be modified. Since the present model fits the data, any significant modification would serve to remove the mantle input model as a satisfactory explanation of the chert data.

6.15 Exchange with Ground Waters

The preceding discussion has been based upon the

assumption that the δ-values are original and reflect conditions associated with crystallization of the original chert. This assumption is contrary to the previous work of Degens and Epstein (1962) who suggested that δO^{18}-values for cherts at the time of their formation are approximately 30‰ to 34‰ and are lowered during post-depositional exchange with isotopically light ground waters.

If their interpretation is correct, then cherts at the time of their original crystallization should ideally define a domain shown as "B" in figure 6-17. If subsequent equilibration with light ground waters occurs at similar temperatures to the original crystallization, then, as shown in the figure, the δ-values of the exchanged cherts will fall along a band parallel to the meteoric water line with the oldest samples lying lower in the band. However, it has been shown that the δ-values of cherts are not distributed in this manner. It is therefore highly unlikely that the variations observed are due to later equilibration with low temperature ground waters.

If exchange occurs at higher temperatures, the δ-values would move toward the meteoric water line and would fall within the region below line AB. Figure 6-18 compares this region with the observed range of δ-values. It is apparent that many cherts lie <u>above</u> the region, being enriched in deuterium relative to the more recent cherts

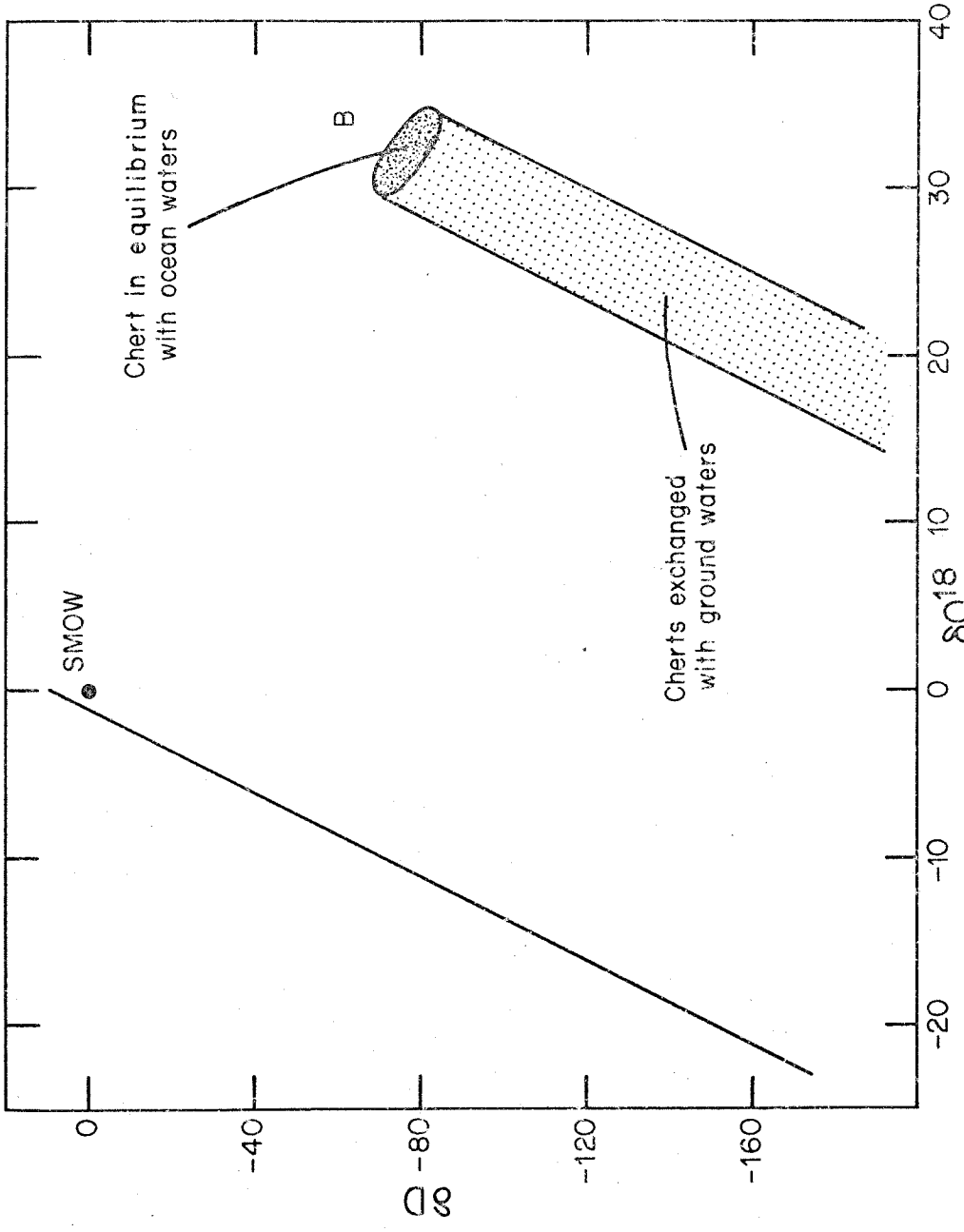

Figure 6-17: $\delta D - \delta O^{18}$ RELATIONSHIPS FOR CHERTS WHICH FORM IN EQUILIBRIUM WITH OCEAN WATER AND SUBSEQUENTLY EXCHANGE WITH GROUND WATERS AT LOW TEMPERATURES.

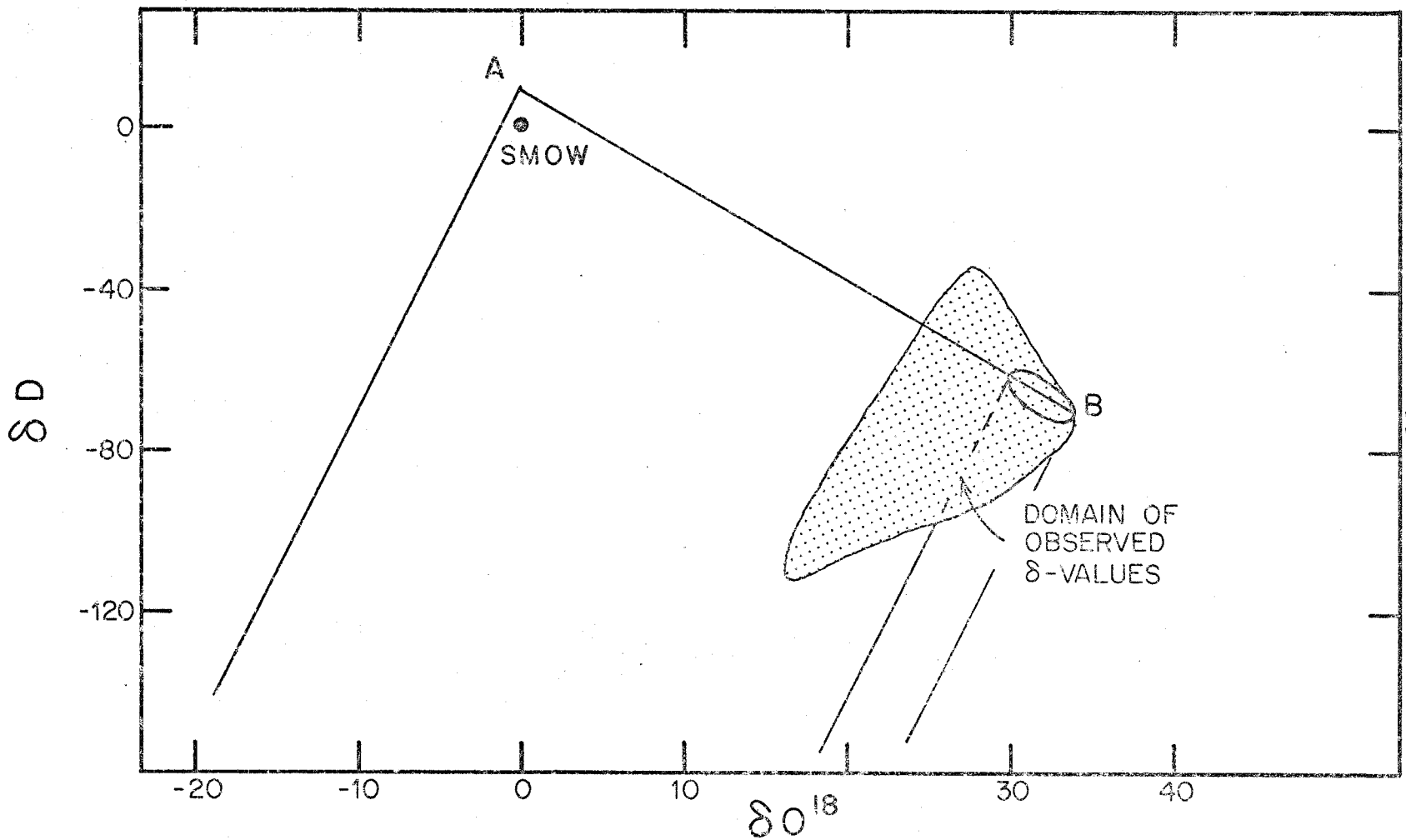

Figure 6-18: RELATIONSHIP OF OBSERVED δ-VALUES TO METEORIC WATER LINE AND HYPOTHETICAL BAND OF δ-VALUES FOR CHERTS EQUILIBRATED WITH METEORIC WATERS

(post-Jurassic). This can nevertheless be explained by the exchange model if the ground waters involved usually had isotopic composition near that of ocean water. Cherts which equilibrated with these waters would be carried above line AB if the hydrogen fractionation is more sensitive to temperature than that of oxygen, or if hydrogen exchanges more readily than oxygen. In other words, as the temperature of exchange increases, the hydrogen-water fractionation decreases at a rate disproportionate to the oxygen-water fractionation. The exchange "trajectory" in δD-δO^{18} space would thus carry the isotopic composition of cherts above line AB. The region below line AB can be filled by cherts which exchanged with lighter waters at similar temperatures.

The model must also explain why the loci of δ-values for cherts of the same age which have exchanged with warm ground waters are approximately parallel to the meteoric water line and shift with time. A possible explanation lies in the fact that older cherts, having been buried to greater depths, have had greater chance for exchange at elevated temperatures and should thus be more strongly displaced toward the meteoric water line. It has been shown that, in general, older cherts do tend to lie closest to the meteoric water line.

The fact that cherts for a given age tend to cluster

about a line parallel to the meteoric water line can be explained by saying that these cherts have been buried to similar depths and have thus exchanged with meteoric waters at similar temperatures. According to this mechanism, the proposed isotherms of figure 6-14 thus reflect temperatures of post-depositional exchange rather than original temperatures of crystallization.

The critical test of this interpretation lies in a possible correlation of depth of burial with displacement toward the meteoric water line. Unfortunately, it is extremely difficult to accurately assess the maximum depth to which various cherts have been buried. However, such an estimate has been attempted for cherts from the Upper Cambrian and is shown in table 6-10. The Upper Cambrian was selected because the cherts form a single, well-defined linear array and thus should all have experienced the same depth of burial according to this interpretation.

In the case of the Upper Cambrian cherts, the overlying sediment thicknesses can be estimated from published stratigraphic information. The depth of burial was assumed equal to the total thickness of younger sediments which occur in the areas from which the samples were taken. This assumption is not always a good one, but reference to the table shows that the differences in thickness at the different localities are so great as to make an accurate

Table 6-10

COMPARISON OF DEPTH OF BURIAL WITH ISOTOPIC COMPOSITION FOR UPPER CAMBRIAN CHERTS

Chert #	Depth of Burial	Reference	δO^{18}	δD
1	6,307 ft.	Hazzard (1937)	26.68	-60.4
3	6,307	Hazzard (1937)	25.95	-71.5
259	15,200	Hazzard (1937)	20.06	-105.3
160	2,485-3,808	Weller & St. Clair (1928)	28.30	-50.1
161	2,485-3,808	Weller & St. Clair (1928)	24.08	-67.9
221	11,295-46,000	Rogers (1927)	26.4	-74.5
325	22,000-39,000	Ham (1969, figure 17)	27.8	-50.5

assessment unnecessary. It is clear that the Missouri platform sediments (# 160, 161) could not have been buried to the depth of the eugeosynclinal sediments from which samples #259, 221, and 325 were collected, yet their δ-values are all linearly related. #160 and #325 have identical isotopic compositions, even though #325 was at one time buried at least 18,000 feet deeper than #160. The tabulation is thus sufficient to show that co-linear points in the array are for cherts which have been buried to drastically different depths. In this case, there is clearly no correlation of depth of burial with displacement toward the meteoric water line. It is, therefore, unlikely that the cherts analyzed have exchanged with heated ground waters to produce an array parallel to the meteoric water line.

The post-depositional exchange model fails completely when the time variations are considered in detail. δ-values for the Upper Cambrian, Ordovician, and Triassic cherts all cluster about the same line in a δD- δO^{18} plot. This is not to be expected if cherts exchange to a greater extent with time, particularly for such a long period of time as represented by the interval between Ordovician and Triassic. Furthermore, the Arizona Precambrian cherts are similar to Upper Paleozoic cherts. If exchange occurs at a rate fast enough to yield the large variation seen in the Phanerozoic samples, then these 1.2 billion year old cherts should

surely have also exchanged. Apparently they have not.

The interpretation invoking heated ground waters cannot be ruled out, but coincidence and special circumstances must be invoked to fully explain the data. It is thus considered unlikely.

Chapter 7

COEXISTING CARBONATES AND CHERTS

7.1 Introduction

Most of the cherts on which oxygen and hydrogen isotope analyses were made were collected from limestones and dolomites. The cherts enclosed small amounts of calcite and dolomite, and some contained well-preserved fragments of calcitic fossils. The chert-bearing carbonate strata will be referred to hereafter as the "host-carbonate". Carbonate contained within the chert will be called "included" carbonate. Oxygen and carbon isotope analyses were obtained on a number of host and included carbonates to (1) evaluate the possibility of using Δ^{OX} quartz-calcite as a temperature indicator, (2) determine if δO^{18} and δC^{13} values of included carbonates indicate preservation of original carbonate in contrast to post-depositional exchange for the host-carbonate, and (3) provide additional data which might assist in evaluating the δD- δO^{18} relationships in cherts. Item (2) is of particular interest since most pre-Permian calcitic fossils in limestones are too poorly preserved to give reliable paleotemperatures by the oxygen isotope method. If calcitic fossils in cherts are better preserved, it may be possible to greatly extend the age-range of this method.

7.2 Procedure

Samples of the host-carbonate were collected in the immediate vicinity of the chert, usually within a few centimeters, and often as part of the same hand-specimen. The δO^{18} and δC^{13} analyses were done in the usual way on carbonate samples ground to <200 mesh and reacted with phosphoric acid in the manner described by McCrea (1950).

Included carbonates were frequently finely dispersed throughout the chert. These were sampled by grinding the <200 mesh chert fraction in a sapphire mortar to the consistency of facial powder and then reacting with phosphoric acid in the standard manner. In several cases the included carbonate was concentrated to such an extent that it could be scraped out with a knife, but such occurrences were unusual.

Chemical staining techniques showed that both host and included carbonate frequently consisted of physically inseparable mixtures of calcite and dolomite. The chemical separation technique of Epstein et al. (1963) which makes use of the differing reaction rates of carbonates was used to obtain CO_2 from the calcite and dolomite separately. The powders were reacted for one hour, after which the CO_2 evolved from calcite was collected and analyzed. This fraction is referred to as the calcite fraction. CO_2 evolved during the next 72 hours will be

referred to as the dolomite fraction. As mentioned by Epstein et al., this method is less accurate when one phase predominates. This was often the case, and the results should be viewed with caution. Also, it is possible that extensive grinding of the chert fraction did not completely separate the carbonate from the chert, and that reaction rates for such "imbedded" carbonate are slower. The dolomite fraction of included carbonate may thus be slightly contaminated with the calcite fraction.

7.3 Results

δ -values for cherts, host carbonate, and included carbonate are given in table 7-1. Included in the table are the percentage yields of CO_2 evolved from the dolomite and calcite fractions. Yields from the host-carbonate almost never equaled 100% of the theoretical carbonate yield. Residues from the phosphoric acid reaction usually contained chert grains, indicating that limestone and dolomite close to chert nodules are generally somewhat silicified. This accounts for the low CO_2 yields.

The data are presented graphically in figures 7-1 to 7-7. Figures 7-1 and 7-2 show the δO^{18}-values for chert and coexisting carbonates plotted against geologic time. Figures 7-3 through 7-7 illustrate the carbon and oxygen isotope data for the individual host and included carbonates.

Table 7-1

ISOTOPIC COMPOSITION OF CARBONATES COEXISTING WITH CHERTS

Chert #	Age	δO^{18} Chert ‰	Host-Carbonate: Carbonate Phase % Calcite(C) % Dolomite(D)	Host-Carbonate: δO^{18} ‰	Host-Carbonate: δC^{13} ‰	Included-Carbonate: Carbonate Phase % Calcite(C) % Dolomite(D)	Included-Carbonate: δO^{18} ‰	Included-Carbonate: δC^{13} ‰
354	T	+35.19	67 C	+30.70	+2.34			
263	K	+32.60	91 C	+25.04	-7.27	2 C	+23.62	-4.03
			7.2D	+24.36	-4.39			
267	K	+33.00				7 C	+25.91	-8.64
249	Tr	+17.77	7.2C	+22.40	+1.00			
			82.3D	+22.82	+1.83			
28	P	+29.93	11 C	+18.00	+0.76	8 C	+26.64	+2.67
			28 D	+25.79	+2.17	3.7D	+26.77	+1.68
9	P	+33.18	23 C	+27.49	+2.22			
8	M	+28.63	13.3C	+25.4	+1.05			
			79 D	+24.94	+1.19			
25	M	+28.91	94.3C	+26.03	+0.03			
			5 D	+25.15	-0.51			
35	M	+16.10	82 C	+ 4.09	-0.39	6.4C	+ 2.60	-1.20
36	M	+22.08	60 C	+14.08	-0.67	7.8C	+13.53	-0.92
171	M	+32.45	91.7C	+26.31	+2.50	26.6C	+29.14	+3.11
153-White	M	+34.32	92 C	+26.42	+2.98	.7C	+25.29	+1.18

Table 7-1 (continued)

Chert #	Age	δO^{18} Chert ‰	Host-Carbonate: Carbonate Phase % Calcite(C) % Dolomite(D)	Host-Carbonate: δO^{18} ‰	Host-Carbonate: δC^{13} ‰	Included-Carbonate: Carbonate Phase % Calcite(C) % Dolomite(D)	Included-Carbonate: δO^{18} ‰	Included-Carbonate: δC^{13} ‰
153-Grey	M	+34.04		+26.42	+2.98	2 C	+29.06	+4.03
128	M	+29.62	100 C	+25.17	+2.82	9.7C	+25.41	+2.56
127	M	+29.00	94 C (Clam)	+25.93	+2.10	92 C (Clam)	-25.59	+1.06
						37 C	+23.24	+1.70
216	M		91.3C	+26.69	+1.88	46 C	+25.65	+1.45
138	M	+31.40	94 C	+25.97	+3.12	15.6C	+22.96	+2.82
			6 D	+25.42	+2.91			
156	M	+31.39	85.2C	+26.35	+3.38	6.1C	+23.64	+2.97
			13.5D	+26.00	+3.57			
123	M	+29.0				42 C	+21.62	+1.95
76	O	+29.66	91 C	+26.63	-0.38			
			9 D	+25.73	-0.34			
159	O	+28.34	5.3C	+25.44	-1.27			
			79.3D	+24.99	-1.03			
94	O	+28.92	91 C	+26.56	-0.05	18.7C	+26.09	-0.58
			7.6D	+24.82	-0.08	20.7D	+25.99	-0.29
101	O	+31.14	75.1C	+25.11	-1.13	5.4C	+26.61	-0.77
			13 D	+25.44	-1.03	5.5D	+26.66	-0.58
3	Є	+25.95	11.2C	+24.54	-1.05			
			77.9D	+24.57	-0.74			

Table 7-1 (continued)

Chert #	Age	δO^{18} Chert ‰	Host-Carbonate: Carbonate Phase % Calcite(C) % Dolomite(D)	Host-Carbonate: δO^{18} ‰	Host-Carbonate: δC^{13} ‰	Included-Carbonate: Carbonate Phase % Calcite(C) % Dolomite(D)	Included-Carbonate: δO^{18} ‰	Included-Carbonate: δC^{13} ‰
1	Є	+26.68	4.8C	+23.80	-2.66			
			67 D	+26.72	-1.14			
221	Є	+26.40	81 D	+24.28	+0.49			
220	Є	+26.02	6.4C	+24.80	+0.17	1.86C	+23.66	-0.25
			59.4D	+24.57	+0.04	6.13D	+23.01	+0.59
259	Є	+20.06	97.4D	+23.28	+0.90	1.7 C	+21.76	-0.69
						10.7 D	+21.54	+0.38
26	pЄ	+30.80	5.1C	+24.40	-0.57			
			81.4D	+23.41	-0.23			
34	pЄ	+29.91	21.5D	+25.70	+2.61	1 C	+25.35	+1.55
188	pЄ	+19.30	78.5D	+25.01	+1.68			

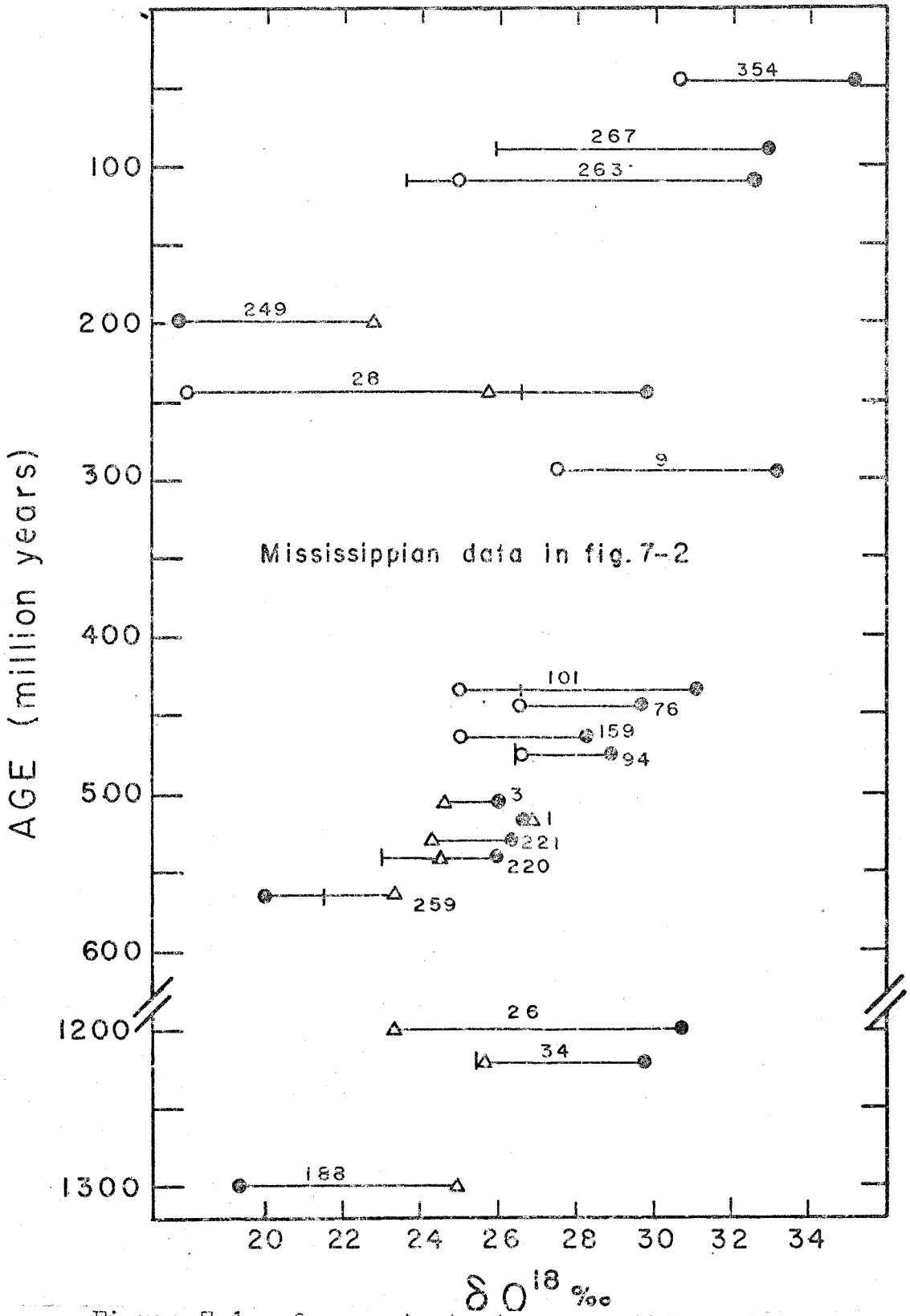

Figure 7-1. Oxygen isotopic composition of calcites and dolomites coexisting with chert. ● = chert, o = host calcite, Δ = host dolomite, I = included carbonate.

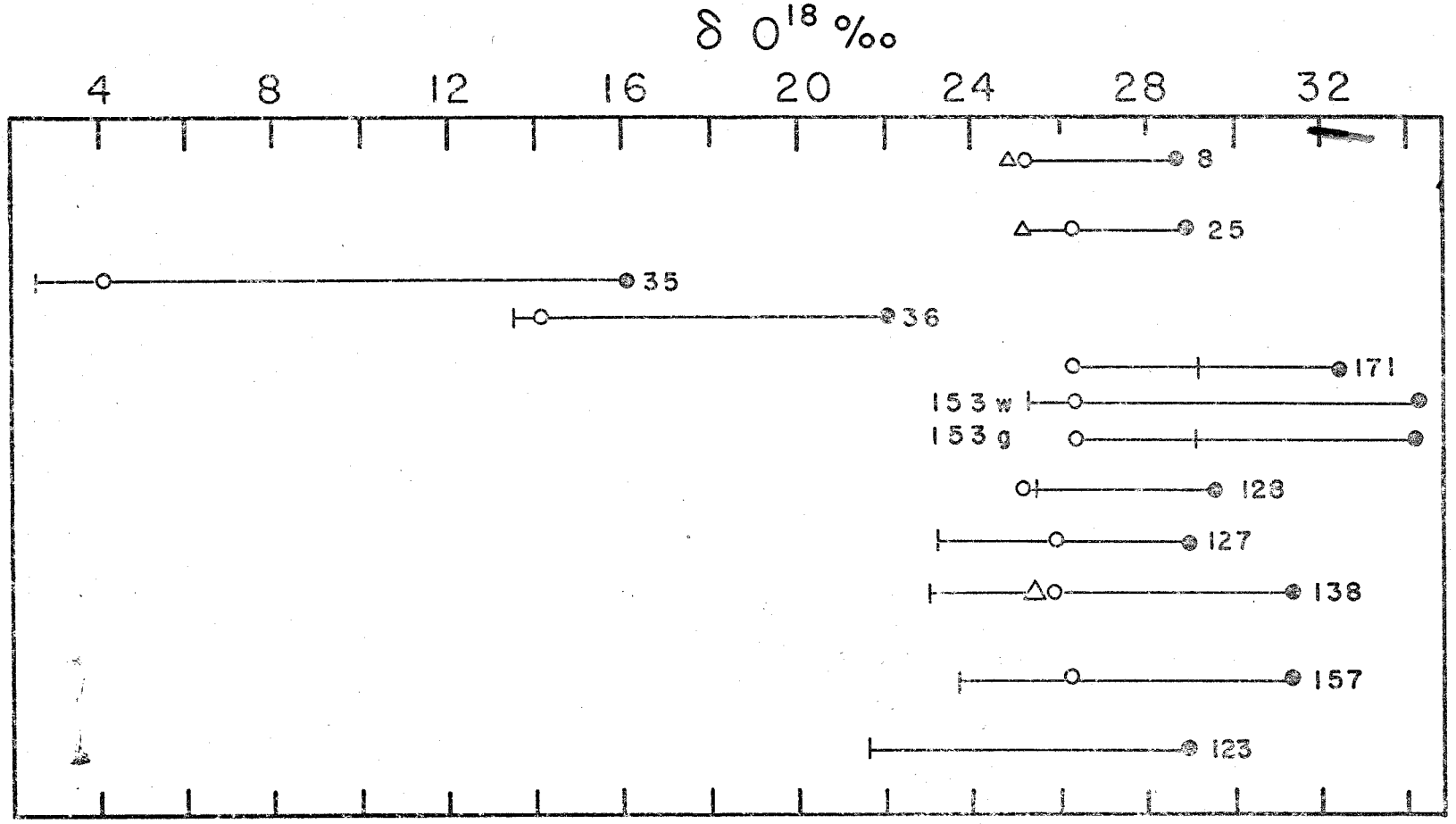

Figure 7-2. Oxygen isotopic composition of calcites and dolomites coexisting with Mississippian cherts. ● = chert, ○ = host calcite, △ = host dolomite, | = included carbonate.

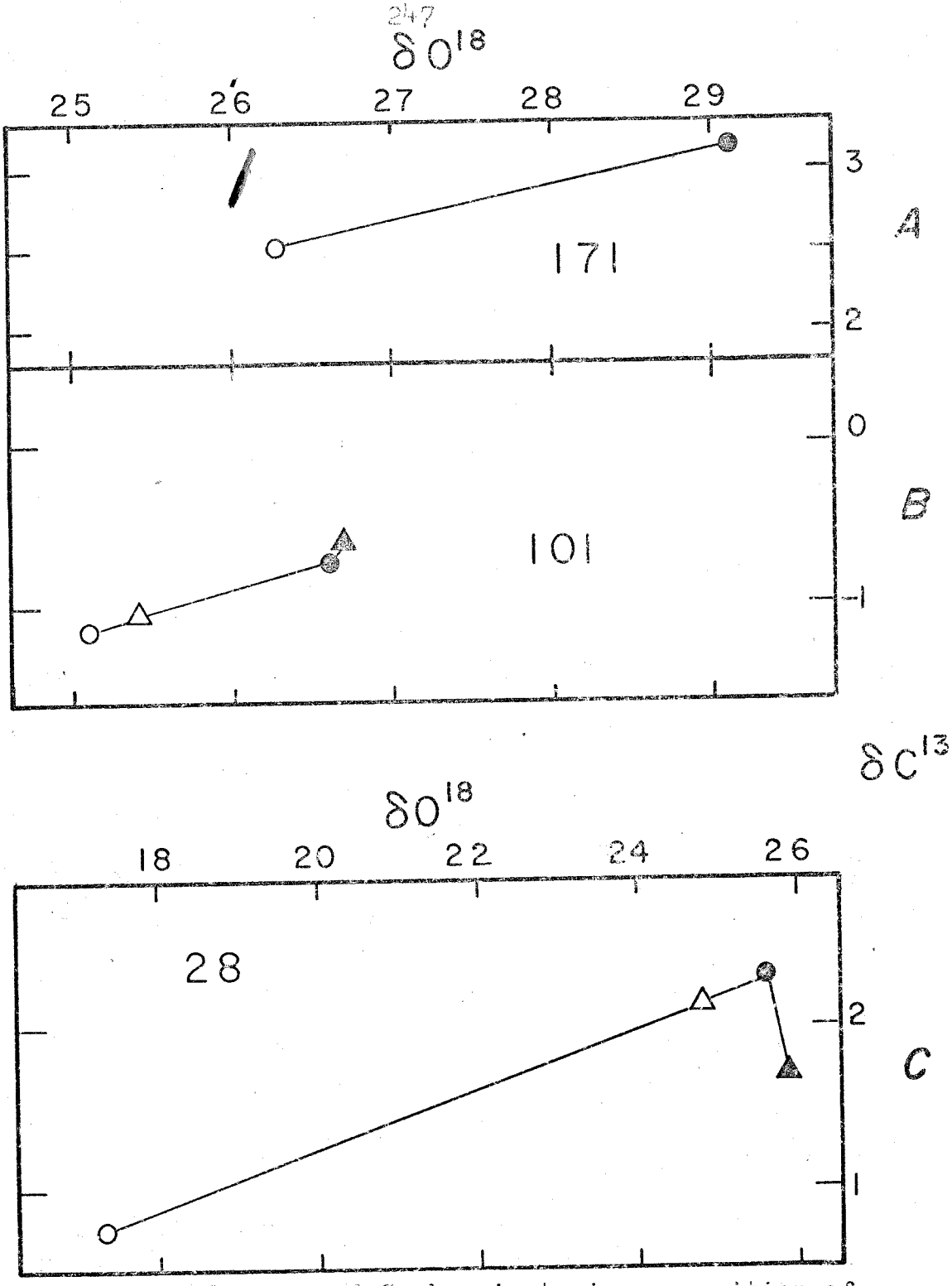

Figure 7-3. Oxygen and Carbon isotopic composition of Host and Included carbonates. ● = included calcite, ○ = host calcite, ▲ = included dolomite, △ = host dolomite.

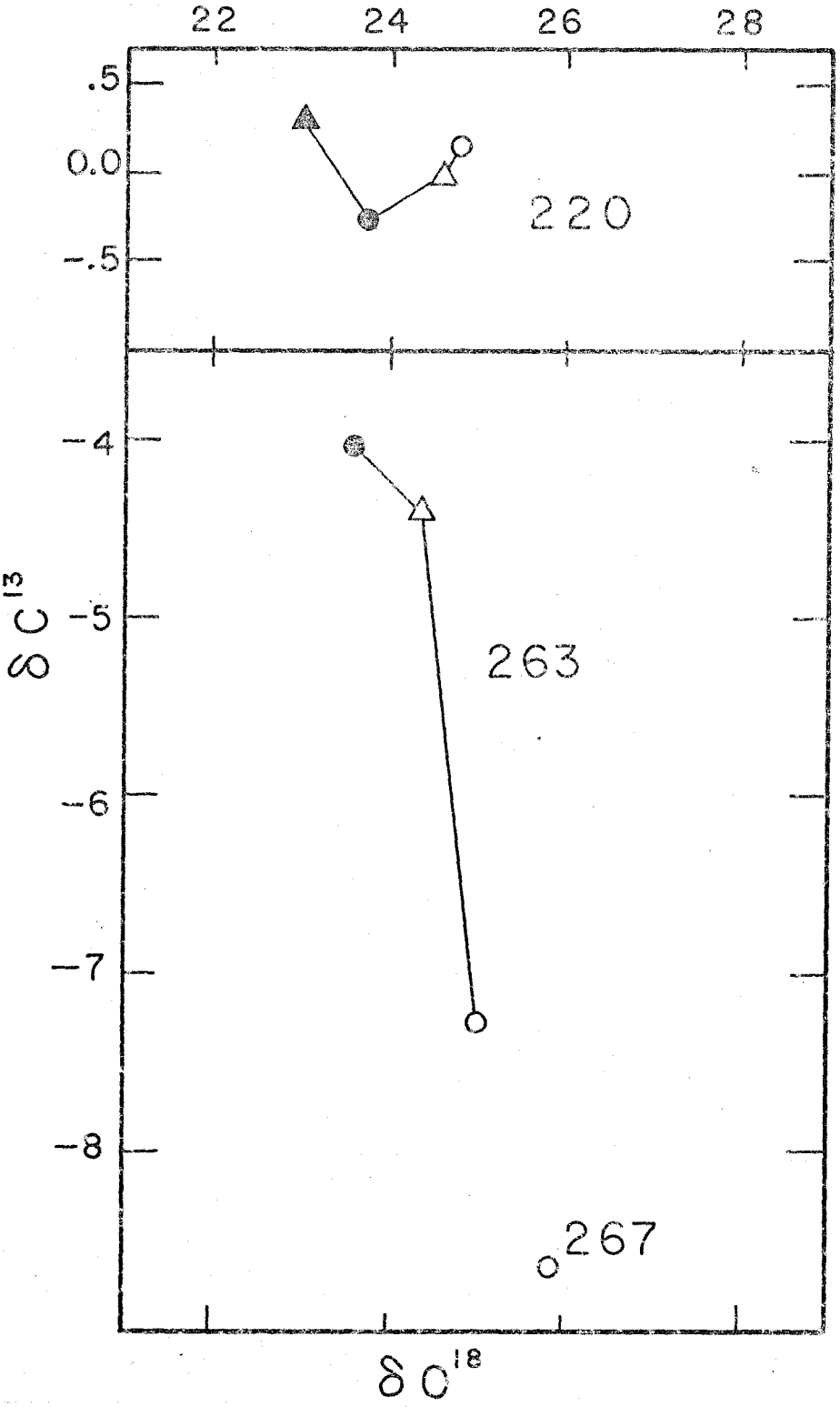

Figure 7-4. Oxygen and Carbon Isotopic composition of Host and Included carbonates. ○ = host calcite, ● = included calcite, △ = host dolomite, ▲ = included dolomite.

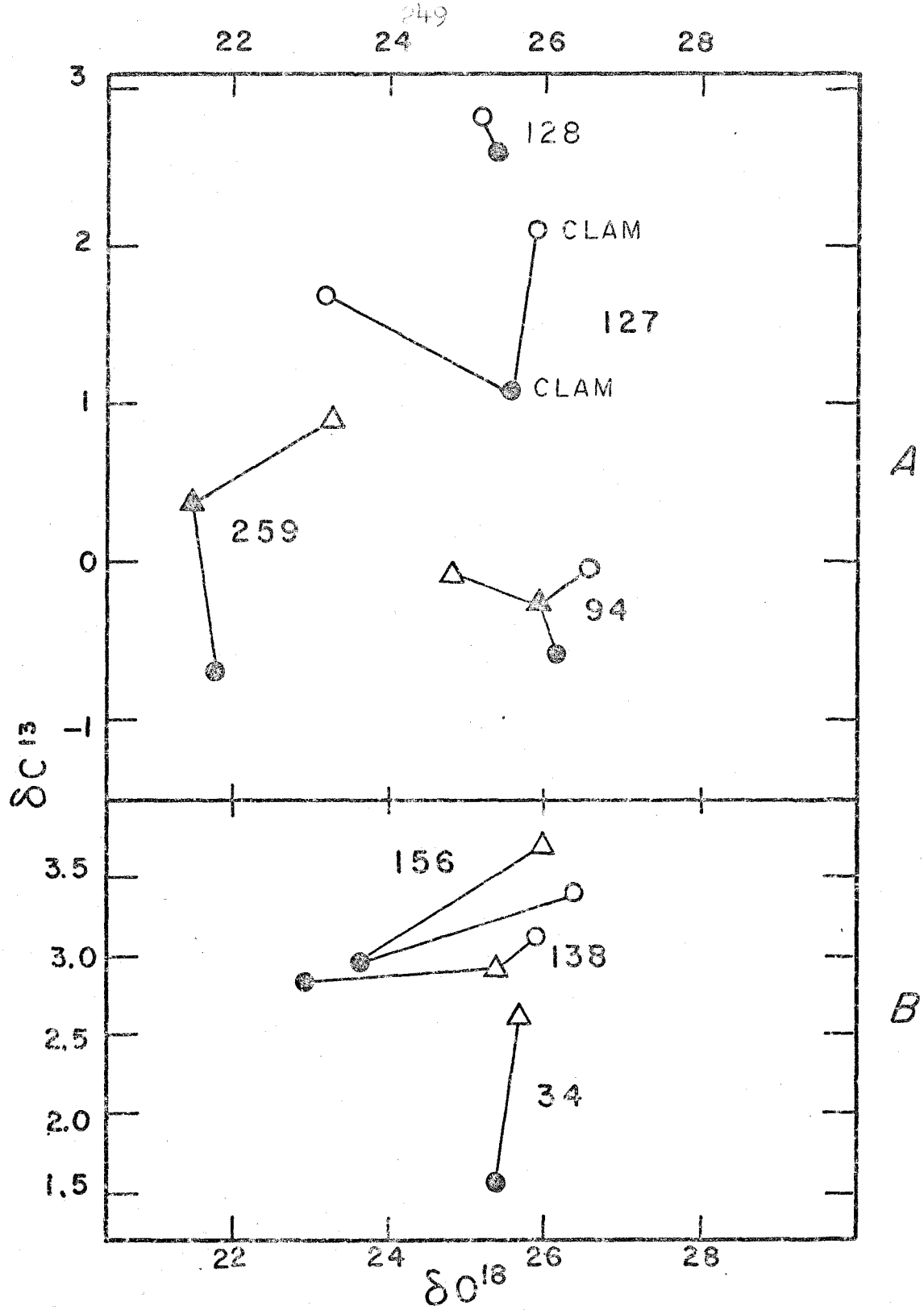

Figure 7-5. Oxygen and Carbon isotopic composition of Host and Included carbonates. ● = included calcite, ○ = host calcite, ▲ = included dolomite, △ host dolomite.

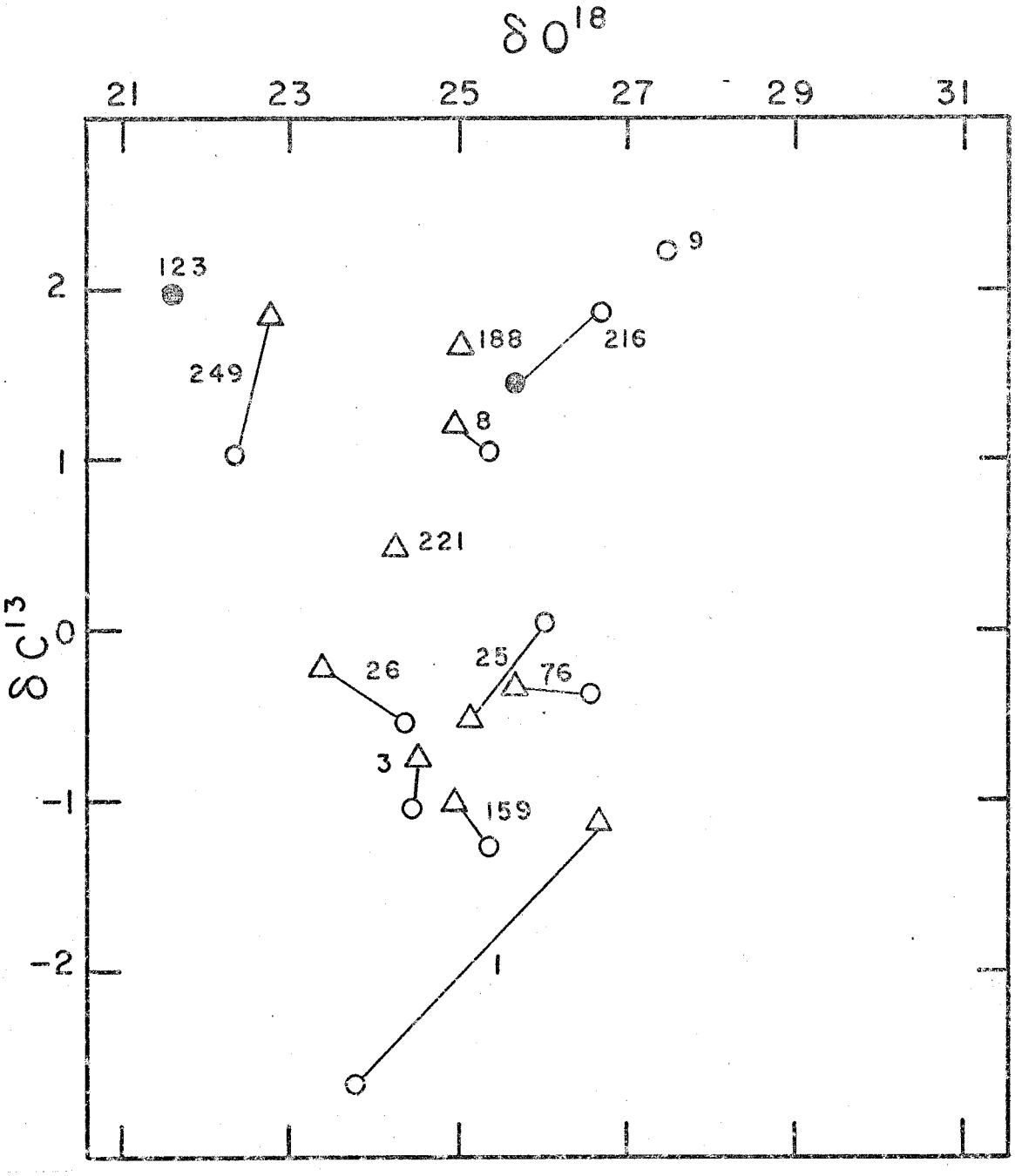

Figure 7-6. Oxygen and Carbon isotopic composition of Host and Included carbonates. ● = included calcite, ○ = host calcite, △ = host dolomite.

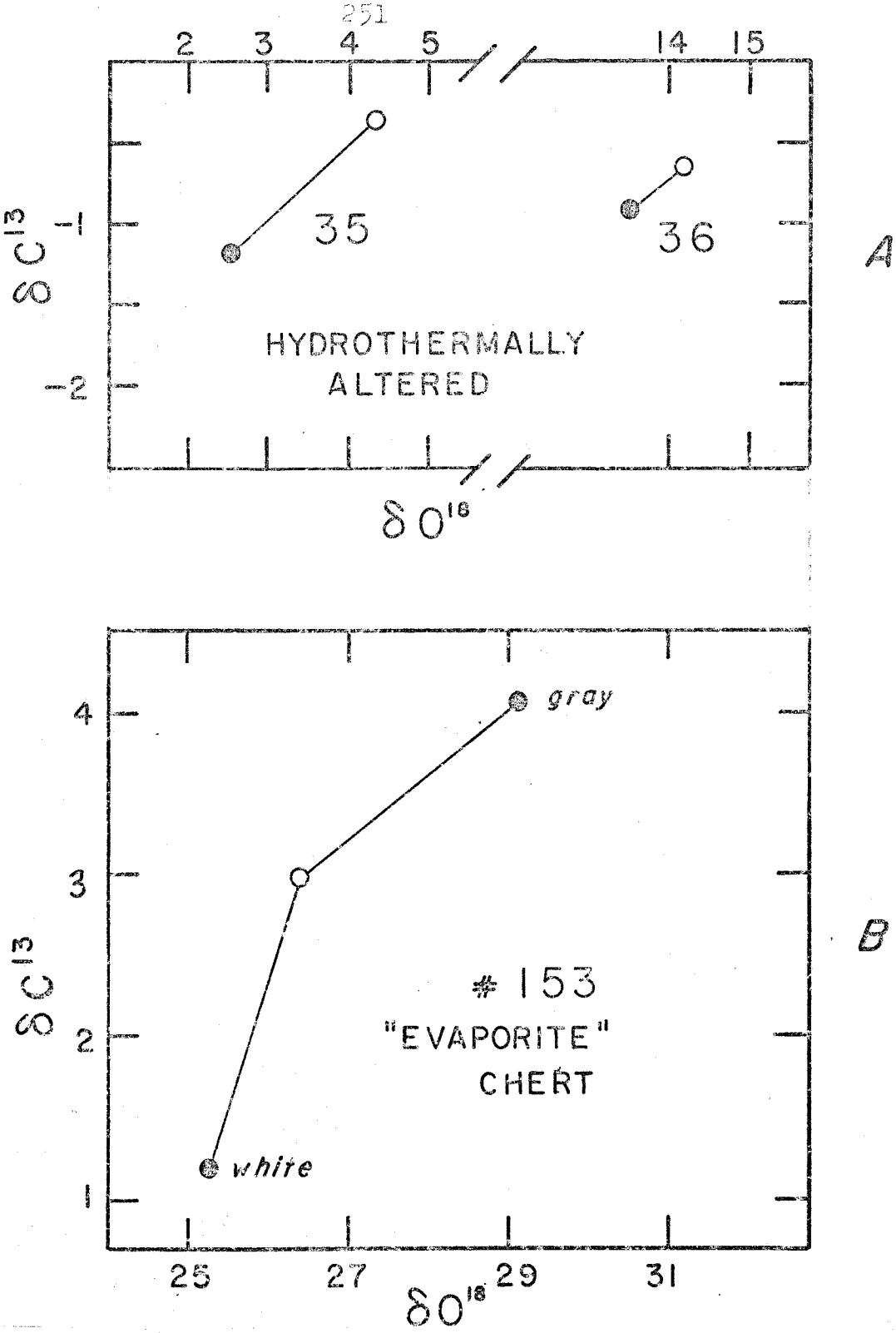

Figure 7-7. Oxygen and Carbon isotopic composition of Host and Included carbonates. ● = included calcite, O = host calcite.

7.4 Discussion

The data given in figures 7-1 and 7-2 show clearly that the chert-carbonate fractionation for δO^{18} is variable, ranging from -4.5 (#188) to +14 (#35). No systematic increase or decrease of this fractionation with geologic time is apparent.

A. Possible equilibration of chert and coexisting carbonate. The proposed δO^{18}-values for calcite, dolomite, and chert in equilibrium with ocean water at 20°C are respectively 29.5‰ (Epstein et al., 1953), 34.5‰ (Clayton et al., 1968), and 31 - 34‰ (see Chapter 6). At 20°C, Δ^{OX} chert-calcite should thus be about 2 - 5‰ and Δ^{OX} chert-dolomite about -4 - 0‰. These fractionations decrease with increasing temperature.

As shown in figures 7-1 and 7-2, Δ^{OX} chert-calcite is extremely variable, ranging from 2.5‰ to 14‰. It is obvious that the differences in δO^{18} for cherts and calcite do not represent precise equilibrium values for various temperatures of isotopic equilibration. Nevertheless, for the purpose of quantitative evaluation of this relationship, oxygen isotopic temperatures were computed for coexisting chert-calcite pairs for both host and included calcite. Two temperatures for each pair are shown in table 7-2. One was obtained using the quartz-calcite temperature fractionation equation given by Clayton et al. (1972). The other was

Table 7-2

EQUILIBRIUM ISOTOPIC TEMPERATURE FOR COEXISTING CHERT-CALCITE AND δO^{18} OF WATER IN ISOTOPIC EQUILIBRIUM WITH CALCITE AT THIS TEMPERATURE

A: Values based on quartz-calcite fractionation of Clayton et al. (1972)

B: Values based on quartz-calcite fractionation: $1000\ n\alpha = (10^6 T^{-2}) - 3.29$
T = temperature in $^\circ K$

	A				B			
	Included		Host		Included		Host	
Sample #	δH_2O ‰	°C	δH_2O ‰	°C	δH_2O ‰	°C	δH_2O ‰	°C
354							- 4.5	- 3
263	-13.6	- 11	- 5.9	+ 13	-49.4	- 84	-36.2	- 66
267	- 2.9	+ 22			-31.4	- 59		
249	I M P O S S I B L E				I M P O S S I B L E			
9			+ 4.9	+ 57			-18.0	- 34
8			+13.7	+160			+ 0.6	+ 43
25			+16.2	+190			+ 4.9	+ 66
35	-54.4	- 61	-46.5	- 48	-107	-120	-93.4	-111
171	+17.4	+159	+ 1.7	+ 44	+ 4.2	+ 43	-23.0	- 43
36					-56.0	- 80	-50.9	- 73
153 white	-12.2	- 11	- 6.0	+ 7	-48.2	- 84	-37.7	- 71
153 grey	+ 9.7	+ 80	- 4.8	+ 12	-10.3	- 17	-35.3	- 67

Table 7-2 (continued)

Sample #	A				B			
	Included		Host		Included		Host	
	δH_2O ‰	°C	δH_2O ‰	°C	δH_2O ‰	°C	δH_2O ‰	°C
128	+ 9.6	+110	+ 8.2	+ 99	- 7.3	+ 5	- 9.7	- 2
127	+13.4	+152	+15.3	+175	- 0.2	+ 37	+ 3.1	+ 55
138	-11.9	- 3	+ 4.6	+ 64	- 45.6	- 78	-17.3	- 28
76			+16.2	+178			+ 4.5	+ 57
159			+15.6	+188			- 4.1	+ 64
94	+16.5	+194	+19.2	+238	+ 5.4	+ 69	+10.0	+103
101	+ 9.3	+ 96	+ 1.0	+ 47	- 8.9	- 5	-23.2	- 41
3			+21.5	+388			+16.3	+220
1			+14.0	+189			+ 2.6	+ 65
220	+16.3	+237	+22.6	+437	+ 7.1	+102	+18.3	+260
259	I M P O S S I B L E				I M P O S S I B L E			
26			- 1.4	+ 37			-27.1	- 48
34	+ 7.9	+ 95			-10.4	- 6		

obtained by combining the calcite-water equation given by O'Neil et al. (1969) with the chert-water equation proposed in section 6.13 to give

$$1000\ \ell n\alpha \text{ chert-calcite} = .31\ (10^6\ {}^{o}K^{-2}) + .1$$

The δO^{18} of the water in equilibrium with the two phases was also computed.

The results of the computation shown in table 7-2 are on the whole unreasonable, giving δO^{18} values for water well outside the natural range and temperatures which are frequently below freezing. It is concluded that most coexisting cherts and calcites are out of isotopic equilibrium with one another and that the difference in δO^{18}-values between the two cannot be used to deduce isotope temperatures. This result is not surprising, since a small numerical deviation from true equilibrium δO^{18}-values of the chert or calcite gives rise to large variations in the calculated temperatures.

Δ^{OX} chert-dolomite for these data is usually positive, but varies from -5 to +6‰ and likewise indicates isotopic disequilibrium for most of the samples. It is possible that chert-dolomite pairs with negative δ-values represent approximate isotopic equilibrium. If so, both minerals must have last equilibrated with fresh waters, since the δO^{18}-values are less positive than nearly all the others obtained in this study.

An intriguing possibility is that negative values for Δ^{OX} chert-dolomite indicate cases where dolomite crystallized directly from solution, while positive values indicate cases in which the dolomite formed as a metasomatic replacement of calcite without isotopic exchange as proposed by Epstein et al. (1963). However, a more likely interpretation of this relationship between δO^{18} of dolomite and chert is discussed in section 7.4-C.

B. Possible post-depositional exchange of cherts and carbonates with ground waters. The average trend in δO^{18}-values for the 30 cherts and limestones analyzed by Degens and Epstein (1962) is superimposed upon the present data for cherts and coexisting calcite in figure 7-8. This trend suggested to Degens and Epstein that cherts and carbonates are initially deposited with δ-values in the range for those of Cretaceous age. Subsequent exchange with isotopically light meteoric water (possibly at warmer temperatures) is responsible for the lighter values. Older rocks should, in general, have suffered the most exchange, thereby producing the observed trend.

With the exception of the Cretaceous samples, all of the present δ-values are more positive than those examined by Degens and Epstein. No systematic time-trends in δ-values are observed in the present data. Instead, calcites from Ordovician to Cretaceous nearly all fall in the range

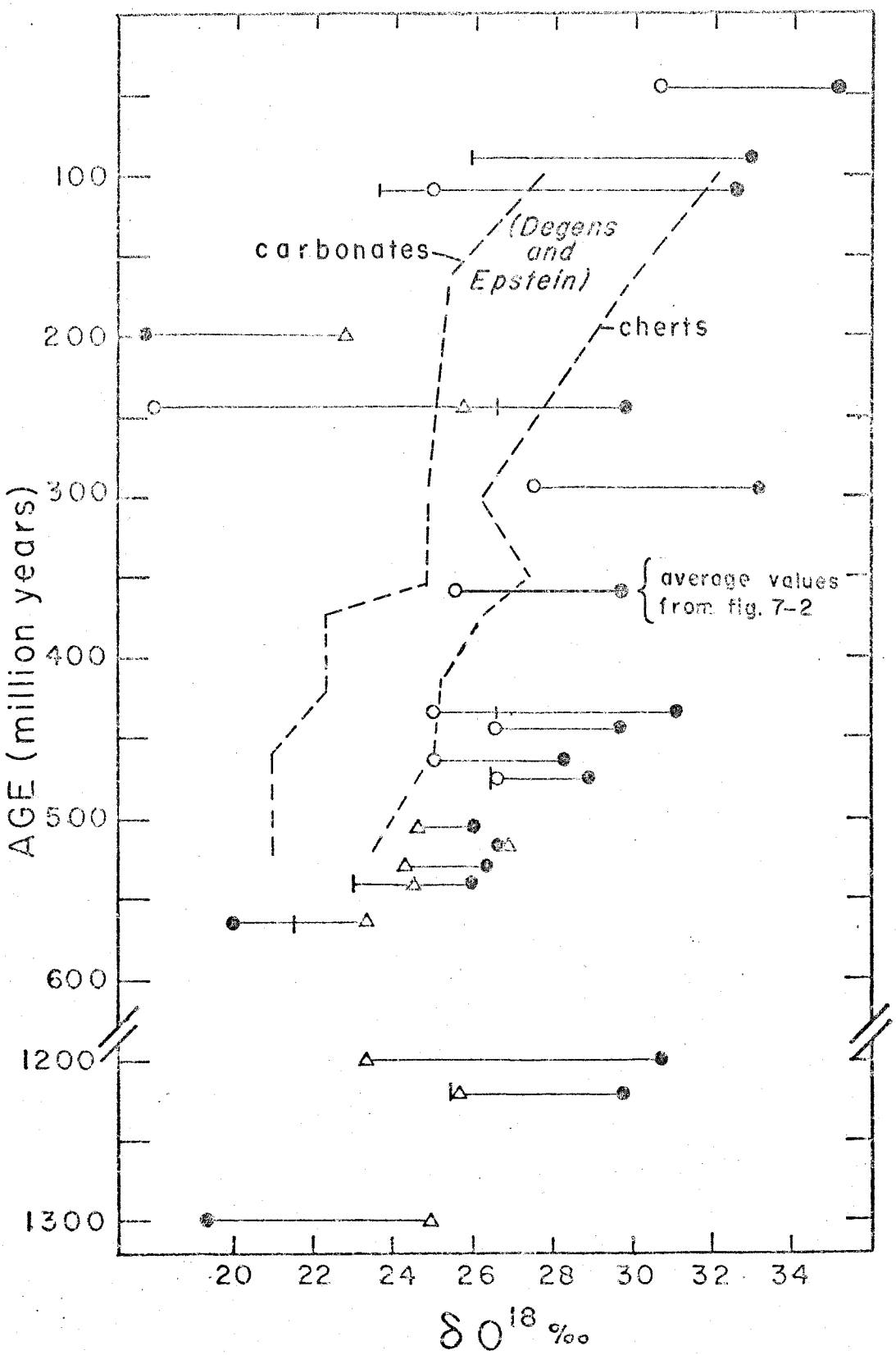

Figure 7-8. Comparison of average δ-values for cherts and coexisting carbonates as reported by Degens and Epstein (1962) with the data shown in figure 7-1.

of +25 to +27‰. Cherts coexisting with these carbonates are more variable, ranging from +28 to +33‰, but there is no correlation between carbonate and chert δ-values. It is, therefore, not possible to use the same arguments which Degens and Epstein used to suggest that post-depositional exchange with ground waters is the cause of δO^{18} variations in these cherts and carbonates.

Particularly difficult to explain in terms of post-depositional exchange are the three samples, #249, #259, and #188, for which δO^{18} of the chert is lower than δO^{18} for the host dolomite. Quartz has been shown to be one of the most resistant minerals to isotopic exchange, even at temperatures above 400°C (Clayton, Muffler et al., 1968; Garlick and Epstein, 1966; Taylor, 1968; Taylor and Forester, 1971). It therefore is unlikely that the δO^{18} of chert could be reduced to a lower value than the coexisting carbonate by exchange with ground waters. Of course, it is possible that exposure to ground waters with pH >9 could cause significant dissolution and exchange, leaving the carbonate relatively unaffected. Cases in which chert has been replaced by carbonate are well documented (Walker, 1962), and indicate that diagenetic environments possibly conducive to the preferential isotopic exchange of quartz can exist. One of these must be invoked if it is desired to explain the data by post-depositional exchange with ground waters.

It is also possible that the fine-grained granular microcrystalline quartz found in cherts is less resistant to exchange than normal quartz. Due to its peculiar structure, this would undoubtedly be true if the fine-grains were disseminated throughout a permeable rock unit. However, grains of granular microcrystalline quartz in chert nodules and beds are intergrown, giving chert an extraordinarily low permeability. Precise values for the permeability of cherts are not available, but Nagy (1970) has reported a value of 5.7×10^{-7} millidarcy for carbonaceous cherts from the Precambrian Onverwacht Series. Thus, at present there is no basis for arguing that granular microcrystalline quartz in cherts is less resistant to exchange than normal quartz.

The fact that some cherts are lighter than the host carbonate and the lack of correlation between δ-values for cherts and carbonates raises serious questions as to whether it is even possible that the variations in δO^{18}-values observed in these cherts and carbonates are due entirely to post-depositional exchange with ground waters over geologic time.

C. Possible role of meteoric water in chert genesis. An alternative explanation for these data is suggested by the results described in Chapter 6. There it was shown that the linear relationship of δD and δO^{18} for cherts was roughly parallel to the meteoric water line suggesting that many cherts

crystallize in the presence of diagenetic meteoric waters. According to this interpretation, opaline silica is deposited with carbonate under marine conditions. Subsequent diagenesis in the presence of marine or fresh waters causes the opaline silica to be mobilized and to replace portions of the carbonate unit forming as nodules, beds, etc. These new accumulations of silica may be initially opaline, but they gradually crystallize to form granular microcrystalline quartz. The δO^{18} of the chert may thus range from values characteristic of deposition under marine conditions to lighter values, depending upon the amount and isotopic composition of any meteoric waters involved. Since the carbonates are marine, δO^{18} of the carbonate is originally high (about +30‰), but is lowered during diagenesis and subsequent exposure to ground waters. This model allows all of the oxygen and carbon isotope data for coexisting cherts and carbonates to be readily explained since there is no requirement that the two formed from waters of the same isotopic composition.

In figure 6-1, sample #259 lies at the lower left of the δD- δO^{18} chert locus. It was therefore suggested that this chert had formed diagenetically from light meteoric waters, even though it is contained in a marine carbonate unit. The host carbonate for this chert has a greater δO^{18} than the chert (figure 7-1). This is in complete accord

with the proposed mechanism for chert formation.

The same argument can be made for samples #249 (figure 6-7) and #188 (figure 6-9). These cherts lie on the δD- δO^{18} diagram in positions indicative of formation from very light meteoric waters and coexist with carbonates richer in O^{18}.

The small fractionations between chert and host dolomite for samples #1, 2, 220, and 221 (figure 6-1) are best explained by this mechanism, since the cherts for these samples have δD and δO^{18}-values indicating deposition from light waters. The small fractionation is not a result of re-equilibration at higher temperatures or post-depositional exchange, but rather is considered the result of the two phases having precipitated from separate waters of different isotopic composition. This interpretation is similarly consistent with all the data for cherts and coexisting host carbonates shown in figures 7-1 and 7-2. As a working hypothesis, this mechanism is considered more probable than the mechanisms assuming equilibrium or post-depositional exchange with ground waters.

D. Relationship between included and host carbonates. In general, δO^{18} of included carbonate is approximately the same or lower than that of the host carbonate. In a few cases it is higher. The explanations for these relationships are based upon the idea that the included carbonate can be either relict host carbonate (host carbonate which was not

replaced but completely enclosed by chert) or carbonate which has precipitated during the episode of silica replacement. It is usually difficult to decide petrographically which of the included carbonate is relict or newly precipitated. The only included carbonate which is obviously relict host carbonate is that which occurs as well preserved fossil fragments.

Mississippian cherts #171 and #127 contain calcitic fossil fragments. #171 contains numerous crinoid plates within well-defined chert nodules of the Burlington limestone. The nodules do not contain significant amounts of calcite in other forms such as drusy calcite, pellets, etc. The original microfabric of many of the crinoid plates has been partially preserved. However, much of the calcite is twinned and the microfabric destroyed, indicating that some recrystallization has occurred. The δO^{18}-value of this carbonate is +29.14‰, and is the most positive calcite δO^{18}-value yet reported for Mississippian samples. The host limestone yields δO^{18} = 25.4‰, a lower value typical of Carboniferous limestones (Keith and Weber, 1964). Figure 7-3A shows δC^{13} and δO^{18} values for these included and host carbonates. δC^{13} is also less positive in the host than in the included crinoids. It is likely that both the included crinoids and the host carbonate were originally deposited with $\delta O^{18} \geq 29.14‰$, $\delta C^{13} \geq 3.11‰$. Ground waters subsequently exchanged with the host carbonate, lowering its

δ-values but leaving the chert-encased crinoids unaffected. Some exchange of the crinoid plates with diagenetic waters previous to and during silicification probably occurred. The δ-values are thus minimum values, but their similarity to present day carbonate δO^{18}-values suggests that they have not been lowered by more than 2 or 3‰ since deposition.

The result is of some significance since it suggests that many calcitic fossils encased in chert nodules are probably suitable for paleotemperature analysis. In the present work, the crinoids were obtained from bulk samples of the chert. Judicious selection of fossil fragments which retain the original calcite microarchitecture and original trace element content could very well give accurate paleotemperature determinations for very ancient fossils. In addition, these δO^{18}-values can be used to place a constraint on the quartz-water fractionation shown in figure 6-13. This is done by first assuming that the included crinoids formed in ocean water with $\delta D = 0.0 \pm 1‰$, equal to the "world average surface water during times when no ice is present" (Craig, 1965). If the crinoids have been preserved, then the temperature obtained by the paleotemperature equation of Epstein et al. (1953), as modified by Craig (1965), is $+25.0^{\circ} \pm 5^{\circ}C$. The $5^{\circ}C$ uncertainty arises because of a $\pm 1‰$ uncertainty in the isotopic composition of surface (or shallow) ocean water.

Assuming that chert #171 formed at the same temperature as the crinoids and under marine conditions as suggested by its position in the δD- δO^{18} plot in figure 6-5, then 1000 $\ell n \alpha$ for quartz-water can be given for that temperature. The results for the three temperatures corresponding to three possible oceanic δ-values are given below.

δO^{18} ocean water ‰	-1	0	+1
temperature for calcite °C	20.3	25.0	29.7
1000 $\ell n \alpha$ chert-ocean	34.85	33.9	32.9

The three values for 1000 $\ell n \alpha$ vs. temperature are plotted in figure 6-13 (connected by curve 1). Since the crinoid δO^{18}-values are minimum values, the temperatures deduced by the paleotemperature equation are maximum temperatures. Therefore, the temperatures for the three corresponding 1000 $\ell n \alpha$ quartz-water values are also maximum temperatures. Given the assumption above, it follows that the true chert-water temperature fractionation curve must fall to the right of the three points in figure 6-13.

It is not known how much the δO^{18}-value of the crinoids has been lowered, but it is instructive to see that if they were originally equal to PDB carbonate ($\delta O^{18} = 30.6$), then the above calculation would yield the three points connected by curve 2, figure 6-13. The numerical results are (on following page)

δO^{18} ocean water ‰	-1	0	+1
temperature for calcite °C	12.8	16.9	21
1000 $\ell n \alpha$ chert-ocean	34.85	33.9	32.9

Sample #127 is a chert nodule containing large fragments of calcitic clam shells, much invertebrate debris, and drusy calcite. The clam shells are also abundant in the host carbonate. δO^{18}-values for a single shell in the chert containing some fibrous calcite and one from the host (fabric not examined) are +25.59‰ and +25.93‰ respectively. The δO^{18}-value for the bulk included carbonate is +23.2‰. These data indicate that the included and host clam shells are similar in δO^{18} while the included bulk carbonate is much lighter, this probably because the drusy calcite has a low δO^{18}-value. As discussed in Chapter 6, the isotopic composition of the chert suggests a marine origin, but a higher temperature origin than for sample #171. The carbonate δ-values are also lower than for sample #171 and are thus compatible with this interpretation.

Assuming that the clam δO^{18}-values have not been significantly lowered since the original crystallization of the clam, then the paleotemperature equations can be applied as above. The calculated temperatures and the corresponding 1000 $\ell n \alpha$'s for the chert are given below and plotted in figure 6-13 as curve 3. As in the previous case, these are

maximum temperatures and the chert-water curve must fall on or to the right of the points in figure 6-13.

δO^{18} ocean water ‰	-1	0	+1
temperature for calcite °C	37.9	43.4	49.0
1000 $\ell n \alpha$ chert-ocean	29.6	28.6	27.6

Two additional cherts, #101 (Ordovician) and #28 (Permain) contain included carbonates (both dolomite and calcite) which are isotopically heavier than the host carbonate. δ-values for these are shown in figure 7-3. The carbonates were not examined petrographically, and it is not known in what form they occur. Fossil fragments were not seen by hand lens examination.

Chert #28 contains dolomite and calcite which is isotopically only slightly different from the host dolomite, but the host calcite is greatly depleted in O^{18}. It seems likely that δ-values of the original carbonate were equal to or greater than those presently observed in the included carbonate. Subsequent exchange lowered the host dolomite slightly, and the host calcite greatly.

Sample #101 shows similar relationships, except that the δO^{18}-value for the host calcite has not been exchanged to a very low value.

Most of the chert samples do not contain large, well-preserved calcite fossil fragments. The carbonate in these

cherts occurs as finely-disseminated irregular grains, dolomite rhombohedra, fracture fillings, and recrystallized blocky calcite. This included carbonate is either isotopically similar to the host or somewhat depleted in O^{18} and C^{13}.

Samples #220, 263, 259, 127, 94, 156, 138, and 34 are cherts which contain included carbonate with δ-values lower than the host carbonate. Several of these cherts, #259, 220, and 34, probably formed from light meteoric waters on the basis of their δD- δO^{18} relationships, pointed out in sections 6.3 and 6.11. For these cherts, the low δO^{18}-values probably resulted by precipitation and exchange of included carbonate with the light waters during silicification. The fact that host carbonate has not been lowered to the same values indicates that exchange and recrystallization of carbonate were more intensive in the localized portions of the limestone which were being silicified.

Three of the other cherts, all from the Burlington limestone, #127, 138, and 157 (figure 7-5), are considered to be marine, but contain included carbonate which has apparently exchanged with isotopically light waters. The fact that the host limestone has apparently not exchanged to the same extent presents a difficult problem for interpretation. One possibility is that the carbonate contained within chert is more susceptible to post-depositional exchange, but this seems unlikely in view of the data for

most of the other cherts. Another possibility is that the Burlington limestone at these localities was subjected to a period of fresh water diagenesis prior to silicification. The portions of the limestone most susceptible to alteration during this episode may have been the most susceptible to silicification under the later marine conditions. This might be the case if the fine-grained portions of the limestone exchanged more readily during diagenesis and were replaced more easily during silicification. In the case of sample #127, this interpretation could explain why the large included and host fossil fragments have similar δ-values, while the fine-grained included carbonate (bulk sample) has a lower δO^{18}-value. Other ad hoc explanations are possible, but it is clear that additional work is required.

δC^{13}-values for sample #263 and #267 (both from the same outcrop) are very low and indicate deposition under fresh water conditions (Clayton and Degens, 1959). However, in section 6.9, it was argued on the basis of δD- δO^{18}-values that chert #263 formed from ocean water. These data can be reconciled if it is assumed that the chert formed diagenetically under marine conditions following a period of fresh water limestone deposition.

E. Hydrothermally altered samples. δ-values for the included and host carbonates coexisting with the hydrothermally altered cherts, #35 and #36, are shown in

figure 7-7A. These δ-values are very much lower than those for other Mississippian samples. Exchange at high temperatures with light meteoric waters is undoubtedly responsible for the low δ-values. The lowering of carbonate δ-values in response to hydrothermal alteration has been well documented in studies by Engel et al. (1958), Lovering et al. (1963), Hall and Friedman (1969), and Pinckney and Rye (1972).

As previously mentioned in section 7.4-A, the chert and calcite are apparently not in isotopic equilibrium and thus cannot be used to indicate temperatures of hydrothermal alteration.

F. Carbonate coexisting with "evaporite" chert #153. Chert #153 was shown in section 6.6 to be anomalously enriched in deuterium and O^{18} relative to the other Carboniferous cherts. A diagenetic origin in the presence of waters which had been extensively evaporated was indicated. The limestone and cherts at this collection locality are severely weathered. The chert nodules contain concentric white and gray bands which apparently result when the gray included carbonate is leached out during weathering. δ-values for included carbonate from the white bands, gray bands, and for the host are shown in figure 7-7. A relatively unweathered sample of the host was obtained from the interior of a large block of carbonate laboriously broken off the outcrop.

δO^{18}-values for included carbonate from gray portions of the chert are heavier than any other Carboniferous calcite with the exception of the well preserved crinoid plates in chert #171. Some exchange has probably occurred during the intensive weathering of this sample and the original δ-value was undoubtedly even more positive. Since the chert probably formed from waters enriched in O^{18}, it is not unlikely that some exchange of the included carbonate also occurred, resulting in an anomalously high δO^{18}-value.

White portions of the chert contain 0.72% calcite, less than half the amount of included calcite in the gray portions. This calcite is considerably depleted in O^{18} and C^{13}. These data are consistent with the idea that the white bands are the more weathered and leached portions of the chert. The host carbonate yields δ-values typical of the Carboniferous limestones analyzed by Keith and Weber (1964). The relationships in the figure suggest that this sample of the host is better preserved than the included carbonate from the leached portion of the chert.

The conclusion that this chert and its included carbonate have interacted with evaporite waters does not necessarily indicate that the host limestone is an evaporite unit. It indicates only that the diagenetic waters were derived from waters which had been extensively evaporated. Abundant fossil outlines are visible within the chert,

suggesting replacement of a normal limestone rather than replacement of evaporite minerals.

Chapter 8

THE ISOTOPIC COMPOSITION OF AMORPHOUS SILICA AND GEODE QUARTZ

8.1 Introduction

Most of the previous discussion on the O^{18}/O^{16} and D/H ratio variations in naturally occurring hydrous silica has been concerned with cherts composed of granular microcrystalline quartz. In this chapter, the results of a brief isotopic investigation of opaline silica and geode quartz are considered.

Opaline silica is commonly found in sediments of Cenozoic age. Much of the opal occurs as biogenic silica which has not been diagenetically mobilized. It is of particular interest to determine if the isotopic composition of both biogenic and inorganic opals is original and if it is a function of temperature.

In the case of megaquartz, the best developed examples are geodes. The complexities of geode formation were discussed in section 2.6-J. It seems likely that an understanding of isotopic relationships in these materials could contribute significantly to an understanding of their origin.

8.2 Isotope Results for Amorphous Silica (Opal)

Ten samples of amorphous silica were investigated.

Descriptions and collection localities for these samples are given in Appendix I. Two of these are samples of hyalite, the purest form of opal. Another is common milky opal, and the remainder are samples of biogenic silica--four Tertiary diatomites, one sample of deep sea radiolarian ooze, and modern sponge spicules.

A. Sample treatment. The samples of diatomite and radiolarian ooze were unlithified and free of visable organic matter. Before analysis, the diatomites were allowed to dry in laboratory air. The radiolarians were obtained from a deep sea core sample. They were not allowed to dry in air, but were stored in a sealed container upon removal from the core.

The sponge spicules were obtained by dissolving a silica sponge in chlorox. This removed all organic matter and left a mesh of silica resembling glass-wool.

The opals were similarly crushed to <200 mesh and were then considered to be ready for isotopic analysis.

B. Procedure. The isotopic composition of hydrogen in these materials was determined using the D.I.A. technique described in section 5.2-A. δO^{18} was determined on the dehydrated silica. In several cases, oxygen isotope analyses were also made on samples which had not been dehydrated.

C. Results. D.I.A. results for sample #287 were previously discussed and can be examined in table 5-1 and figure 5-2. Results for the rest of the samples are given in table 8-1. Table 8-2 gives the total water contents for water outgassed above room temperature, δO^{18} determinations, and δD values for the total water and for water outgassed above 200°C. The total water contents are shown graphically in figure 8-1.

D. Discussion. In figure 8-1, it is apparent that marine biogenic silica is the most hydrous form of opal. The pure hyalites contain the least amount of water. Since the presence of large amounts of water inhibits accurate determination of δ-values for opal (see Chapter 5), it follows that hyalite should be the most suitable form of amorphous silica for isotopic studies. Marine biogenic silica should be the least suitable.

δD total and δO^{18} for each sample is plotted in figure 8-2. A comparison of the δO^{18} for undehydrated and dehydrated samples shows that δO^{18} values for dehydrated samples are more positive than for the same samples which have not been dehydrated. The effect of dehydration on the δO^{18}-values appears to be roughly proportional to the water content of the sample. Sample #355 has a large water content and shows a difference of 6.5‰. Sample #286, the least hydrous, shows a difference of only 1.2‰.

Table 8-1

DIFFERENTIAL ISOTOPIC ANALYSES FOR SAMPLES OF OPALINE SILICA

Sample	Fraction	Temperature Interval	Time Interval	µm water/ mg SiO_2	δD‰
286	1	25-103°C	2^h	sample lost	
	2	103-208	12^h	.32	-110.3
	3	208-1000	3^h	.787	-146.7
202	1	25-210	15^h	.851	-177.6
	2	210-1000	3^h30^m	.987	-219.4
261	1	25-66	13^h30^m	1.35	- 77.8
	2	66-195	4^h05^m	.49	- 45.5
	3	195-266	5^h20^m	.19	- 75.0
	4	266-1000	3^h06^m	1.01	-130.2
288	1	22	51^h35^m	1.16	- 47.1
	2	22-110	52^h25^m	1.23	- 37.1
	3	110-179	13^h20^m	1.70	- 83.0
	4	179-425	3^h45^m	1.52	-119.1
	5	425-649	5^h	.57	-120.4
	6	649-1029	2^h50^m	.13	- 95.4
285	1	20	1^h48^m	4.15	- 58.2
	2	20-56	19^h45^m	4.04	- 87.3
	3	56-107	3^h05^m	3.37	- 94.1
	4	107-157	2^h50^m	3.02	-100.8
	5	157-158	24^h40^m	2.22	-106.7
	6	158-209	4^h	1.29	-112.5
	7	209-372	14^h35^m	1.01	-117.8
	8	372-568	2^h50^m	.26	-126.0
	9	568-767	20^h15^m	.17	-137.4
	10	767-1014	4^h20^m	.02	-112.7
245	1	25-66	9^h25^m	1.61	- 32.0
	2	66-170	2^h15^m	1.71	- 84.1
	3	170-266	3^h	.16	-104.0
	4	266-1000	2^h	1.24	- 21.4

Table 8-1 (continued)

Sample	Fraction	Temperature Interval	Time Interval	μm water/ mg SiO_2	δD‰
355	1	24°C	2^h	.642	- 16.0
	2	24-35	12^h	.472	17.2
	3	35-75	4^h	.213	19.7
	4	75-115	22^h50^m	5.536	- 8.5
	5	115-185	1^h50^m	.557	- 16.7
	6	185-290	1^h45^m	1.466	- 24.4
	7	290-435	1^h50^m	.654	- 50.0
	8	435-541	2^h10^m	.201	- 38.9
	9	541-780	14^h30^m	.186	- 2.1
	10	780-1000	3^h30^m	.054	- 43.0
289	1	25	15^h40^m	3.66	- 61.4
	2	25-112	4^h48^m	.51	- 29.0
	3	112-188	4^h22^m	1.91	- 37.0
	4	188-407	11^h42^m	1.52	- 90.8
	5	407-801	15^h40^m	.43	-134.4
	6	801-1000	3^h35^m	no yield	

Table 8-2

ISOTOPIC COMPOSITION OF OPALINE SILICA

Sample	δD Total	$\delta D > 200^{\circ}$	δO^{18}	δO^{18} Dehydrated	wt.% H_2O
202	-200.0	-219.4		23.05	3.18
245	- 50.5	- 30.8	20.02	22.05	7.13
261	- 89.8	-121.4		29.30	5.08
285	-104.0	-119.4	17.5	20.55	6.94
286	-135.3	-146.7	26.27	27.46	2.02
355	- 15.6	- 31.4	35.83	42.4	9.1
287	- 52.1	- 91.5		34.87	7.5
289	- 76.9	-103.2	35.14	37.46	9.4
288	- 71.9	-117.4		23.62	6.9

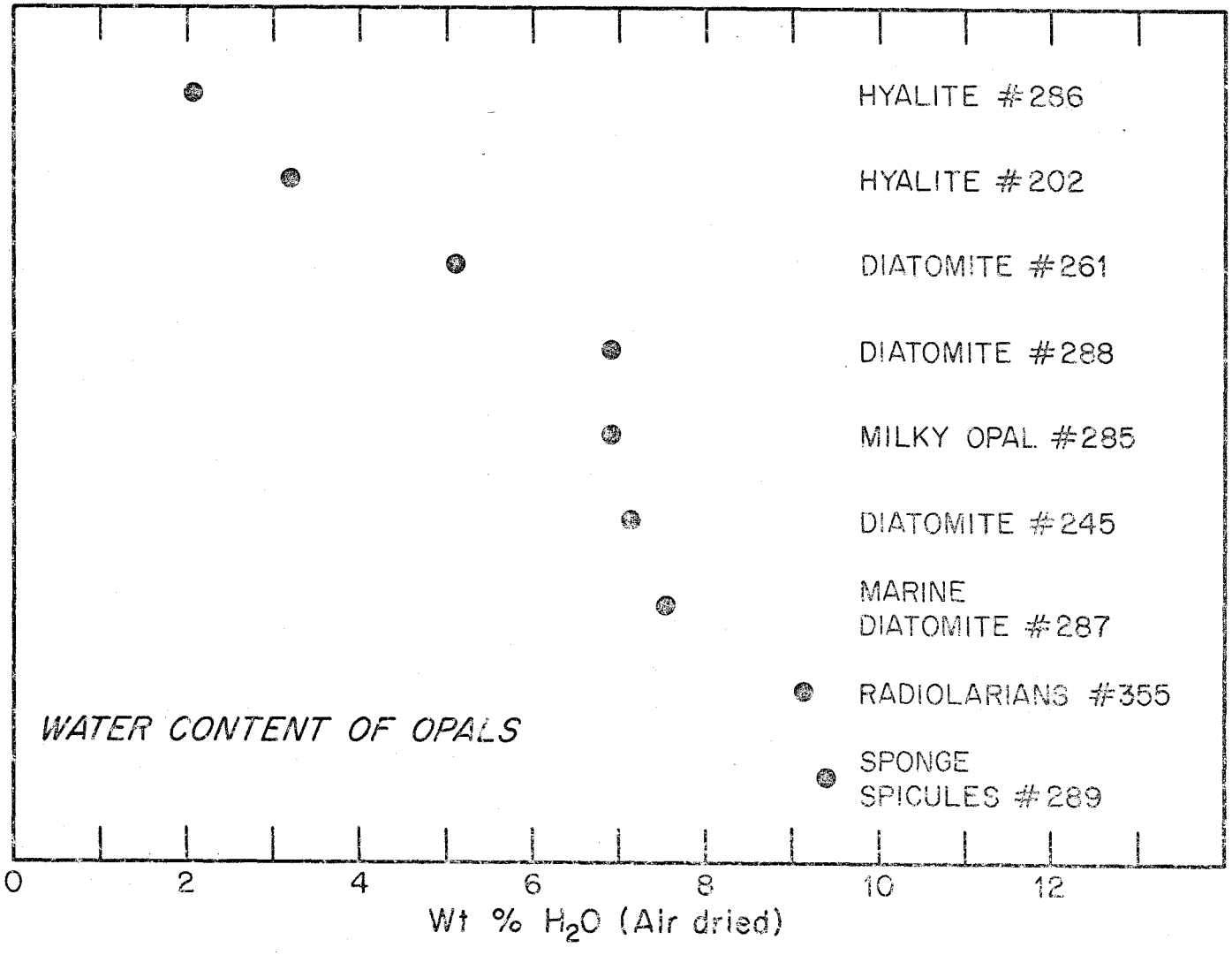
HYALITE #286
HYALITE #202
DIATOMITE #261
DIATOMITE #288
MILKY OPAL #285
DIATOMITE #245
MARINE DIATOMITE #287
RADIOLARIANS #355
SPONGE SPICULES #289
WATER CONTENT OF OPALS
0
2
4
6
8
10
12
Wt % H_2O (Air dried)

Figure 8-1

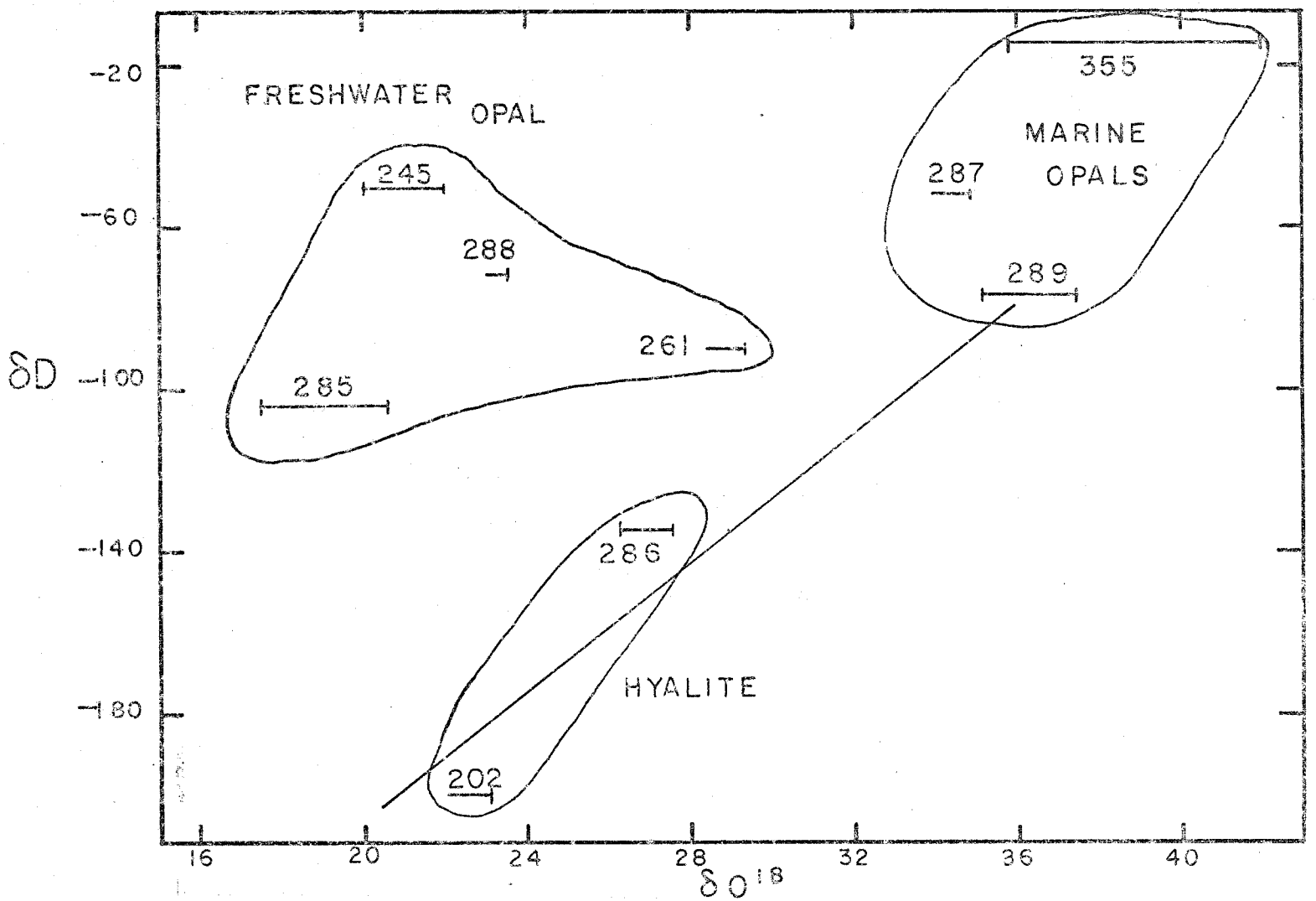

Figure 8-3. ISOTOPIC COMPOSITION OF AMORPHOUS SILICA. δ D-VALUES ARE FOR TOTAL WATER RELEASED ABOVE 25°. THE BAR CONNECTS δO^{18}-VALUES FOR THE SAMPLE BEFORE AND AFTER DEHYDRATION. THE LINE SHOWN IS PARALLEL TO THE METEORIC WATER LINE.

In several cases δO^{18}-values were determined only for the dehydrated samples. Since δ-values from dehydrated samples are more positive than those from undehydrated samples, these measurements are maximum values only.

As shown in figure 8-2, the δ-values for the samples fall into three groups. Marine silica is the most enriched in O^{18} and this undoubtedly results from the fact that ocean water has more positive δ-values than fresh water. δ-values for a second group, composed of the two hyalites, fall roughly on a line parallel to the meteoric water line which passes through the group of marine samples. This line is shown in figure 8-2 and is drawn to pass through the δ-values for present day sponge spicules. Formation of all these samples at similar temperatures is suggested.

The third group, composed mainly of δ-values for fresh water Tertiary diatomites, lies to the upper left of the "sponge-hyalite" line. This may indicate that these samples formed at higher temperatures. The large uncertainties in δ-values prevents any precise temperature assignment.

In Chapter 5 it was suggested that water outgassed from silica above 200°C was derived almost entirely from hydroxyl groups. It therefore is of interest to examine the δD-δO^{18} relationships using the δD-value for this

water fraction rather than for the total water. The fractions above 200°C were combined for each sample (table 8-2) and are plotted with the corresponding δO^{18}-values in figure 8-3. The δ-values again fall into three groups, and are related to one another in the same manner as the plot using δD total water. There is thus no reduction in the data scatter if δD is taken for the $>200^{\circ}$ fraction only.

E. Conclusions. Of all the varieties of amorphous hydrous silica analyzed, hyalite presents the fewest difficulties for isotopic analysis. Present techniques for the isotopic analyses of this form of opal are probably sufficient to indicate relative temperatures of formation and the probable isotopic compositions of the water from which it formed. Measurements of δ-values on these opals may thus be useful for investigating Cenozoic climates. Other forms of opal are so hydrous that meaningful δ-values cannot be ascertained with the existing analytical techniques. However, in spite of these uncertainties, the δ-values seem to fall into groups which qualitatively reflect the isotopic composition of the waters and the temperatures of formation.

The great dissimilarity between δD-values for radiolarians and other marine biogenic silica suggests a possible difference in the structure of these opals. Since

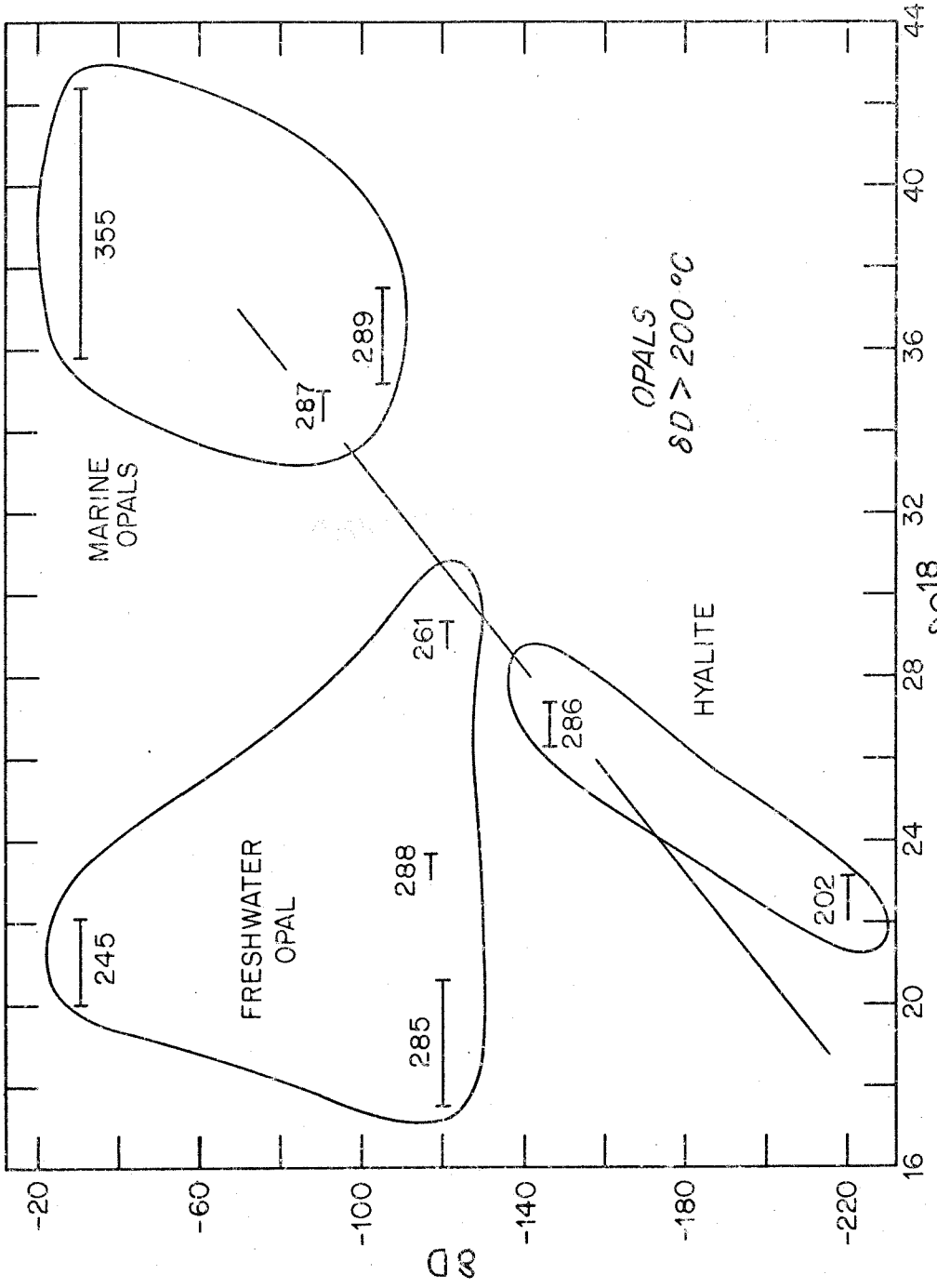

Figure 8-3. ISOTOPIC COMPOSITION OF AMORPHOUS SILICA.
δD-VALUES ARE FOR WATER RELEASED ABOVE 200°C. THE BAR CONNECTS
δO^{18}-VALUES FOR THE SAMPLE BEFORE AND AFTER DEHYDRATION.
THE LINE SHOWN IS PARALLEL TO THE METEORIC WATER LINE.

α^{hy} silica-water is negative for hydroxyl groups at low temperatures, the lower δD for sponges and diatoms may indicate that these forms of biogenic silica contain a greater proportion of hydroxyls than do the radiolarians. Unfortunately, the samples are of different ages, have had different geologic histories, and were treated differently in the laboratory. The suggestion that they may have different hydration states must therefore be viewed with caution.

8.3 Geodes

Isotopic data were obtained for several samples of megaquartz in geodes to evaluate the possibility of making meaningful δD measurements on this type of silica and to better understand the mechanism of geode formation.

Permian sample #209 was collected from an argillaceous carbonate deposit in the Phosphoria formation in Wyoming. δ-values for this sample and its coexisting carbonates are shown in table 8-3.

δO^{18}-values for the quartz and the host carbonate are very positive. The only reported δO^{18}-values for quartz which exceed this value of +38.9‰ are those reported by O'Neil and Hay (1971) for the cherts at Lake Magadii. Either this sample formed from ocean water at very low temperatures, or it formed from waters enriched in O^{18} by

Table 8-3

ISOTOPIC COMPOSITION OF QUARTZ AND CARBONATE IN PERMIAN GEODE #209 FROM PHOSPHORIA FORMATION

Phase	δO^{18}	δD	δC^{13}	wt.% H_2O
Megaquartz	38.90	-96.1		.19
Host calcite	32.29		-11.84	
Host containing translucent calcite	26.50		-14.25	
Calcite core	15.16		- 5.83	

evaporation.

Water was extracted from the quartz in the same manner as for cherts and had a δD-value of -96.1‰. The δD and δO^{18}-values of this quartz, if referred to figure 6-14, fall on the curve interpreted as the locus of δ-values for cherts in equilibrium with ocean water at various temperatures. This result suggests that δ-values of megaquartz can be interpreted in the same way as those of granular microcrystalline quartz; namely, that this geode formed in the presence of ocean water at a temperature of about $0^{\circ}C \pm 3^{\circ}C$. If this interpretation is correct, it implies that water occurs in megaquartz as hydroxyl and can be analyzed for δD in the same manner as for granular microcrystalline quartz.

The δO^{18}-values for the host carbonate is +32.29‰, giving an oxygen isotope temperature of 11.4°C, assuming δO^{18} of the water = 0‰. Since post-depositional exchange of the calcite with meteoric waters has probably lowered this δO^{18}-value, the original temperature of formation could have been approximately 0°C, as suggested by the megaquartz data.

Small pieces broked off hand specimens of the host carbonate contain translucent calcite on their surfaces. Both O^{18} and C^{13} of these pieces are depleted relative to normal marine samples, suggesting that the translucent calcite has been precipitated from meteoric waters. This beautiful translucent calcite was crystallized in the presence of water which fell from the sky and is therefore termed the "heavenly host".

The above results suggest that at least part of the Phosphoria formation was deposited at 0 or near-0°C temperatures under marine conditions. Such temperatures are usually atypical for any but deep sea sediments. Geologically, the Phosphoria formation is unusual. It contains a vast amount of phosphorite, phosphatic shales, bedded cherts, and geodiferous carbonates. It is not inconceivable that the remarkably low temperatures indicated by the isotopic data is partially responsible for the unusual character of this deposit.

The coarsely crystalline calcite core of this geode yields a very low δO^{18}-value of +15.16‰, indicating formation from light meteoric waters.

In section 2.6-J, the sequence of geode formation in the Warsaw formation, as proposed by Hayes (1964), was summarized. Following the sequence given by Hayes, the isotope record would be acquired in the following way: (1) deposition of heavy host carbonate due to low temperature or evaporite environment, (2) growth of carbonate in the presence of light meteoric waters, and (3) replacement of carbonate by quartz from evaporite waters or ocean waters at low temperature.

It is also possible that the sequence observed by Hayes did not occur for this geode. The isotope data are compatible with the following sequence which involves fewer steps than Hayes'. (1) Deposition from ocean water of host carbonate and shale at temperatures below 12°C, (2) growth of quartz at about 0°C in the presence of interstitial or ocean water with $\delta O^{18} = 0$, and (3) deposition of calcite in the hollow core at a much later time in the presence of meteoric waters.

The important difference between the two sequences is that in the latter sequence formation of the core calcite follows rather than precedes formation of the quartz geode. Since the latter sequence requires only one

large change in the isotopic composition of the interstitial or overlying waters, it is considered to be the more probable interpretation.

δC^{13}-values for the carbonates associated with the geode are given in table 8-3. The low δC^{13}-values for the host may mean that the carbonate was deposited from fresh waters which had become enriched in O^{18} by extensive evaporation. However, the use of carbon isotope analyses of carbonates for differentiating fresh water and marine sediments is much less reliable for shales than for limestones (Clayton and Degens, 1959). The significance of this δC^{13}-value is therfore difficult to assess.

δ-values for a geode, sample #284, collected from weathered Tertiary volcanic rocks in the Orocopia Mtns., California, are

δO^{18}: 21.87‰ δD: -67.5‰ water content: .39%
22.00

This isotopic composition, if referred to figure 6-14, suggests deposition at temperatures of ≈44°C in the presence of fresh waters. This temperature is probably high for Tertiary climatic temperatures, indicating that heated ground waters were at least partially responsible for the formation of this geode. A single δO^{18} measurement was obtained for large euhedral quartz crystals in a geode from the same area (sample #310). The value, +21.54,

is similar to sample #284.

In summary, it appears that significant amounts of water are contained in geode megaquartz in the form of hydroxyls which are suitable for isotopic investigation. The oxygen isotopic composition is certainly preserved over geologic time, since the crystal size equals or exceeds that of minerals in plutonic rocks which are known to have preserved their original δO^{18}-values. Isotopic analyses of hydrogen, oxygen, and carbon for geode quartz and its coexisting carbonates can be used to obtain the approximate temperature of their formation, the marine or fresh water nature of the diagenetic environment, and the probable mineral paragenesis.

Chapter 9

SILICA IN DEEP SEA SEDIMENTS

9.1 Introduction

Silica from deep sea sediments is particularly important for this study because it has not been exposed to meteoric waters. It is therefore possible to assume that the interstitial water in which the silica formed was isotopically similar to ocean water. Any variations in the isotopic composition of the silica may then be related to temperature, mineralogy, and possible vital effects in the case of biogenic silica.

9.2 Sample Descriptions and Isotopic Results

Samples were selected from cores for 4 drill sites of the Deep Sea Drilling Project. These samples included radiolarian ooze, opal-CT, granular microcrystalline quartz, chalcedony, and drusy quartz. Also obtained was a hand specimen of granular microcrystalline quartz from a seven-foot long chert nodule dredged from Horizon Guyot.* With the exception of the radiolarians, all of this silica formed diagenetically in the sediments.

---

* This sample was dredged during an investigation of Horizon Guyot conducted by Dr. William Newman of the Scripps Institution of Oceanography. It was transmitted to the author by Dr. Harmon Craig.

In table 9-1, the JOIDES sample numbers, the age of the sediments in which the silica occurs, the mineralogy, and the isotopic results are listed. Descriptions, locations, and literature references for these samples are given in the appendix. The literature references give complete discussions of the drill sites, cores, regional geology, and analytical data.

Where possible, the different silica phases were separated before isotopic analysis. Percentages of the different constituents are given for unseparated mixtures. All samples except the radiolarian ooze was crushed to <200 mesh. δO^{18} determinations on samples which were not dehydrated prior to analysis are minimum δO^{18}-values, due to their possible water contents (see Chapter 8). Unless otherwise indicated, δD is for the total water outgassed between 25° and 1000°C after the sample had been exposed to high vacuum over night.

9.3 Oxygen Isotope Results

Figure 9-1 shows δO^{18}-values of the silica phases and coexisting carbonates plotted against the sediment depth at which the samples were cored. The samples come from 4 separate localities in the Pacific Ocean and from one locality in the Caribbean Sea (#370). All were recovered from mid-Eocene horizons except for sample #356, which was found in an Upper Cretaceous horizon.

Table 9-1

DEEP SEA SILICA

Sample #	JOIDES #	Sediment Depth, Meters	Mineralogy*	δO^{18}	Temp. °C	δC^{13}	wt.% H_2O	δD
352	8-70B-4cc	388	95% chert, 5% opal	33.24	18			
353	"	"	Drusy Quartz	29.83	32			
353-F	"	"	Pure chalcedony	35.19	11		1.09	-85.6
354	7-64-1-11	984	>95% gmc qtz	35.19	11		.92	-78.9
354-L	"	"	67% calcite	30.78		+2.34		
"	"	"	65% calcite	30.62		+2.34		
"	"	"	Acid residue: >80% opal	37.22	4			
355	8-69-6-5	190	100% opal, air-dried	35.83			9.0 (>25°C)	-32.1
"	"	"	" " , dehydrated	42.43			See table 8-1 for D.I.A.	
356	7-61-1cc	86	>98% gmc qtz	35.62	9		1.0	-79.1
"	"	"	" " "	35.90	8			
356-0	"	"	>98% opal	36.14	7		1.2	-56.5
"	"	"	" " , dehydrated	36.79	5		See table 9-2 for D.I.A.	
"	"	"	" " , dehydrated	36.87				

* gmc qtz = granular microcrystalline quartz
opal = opal-CT (?)

Table 9-1 (continued)

Sample #	JOIDES #	Sediment Depth, Meters	Mineralogy*	δO^{18}	Temp. °C	δC^{13}	wt.% H_2O	δD
367	8-70B-1B-1	383	7% calcite	29.52		+2.35		
"	"	"	Acid residue:					
			>90% opal	34.89				
368	8-70B-2B-1	385	>98% gmc qtz	32.58	20			
"	"	"	5% gmc qtz, 95% opal	34.67	12			
"	"	"	>98% gmc qtz, porous	32.46	21			
369	8-70B-1B-1	383	>98% opal	34.71	12			
370	15-149-43-1	390	Acid residue:					
			>90% opal	34.32	14			
"	"	"	25% calcite	29.10		+2.21		
"	"	"	27% calcite	28.88		+2.13		
343	Horizon Guyot	Dredge Haul	>98% gmc qtz	38.85				

* gmc qtz - granular microcrystalline quartz
opal = opal-CT (?)

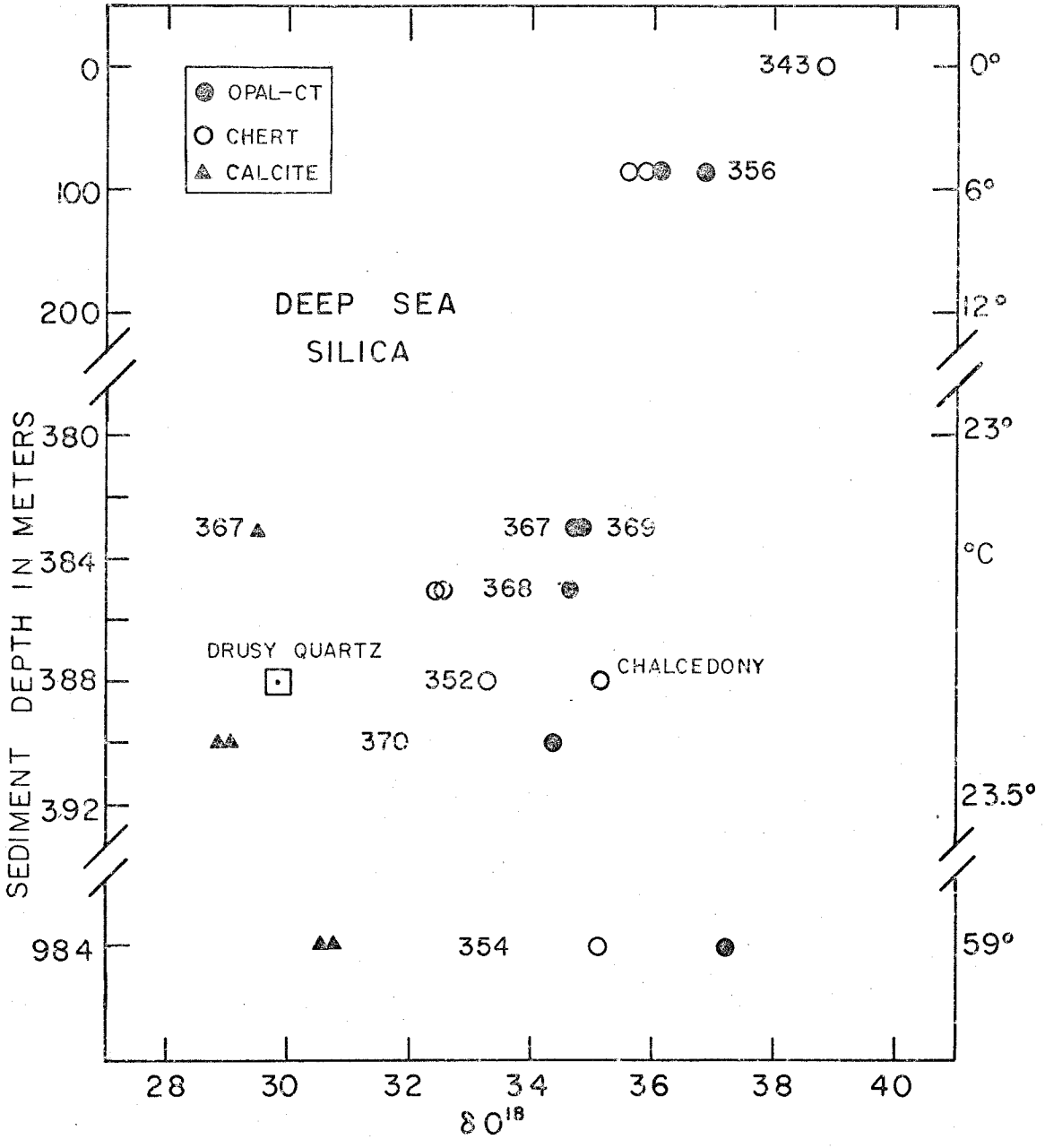

Figure 9-1

OXYGEN ISOTOPIC COMPOSITION OF DEEP SEA SILICA. "OPAL-CT" REFERS TO SAMPLES COMPOSED PREDOMINANTLY OF ISOTROPIC SILICA.

From figure 9-1, it is apparent that δO^{18}-values for deep sea silica are generally very positive. This probably indicates formation at very low temperatures in the presence of interstitial waters isotopically similar to ocean water. δO^{18}-values for silica obtained from the drill holes are significantly lower than that measured for the dredge-haul sample, #343. This may mean that the silica obtained from deep sediment depths formed during diagenesis at the warmer temperatures characteristic of burial. On the other hand, it is possible that silica forms before significant burial at ocean bottom temperatures. The less positive δO^{18}-values for silica in the more deeply buried sediments may represent silica formation at past times when the bottom waters were warmer than the time at which the dredge haul sample formed.

A. Relationships between δO^{18}-values and depth of burial. Estimated sediment temperatures, assuming bottom water temperatures of $0^{\circ}C$ and a normal oceanic geothermal gradient of $.06^{\circ}C$/meter (Von Herzen and Langseth, 1965), are shown in figure 9-1. A very significant increase in temperature with depth of burial is apparent. However, the δO^{18}-values do not decrease accordingly. In particular, the most deeply buried sample (#354) yields δO^{18}-values similar to the least deeply buried sample (#356). It must be concluded that much of the silica diagenesis occurs before or during shallow burial and at ocean bottom temperatures.

δ-values acquired at these temperatures must then be preserved during deep burial.

In samples #356, 368, and 354, the δO^{18} of the opal-CT is 1 to 3‰ more positive than that of the coexisting granular microcrystalline quartz of these samples. Such a result is possible if opal-CT forms during shallow burial and is transformed to granular microcrystalline quartz in the presence of water with $\delta O^{18} \cong 0$ at the higher temperatures encountered during burial. Granular microcrystalline quartz, which equilibrates or exchanges with this water at the warmer temperatures, would thus have lower δO^{18}-values.

Sample #356 has been buried the least amount and shows the smallest δ-value difference. Presumably, the two kinds of silica had to form within 6°C of each other, since they have only been buried 86 meters where the sediment temperature is 6°C greater than at the sediment-ocean interface. Sample #368 has been buried to greater depths and presumably was subjected to higher temperatures and consequently shows a larger δO^{18} difference between the two types of silica, suggesting that the granular microcrystalline quartz formed at these higher temperatures. Significantly, this δO^{18} difference between the opal-CT and granular microcrystalline quartz is not larger for sample #354, in spite of the fact that this sample has been buried twice as deep. The results indicate that the granular

microcrystalline quartz in sample #354 formed at about the same depth as the granular microcrystalline quartz in sample #368 and has remained isotopically unchanged while suffering deeper burial.

Drusy quartz crystals in a cavity in sample #353 have the least positive δO^{18}-value of deep sea silica. These crystals had grown upon a layer of fibrous quartz which lined the cavity. The chalcedony has a more positive δO^{18}-value, similar to that of sample #356. It therefore seems likely that the cavity formed and was lined with chalcedony before it had reached a depth of 100 meters. Subsequent growth of the drusy quartz probably occurred at greater sediment depths and higher temperatures.

Carbonates coexisting with silica in these sediments consist of indurated calcareous oozes of pelagic origin which have been partially silicified. In thin-section, minor calcite overgrowths can be seen on foraminifera and nannofossils, indicating at least some diagenetic change in the condition of the original calcite (Moberly and Heath, 1971). However, no correlation of δO^{18}-value with depth of burial is apparent for the three carbonate samples analyzed. Carbonate sample #354-L (mid-Eocene), buried to the greatest depth (984 meters) has a δO^{18}-value of +30.7‰, almost identical to the δO^{18}-value of +30.3‰ obtained by Douglas and Savin (1971) for well preserved, middle Eocene planktonic Foraminifera from the

western Pacific. At least in the case of this sample, major isotopic change has not resulted due to induration of the calcareous ooze. The other two carbonate samples have less positive δO^{18}-values, but it is difficult to attribute these to diagenesis at higher temperatures during burial since the inferred sediment temperature of 20 - 25°C cannot have greatly exceeded the surface-water temperatures at which the pelagic calcite originally formed (15 - 30°C).

For the three samples analyzed, there is a correspondence between the variation of δO^{18}-values for the opal-CT and variation of the δO^{18}-values for the coexisting carbonate. In other words, the more positive the opal-CT δO^{18}-value, the more positive the carbonate δO^{18}-value. Since the variations in carbonate δO^{18}-values are probably related to the temperature variations of the ocean water in which they formed, this correspondence suggests that the opal-CT δO^{18}-values may also be related to ocean temperatures. This is a weak argument, but it further supports the idea that δO^{18}-values for opal-CT are fixed during shallow burial.

B. Deep sea cherts as calibration points for the quartz-water oxygen isotope fractionation curve. Two natural calibration points in the quartz-water oxygen isotope temperature scale can be proposed utilizing δO^{18}-values for deep sea silica. These are based upon sample #343 and the drusy quartz sample #353.

Sample #343. Since this sample is a dredge-haul sample, it has not been deeply buried and it is likely that the interstitial waters from which it formed were isotopically similar to ocean waters. The dredge-haul was recovered from a water depth of about 1700 meters, where the temperature is probably about 2°C (Sverdrup et al., 1942, p. 746).

Present day Pacific deep water has a δO^{18}-value of -0.2‰ (Craig and Gordon, 1965). However, the chert could have formed at any time since mid-Eocene, and may have formed at a time when no ice cap was present. The isotopic composition of deep ocean water at such times was probably δO^{18} = -0.6‰, according to Craig and Gordon. On the other hand, the chert may have formed during the peak of the Pleistocene glaciations, at which time the water may have been +0.9‰. Therefore, the range of isotopic compositions of water from which the chert formed was probably -0.6 to +0.9‰. The temperature could range from the present day ocean minimum of -1°C to the mid-Eocene value of 13°C, suggested by the data of Emiliani (1954) and Lowenstam and Epstein (1956). The range in values of $1000 \ell n \alpha$ quartz-water defined by these temperatures and waters is shown by rectangle A in figure 6-13. It is very probable that the quartz-water curve passes through this rectangle.

This chert is several per mil heavier than any of the other Cenozoic deep sea cherts, suggesting that it may have formed during a glacial maximum when the temperature of the oceans was near a minimum. If so, then the calibration point for the quartz-water curve suggested by this sample should lie toward the lower right corner of rectangle A in figure 6-13. Specifically, it would lie between the two values given below:

	$\%o\delta O^{18}_{water}$	T°C	$10^3 \ell n \alpha$	$10^6/°K^2$
chert in equilibrium with ocean today	-.2	+2	38.3	13.2
chert in equilibrium with ocean during glacial maximum	+.9	-1	37.2	13.6

A line segment connecting these two points is shown in figure 6-13 and is labeled "C".

Drusy quartz, sample #353. As indicated in figure 9-1, the temperature reached during burial of sample #353 is about 23°C if the geothermal gradient is 6°/100 meters. Assuming that the drusy quartz formed in the temperature range 20° - 30°C from waters with the same isotopic range of -0.6 to -0.9‰, then the range of $1000 \ell n \alpha$ -temperature points can be shown as rectangle B in figure 6-13. The temperature at which the quartz formed is extremely uncertain due to possible variations in the geothermal gradient and the possibility that the quartz formed at shallower sediment depths or from ascending hydrothermal

solutions. Also, the temperature in the sediments could have been higher if bottom waters were warmer in the past.

C. Temperatures of silica formation and their relevance to Cenozoic ocean bottom temperatures. Perhaps the single greatest uncertainly in using δO^{18}-values of deep sea silica as temperature indicators for deep sea sediment diagenesis is the great time interval over which the silica transformations can occur. For example, the Upper Cretaceous sample is still incompletely transformed from opal-CT to granular microcrystalline quartz, after a period of possibly 60 million years. The granular microcrystalline quartz which has formed is probably a composite sample of chert which formed at various bottom temperatures, sediment temperatures, and isotopic compositions of interstitial water. The prospect of obtaining isotopic temperatures for opal-CT is better since it probably forms earlier in the diagenetic sequence, probably shortly after burial.

The use of radiolarians and diatoms for isotopic temperatures would relate directly to ocean water temperatures at a specified age, but accurate δO^{18} measurements of these materials cannot presently be obtained because of the unusually large water content of biogenic opal.

Fortunately, the water content of opal-CT is apparently small, and only slightly exceeds that of coexisting granular

microcrystalline quartz (see sample #356). δO^{18} can probably be determined with an accuracy of $\pm$.5‰ for opal-CT.

Table 9-1 contains a tabulation of isotopic temperatures assuming δO^{18} of the interstitial waters to be -.6‰. The quartz-water oxygen isotope temperature-fractionation curve used is curve I of figure 6-13. Since opal-CT is apparently composed of hydrous cristobalite and not a quartz, the temperatures deduced from this curve should be viewed as uncertain approximations.

Temperatures obtained in this fashion for mid-Eocene opal-cristobalite are approximately 4 - 16°C. The Caribbean sample (#370) and the Pacific samples at site 70B (#368 and #369) define the upper end of this range and agree well with the Tertiary deep sea temperature trend given by Emiliani(1954) and Lowenstam and Epstein (1956). Their data is shown in figure 9-2, together with the opal-CT temperatures.

The low temperature indicated for sample #354 can be explained if this opal-cristobalite formed after mid-Eocene times when bottom water was possibly cooler, say, during Pliocene time. However, during this time period, the sample was already buried to a depth of at least 800 meters (Winterer et al., 1971, Chapter 6, figure 7) and, therefore, a probable temperature of around 50°C. The sample had to form before burial to a depth sufficient to heat the

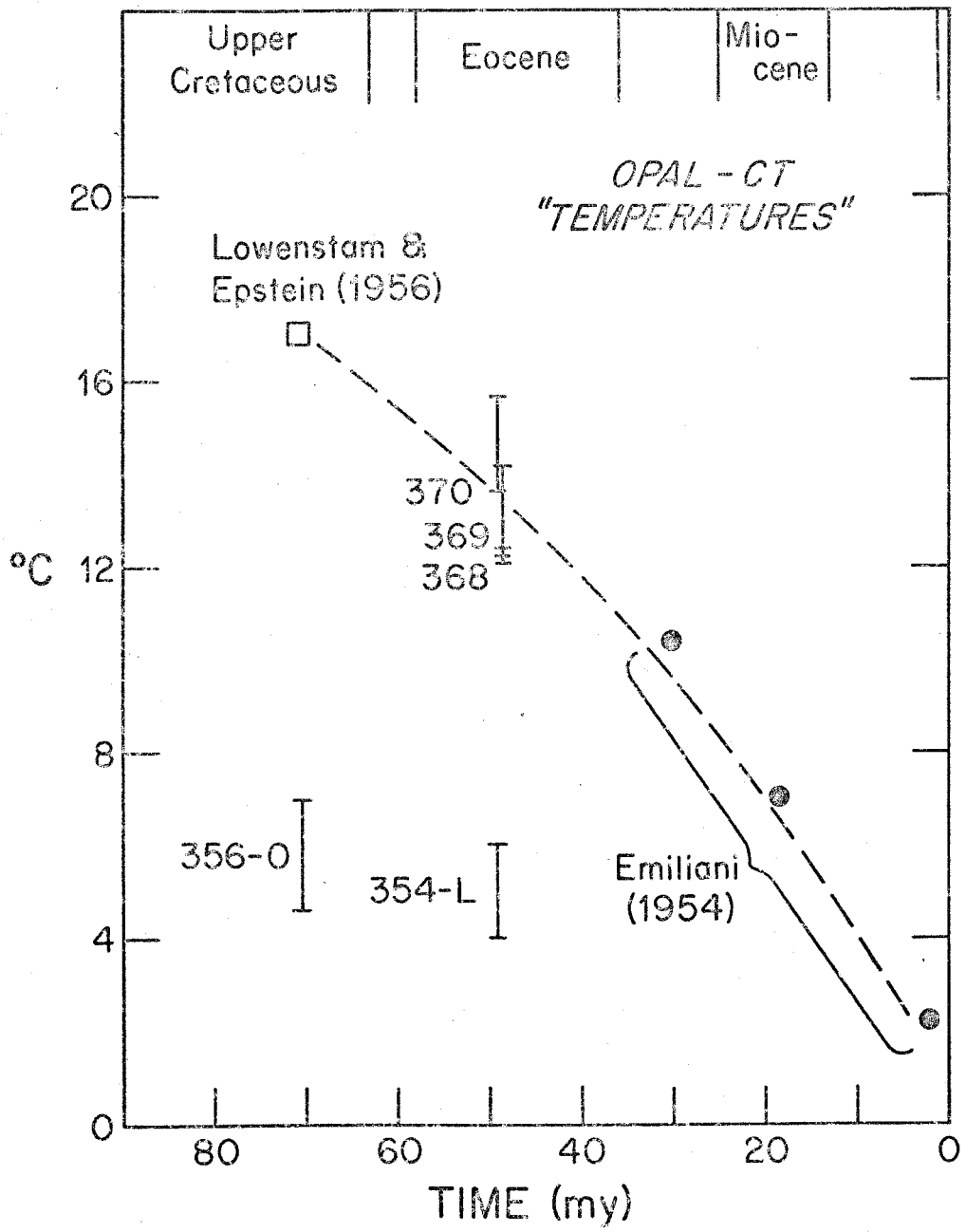

Figure 9-2

DEEP SEA TEMPERATURES CALCULATED FROM THE δO^{18} OF OPAL-CT IN DEEP SEA SEDIMENTS

sediments to 6°C--about 100 meters. Sediments 100 meters above this sample have ages of Upper Eocene-Lower Oligocene. Thus, at some time between mid-Eocene and Lower Oligocene, cold bottom waters had to be present, implying possible glaciations during this interval. It is interesting in this respect that the oxygen isotope paleotemperature determinations for Pacific Planktonic Foraminifera indicate a temperature minimum during the Oligocene (Douglas and Savin, 1971).

Sample #356-O from a Cretaceous horizon yields temperatures far below the result of Lowenstam and Epstein for Cretaceous bottom water. However, this sample has only been buried to a depth of 86 meters. The increase in temperature due to burial is probably less than 6°C. Thus, at any time since the Upper Cretaceous, when the bottom temperatures reached near 0°C, the opal-cristobalite could have formed at the indicated temperature.

It is also possible that the opal-CT formed in the Upper Cretaceous or Paleocene. If so, the low isotopic temperature given by this sample indicates that cold bottom waters were present at these times and that the general cooling trend for bottom water from Cretaceous to Pleistocene proposed by Emiliani , Lowenstam, and Epstein is not correct.

9.4 Hydrogen Isotope Results

A. Interstitial waters. An attempt was made to determine the approximate δD-value of interstitial waters in the Radiolarian ooze, sample #355.

2.2 gm of ooze was placed in the vessel shown in figure 5-6. The stopcock was closed and the sample frozen with liquid nitrogen. Air in the vessel was pumped out and the stopcock was again closed. The cold-trap was then transferred to the side arm. As the sample warmed up, the interstitial water was frozen into the side arm. After the sample was completely dry, the cold-trap was removed from the side arm and the ice allowed to melt, yielding 1.4 ml of water. The vessel was then vented and capillary samples of the water were obtained and analyzed for δD. The dry radiolarians weighed .83 grams. The interstitial water content of this sample is therefore 63.5 wt.%.

δD for the interstitial water is -4.5‰ on the SMOW scale. This value is only an approximate one for the following reasons:

(1) Contamination of the very permeable ooze by waters used in the drilling operation is probable.

(2) Isotopic exchange with water vapor during shipboard examination, subsequent storage, and laboratory handling is probable and serves to reduce the δ-value.

(3) Very small amounts of isotopically light water

vapor in the reaction vessel are frozen in with the sample and therefore included in the analysis.

(4) Much water adsorbed on the radiolarians is probably removed during distillation into the sidearm. This water may have been fractionated during the initial adsorption.

Because the amount of water is large, the error due to points 1 - 4 is probably minor. Contamination during drilling is probably the most serious effect.

The most important conclusion is that interstitial waters in siliceous sediments buried to a depth of 200 meters are isotopically similar to present day ocean water. Large fractionations of hydrogen isotopes associated with possible early diagenesis in these sediments are not indicated.

B. Changes in isotopic composition and hydration states during silica diagenesis. The sequence of mineralogical transformations in deep sea silica diagenesis can be considered to be the following: biogenic silica ⟶ opal-CT ⟶ granular microcrystalline quartz (Heath and Moberly, 1971). It was, therefore, of interest to compare the D.I.A. patterns for these three mineralogical forms to see if any changes in the hydration characteristics and δ-values occurred during the transformation.

Standard D.I.A. patterns were obtained on the radiolarians dried in the manner described above and on the opal-CT crushed to <200 mesh. The opal-cristobalite sample (#356-O) was part of the Cretaceous chert nodule, #356. δ-values for the granular microcrystalline quartz in this sample were given previously in section 6.10.

Data for the radiolarian D.I.A. were given in table 8-1 and are plotted in figure 9-3. Water given off below 115°C is isotopically similar to the interstitial waters. This water is therefore probably adsorbed and mechanically trapped. Water fractions given off above 115°C have lower δD-values, suggesting a mixture of much lighter hydroxyls and adsorbed water as in the case of diatomite (see Chapter 5).

Data for the D.I.A. of opal-cristobalite are given in table 9-2 and plotted in figure 9-4. Opal-CT is much less hydrous than biogenic silica. However, it is apparently not the dehydration product of biogenic silica. This can be seen by comparing the two D.I.A. patterns in figures 9-3 and 9-4. The D.I.A. of opal-CT does not correspond to the last fractions of the D.I.A. for radiolarians, as might be expected if all the loosely-bound water in ratiolarians were removed during opal-CT formation. This result is not unexpected, since petrographic and scanning electron microscope observations show that opal-CT forms

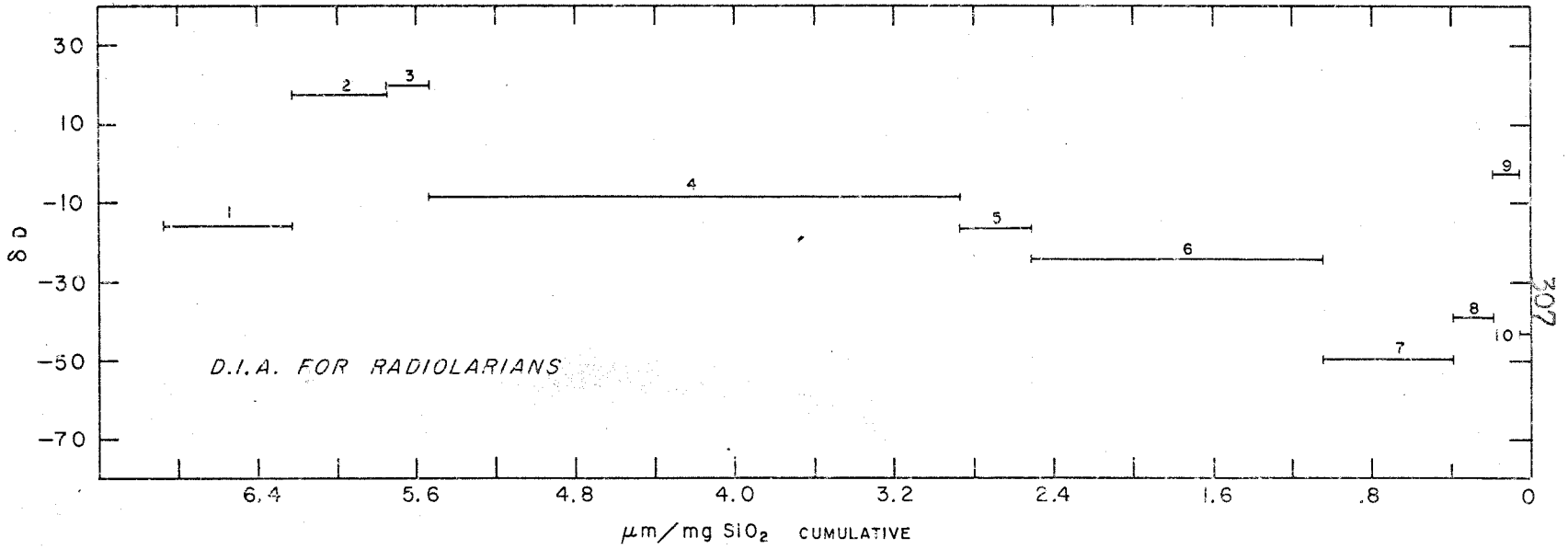

Figure 9-3

DIFFERENTIAL ISOTOPIC ANALYSIS OF RADIOLARIAN OOZE RECOVERED FROM SITE 69 OF THE DEEP SEA DRILLING PROJECT

Table 9-2

DIFFERENTIAL ISOTOPIC ANALYSIS FOR OPAL-CT, #356-O

Fraction	Temperature Interval	Time Interval	μm water / mg SiO_2	δD‰
1	25°C	18^h45^m	.313	-17.6
2	25-126	3^h	.141	-13.1
3	126-228	4^h05^m	.109	-36.4
4	228-308	3^h25^m	.077	-60.8
5	308-416	2^h30^m	.113	-74.3
6	416-1000	4^h30^m	.257	-79.6

as a result of diagenetic silica mobilization rather than the in situ transformation of biogenic silica (Heath and Moberly, 1971; Weaver and Wise, 1972; von der Borch et al., 1971).

The last fraction of the D.I.A. for opal-CT is isotopically similar to the δD-value of the coexisting granular microcrystalline quartz. Above 416°C, most water appears to be coming from sites containing hydroxyls with a δD-value of approximately -80‰. The D.I.A. pattern for opal-CT can be explained if opal-CT has water in two "sites", one composed of H_2O and OH which outgasses at lower temperatures with δD-values near zero, and the other composed of OH with δD-values of -80‰, which outgasses primarily at high temperatures. It is thus possible that a simple dehydration of this opal-CT in which the low temperature

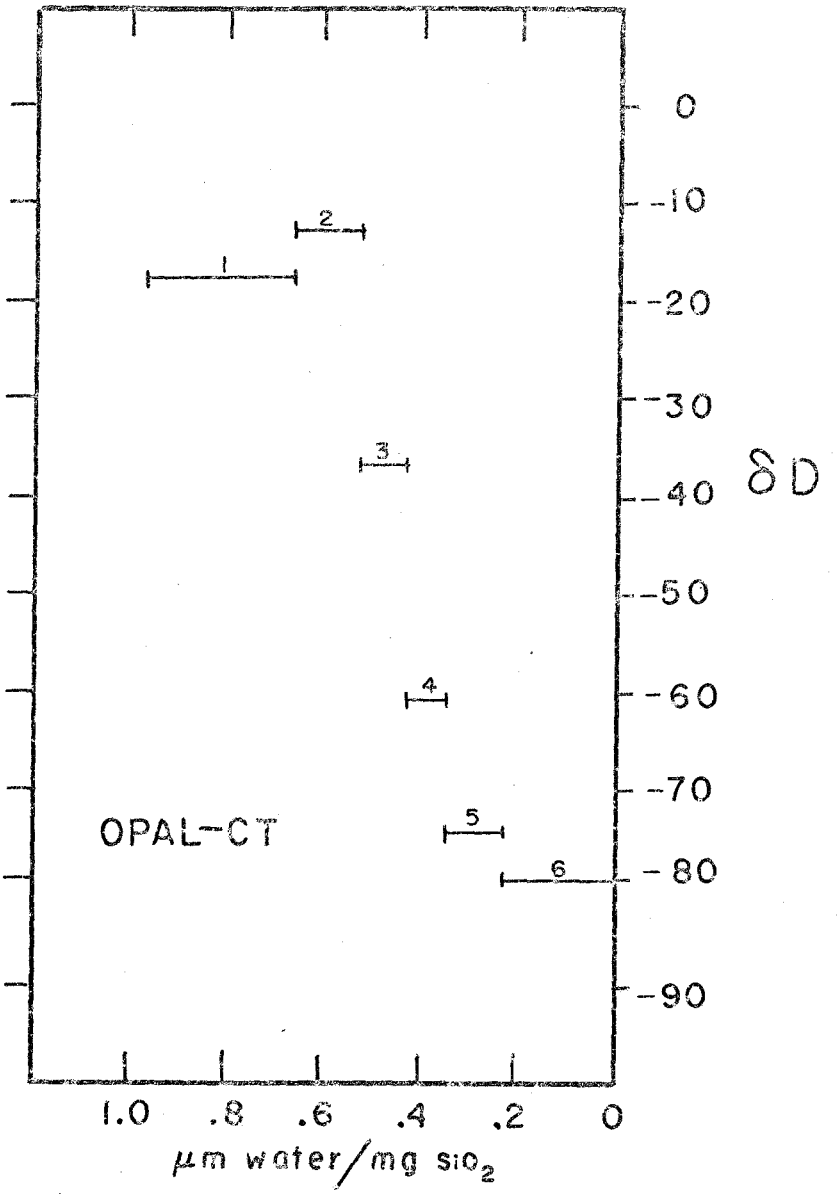

Figure9-4. DIFFERENTIAL ISOTOPIC ANALYSIS FOR OPAL-CT FROM SITE 61 OF THE DEEP SEA DRILLING PROJECT.

water (δD-values near zero) is lost could result in granular microcrystalline quartz with δD-values very close to those observed for the coexisting granular microcrystalline quartz. However, since the two forms of silica had to form within about $6^{o}C$ of one another, complete exchange of the hydroxyl component during conversion of opal-CT to granular microcrystalline quartz would result in little change of δD-value. It is thus not possible to use hydrogen isotope data for this sample to decide whether the mechanism of conversion from opal-CT to granular microcrystalline quartz is a solid state transformation or a solution-reprecipitation mechanism.

Chapter 10

CONCLUSIONS AND SUMMARY DISCUSSION

10.1 The D/H Ratio in Hydrous Silica

Sedimentary silica contains water of various amounts ranging from 10 wt.% in marine biogenic opal to 0.03 wt.% in some cherts. Adsorbed, mechanically trapped, and readily exchangeable water in biogenic opal, fibrous quartz, granular microcrystalline quartz, and megaquartz can be largely removed from the samples if they are crushed to <200 mesh and vacuum-pumped for several hours at room temperature.

In the case of biogenic silica, water released at temperatures above 25°C is derived from bonded H_2O and hydroxyls from at least 5 sites. The relative amounts of water in these 5 sites is shown by the histogram in figure 5-18. Most of these waters exchange at 100°C in the laboratory with deuterium enriched water, indicating that many natural samples of biogenic opal may not preserve their D/H ratios over geologic time.

Vacuum pumping at room temperature removes nearly all of the readily exchangeable water in granular microcrystalline quartz. Water extracted from this material above 25°C is derived almost entirely from hydroxyl groups within the silica structure. Most cherts are composed predominantly of granular microcrystalline quartz and thus contain hydroxyl

groups suitable for hydrogen isotope analyses. The question of preservation of these ratios over geologic time must be treated by examination of natural data.

In the case of cherts which are composed mostly of chalcedony, approximately 14% of the water extracted after they have been pumped under high vacuum is water which can be exchanged in the laboratory. The remaining 86% of the water extracted is probably derived from hydroxyl groups within the silica structure and not from fluid-filled bubbles as proposed by Folk and Weaver (1952).

10.2 δD-δO^{18} Relationships in Cherts

When plotted on a δD-δO^{18} diagram, δ-values for cherts of a given age collected from the central and western United States and consisting predominantly of granular microcrystalline quartz free of organic matter define a domain which is greatly elongated in a direction parallel to the meteoric water line. As shown in figures 6-10 and 6-11, the domains of δ-values for cherts from the Upper Cambrian, Ordovician, and Triassic are similar. The domains for δ-values of cherts from the Devonian, Carboniferous, and post-Jurassic cherts are separate from those of the Upper Cambrian, Ordovician, and Triassic, but overlap to some extent. δ-values for several Precambrian cherts fall within the domains of the Phanerozoic samples, while those for several

other Precambrian cherts lie well outside these domains.

These data indicate that, for many cherts, the diagenetic transformation of opal to granular microcrystalline quartz occurred in the presence of meteoric waters. δ-values for cherts which may have formed directly or diagenetically from marine waters lie on or near a line given by the equation

$$\delta D = -6\delta O^{18} + 135$$

This is shown as line A in figure 6-11. Samples with δ-values significantly above this line have probably been derived from evaporite waters.

Unlike the δO^{18}-values of limestones, the δ-values of cherts appear to have been preserved over geologic time. The variation with time of the domain of δ-values in δD-δO^{18} space is best understood in terms of climatic temperature variations over geologic time in the central and western United States. δ-values for cherts formed in warm climates lie closer to the meteoric water line than those formed in cooler climates due to the temperature dependence of isotopic fractionation factors for the chert-water system. In this interpretation, Cambrian, Ordovician, and Triassic cherts formed from waters about 15°C warmer than those of the Cretaceous and Tertiary cherts. Assuming no large change in the isotopic composition of ocean water, figure 6-14 shows the approximate range of temperatures proposed for the

formation of cherts studied in this investigation. The total range of temperatures is about 40°C.

The presence of large amounts of megaquartz in cherts, when unrelated to cavities and veins, usually indicates that the chert has been recrystallized in response to thermal metamorphism or hydrothermal activity. δ-values for such recrystallized cherts are frequently, but not always, greatly altered.

10.3 Deep Sea Silica

Silica in deep sea sediments occurs as biogenic opal, opal-CT, chalcedony, granular microcrystalline quartz, and drusy quartz. Biogenic opal is dissolved and reprecipitated to form opal-CT during shallow burial of the sediments. Temperatures based on the quartz-water oxygen isotope fractionation can be calculated for the formation of this opal-CT. Because the opal-CT is forming near the sediment-ocean interface, the temperature so calculated is approximately equal to the temperature of deep ocean water. Temperatures calculated for several samples of post-Jurassic opal-CT are shown in figure 9-2. These temperatures are in partial agreement with the results of Emiliani (1954) and Lowenstam and Epstein (1956), but suggest the possibility of extremely cold bottom water near the close of the Cretaceous and near the beginning of the Oligocene, implying possible

glaciations during these intervals.

Opal-CT is transformed to granular microcrystalline quartz during subsequent burial of the samples. The isotopic composition of granular microcrystalline quartz in deep sea sediments may thus reflect the temperature of burial and isotopic variations in the interstitial waters.

10.4 Carbonates Coexisting with Cherts

The chert-carbonate fractionation for O^{18}/O^{16} is highly variable, ranging from -4.5‰ to +14‰. Most coexisting cherts and calcites are out of isotopic equilibrium with one another and the difference in δO^{18}-values between the two cannot be used to deduce isotopic temperatures.

The observed variation in values for Δchert-calcite can be readily understood if, as suggested by the δD-δO^{18} data, many cherts form diagenetically from fresh waters in strata which were originally of marine origin. Negative Δ-values for chert-carbonate correspond to situations where the chert formed in the presence of low O^{18} meteoric waters in marine carbonate rocks which have partially preserved their originally high δO^{18}-values.

In a few cases, cherts contain well preserved calcitic fossils. In one of these, Mississippian Crinoids yielded δO^{18}-values of +29.14‰, the highest δO^{18}-value yet measured for Mississippian calcite. The oxygen isotope

temperature for this calcite is 25°C. This result suggests that many calcitic fossils encased in chert nodules might be suitable for isotopic paleotemperature analysis.

10.5 Isotopic History of the Hydrosphere

It is very unlikely that large changes in the isotopic composition of the oceans could occur at a fast enough rate to account for the rather large displacements observed between different time periods for the isotopic compositions of Phanerozoic cherts, particularly the large change between Carboniferous-Triassic and Triassic-Cretaceous. Therefore, it is clear that changes in the isotopic composition of ocean water are not the primary cause of variations in the isotopic compositions of cherts. In fact, the data can be satisfactorily explained without the necessity of invoking past changes in the isotopic history of ocean water.

The explanations advanced in this thesis for variations of D/H and O^{18}/O^{16} ratios in cherts are directly at odds with the explanation proposed by Perry (1967). Perry assumed that the cherts he had analyzed had formed directly from ocean water at the same temperature as the Cretaceous cherts analyzed by Degens and Epstein (1962). In this thesis it has been argued on the basis of relationships between δD and δO^{18} that many, if not most, cherts are not marine cherts, but have formed diagenetically from fresh waters.

Furthermore, as discussed in Chapter 6, it is extremely likely that climatic temperatures at which the cherts formed have varied by at least 15°C throughout the Phanerozoic, and probably by greater amounts throughout the Precambrian. If these interpretations are correct, then the basic assumptions underlying Perry's hypothesis are invalid.

As discussed in Chapter 6, it is possible that part of the variation in the isotopic composition of cherts with time may be due to long term changes (>2 billion years) in the isotopic composition of the oceans in which δO^{18} has increased by several per mil and δD has decreased by several percent. At present, however, there is no compelling evidence that this is so.

In figure 10-1 are plotted most of the known δO^{18} analyses of cherts. Included also are two analyses of cherts kindly sent to the author by Dr. Perry. Sample #372, from the 700-1000 million year old Bitter Springs Formation, Australia, yields a δO^{18}-value of +30.45‰. This is about 4‰ heavier than the value reported by Perry (1967) and is similar to the δO^{18}-values for 1.2 billion year old cherts in Arizona (see Chapter 6).

Figure 10-1 shows that, with the exception of some of the 3 billion year old Fig-Tree cherts, all of the δO^{18}-values for Precambrian cherts fall within the range of those

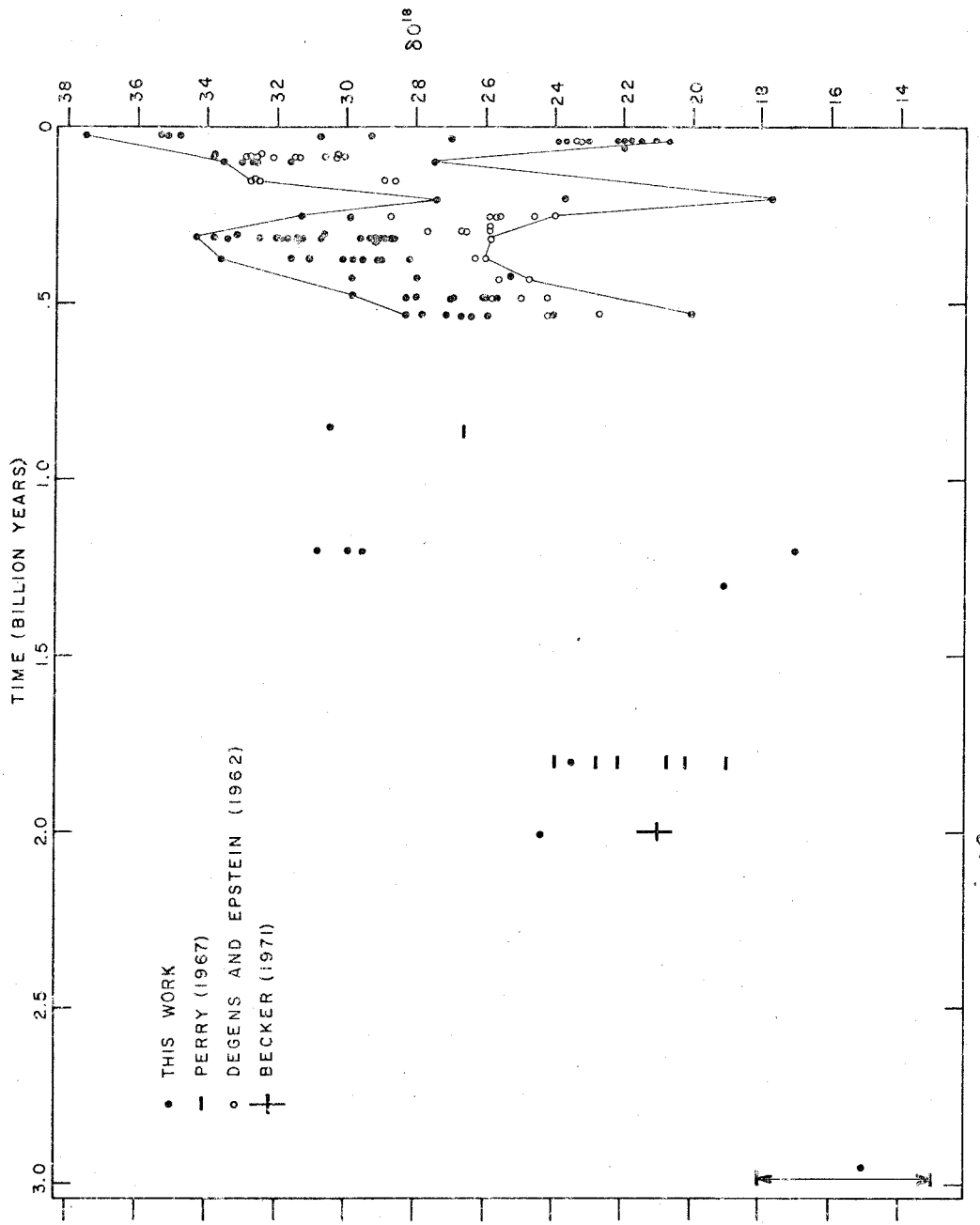

Figure 10-1: δO^{18} ANALYSES OF CHERTS VS. AGE OF THE SAMPLES. ALL SAMPLES OLDER THEN 1.5 BILLION YEARS ARE FROM IRON FORMATIONS. THE VARIATION IN MAXIMUM AND MINIMUM δO^{18} VALUES FOR PHANEROZOIC CHERTS IS INTERPRETED AS BEING DUE TO CLIMATIC TEMPERATURE VARIATIONS.

observed for cherts as young as the Tertiary. There is thus no necessity of assuming that the Precambrian oceans were greatly depleted in O^{18} in order to account for low δO^{18}-values for cherts. The iron formation cherts (Transvaal, Gunflint, and Hamersley) have δO^{18}-values similar to Tertiary fresh water cherts and may, themselves, be fresh water deposits. Indeed, the combined δD-δO^{18} data for a sample of the Gunflint chert suggest that it formed from meteoric waters.

10.6 Climatic Temperatures of the Past Based on the Isotopic Composition of Cherts

It is of interest to compare the temperatures of formation deduced for cherts as shown in figure 6-14 with past climatic temperatures proposed by other authors. In order to obtain temperatures for each sample analyzed in this investigation, it was desirable to derive an equation from the geometrical relationships in figure 6-14 which would give temperature as a function of δD and δO^{18}. Such an equation eliminates the need for geometrical extrapolations in order to obtain a temperature for a chert with an isotopic composition which does not lie on one of the "isotherms" in figure 6-14. The derivation and the equation are given in Appendix III. The calculated temperatures are given in tables 6-1 to 6-8.

Cherts with δ-values lying on or near line A, figure 6-14, can be either marine or non-marine. It is necessary to assign two temperatures to such cherts, corresponding to a possible marine or fresh water origin. For example, as shown in figure 6-14, a chert with δO^{18} = 32, δD = -57 can be either a marine chert which formed at 25°C or a fresh water chert which formed at 22°C. Temperatures for cherts are listed in tables 6-1 to 6-8 under the headings "T°C(FW)" and "T°C(Marine)", depending upon whether the cherts formed from meteoric waters (FW) or possible marine waters (Marine).

The temperatures derived for all cherts collected from the central and western United States are plotted in figure 10-2 against the ages of the samples. This figure gives a rough outline of the climatic temperature history for the central and western United States for the last two billion years. The following aspects of this history are noteworthy:

(1) Temperature variations over the area of sampling can vary by 20°C within an individual Geologic Period. These variations were probably due to geographical variations in climate and climatic changes during the 30 - 75 million year time interval represented by each interval.

(2) Nearly all temperatures in the past were warmer than the present day average temperature of 13° - 15°C.

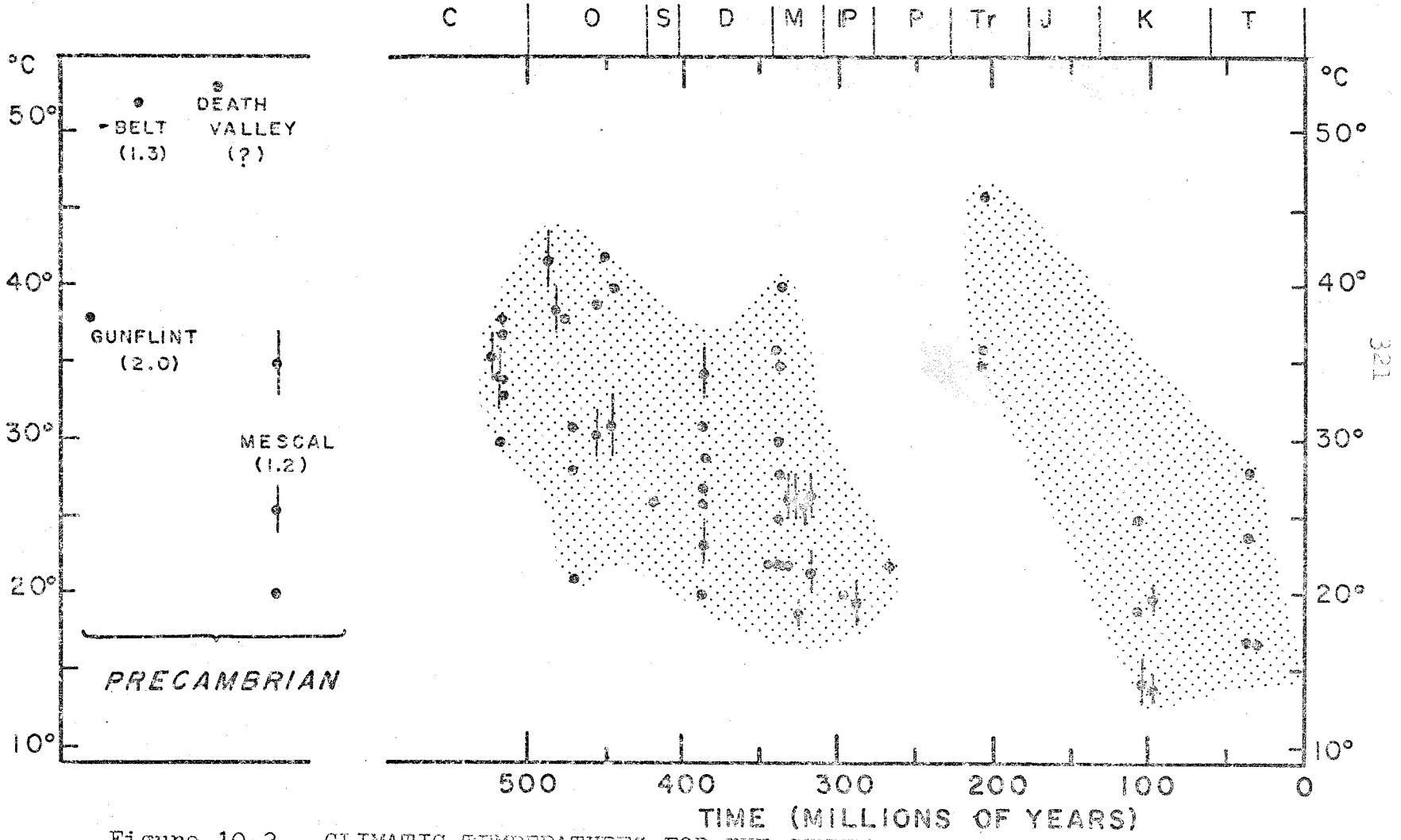

Figure 10-2. CLIMATIC TEMPERATURES FOR THE CENTRAL AND WESTERN UNITED STATES OVER GEOLOGIC TIME AS DEDUCED FROM THE ISOTOPIC COMPOSITION OF CHERTS. AGES FOR PRECAMBRIAN CHERTS ARE GIVEN IN BILLIONS OF YEARS.

(3) Temperatures dropped continuously from about 35°C to 20°C during the Paleozoic Era. Presumably, the great Permian ice ages were the culmination of this declining temperature trend.

(4) By Triassic times, the temperatures once again equaled or surpassed those of the Upper Cambrian (≈35°C).

(5) Temperatures decreased from the Triassic through the Tertiary, culminating once again in a series of ice ages.

(6) The temperature spread shown by the 1.2 billion year old Arizona cherts is almost identical to that shown by the Devonian. Thus, in at least one part of the Precambrian, climatic temperatures were similar to those of the Phanerozoic.

(7) Several intervals in the Precambrian were much warmer than climates of the Phanerozoic. The Belt Series chert and the Death Valley chert apparently formed in climates with temperatures of about 50°C. The Gunflint chert appears to have formed at 38°C.

The extremely warm temperatures proposed here for most of geologic time are not incompatible with the temperature tolerances of living organisms. Brock (1967) has given the following approximate upper thermal limits for different groups of organisms:

Animals, including protozoa: 45° - 51°C

Eucaryotic microorganisms:	56° - 60°C
Photosynthetic procaryotes (blue-green algae)	73° - 75°C
Nonphotosynthetic procaryotes (bacteria)	>90°C

The only climatic temperatures proposed here that exceed 50°C, and thus the upper tolerance for any animals which might occur as fossils, are those of the Precambrian, where there are no such fossils. The 52° - 53°C temperatures assigned to the Belt and Death Valley cherts which occur in stromatilitic dolomites, while surprisingly high, are well below the 73° - 75°C maximum temperature tolerance for blue-green algae.

Brooks (1951) has summarized the geologic and historical aspects of climatic change and has given two estimates of the variations of temperature over geologic time based on the fossil record and on geographic factors. This estimate is shown in figure 10-3. The actual temperatures given by Brooks for each Period are about 15° - 25°C lower than those deduced from the isotopic composition of the cherts. However, qualitatively, the temperature variations in figure 10-3 bear a remarkable resemblance to those deduced from the cherts. All three approaches show a cooling trend through the Paleozoic followed by a warm interval in the Triassic which was then followed by a cooling trend.

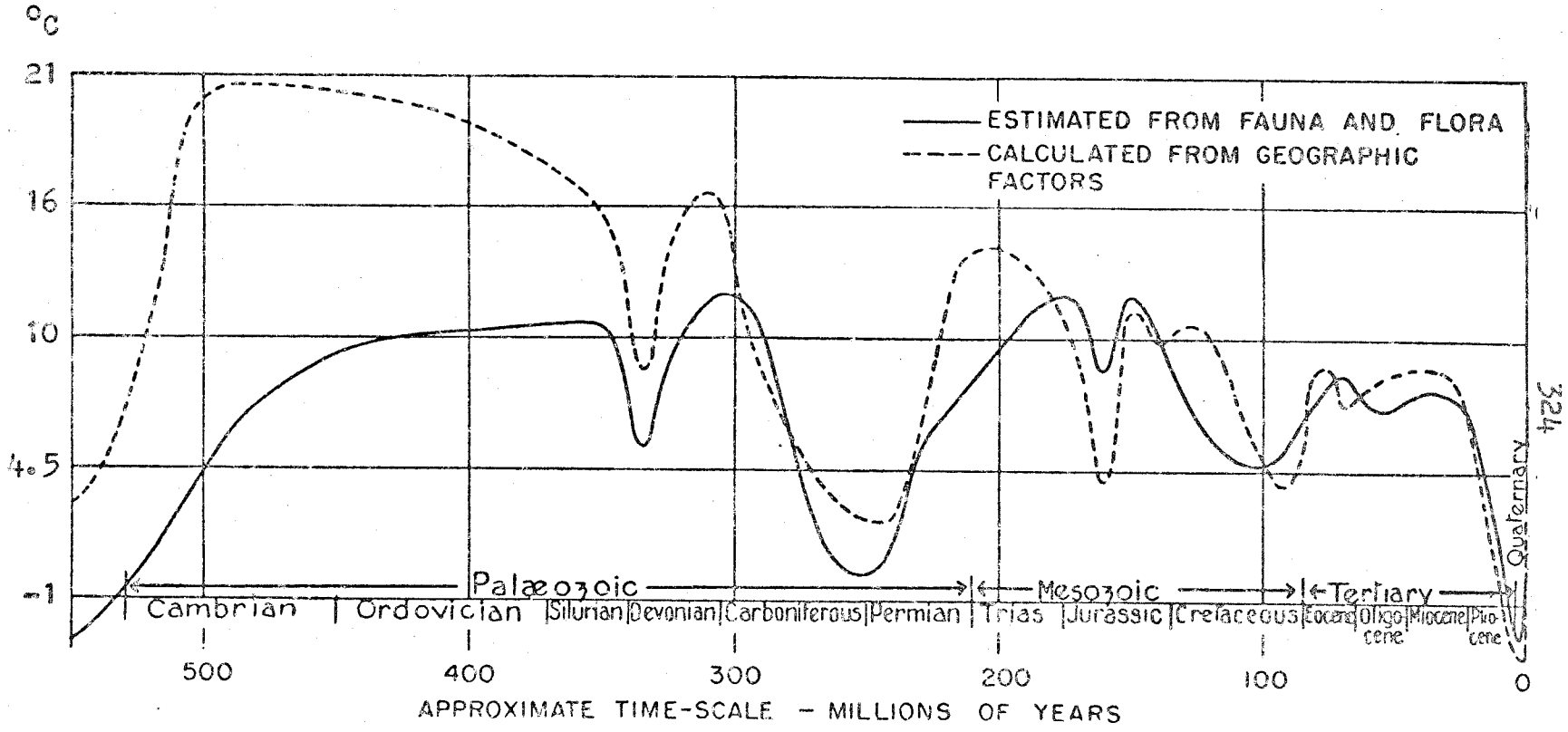

Figure 10-3

VARIATIONS OF TEMPERATURE OVER GEOLOGIC TIME AS GIVEN BY BROOKS (1951)

Few workers have proposed temperatures for Pre-cambrian climates, since little fossil evidence is available. Recently, Sagan and Mullen (1972) derived theoretical trends for the temperature history of the earth based on the luminosity history of the sun and various atmospheric "greenhouse" models. Their results are shown in figure 10-4 together with the temperatures deduced from the isotopic compositions of the Precambrian cherts. It should be emphasized that all of the temperatures based on the cherts are for the central and western United States, with the exception of the South African chert (#304) at 3 billion years. Sagan and Mullen's trends are for the whole earth.

As shown in figure 10-4, the chert temperatures lie near the "equilibrium NH_3 evolutionary track" of Sagan and Mullen. The "track" is based on a model history of the early atmosphere in which insignificant H_2 was present and the atmospheric greenhouse was dominated by H_2O and an equilibrium abundance of NH_3. The decline in temperature corresponds to the decline in ammonia abundance due to photodissociation and reaction with other atmospheric constituents. The "subequilibrium NH_3 track" is for the same situation, except that the NH_3 abundance is in sub-equilibrium abundances because of photodissociation and

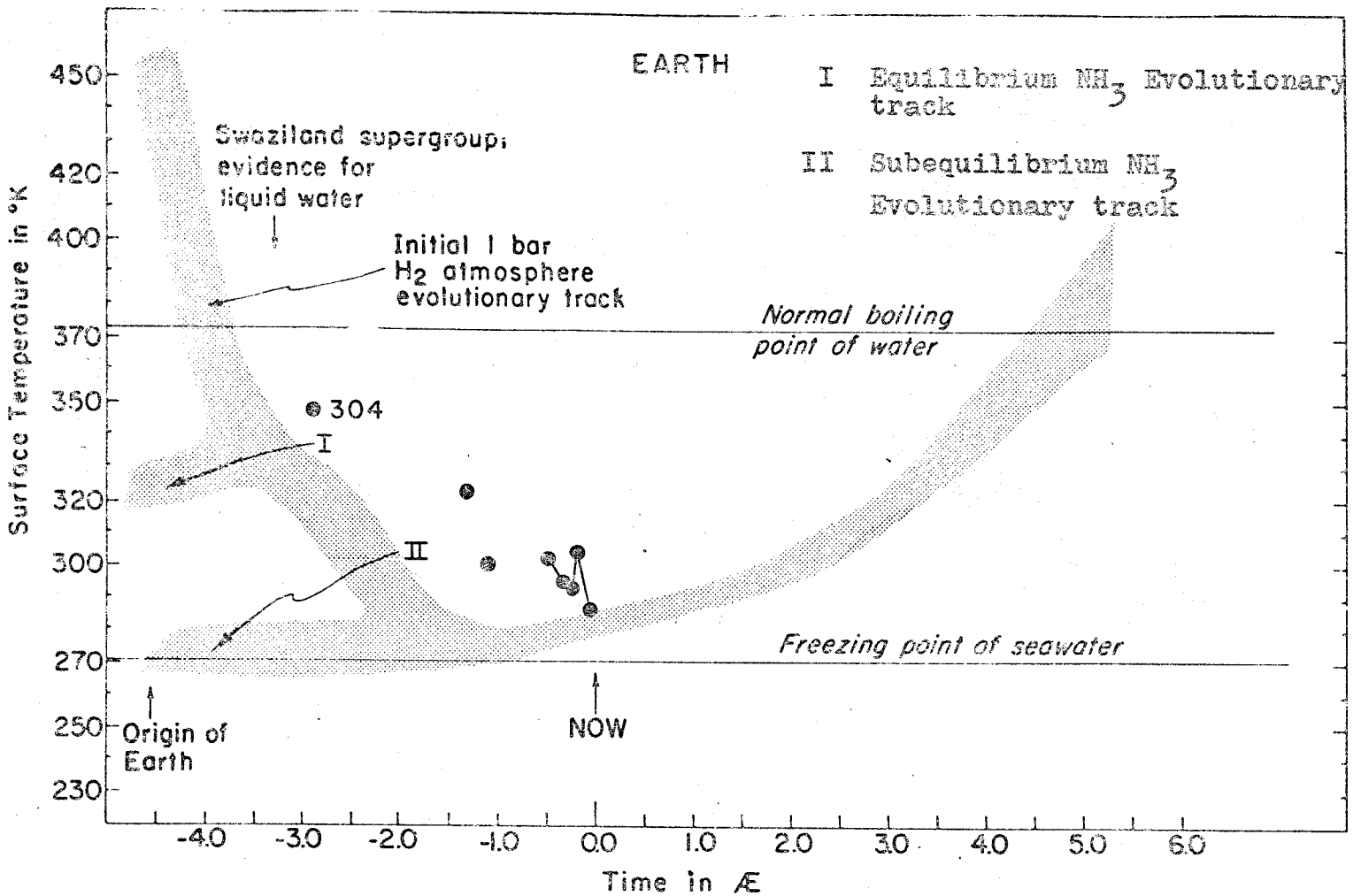

Figure 10-4: COMPARISON OF TEMPERATURES DEDUCED FROM THE ISOTOPIC COMPOSITION OF CHERTS WITH THE THREE EVOLUTIONARY TRACKS FOR THE TEMPERATURE OF THE EARTH DERIVED BY SAGAN AND MULLEN (1972). THE FILLED CIRCLES ARE THE CHERT TEMPERATURES.

reaction with other atmospheric constituents. Sagan and Mullen consider this latter track to be the most likely of those shown, but the chert temperatures are incompatible with this track.

10.7 Conclusion Concerning Temperatures Based on the Isotopic Composition of Cherts

The most plausible interpretation of variations of the D/H and O^{18}/O^{16} ratios in cherts of all ages is that they reflect (1) changes in past climatic temperatures and (2) differing amounts of meteoric waters involved in their genesis. Temperatures deduced from the isotopic compositions of cherts suggest that past temperatures for the central and western United States have, in general, declined from extremely warm values of 50°C in the Precambrian to the present day values of about 15°C. An outline, with many gaps, of this climatic temperature history was shown in figure 10-2. It is felt that additional analyses of the isotopic compositions of carefully sampled cherts from numerous localities around the world could result in nothing less than a detailed record of the temperature history of the earth's surface for all of geologic time.

BIBLIOGRAPHY

Bain, H. F. and E. O. Ulrich, 1905, The copper deposits of Missouri: U.S.G.S. Bull.,267.

Barghoom, E. S. and S. A. Tyler, 1965, Microorganisms from the Gunflint chert: Science, 147, p. 563-577.

Barnes, V. E. et al., 1956, San Agnelo Geological Society, Four Provinces Field Trip, Guidebook.

Becker, R. H., 1971, Carbon and oxygen isotope ratios in iron-formation and associated rocks from the Hamersley Range of western Australia and their implications: PhD thesis, Univ. of Chicago.

Bein, G. S., D. E. Contois and W. H. Thomas, 1958, The removal of soluble silica from fresh water entering the sea: Geochim. et Cosmochim. Acta, 14, p. 35-54.

Bigeleisen, J. and M. G. Mayer, 1947, Calculation of equilibrium constants for isotopic exchange reactions: Jour. Chem. Phys., 15, p. 261-271.

Biggs, D. L., 1957, Petrography and origin of Illinois nodular cherts: Illinois State Geol. Survey Circ. 245, p. 25.

Bissell, H. J., 1959, Silica in sediments of the Upper Paleozoic of the Cordilleran area, in Silica in sediments, Soc. Econ. Paleontologists Mineralogists, Spec. Public., 7, p. 150-185.

Bowen, R., 1966, Paleotemperature analysis, Elsevier Publishing Company

Bramlette, M. N., 1946, The Monterey formation of California and the origin of its siliceous rocks: U.S.G.S. Prof. Paper 212.

Brewster, E. B. and N. F. Williams, 1951, Arkansas Geol. Survey Guidebook to Paleozoic rocks of northwest Arkansas.

Brock, T. D., 1967, Life at high temperatures, Science, 158, p. 1012-1019.

Brooks, C. E. P., 1951, Geological and historical aspects of climatic change, in Compendium of Meteorology, T. F. Malone, ed., Am. Meteorological Society, Boston, p. 1004-1018.

Burton, J. D. and P. S. Liss, 1968, Oceanic budget of dissolved silicon: Nature, 220, p. 905-906.

Calvert, S. E., 1968, Silica balance in the ocean and diagenesis: Nature, 219, p. 919-920.

Carozzi, A. V., 1960, Microscopic Sedimentary Petrography, Wiley, New York, N. Y., p. 291-343.

Chase, C. G. and E. C. Perry, Jr., 1972, The oceans: Growth and oxygen isotope evolution: manuscript in preparation.

Clayton, R. N., 1971, Stable isotope geochemistry: EOS, Trans. Am. Geophys. Union, 52, No. 5, p. 106.

Clayton, R. N. and E. T. Degens, 1959, Use of carbon isotope analyses of carbonates for differentiating fresh-water and marine sediments: Amer. Assoc. Petroleum Geologists Bull., 43, p. 890.

Clayton, R. N. and S. Epstein, 1958, The relationship between O^{18}/O^{16} ratios in coexisting quartz, carbonate, and iron oxides from various geological deposits: Jour. Geology, 66, p. 352-373.

Clayton, R. N., J. R. Goldsmith, K. Johnson and R. C. Newton, 1972, Pressure effects on stable isotope fractionation: Abstract in EOS, Trans. Am. Geophys. Union, 53, p. 555.

Clayton, R. N., B. F. Jones and R. A. Berner, 1968, Isotope studies of dolomite formation under sedimentary conditions: Geochim. et Cosmochim. Acta, 32, p. 415-432.

Clayton, R. N. and T. K. Mayeda, 1963, The use of bromine pentafluoride in the extraction of oxygen from oxides and silicates for isotopic analysis: Geochim. et Cosmochim. Acta, 27, p. 43.

Clayton, R. N., L. J. P. Muffler and D. E. White, 1968, Oxygen isotope study of calcite and silicates of the River Ranch No. 1 well, Salton Sea geothermal field, California: Amer. Jour. Science, 266, p. 968-979.

Clayton, R. N., J. R. O'Neil and T. K. Mayeda, 1972, Oxygen isotope exchange between quartz and water: Jour. Geophys. Research, 77, p. 3057.

Cleveland, G. B., 1961, Economic geology of the Long Valley diatomaceous earth deposit, Mono County, California: California Div. of Mines and Geology Map Sheep No. 1.

Cloud, P. E. and V. E. Barnes, 1946, The Ellenburger group of central Texas: Univ. of Texas Public., 4621.

Compston, W., 1960, The carbon isotopic compositions of certain marine invertebrates and coals from the Australian Permian: Geochim. et Cosmochim. Acta, 18, p. 1-22.

Correns, C. W., 1969, Introduction to Mineralogy, Springer-Verlag, New York, p. 306.

Craig, H., 1957, Isotopic standards for carbon and oxygen and correction factors for mass-spectrometric analysis of carbon dioxide: Geochim. et Cosmochim. Acta, 12, p. 133-149.

Craig, H., 1961a, Isotopic variations in meteoric waters: Science, 133, p. 1702-1703.

Craig, H., 1961b, Standard for reporting concentrations of deuterium and oxygen 18 in natural water: Science, 133, p. 1833.

Craig, H., 1965, The measurement of oxygen isotope paleo-temperatures: Proc. Spoleto Conf. on Stable Isotopes in Oceanographic Studies and Paleotemperatures, 2.

Craig, H. and L. I. Gordon, 1965, Deuterium and oxygen 18 variations in the ocean and the marine atmosphere: Proc. Spoleto Conf. on Stable Isotopes in Oceanographic Studies and Paleotemperatures, p. 9-130.

Dake, C. L., 1930, The geology of the Potosi and Edgehill Quadrangles: Missouri Bureau of Geology and Mines, XXIII, Second Series.

Dansgaard, W., 1964, Stable isotopes in precipitation: Tellus, 16, p. 436.

Dansgaard, W. and H. Tauber, 1969, Glacier oxygen-18 content and Pleistocene ocean temperatures: Science, 166, p. 499-502.

Dapples, E. D., 1959, The behavior of silica in diagenesis: in Silica in Sediments, H. A. Ireland, ed., Soc. Econ. Paleontologists Mineralogists Spec. Public. 7, p. 36-54.

Dapples, E. C., 1967, Silica as an agent in diagenesis: in Diagenesis of Sediments, Developments in Sedimentology, 8, Elsevier Publishing Company, New York.

Davis, E. F., 1918, The radiolarian cherts of the Franciscan group: Calif. Univ. Dept. Geol. Bull. 11, No. 3, p. 235-432.

Degens, E. T. and S. Epstein, 1962, Relationship between O^{18}/O^{16} ratios in coexisting carbonates, cherts, and dolomites: AAPG Bull., 46, p. 534-542.

Degens, E. T. and S. Epstein, 1964, Oxygen and carbon isotope ratios in coexisting calcites and dolomites from recent and ancient sediments: Geochim. et Cosmochim. Acta, 28, p. 23-44.

Douglas, R. G. and S. M. Savin, 1971, Isotopic analyses of planktonic Foraminifera from the Cenozoic of the northwest Pacific, Leg 6: in Initial Reports of the Deep Sea Drilling Project, 6, A. G. Fischer et al., ed., p. 1123-1127.

Dunbar and Waage, 1969, Historical Geology, John Wiley & Sons, New York.

Emiliani, C., 1954, Temperatures of Pacific bottom waters and polar superficial waters during the Tertiary: Science, 119, p. 853-855.

Emiliani, C., 1966, Isotopic paleotemperatures: Science, 154, p. 851.

Emiliani, C., 1970, Pleistocene paleotemperatures: Science, 168, p. 822-825.

Engel, A. E. J., 1970, The Barbeton Mountain land: in Adventures of Earth History, P. Cloud, ed., Freeman.

Engel, A. E. J., R. N. Clayton and S. Epstein, 1958, Variations in the isotopic composition of oxygen and carbon in Leadville limestone (Mississippian, Colorado) and in its hydrothermal and metamorphic phases: Jour. Geology, 66, p. 374-393.

Epstein, S., R. Buchsbaum, H. Lowenstam and H. Urey, 1951, Carbonate-water isotopic temperature scale: Bull. Geol. Soc. of Amer., 62, p. 417-426.

Epstein, S., R. Buchsbaum, H. Lowenstam and H. Urey, 1953, Revised carbonate-water isotopic temperature scale: Bull. Geol. Soc. of Amer., 64, p. 1315-1326.

Epstein, S., D. Graf and E. T. Degens, 1963, Oxygen isotope studies on the origin of dolomites: in Isotopic and Cosmic Chemistry, Craig et al., ed., North Holland Publishing Company, Amsterdam.

Epstein, S. and T. Mayeda, 1953, The variation in O^{18} content of water from natural sources: Geochim. et Cosmochim. Acta, 4, p. 213.

Epstein, S and H. P. Taylor, Jr., 1967, Variation of O^{18}/O^{16} in minerals and rocks: in Researches in Geochemistry, 2, P. H. Abelson, ed., John Wiley & Sons, New York.

Ernst, W. G. and S. E. Calvert, 1969, An experimental study of the recrystallization of Porcelanite and its bearing on the origin of some bedded cherts: Amer. Jour. Sci., 267-A, p. 114-133.

Eslinger, E. V. and S. Savin, 1971, Oxygen isotope studies of burial metamorphism of the Belt Supergroup, Glacier National Park, Montana: Geol. Soc. Amer., Abstracts, 3, No. 7, p. 558.

Eugster, H. P., 1969, Inorganic bedded cherts from the Magadi area, Kenya: Contr. Mineral. Petrol., 22, p. 1-31.

Fagin, J. J., 1963, Carboniferous cherts, turbidites, and volcanic rocks in northern Independence Range, Nevada: Geol. Soc. Amer. Bull., 73, p. 595-612.

Fanning, K. A. and D. R. Schink, 1969, Interaction of marine sediments and dissolved silica: in Limnology and Oceanography, 14, p. 59-68.

Folk, R. L., 1950, Petrology of authigenic silica in the Beckmantown group of central Pennsylvania: MS thesis, Pennsylvania State College, as reported in Pittman (1959).

Folk, R. L., 1970, Evidence of peritidal origin for part of the Caballos novaculite: G.S.A. Annual Meeting, Abstracts, 2, No. 7.

Folk, R. L. and E. Weaver, 1952, A study of the texture and composition of chert: Amer. Jour. Sci.,250, p. 498-510.

Friedman, I., 1953, Deuterium content of natural waters and other substances: Geochim. et Cosmochim. Acta, 4, p. 89-103.

Friedman, I., A. C. Redfield, B. Schoen and J. Harris, 1964, The variation of the deuterium content of natural waters in the hydrologic cycle: Reviews of Geophy., 2, p. 177.

Fritz, P., 1971, Geochemical characteristics of dolomites and the O^{18} content of Middle Devonian oceans: Earth and Planet. Sci. Letters, 11, p. 277-282.

Garlick, G. D., 1969, The stable isotopes of oxygen: in Handbook of Geochemistry, Vol. II/1, K. H. Wedepohl, ed., p. 8-B-1 to 8-B-27, Springer-Verlag, Berlin.

Garlick, G. D. and S. Epstein, 1966, The isotopic composition of oxygen and carbon in hydrothermal minerals at Butte, Montana: Econ. Geol., 61, p. 1325-1335.

Garlick, G. D. and S. Epstein, 1967, Oxygen isotope ratios in coexisting minerals of regionally metamorphosed rocks: Geochim. et Cosmochim. Acta, 31, p. 181-214.

Garlick, G. D., I. D. MacGregor and D. E. Vogel, 1971, Oxygen isotope ratios in Eclogites from Kimberlites: Science, 172, p. 1025-1027.

Gilluly, J., J. R. Cooper and J. S. Williams, 1954, Late Paleozoic stratigraphy of central Cochise County, Arizona: U.S.G.S. Prof. Paper 226.

Godfrey, J. D., 1962, The deuterium content of hydrous minerals from the east-central Sierra Nevada and Yosemite National Park: Geochim.et Cosmochim. Acta, 26, p. 1215-1245.

Goldstein, A., Jr., 1959, Cherts and novaculites of the Ouachita facies: in Silica in Sediments, H. A. Ireland, ed., Soc. Econ. Paleontologists and Mineralogists Spec. Public. 7, p. 185.

Govett, G. J. S., 1966, Origin of banded iron formations: Bull. Geol. Soc. Amer. 77, p. 1191-1212.

Gregory, H. E., 1950, Geology and geography of the Zion Park region, Utah and Arizona: U.S.G.S. Prof. Paper 220.

Hall, W. E. and I. Friedman, 1969, Oxygen and carbon isotopic composition of ore and host rock of selected Mississippi Valley deposits: U.S.G.S. Prof. Paper 650-C, p. C140-C148.

Ham, W. E., 1969, Regional geology of the Arbuckle Mountains, Oklahoma: in Oklahoma Geol. Survey Guidebook XVII.

Harris, L. D., 1958, Syngenetic chert in the Middle Ordovician Hardy Creek limestone of southwest Virginia: Jour. Sed. Petrology, 28, p. 205-208.

Harrison, J. E., 1972, Precambrian Belt Basin of northwestern United States: its geometry, sedimentation and copper occurrences: Bull. Geol. Soc. Amer. 83, p. 1215-1240.

Harriss, R. C., 1966, Biological buffering of oceanic silica: Nature, 212, p. 275-276.

Hatch, F. H., R. H. Rastall and M. Black, 1938, The petrology of the sedimentary rocks, 3rd Ed., George Allen & Unwin, London.

Hayes, J. B., 1964, Geodes and concretions from the Mississippian Warsaw Formation, Keokuk region, Iowa, Illinois, Missouri, Jour. Sed. Pet. v. 34, p. 123-133.

Hay, R. L., 1968, Chert and its sodium-silicate precursors in sodium-carbonate lakes of East Africa: Contr. Mineral. Petrol., 17, p. 225.

Hazzard, J. C., 1937, Paleozoic section in the Nopah and Resting Springs Mountains, Inyo County, California: California Jour. Mines and Geology, 33, p. 289.

Heath, G. R. and R. Moberly, 1971, Cherts from the western Pacific, Leg 7, Deep Sea Drilling Project: in Initial Reports Deep Sea Drilling Project, 7, E. L. Winterer et al., ed., p. 991.

Hendricks, T. A., M. M. Knechtel and J. Bridge, 1937, Geology of Black Knob Ridge, Oklahoma: AAPG Bull. 21, p. 1.

Hoering, T. C., 1961, The physical chemistry of isotopic substances: Annual Report of the Director of the Geophys. Lab., p. 201.

Holland, R. E., 1969, Seasonal fluctuations of Lake Michigan diatoms: Limnology and Oceanography, 14, No. 3.

Hough, J. L., 1958, Fresh-water environment of deposition of Precambrian iron formations: Jour. Sed. Petrology, 28, p. 414-430.

Hurley, P. M., H. W. Fairbairn, W. H. Pinson and J. Hower, 1962, Unmetamorphosed minerals in the Gunflint Formation used to test the age of the Animikie: Jour. Geology, 70 p. 489.

Iler, R. K., 1955, The colloid chemistry of silica and silicates: Cornell University Press, New York.

James, H. L., 1954, Sedimentary facies of iron formation: Econ. Geol., 49, p. 235-293.

James, H. L., 1960, Problems of stratigraphy and correlation of Precambrian rocks: Amer. Jour. Science, 258A, p. 104-114.

James, H. L., 1966, Chemistry of the iron-rich sedimentary rocks: U.S.G.S. Prof. Paper 440-W, p. 61.

James, H. L. and R. N. Clayton, 1962, Oxygen isotope fractionation in metamorphosed iron formations of the Lake Superior region and in other iron-rich rocks: in Petrologic studies: a volume to honor A. F. Buddington, Geol. Soc. Amer., p. 217-239.

Jensen, A. T., C. J. Wohlk, K. Drenck and E. K. Andersen, 1957, A classification of Danish flints, etc., based on X-ray diffractometry: Com. alkali reactions in concrete, Copenhagen, Progress Rep. D 1, p. 37.

Jicha, H. L., Jr., 1954, Geology and mineral deposits of Lake Valley Quadrangle, Grant, Luna, and Sierra Counties, New Mexico: New Mexico Geol. Survey Bull. 37.

Jones, J. B., J. V. Sanders and E. R. Segnit, 1964, Structure of opal: Nature, 204, p. 990.

Jones, J. B., E. R. Segnit and N. M. Nickson, 1963, DTA of opal: Nature, 198, p. 1191.

Jones, J. B. and E. R. Segnit, 1971, The nature of opal: I. Nomenclature and constituent phases: Jour. Geol. Soc. Australia, 18, p. 57-68.

Keith, M. L. and J. N. Weber, 1964, Carbon and oxygen isotopic composition of selected limetones and fossils: Geochim. et Cosmochim. Acta, 28, p. 1787-1816.

Keller, W. D., 1941, Petrography and origin of the Rex chert: Bull. Geol. Soc. of Amer., 52, p. 1279-1297.

Keller, W. D. and E. E. Pickett, 1949, Absorption of infrared radiation by powdered silica minerals: Amer. Mineralogist, 34, p. 855.

Keller, W. D., J. H. Spotts, and D. L. Biggs, 1952, Infrared spectra of some rock-forming minerals: Amer. Jour. Science, 250, No. 6, p. 453.

King, P. B., 1938, Geology of the Marathon Region, Texas: U.S.G.S. Prof. Paper 187.

King, P. B., R. E. King and J. B. Knight, 1945, Geology of Hueco Mountains, El Paso and Hudspeth Counties, Texas: U.S.G.S. Oil and Gas Preliminary Investigation Map 36.

Kulp, J. L., 1961, Geologic time scale: Science, 133, p. 1105-1114.

Krauskopf, K. B., 1959, The geochemistry of silica in sedimentary environments: in Silica in Sediments, H. A. Ireland, ed., Soc. Econ. Paleontologists and Mineralogists Spec. Public. 7, p. 4-19.

Lamar, J.E., 1953, Siliceous materials of extreme southern Illinois: Illinois State Geol. Survey Report of Investigations No. 166.

Leith, C. K., 1925, Silicification of erosion surfaces: Econ. Geol., 20, p. 513.

Lewin, J. C., 1961, The dissolution of silica from diatom walls: Geochim. et Cosmochim. Acta, 21, p. 182-198.

Lisitsyn, A. P., 1967, Basic relationships in distribution of modern siliceous sediments and their connection with climatic zonation (English translation): Int. Geol. Rev., 9, p. 631.

Lisitsyn, A. P., Yu. I. Belyayev, Yu. A. Bogdanov and A. N. Bogoyavlenskiy, 1967, Distribution relationships and forms of silicon suspended in waters of the world ocean (English translation): Int. Geol. Rev., 9, p. 253.

Longinelli, A., 1966, Ratios of oxygen-18: oxygen-16 in phosphate and carbonate from living and fossil marine organisms: Nature, 211, p. 923-927.

Longinelli, A. and S. Nuti, 1972, Revised and extended phosphate-water isotopic temperature scale: Abstract in EOS, Trans. Am. Geophys. Union., 53, p. 555.

Longwell, C. R., E. H. Pampeyan, B. Bowyer and R. J. Roberts, 1965, Geology and mineral deposits of Clark County, Nevada: Nevada Bureau of Mines Bull. 62.

Lovering, T. S., J. H. McCarthy and I. Friedman, 1963, Significance of O^{18}/O^{16} and C^{13}/C^{12} ratios in hydrothermally dolomitized limestones and manganese carbonate replacement ores of the Drum Mountains, Juab County, Utah: U.S.G.S. Prof. Paper 475-B, p. B1-B9.

Lowenstam, H. A., 1942, Facies relation and origin of some Niagaran cherts: Abstract in Bull. Geol. Soc. Amer., 53, p. 1805-1806.

Lowenstam, H. A., 1961, Mineralogy, O^{18}/O^{16} ratios, and strontium and magnesium contents of recent and fossil Brachiopods and their bearing on the history of the oceans: Jour. Geol., 69, p. 241-260.

Lowenstam, H. A., 1963, Biologic problems relating to the composition and diagenesis of sediments: in The Earth Sciences, Problems and Progress in Current Research, T. W. Donnelly, ed., Univ. of Chicago Press, Chicago.

Lowenstam, H. A., 1971, Opal-precipitation by marine gastropods (Molluska): Science, 171, p. 487-490.

Lowenstam, H. A. and S. Epstein, 1956, Cretaceous paleotemperatures as determined by the oxygen isotope method, their relations to and the nature of rudistid reefs: 20th Int. Geol. Congress Report, p. 65-76.

MacKenzie, F. T. and R. M. Garrels, 1966, Silica-bicarbonate balance in the ocean and early diagenesis: Jour. Sed. Petrology, 36, p. 1075-1084.

MacKenzie, F. T., R. M. Garrels, O. P. Bricker and F. Bicley, 1967, Silica in sea water: Control by silica minerals: Science, 155, p. 1404-1405.

MacKenzie, F. T. and R. Gees, 1971, Quartz: Synthesis at earth-surface conditions: Science, 173, p. 533-534.

McBride, E. F. and A. Thomson, 1970, The Caballos novaculite, Marathon Region, Texas: Geol. Soc. Amer. Spec. Paper 122.

McCrea, J. M., 1950, The isotopic chemistry of carbonates and a paleotemperature scale: Jour. Chem. Phys., 18, p. 849-857.

McKee, E. H., 1968, Geology of the Magruder Mountain area, Nevada-California: U.S.G.S. Bull. 1251-H.

McKinney, C. R., J. M. McCrea, S. Epstein, H. A. Allen and H. C. Urey, 1950, Improvements in mass spectrometers for the measurement of small differences in isotope abundance ratios: Rev. Sci. Inst., 21, p. 724.

Mansfield, G. R., 1927, Geography, geology, and mineral resources of southeastern Idaho: U.S.G.S. Prof. Paper 152.

Maxson, J. H., 1967, Preliminary geologic map of the Grand Canyon and vicinity, Arizona: Grand Canyon Nat. History Assoc.

Maxwell, R. A., J. T. Lonsdale, R. T. Hazzard and J. A. Wilson, 1967, Geology of Big Bend National Park, Brewster County, Texas: Univ. of Texas Public. No. 6711.

Micheelsen, H., 1966, The structure of dark flint from Stevns, Denmark: Medd. fra Dansk Geol. Forening, København, Bd. 16.

Miser, H. D. and A. H. Purdue, 1929, Geology of the DeQueen and Caddo Gap Quadrangles, Arkansas: U.S.G.S. Bull. 808.

Moberly, R., Jr., and G. R. Heath, 1971, Carbonate sedimentary rocks from the western Pacific: in Initial Report of the Deep Sea Drilling Project, 7, E. L. Winterer et al., ed., p. 977-987.

Mopper, K. and G. D. Garlick, 1971, Oxygen isotope fractionation between biogenic silica and ocean water: Geochim. et Cosmochim. Acta, 35, p. 1185-1187.

Muehlenbachs, K., 1971, The oxygen isotope geochemistry of rocks recovered from the ocean floor: Ph.D. thesis, Univ. of Chicago.

Muller, S. W. and H. G. Ferguson, 1939, Mesozoic stratigraphy of the Hawthorne and Tonopah Quadrangles, Nevada: Bull. Geol. Soc. Amer. 50, p. 1573-1624.

Nagy, B., 1970, Porosity and permeability of the early Precambrian Onverwacht chert: Origin of the hydrocarbon content: Geochim. et Cosmochim. Acta, 34, p. 525-527.

Nier, A. O., 1947, A mass spectrometer for isotope and gas analysis: Rev. Sci. Instr., 18, p. 398-411.

Noble, L. F., 1910, The geology of the Shinumo area, part 2 of Contr. to the geology of the Grand Canyon, Arizona: Amer. Jour. Science, 4th Series, 29, p. 497.

Noble, L. F., 1914, The Shinumo Quadrangle, Grand Canyon district, Arizona: U.S.G.S. Bull. 549, p. 46.

Oehler, J. H. and J. W. Schopf, 1971, Artificial microfossils: Experimental studies of permineralization of blue-green algae in silica: Science, 174, p. 1229-1231.

O'Neil, J. R., R. N. Clayton and T. K. Mayeda, 1969, Oxygen isotope fractionation in divalent metal carbonates: Jour. Chem. Phys., 51, p. 5547-5558.

O'Neil, J. R. and S. Epstein, 1966, A method for oxygen isotope analysis of milligram quantities of water and some of its applications: Jour. Geophys. Research, 71, p. 4955-4961.

O'Neil, J. R. and R. L. Hay, 1971, O^{18}/O^{16} ratios of cherts associated with the Alkaline Lakes of East Africa: EOS Trans. Am. Geophys. Union, 52, No. 4, p. 365.

Palmer, A. R., 1957, Miocene arthropods from the Mojave Desert, California: U.S.G.S. Prof. Paper 294-G.

Perry, E. C., 1967, The oxygen isotopic chemistry of ancient cherts: Earth and Planet. Sci. Letters, 3, p. 62-66.

Perry, E. C. and F. C. Tan, 1972, Significance of oxygen and carbon isotope determinations in early Precambrian cherts and carbonate rocks of Southern Africa: Bull. Geol. Soc. Amer., 83.

Peterson, M. N. A. and C. C. Von der Borch, 1965, Chert: Modern inorganic deposition in a carbonate precipitating locality: Science, 149, p. 1501-1503.

Pettijohn, F. J., 1957, Sedimentary Rocks, 2nd Edition, Harper and Brothers, New York.

Pinckney, D. M. and R. O. Rye, 1972, Variation of O^{18}/O^{16}, C^{13}/C^{12} texture, and mineralogy in altered limestone in the Hill Mine, Cave-in-District, Illinois: Econ. Geol., 67, p. 1-17.

Pitt, W. D. et al., 1963, Oklahoma Geol. Survey Guidebook XI.

Pittman, J. S., Jr., 1959, Silica in Edwards limestone, Travis County, Texas: in Silica in Sediments, H. A. Ireland, ed., Soc. Econ. Paleontologists and Mineralogists Spec. Public. 7.

Pittman, J. S. and R. L. Folk, 1971, Length-slow chalcedony after sulfate evaporite minerals in sedimentary rocks: Nature, 230, p. 64.

Pöhlmann, R., 1886, Gesteine aus Paraguay: Nenes Jahab. fur Min. i., 247, as quoted in Hatch et al., 1938.

Rich, M. 1961, Stratigraphic section and fusulinids of the Bird Spring Formation near Lee Canyon, Clark County, Nevada: Jour. Paleontology, 35, p. 1159.

Robertson, C. E., 1967, The Elsey Formation and its relationship to the Grand Falls chert: Missouri Geol. Survey Report of Investigations No. 38.

Robertson, P., 1944, Silica gel and Warsaw geodes: Ill. Acad. Sci. Trans., 37, p. 93-94.

Robertson, P., 1951, Geode note: Science, 114, p. 215.

Rogers, G. R., 1927, Geography, geology, and mineral resources of part of southeastern Idaho: U.S.G.S. Prof. Paper 152.

Ross, C. P., 1959, Geology of Glacier National Park: U.S.G.S. Prof. Paper 196.

Rubey, W. W., 1952, Geology and mineral resources of the Hardin and Brussels Quadrangles (in Illinois): U.S.G.S. Prof. Paper 218.

Sagan, C. and G. Mullen, 1972, Earth and Mars: Evolution of atmospheres and surface temperatures: Science, 177, p. 52-56.

Sampson, E., 1923, The Ferruginous chert formations of Notre Dame Bay, Newfoundland: Jour. Geology, 31, p. 571.

Savin, S. M., 1967, Oxygen and hydrogen isotope ratios in sedimentary rocks and minerals: Ph.D. thesis, Calif. Institute of Tech.

Savin, S. M. and S. Epstein, 1970a, The oxygen and hydrogen isotope geochemistry of clay minerals: Geochim.et Cosmochim. Acta, 34, p. 25-42.

Savin, S. M. and S. Epstein, 1970b, The oxygen isotopic compositions of coarse grained sedimentary rocks and minerals: Geochim. et Cosmochim. Acta, 34, p. 323-329.

Savin, S. M. and S. Epstein, 1970c, The oxygen and hydrogen isotope geochemistry of ocean sediments and shales: Geochim. et Cosmochim. Acta, 34, p. 43-63.

Shackleton, N., 1967, Oxygen isotope analyses and Pleistocene temperatures reassessed: Nature, 215, p. 15.

Sharma, T. and R. N. Clayton, 1965, Measurement of O^{18}/O^{16} ratios of total oxygen from carbonates: Geochim. et Cosmochim. Acta, 29, p. 1347.

Sharma, T., R. F. Mueller and R. N. Clayton, 1965, O^{18}/O^{16} ratios of minerals from the iron formations of Quebec: Jour. Geology, 73, p. 664-667.

Sharp, R. P., 1939, The Miocene Humboldt Formation in northeastern Nevada: Jour. Geology, 47, p. 133-160.

Sharp, R. P., 1942, Stratigraphy and structure of the southern Ruby Mountains, Nevada: Bull. Geol. Soc. Amer., 53, p. 647-690.

Sheppard, S. M. F. and S. Epstein, 1970, D/H and O^{18}/O^{16} ratios of minerals of possible mantle or lower crustal origin: Earth and Planet. Sci. Letters, 9, p. 232-239.

Shride, A. F., 1967, Younger Precambrian geology in southern Arizona: U.S.G.S. Prof. Paper 566.

Siever, R., 1959, Petrology and geochemistry of silica cementation in some Pennsylvanian Sandstones: in Silica in Sediments, H. A. Ireland, ed., Soc. Econ. Paleontologists and Mineralogists Spec. Public. 7, p. 55-79.

Silberling, N. J. and R. E. Wallace, 1969, Stratigraphy of the Star Peak Group (Triassic) and overlying Lower Mesozoic rocks, Humboldt Range, Nevada: U.S.G.S. Prof. Paper 592.

Silver, L. T., 1960, Age determinations of Precambrian diabase differentiates in the Sierra Ancha, Gila County, Arizona: Bull. Geol. Soc. Amer. 71, p. 1973-1974.

Silverman, S. R., 1951, The isotopic geology of oxygen: Geochim. et Cosmochim. Acta, 2, p. 26-42.

Stöber, W., 1967, Formation of silicic acid in aqueous suspensions of different silica modification: in Equilibrium Concepts in Natural Water Systems, Am. Chem. Soc. Advances in Chemistry, Series 67.

Strahler, A. N., 1963, The Earth Sciences, Harper and Row Publishers.

Sun, M-S, 1962, Tridymite (low form) in some opal of New Mexico: Amer. Mineralogist, 47, p. 1453.

Suzuoki, T and S. Epstein, 1972, Hydrogen isotope fractionation between OH-bearing silicate minerals and water: manuscript in preparation.

Swineford, A. and P. C. Franks, 1959, Opal in the Ogallala Formation in Kansas: in Silica in Sediments, H. A. Ireland, ed., Soc. Econ. Paleontologists and Mineralogists Spec. Public. 7, p. 185.

Sverdrup, H. U., M. W. Johnson and R. H. Fleming, 1942, The Oceans, Prentice-Hall, Inc., New York.

Tallman, S. L., 1949, Sandstone types: Their abundance and cementing agents: Jour. Geology, 57, p. 582-591.

Tarr, W. A., 1926, The origin of chert and flint: Univ. Missouri Studies 1, No. 2.

Taylor, H. P., Jr., 1968, The oxygen isotope geochemistry of igneous rocks: Contr. Mineral. Petrol., 19, p. 1-71.

Taylor, H. P., Jr., and R. G. Coleman, 1968, O^{18}/O^{16} ratios of coexisting minerals in glaucophane-bearing metamorphic rocks: Bull. Geol. Soc. Amer. 79, p. 1727-1756.

Taylor, H. P., Jr., and S. Epstein, 1962, Relationship between O^{18}/O^{16} ratios in coexisting minerals of igneous and metamorphic rocks, Part I: Principles and experimental results: Bull. Geol. Soc. Amer., 73, p. 461.

Taylor, H. P., Jr., and R. W. Forester, 1971, Low-O^{18} igneous rocks from the intrusive complexes of Skye, Mull, and Ardnamurchan, Western Scotland: Jour. Petrol., 12, No. 3, p. 465-497.

Thompson T. L. and L. D. Fellows, 1969, Stratigraphy and conodont biostratigraphy of kinderhookian and osagean rocks of southwestern Missouri and adjacent areas: Missouri Geol. Survey Report of Investigations No. 45.

Tracey, J. I., Jr. et al., 1971, Site report 70: in Initial Report of the Deep Sea Drilling Project, 8, p. 135.

Trendall, A. F., 1968, Three great basins of Precambrian banded iron formation: A systematic comparison: Bull. Geol. Soc. Amer., 79, p. 1527-1544.

Trendall, A. F. and J. G. Blockley, 1970, The iron formations of the Precambrian Hamersley group, Western Australia, with special reference to the crocidolite: Western Australia Geol. Survey Bull. No. 119.

Urey, H. C., 1947, The thermodynamic properties of isotopic substances: Jour. Chem. Soc., p. 562-580.

Urey, H. C., H. A. Lowenstam, S. Epstein and C. R. McKinney, 1951, Measurement of paleotemperatures and temperature of the Upper Cretaceous of England, Denmark, and the southeastern United States: Bull. Geol. Soc. Amer., 62, p. 399-416.

Van Tuyl, F. M., 1916, The geodes of the Keokuk bed: Amer. Jour. Science, 4th series, 42, p. 34-42.

Van Tuyl, F. M., 1918, The origin of chert: Amer. Jour. Science, 4th series, 45, p. 449-456.

Van Tuyl, F. M., 1925, The stratigraphy of the Mississippian formations of Iowa: Iowa Geol. Survey Annual Report, 30, p. 33-349.

Von der Borch, C. C., J. Galehouse and W. D. Nesteroff, 1971, Silicified limestone-chert sequences cored during Leg 8 of the Deep Sea Drilling Project: A petrologic study: in Initial Reports of the Deep Sea Drilling Project, 8, J. I. Tracy Jr., et al., ed., p.819.

Von Herzen, R. P. and M. G. Langseth, 1965, Present status of oceanic heat-flow measurements: in Physics and Chemistry of the Earth, 6, p. 365-407, Pergamon Press, London.

Walker, T. R., 1960, Carbonate replacement of detrital crystalline silicate minerals as a source of authigenic silica in sedimentary rocks: Bull. Geol. Soc. Amer., 71, p. 145-157.

Walker, T. R., 1962, Reversible nature of chert-carbonate replacement in sedimentary rocks: Bull. Geol. Soc. Amer., 73, p. 237-242.

Wang, W-C and R. L. Evans, 1969, Variation of silica and diatoms in a stream: Limnology and Oceanography, 14, No. 6, p. 941-944.

Wanless, H. R., R. L. Belknap and H. Foster, 1955, Paleozoic and Mesozoic rocks of Gros Ventre, Tenton, Hoback, and Snake River Ranges, Wyoming: Geol. Soc. Amer. Memoir 63.

Ward, L. F., 1895, The Potomac formation: U.S.G.S. Annual Report, 15th, p. 323.

Weaver, F. M. and S. W. Wise, 1972, Ultramorphology of Deep Sea Crisobalitic chert, Nature Phys. Sci., 237, p. 56-57.

Weber, J. N., 1965, Evolution of the oceans and the origin of fine-grained dolomites: Nature, 207, p. 930-933.

Weller, J. M. and G. E. Ekblaw, 1940, Preliminary geologic map of parts of the Alto Pass, Jonesboro, and Thebes Quadrangles: Ill. State Geol. Survey Report of Investigations No. 70.

Weller, S. and S. St. Clair, 1928, Geology of St. Genevieve County, Missouri: Missouri Bureau of Geology and Mines, 2nd series, 22.

Wenner, D. B. and H. P. Taylor, Jr., 1972, O^{18}/O^{16} and D/H studies of a Precambrian granite-rhyolite terrane in southeastern Missouri: Trans. Amer. Geophys. Union, 53, No. 4, p. 534.

White, D. E., 1947, Diagenetic origin of chert lenses in limestone at Soyatal, State of Queretaro, Mexico: Amer. Jour. of Science, 245, p. 49.

Winterer, E. L. et al., ed., 1971, Initial Reports of the Deep Sea Drilling Project, 7, Washington.

Wrucke, C. T. and A. F. Shride, 1972, Correlation of Precambrian diabase in Arizona and southern California: Abstract in Geol. Soc. Amer. Abstracts with Programs, 4, No. 3, p. 265.

APPENDIX I

SAMPLE LOCALITIES AND DESCRIPTIONS

gmc qtz = granular microcrystalline quartz

1 Nodular chert in dolomite bed. Nopah Formation, Nopah Mtns., Calif. Coll. from unit 8 G or 8 F of measured section E-E' of Hazzard (1937). >95% gmc qtz, remainder is megaquartz and chalcedony. Some dolomite rhombs along fractures. Upper Cambrian.

2 Nodular chert from same unit, same location as #1 gmc qtz.

3 Irregular chert accumulation ("stringy" chert) from same unit, same location as #1 gmc qtz. Weathers white.

4 Irregular chert nodule from base of section E-E' of Hazzard (1937). Cornfield Springs Formation, Mid-Cambrian gmc qtz.

6 Irregular chert accumulation, Pogonip Group, Lower Ordovician, Charleston Peak Quadrangle, Nevada. NE 1/4, SW 1/4, sec. 3, T 19S, R 56 E. Ref. Longwell et al., (1965). Sample collected about 100 feet below the Eureka Quartzite. gmc qtz.

8 Thin beds (1" - 2") of chert in limestone ("Lunch Meat" chert). Monte Cristo Limestone. SW 1/4, NE 1/4, sec. 9, T 18S, R 57E, Charleston Peak Quadrangle, Nevada. Ref. Longwell et al. (1965). Mississippian gmc qtz.

9 Irregular chert nodule from bed 180 of section measured by Rich (1961), Lee Canyon, Nevada. 60% gmc qtz, 5% megaquartz, 35% carbonate. Pennsylvanian.

12 Chert nodule, Monte Cristo Limestone. On line of measured section by Rich (1961). Mississippian. Collected just below Pennsylvanian contact. gmc qtz.

15 Petrified wood from Chinle Formation. Sample coll. from purple bentonite beneath Springdale Sandstone member. Upper Triassic. SW 1/4, NE 1/4, sec. 29, T 41S, R 10W, topographic map of Zion Nat'l Park. gmc qtz with red stains from iron oxides and organic matter (?).

22 White irregular chert from limestone in Supai Formation. Collected in saddle east of Burro Spring along Kaibab Trail, Grand Canyon Nat'l Park, Arizona. Probably Pennsylvanian. About 70% gmc qtz, 2% megaquartz, 28% carbonate. Ref. map: Maxson (1967).

24 Irregular chert bed in Thunder Springs member of Redwall Limestone. Coll. at the 5,030' contour at the Kaibab Trail, Grand Canyon Nat'l Park, Arizona. 80% gmc qtz, 20% carbonate. Numerous molds of crinoid columns on weathered surfaces. Mississippian. Ref. Map: Maxson (1967).

25 Irregular chert nodule coll. at sample horizon and loc. as #24. gmc qtz.

26 Irregular chert nodule in the Bass Limestone. Precambrian. Coll. at 2,850' ± 50' contour on Kaibab Trail, Grand Canyon Nat'l Park, Arizona, just south of the Suspension Bridge. Chert occurs as scattered, irregular nodules in one three foot thick horizon. Well defined algal structures are abundant in the limestone. No diabase sills visable here. 85% megaquartz, 5% gmc qtz, 10% reddish carbonate. Ref. map: Maxson (1967).

28 Chert nodule from Kaibab Limestone. Collected at the 6,580' level on the Bright Angel Trail, Grand Canyon Nat'l Park, Arizona. gmc qtz. Permain. Ref.map: Maxson (1967).

31 Lunch meat chert, black. 1" thick chert beds, Mescal Limestone. Coll. from roadcut immediately south of Roosevelt Dam, Arizona. gmc qtz. Ref: Shride (1967). Precambrian.

34 White stringy lunch meat chert collected from ledgy outcrop south of Roosevelt Dam, Arizona. 90% gmc qtz, 5% megaquartz, 5% carbonate. Precambrian. Shride (1967).

35 Irregular chert bed in Escabrosa Limestone, near Tombstone, Arizona. SW 1/4, SW 1/4, sec. 23, T 20S, R 22E, Tombstone Quadrangle. Lower Mississippian. Ref: Gilluly et al. (1954). 75% gmc qtz (?), 10% megaquartz, 15% carbonate, numerous carbonate veinlets.

36 Thin bed of white chert with a black nodular core. Escabrosa Limestone, near Tombstone, Arizona. Coll. from saddle on middle of western half of north edge of sec. 26, T 20S, R 22E, Tombstone Quadrangle. Lower Mississippian. Ref: Gilluly et al. (1954). Extraordinarily fine-grained gmc qtz (?), network of veinlets.

37 Chert nodule 1' x 3'. Horquilla limestone near Tombstone, Arizona. Loc: center of west edge of NE 1/4 of sec. 26, T 20S, R 22E, Tombstone Quadrangle. Pennsylvanian. Ref: Gilluly et al. (1954). gmc qtz.

41 Black nodular chert, Lake Valley Formation, near Lake Valley, New Mexico. Coll. at middle of north edge of SW 1/4, sec. 21, R 7W, T 18S, Lake Valley Quadrangle. Mississippian (Osagian). 80% gmc qtz, 20% carbonate, several carbonate veins present, numerous invertebrate fragments. Ref: Jicha (1954).

59 Black bedded chert in carbonate. Helms Formation. Mississippian. Coll. on line of measured section C of King (1945). gmc qtz, organic matter (?) visable. Hueco Mountains, Texas.

62 Pinkish-gray nodule in limestone. Permain. Hueco Canyon Formation. Coll. from roadcut on Highway 180, .8 mile NE of the Roadside Park in Pow Wow Canyon, Hueco Mountains, Texas. Ref: King (1945). gmc qtz.

70 Silicified wood, white. Weathered free from a bentonite slope. Cretaceous Aguja Formaton. Collected about 1 1/2 miles west of B. M. 1881 near Hot Springs, Big Bend Nat'l Park, Texas. Ref: Maxwell et al. (1967). gmc qtz.

76 Black nodular chert in limestone. Maravillis chert. Coll. about 10' below contact with Caballos Novaculite at County Picnic grounds, south of Marathon, Texas, near old Fort Pena. Ordovician. gmc qtz. Ref: King et al. (1938).

81 Black bedded chert. Fort Pena chert. Mid-Ordovician. Coll. at bend in road to Picnic grounds about 2 miles south of Marathon, Texas. Ref: King et al. (1938). 95% gmc qtz, 2% organic matter (?), 1% detrital quartz, 2% calcite, mainly as cross-cutting veins.

85 4" thick bed of white chert in carbonate, Gorman Formation. Lower Ordovician. Roadcut on Texas Ranch Road, 2.5 miles east of Highway 290, near Johnson City, Texas. Ref: Cloud and Barnes (1946). gmc qtz.

93 Gray bed of chert in dolomite. Tanyard Formation. Lower Ordovician. Coll. from roadcut 2 miles west of Longhorn Cavern, Texas, in the "fault wedge" described by Cloud and Barnes (1946). gmc qtz.

94 8" thick bed of chert in Viola Limestone. Mid to Late Ordovician. Coll. in roadcut on Highway 77 described in Ham (1969). gmc qtz. Arbuckle Mountains, Oklahoma.

95 Irregular gray nodule collected at the same locality as #94.

101 Black bedded chert, Bigfork chert. Ordovician. Exposure in stream bottom at Granite Gap, about 8 miles north of Atoka, Oklahoma. Unit 14 of measured section in Hendricks et al. (1937). gmc qtz.

107 Gray novaculite. Arkansas Novaculite. Devonian. Roadcut about 3/4 west of Park headquarters, Beavers Bend State Park, Oklahoma. Ref: Pitt et al. (1963). 100% very fine-grained megaquartz, numerous veins of megaquartz.

111 Pure white novaculite, Arkansas Novaculite. In roadcut at Caddo Gap, Arkansas. Lower division of measured section in Miser and Purdue (1929, p. 55). 97% gmc qtz, 2% megaquartz, 1% detrital quartz grains.

120 Black bedded chert in limestone. Boone chert. Mississippian. Coll. from measured section at Buffalo River Bridge in Brewster and Williams (1951, p. 17). Near Jasper, Arkansas. gmc qtz, organic matter (?).

121 Black chert bed (8" thick) in limestone. Boone chert. Same measured section as #120. 98% gmc qtz, 2% carbonate, <1% pyrite, <1% organic matter (?). Beautiful euhedral pyrite crystals at contact with host limestone.

124 4" thick bed of light gray chert in the Cotter Dolomite. Roadcut about 1/4 mile north of the Busch Post Office, Arkansas. Badly weathered outcrop. 50% gmc qtz, 50% carbonate. Ref: Brewster and Williams (1951). Ordovician.

127 Irregular white nodular chert in Burlington-Keokuk Formation. Coll. in unnamed quarry about 1 mile due south of Grand Falls at Joplin, Missouri. Mississippian. Ref: Robertson (1967). 20% gmc qtz, 80% calcite invertebrate fragments.

128 Chert nodule in limestone of Burlington-Keokuk. Mississippian. Same locality as #127. 60% calcite as invertebrate debris, 5% sparry calcite along fractures, 34% gmc qtz, <1% dark brown material unidentified at limit of optical resolution, possibly organic matter.

136 6" thick bed of pure white chert in limestone of Elsey Formation at Lake Springfield Bridge, Missouri. Unit 1 of measured section Y in Thompson and Fellows (1969). gmc qtz.

137 8" thick bed of pure white chert collected about 5' stratigraphically above #136. 98% gmc qtz, 2% very fine-grained carbonate.

138 Gray nodular chert from the Burlington Limestone at Lake Springfield, Missouri. Measured section Y in Thompson and Fellows (1969). 59% well preserved calcite crinoid fragments, 1% sparry calcite, 30% gmc qtz, 10% megaquartz.

139 Black bedded chert in Bailey limestone. Devonian. Roadcut 2 miles south of Thebes, Illinois in State Highway 3. Field relations exposed in this roadcut are described in Weller and Ekblaw (1940). gmc qtz. Parts of this exposure are deeply weathered and parts are relatively unweathered. Sample coll. from unweathered limestone.

152 "Tripoli". Very pure, white silica earth. Coll. about 30' inside of a mine shaft. SE 1/4, sec. 10, T 14S, R 2W, Jonesburo Quadrangle, west of Elco, Illinois. Ref: Weller and Ekblaw (1940). 100% disaggregated gmc qtz. Mississippian (?).

153 Nodular chert. Concentrally banded gray and white. Krazinger Hollow. W 1/2 of sec. 18, T 12S, R 1W, Jonesburo Quadrangle, Illinois. Badly weathered outcrop, St. Louis Limestone. 5% carbonate, 2% megaquartz, 25% chalcedony, 78% gmc qtz. Mississippian.

154 Nodular chert from same locality as #153.

156 White to gray fossilferous chert. Burlington Limestone. Discontinuous bed about 12" thick. Coll. from railroad cut at section measured by Weller and St. Clair (1928) near "Clement" on the south side of Establishment Creek, Missouri. 90% gmc qtz, 5% chalcedony, 1% megaquartz, 4% carbonate. Mississippian.

157 Small chert nodule from same locality as #156.

158 Oolitic chert, Gasconade Formation. Ordovician. Roadcut about 1 mile northeast of Lawrenceton, Missouri. gmc qtz. Ref: Weller and St. Clair (1928).

160 5" bed of oolitic chert. Potosi Formation. Cambrian. NW 1/4, SE 1/4, sec. 36, R 6E, T 38N, near Lawrenceton, Missouri. Ref: Weller and St. Clair (1928).

161 Chert with abundant drusy quartz. Potosi Formation. Cambrian. Same locality as #160.

165 Nodular chert in 40' thick chert residuum of the Burlington limestone, Western Illinois. Location and description on p. 44 of Rubey (1952). Badly weathered carbonated leached out of chert surface. gmc qtz.

166 Chert with abundant drusy quartz. Same locaity as #165.

167 Irregular bed of chert in the same residuum as was #165 and #166. Carbonate leached from surface, interior gray. gmc qtz.

169 Ultra-weathered chert. Pink-gray with intense red stains, very porous. Coll. from the top of the first hill south of the location for #165 - #167. Burlington limestone residuum (?). The position of this chert at the top of the residuum indicates that it may be from a younger unit. Ref: Ruby (1952). gmc qtz.

171 Nodular chert in the Burlington limestone. Mississippian. Coll. from quarry face on Rocky Hill road just west of Hardin, Illinois. SE 1/4, SE 1/4, sec. 28, T 10S, R 2W, Hardin Quadrangle. 60% well preserved crinoid fragments, 30% chalcedony, 5% gmc qtz, 5% megaquartz. Ref. map: Rubey (1952).

188 6" wide black chert nodule in stromatilitic dolomite in the Siyeh limestone, Belt Supergroup. Precambrian. Coll. from roadcut at the point of the "rising sun" at the "narrows" in St. Mary Lake, Glacier Nat'l Park, Montana. 96% gmc qtz, 1% chalcedony and megaquartz, 3% carbonate along fractures. Ref: Ross (1959).

202 Clear, translucent hyalite opal. Botyroidal. Coll. from the summit of Mt. Blackmore near Bozeman, Montana. Occurs along fractures in weathered volcanic rocks near the summit.

209 Megaquartz geode with yellow, coarsely crystalline calcite in the core. Coll. from an argillaceous carbonate deposit in the Permian Phosphoria Formation. Locality is figure 3, location 6 of Wanless et al. (1955), about 20' from the farthest advance of the famous Gros Ventre landslide.

220 Pink-gray chert seam 1-3 cm thick. St. Charles limestone. Cambrian. Coll. near the summit of the ridge north of Fish Haven Canyon near Bear Lake, Idaho. 30% carbonate, 50% length-slow chalcedony, 20% gmc qtz. Ref: Mansfield (1927).

221 Dark gray chert seam, 3 cm thick. Coll. from summit of ridge mentioned for #220. Cambrian. St. Charles Limestone.

233 Gray nodular chert in fresh water limestone of the Miocene Humboldt Formation near Elko, Nevada. Center SE 1/4, NW 1/4, sec. 36, T 32N, R 55E. Lee, Nevada Quadrangle. 100% gmc qtz. Ref: Sharp (1939).

234 Amber-colored chert nodule from the same outcrop as #233. gmc qtz.

235 Amber and brown colored chert bleb in opal nodule from the same outcrop as #233. 98% gmc qtz, 2% chalcedony.

239 Black-gray chert nodule with deep red interior. gmc qtz. Same outcrop as #233.

244 Black, irregular chert nodule in dolomite, about 1' wide. Ordovician. Pogonip Formation. Coll. from a small bluff on the western edge of sec. 3, T 25N, R 57E. Ruby Mountains, northwest Nevada. Ref: Sharp (1942). gmc qtz.

245 White diatomite from inside mine shaft in SE 1/4 of sec. 18, T 33N, R 53E, about 3 miles northeast of Carlin, Nevada. Fresh water Miocene Humboldt Formation. Ref: Sharp (1939).

248 Black chert nodule in dolomite. Triassic. Upper Prida Formation. NE 1/4, NE 1/4, sec. 17, T 32N, R 35E, Imlay Quadrangle, northern Nevada. gmc qtz. Ref: Silberling and Wallace (1969).

249 Host dolomite for chert #248.

256 Black 10' thick chert bed forming 15' high wall on south side of mouth of canyon 2 - 3 miles due west of Minna, Nevada. Triassic. Excelsion Formation. Ref: Muller and Ferguson (1936). gmc qtz.

259 Black nodular chert in dolomite. Mid-Upper Cambrian. Emigrant Limestone. Coll. about 15 yards north of Nevada Highway 3 in SW 1/4, NE 1/4, NW 1/4, sec. 8, T 6S, R 40E, Magruder Mountain Quadrange, Nevada. gmc qtz. Ref: McKee (1968).

260 Black bedded chert. Palmetto Formation. Late-Mid Ordovician. Summit of hill on SW 1/4, SE 1/4, sec. 6, R 40E, T 6S. Magruder Mountain Quadrange, Nevada. Ref: McKee (1968). gmc qtz.

261 Diatomaceous earth. Late Pleistocene. Fresh water. SE 1/4, NW 1/4, SW 1/4, sec. 18, T 32S, R 29E, near Crowley Lake, California. Ref: Cleveland (1961).

262 Gray nodular chert in limestone. Cretaceous. FredericksburgLimestone. Stop 1, p. 43 of Barnes et al. (1956). Central Texas. 60% carbonate, 40% gmc qtz.

263 6" thick bed of gray chert in limestone at same outcrop as #262. gmc qtz and carbonate.

266 Same chert bed as #263, sampled 10 yards away.

268 Novaculite from upper member of Caballos Novaculite. Devonian. Roadcut 4 miles south of Marathon, Texas, on U. S. Highway 385. Ref: King (1938). 100% gmc qtz.

270 Novaculite from same outcrop as #268.

272 Novaculite from lower member of Caballos Novaculite at the north end of the same roadcut as for #268.

274 Black, bedded chert. Fort Pena Formation. Mid-Ordovician. 2 miles south of Marathon, Texas, in roadcut of U. S. Highway 385. 94% gmc qtz, 3% carbonate, 2% brown organic matter (?), 1% chalcedony. Ref: King (1938).

278 Black, bedded chert at contact between the Beck Spring and Kingston Peak Formation about 1 mile east of Saratoga Springs, Death Valley Nat'l Monument. 95% gmc qtz, 5% megaquartz in fractures.

283 Black chert from the Dover Flint, England. Contr. by J. Verhoogen to S. Epstein. gmc qtz.

284 Megaquartz geode from weathered Tertiary volcanic rocks, Orocopia Mountains, California. Coll. by L. T. Silver.

285 Milky opal from Virgin Valley, northwest Nevada. Coll. by H. Emerson.

286 Hyalite opal in weathered volcanic rock, Goldstone Valley, California (?). Caltech collection.

287 White, pure diatomite. Monterey Formation, Palos Verdes Hills, California. Coll. from quarry face by H. Lowenstam and S. Epstein.

288 "Fresh water diatomite", California. Location and age unknown. Contr. by J. Verhoogen to S. Epstein.

289 Silica Sponge Spicules. Coll. from dredge haul by the Univ. S. Calif. research vessel "Valero IV" near Catalina Island off the coast of Southern California. Sponge dissolved in chlorox.

300 Gunflint chert. Schreiber's Beach, Ontario, on northwest shore of Lake Superior. Coll. by J. Schopf. 97% gmc qtz, 2% megaquartz, 1% opaque organic matter (?). Precambrian. (≈2 billion years).

304 Fig Tree chert. Precambrian. ≈3 billion years. Coll. by J. Schopf. 70% megaquartz, 30% gmc qtz.

325 Blebs of chert in the Arbuckle Limestone. Coll. from an Upper Cambrian horizon on Oklahoma old Highway 77 by H. Lowenstam. 100% gmc qtz.

343 Gray mottled chert nodule dredged from the north shoulder of Horizon Guyot, Pacific Ocean. 168°52.3'W, 10°28.0'N, 1700 meters water depth. Coll. by W. Newman from dredge haul on Scripps expedition Styx, leg 7. Almost pure gmc qtz, some yellow material which may be organic matter is present.

352 Deep sea chert. Black gmc qtz with 5% chalcedony. Abundant organic matter (?) present. Mid-Eocene. JOIDES 8-70B-4cc. Tracey et al. (1971).

353 Deep sea chert from JOIDES DSDP 8-70B-4cc. Black gmc qtz with cross cutting veins of chalcedony, open cavity with fine-grained euhedral drusy quartz. Mid-Eocene. Tracey et al. (1971).

354 Deep sea chert from JOIDES DSDP 7-64-1-II, 4cc. Gray translucent gmc qtz with <1% opal-CT. Occurs as a small nodule in a lithified calcareous ooze. Winterer et al. (1971). Mid-Eocene.

355 White radiolarian ooze from JOIDES DSDP 8-69-6-5. Tracey et al. (1971). Mid-Eocene.

356 Olive green translucent chert from JOIDES DSDP 7-61-1-cc. Pure gmc qtz coexisting with opal-CT. Upper Cretaceous. Winterer et al. (1971).

367 Silicified limestone from JOIDES DSDP 8-70B-1B-1. Mid-Eocene. Sample is >90% carbonate. Silica is isotropic (opal-CT). Tracey et al. (1971).

368 Deep sea chert from JOIDES DSDP 8-70B-2B-1. gmc qtz coexisting with opal-CT. Contains white, porous areas of pure gmc qtz. Tracey et al. (1971). Mid-Eocene.

369 Deep sea silica from JOIDES DSDP 8-70B-1B-1. >98% opal-CT, 2% gmc qtz. Tracey et al. (1971). Mid-Eocene.

370 Deep sea silica from JOIDES DSDP 15-149-43-1. Eocene. >95% carbonate. Acid residue is 90% opal-CT and 10% gmc qtz. Contr. by Jim Lawrence.

371 Chert nodule from the Transvaal system dolomite, South Africa. Precambrian. Coll. by E. C. Perry. Dr. Perry writes that this chert is finer-grained than associated iron-formation cherts and that it may be the result of recent weathering. However, the sample is composed almost entirely of gmc qtz, indistinguishable from normal cherts. Neither the formation of gmc qtz nor the formation of cherts during the weathering cycle has ever been reported. Dr. Perry's suggestion is thus open to question.

372 Chert from the Bitter Springs Formation, Australia. Precambrian. Contr. by E. C. Perry. Dr. Perry writes that the Bitter Springs Formation may be an evaporite deposit.

APPENDIX II

MASS SPECTROSCOPY, CORRECTION FACTORS, AND NUMERICAL CONVERSIONS FOR THE ISOTOPIC ANALYSIS OF OXYGEN

A. C^{13}, O^{17} corrections. The CO_2 derived from silica by the fluorine method or from carbonates treated with H_3PO_4 is analyzed on a mass spectrometer containing a double-collector and a dual gas-leak system (Nier, 1947; McKinney et al., 1950). The instrument measures the ratio of the mass-46 ion beam to the combined mass-44 + mass-45 ion beams. The ratio in terms of isotopic molecules is thus:

$$R = \frac{C^{12}O^{16}O^{18} + C^{13}O^{16}O^{17} + C^{12}O^{17}O^{17}}{C^{12}O^{16}O^{16} + C^{13}O^{16}O^{16} + C^{12}O^{16}O^{17}}$$

However, since the ratio of interest is O^{18}/O^{16}, the above ratio must be corrected for O^{17} and C^{13} in order to obtain the desired ratio: $\frac{C^{12}O^{16}O^{18}}{C^{12}O^{16}O^{16}}$.

Craig (1957) has utilized absolute abundance data for C^{13} and O^{17} to derive correction factors to be applied to carbon and oxygen isotope analyses made against the PDB standard.

For carbon

$$\delta C^{13} = 1.0676\, \delta {}^{C^{13}}_{m} - .0338\, \delta O^{18}$$

For oxygen

$$\delta O^{18} = 1.0014\, \delta_m O^{18} + .009\, \delta C^{13}$$

where δm = δ-value corrected for all instrumental errors.

δ = corrected or raw δ-values (the multiplicative factors here are so small that it makes no difference whether δ is the corrected or uncorrected value).

The equations can be utilized only if PDB is the working standard in the mass spectrometer. However, in order to conserve PDB, various arbitrary standards are used as working standards and new correction equations must be evaluated. This can be done by running PDB against the working standard, and deriving the absolute ratios of the working standard from values and relationships given by Craig (1957). Most of the samples analyzed in this work were analyzed against a working standard for which the approximate correction equations were found to be

$$(1) \quad \delta_c O^{18} = 1.0014\, \delta_m O^{18} + .009 \delta_m C^{13}$$

$$(2) \quad \delta_c C^{13} = 1.0695\, \delta_m C^{13} - .0348 \delta_c O^{18}$$

B. Background corrections. The δ_m-values used in these equations must first be corrected for leakage of the glass inlet valves and the background ion currents of mass-46 and

-44. This is done by closing both inlet valves and measuring the mass-44 beam strength. This beam arises from leakage through the valves and CO_2 degassing from the metal parts of the line. The correction factor for this background is derived as follows:

The desired δ-values in terms of mass beams in the mass-spectrometer is

$$(3) \quad \delta_c = \left[\frac{\frac{46_x}{44_x}}{\frac{46_s}{44_s}} - 1 \right] 10^3$$

where 46 = mass-46 ion beam voltage

44 = mass-44 + -45 ion beams voltage

x = sample

s = standard

δ_c = uncorrected for C^{13}, O^{17}

Garlick (1964) has shown that the approximate δ-value of the mass-spectrometer background ion current is similar to that of ocean water indicating that there is no disproportionate contribution to the mass-46 background. The mass-44 background current is routinely measured and used in the following correction procedure.

The δ-value with the background ion currents included is

$$(4) \qquad \delta_u = \left[\frac{\frac{46_x + 46_B}{44_x + 44_B}}{\frac{46_s + 46_B}{44_s + 44_B}} - 1 \right] 10^3$$

where B = voltage due to background

δ_u = δ-value uncorrected for C^{13}, O^{17}, background

The gas pressures of the sample are always adjusted such that $44_x + 44_B = 44_s + 44_B$, $44_x = 44_s$.

Equation (2) then reduces to

$$\delta_u = \left[\frac{46_x + 46_B}{46_s + 46_B} - 1 \right] 10^3$$

$$\delta_u = \frac{46_s}{46_s + 46_B} \left[\frac{46_x - 46_s}{46_s} \right] 10^3$$

since $44_x = 44_s$

$$\delta_u = \frac{46_s}{46_s + 46_B} \left[\frac{\frac{46_x}{44_x} - \frac{46_s}{44_s}}{\frac{46_s}{44_s}} \right] 10^3$$

$$\delta_u = \frac{46_s}{46_s + 46_B} \cdot \delta_c$$

$$\delta_c = \left[1 + \frac{46_B}{46_s}\right] \delta_u$$

Since the natural abundance of mass-46 $\cong \frac{1}{200}$ (natural abundance of mass-44)

$$\left[1 + \frac{44_B}{44_s}\right] \delta_u = \delta_c$$

Mass $\left[44_s + 44_B\right]$ and mass-44_B are the routinely measured quantities, so the correction factor is

$$(5) \qquad \left[1 + \frac{44_B}{\left[44_B + 44_s\right] - 44_B}\right] \delta_u = \delta_c$$

where 44B = voltage mass-44 beam, both valves closed.

C. Conversion to SMOW. δ-values corrected for C^{13}, O^{17}, and background are the precise isotope ratio differences between the sample and the working standard. The values, however, must be referred to the SMOW standard. This is done using the following relationship:

$$(6) \quad \delta_{x\text{-SMOW}} = \delta_{x\text{-std}} + \delta_{\text{std-SMOW}} + 10^{-3} \delta_{(x\text{-std})} \delta_{(\text{std-SMOW})}$$

where x = sample

std = working standard

Use of this equation and further corrections differ depending on whether the CO_2 was derived from silica by the fluorine method or from carbonates by the phosphoric acid reaction. These will be considered separately.

Further CO_2 corrections for silica. The reduction to SMOW is considerably simplified if a standard with a known δ-value, $\delta_{K\text{-}SMOW}$, is run on the mass-spectrometer on the same day in which the sample(s) are analyzed. The difference between the δ-value of the known sample and the unknown sample multiplied by the appropriate correction factors and added to the δ_{SMOW}-value of the known sample yields a precise δ-value in which many instrumental and analytical errors will cancel out. In particular, for successive samples of CO_2 prepared by the fluorine method using the same carbon rod, the carbon correction in equation (1) is eliminated. A further correction, however, is necessary since a numerical δ-difference on the working-standard-scale is not the same value as a numerical difference on the SMOW scale.

The correction factor is derived from equation (4-5) by setting up the equations

$$(7)\ (4\text{-}6)\quad \delta_{x\text{-}SMOW} = \delta_{x\text{-}std} + \delta_{std\text{-}SMOW} + 10^{-3}\,\delta_{x\text{-}std}\ \delta_{std\text{-}SMOW}$$

$$(8)\quad (4\text{-}7)\quad \delta_{K\text{-}SMOW} = \delta_{K\text{-}std} + \delta_{std\text{-}SMOW} + 10^{-3}\,\delta_{K\text{-}std}\,\delta_{std\text{-}SMOW}$$

Equation (8) is subtracted from (7) to yield the approximate correction factor

$$(9)\quad (4\text{-}8)\quad \delta_{x\text{-}SMOW} - \delta_{K\text{-}SMOW} = \left[1 + \frac{1}{10^3}\,\delta_{std\text{-}SMOW}\right] \left[\delta_{x\text{-}std} - \delta_{K\text{-}std}\right] .$$

D. Blank correction for the fluorine extraction method.

The correction for oxygen impurity in the fluorine may be accomplished with the relation used for combining δ-values of two different samples.

$$(10)\quad \delta_{total} = X_1\delta_1 + (1\text{-}X_1)\,\delta_2$$

where X_1 = mole fraction of substance with δ-value = δ_1

Each sample contained n μm of impurity O_2 with $\delta_{SMOW} = \delta_1$. The correct δ-value is thus

$$\delta_{c'} = \frac{\delta_c - \left(\frac{n}{n + \mu m}\right)(\delta_1)}{1 - \frac{\mu m}{n + \mu m}}$$

where μm = CO_2 yield in μm

δ_c = δ-value for sample with impurity O_2

$\delta_{c'}$ = δ-value corrected for impurity O_2

All of the correction factors may be combined to give the following equation which is appropriate for CO_2 derived from silica by the fluorine extraction method.

$$(11)\quad \delta_f = \frac{A + \delta_{K\text{-}SMOW} - \left(\frac{n\,\delta 1}{n + \mu m}\right)}{1 - \frac{\mu m}{n + \mu m}}$$

where

$$A = \left[1+10^{-3}\,(\delta_{std\text{-}SMOW})\right]\left[1.0014\right]\left[1+\frac{44_B}{44-44_B}\right]\left[\delta_{x\text{-}std} - \delta_{K\text{-}std}\right]$$

$44 = 44B + 44S$

δ_f = final, corrected δ-value

E. Correction factors for carbonates.

Further corrections for carbonates. Raw mass-spectrometric measurements of δC^{13} and δO^{18} for CO_2 derived from carbonates by reaction with phosphoric acid are first corrected for background, C^{13}, and O^{17} by equations (1), (2), and (5). These values are then converted to PDB δ-values using the "change of standard equation".

$$(12)\quad \delta_{x\text{-}PDB} = \delta_{x\text{-}std} + \delta_{std\text{-}PDB} + 10^{-3}\,\delta_{x\text{-}std}\,\delta_{std\text{-}PDB}$$

where std = working standard

$\delta_{std\text{-}PDB}$ is determined by running the working standard against PDB

For carbon isotope corrections this represents the final step.

The δO^{18} of CO_2 of the PDB standard is +.22‰ relative to CO_2 equilibrated at 25°C with SMOW (Craig, 1961). Thus, δO^{18}_{PDB}-values from equation (12) can be converted to δO^{18}_{SMOW}-values by an additional "change-of-standard" calculation.

Comparisons of carbonate δ-values with silica δ-values

are facilitated if the carbonate δ-value is given in terms of the total carbonate relative to SMOW rather than carbonate CO_2 δ-values relative to CO_2 equilibrated with SMOW. This conversion is accomplished by combining the expressions for α of the phosphoric acid reaction with δ where

$$\alpha = \frac{(O^{18}/O^{16})_{CO_2}}{(O^{18}/O^{16})_{carbonate}}$$

to give

$$(13) \quad \delta_{carbonate}O^{18} = \frac{1000 + \delta_{CO_2}O^{18}}{\alpha} - 1000$$

Sharma and Clayton (1965) have determined α for dolomite and calcite and found $\alpha_{dolomite} = 1.01090$, $\alpha_{calcite} = 1.01008$.

This δ-value, however, is still relative to CO_2 equilibrated with SMOW. Unfortunately, the exact fractionation between CO_2 and water at 25°C is poorly known. O'Neil and Epstein (1966) determined a probable value of 1.0407 for this fractionation factor and this number has been adopted for this research. The $\delta_{SMOW\text{-}CO_2}O^{18}$-value can be converted to $\delta_{SMOW}O^{18}$ by use of this number and equation (13) to give the final form of δ-values reported for carbonates in this work.

APPENDIX III

DERIVATION OF CHERT PALEOTEMPERATURE EQUATION

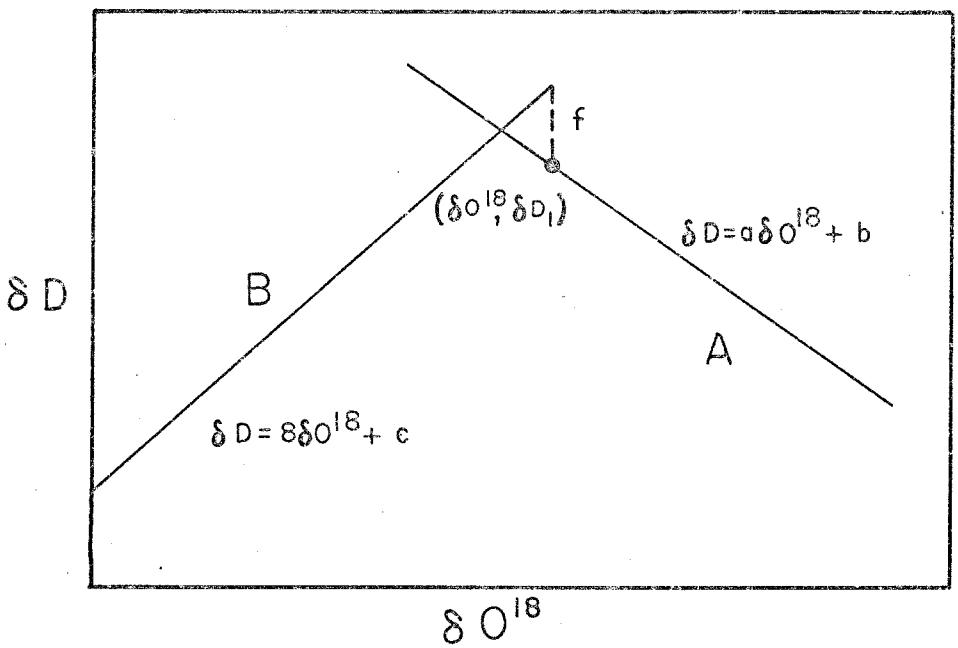

FIGURE A III-1

In figure AIII-1, line B is parallel to the meteoric water line and is given by

$$(1) \quad \delta D = 8\delta O^{18} + C \qquad C = \text{intercept}$$

This line represents the locus of δ-values for cherts in equilibrium with meteoric waters.

Line A is the locus of δ-values for marine cherts in

equilibrium with ocean water at various temperatures. Its equation is

$$(2) \quad \delta D = a\delta O^{18} + b$$

The variation with temperature of points on this line can be obtained in the following way using the chert-water oxygen isotope fraction curve normally given as

$$(3) \quad 1000 \ln \alpha^{OX}_{\text{chert-water}} = d \left(\frac{10^6}{{}^{o}K^2}\right) + g$$

where $= \dfrac{1 + \dfrac{\delta O^{18}_{\text{chert}}}{1000}}{1 + \dfrac{\delta O^{18}_{\text{water}}}{1000}}$

Since climatic temperature changes cause the intercept, C, of line B to change with time, it is possible to relate C to equation (3) to obtain a relationship between the chert δD, δO^{18}-values and temperature.

At a given temperature a point (δO_1^{18}, δD_1) on line A is specified. The intercept, C, for line B is also specified (C_1) and can be related to δO_1^{18} by solving the following two equations simultaneously.

$$\delta D_1 + f = 8\, \delta O_1^{18} + C_1$$

$$\delta D_1 = a\, \delta_1 O^{18} = b$$

where f = offset in δD of SMOW from the meteoric water line. (This may be a function of climatic temperature, but is assumed constant here. See pages 227-228 for a discussion of this quantity).

The result is

$$\delta_1 O^{18} = \frac{f - c_1 + b}{8 - a}$$

In general, then, the δO^{18}-value for a chert in equilibrium with ocean water at the same temperature as those with δ-values defining a line with intercept C (equation (1)) is given by

$$(4) \quad \delta O_m^{18} = \frac{f - c + b}{8 - a}$$

Assuming ocean water has $\delta_w O^{18} = 0.0‰$, equation (4) can be combined with equation (1), substituted into equation (3), and rearranged to give

$$(5) \quad T^{\circ}C = \sqrt{\frac{d \times 10^6}{10^3 \ln \left[1 + \frac{f + b + 8\delta O^{18} - \delta D}{(8 - a)\ 10^3}\right] - g}} - 273$$

This expression gives the temperature of formation of cherts with known δO^{18}- δD-values <u>which formed from meteoric waters</u>. If the chert formed in ocean water the equation can be used if f is set equal to 0.

If the isotopic composition of ocean water at the time of chert formation is different from $\delta O^{18} = 0$, $\delta D = 0$, then the difference in δ-values for D and O^{18} must be subtracted from the δ-values of the cherts before computing the temperature.

The temperatures listed in tables 6-1 to 6-8 were calculated from equation (5) using the following parameters obtained from the equation on page 219 and line A, figure 6-14:

$a = -6.06$,

$b = 136.8$,

$d = 3.09$,

$g = -3.29$,

$f = 10$ for charts designated in the tables as "FW",

and $f = 0$ for those designated "marine".